UNIVERSITÉ DE LIMOGES

ÉCOLE DOCTORALE SISMI n°610

FACULTÉ DES SCIENCES ET TECHNIQUES

Année : 2020 Thèse N °X

Thèse

pour obtenir le grade de

DOCTEUR DE L'UNIVERSITÉ DE LIMOGES

Discipline : Mathématiques et Applications

présentée et soutenue par

Van Duc HOANG

le 12 Février 2020

Distance and geometry of the set of curves and approximation of optimal trajectories

Thèse dirigée par: Olivier RUATTA et Jacques-Arthur WEIL

JURY :

Paul Armand	Professeur, Université de Limoges	Examinateur
Fabien Caubet	Maître de Conférences, Université de Pau	Examinateur
Bernard Mourrain	Directeur de recherche INRIA	Rapporteur
Olivier Ruatta	Maître de Conférences	Directeur de thèse
Jacques-Arthur Weil	Professeur, Université de Limoges	Directeur de thèse
Jean-Claude Yakoubsohn	Professeur, Université de Toulouse	Rapporteur

To my parents,

Acknowledgements

First of all, I would like to express my gratitude to my thesis advisors Assoc. Prof. Dr. Olivier Ruatta and Prof. Jacques-Arthur Weil. I would not be able to accomplish this work without their kind help, their ideas and suggestions they made to me during my study. It is a great honour for me to do mathematical research under their guidance. I am also deeply grateful to Van Ngai HUYNH for his kind helps.

The author is very grateful the jury, who had spent their precious time to read this dissertation, for their insightful comments and counsels. I thank the referees, Prof. Jean-Claude Yakoubsohn and Prof. Bernard Mourrain, who agreed to write a review of my thesis. The heartfelt thanks are due to Prof. Paul Armand and Assoc. Prof. Dr. Fabien Caubet for the acceptance to be a member of the jury.

This thesis has been completed at the Xlim laboratory, Faculty of Sciences and Technologies in the University of Limoges. I greatly appreciate the librarian, the secretariats and other persons at the Xlim laboratory for their kind helps to the work as well as the life in a professional scientific environment. I thank the colleagues and friends at the Xlim Laboratory about their friendly companionship and cooperation.

My sincere acknowledgements are also dedicated to the Government of Vietnam, that has given the financial supports for doing the doctoral thesis.

I thank my Vietnamese friends, who motivate and encourage me continuously: Tran, Vu, Thanh, Nguyen, Nam, Thieu, etc.

Finally, and most importantly, I would like to thank my family for everything they have given to me. My mother can not wait for me anymore. I lost my most loved one.

Contents

List of Figures

Chapter 1

Introduction

English Introduction

Optimization on the set of curves is a ubiquitous problem which has a long history in the literature. Its importance is due to the fact that, optimization on the set of curves appears in many fields of applications, not only mathematics themselves. For example, the trajectory optimization is applied in industry, robotic, walking, path-planning and aerospace ([16, 35–37, 65, 74, 76, 92, 94]). Plane shape optimization can be interpreted as a special case of curve optimization and it arises in many design problems such as structural mechanics, aerospace, automotive, hydraulic, oceanology and wind engineering ([3, 15, 27, 48, 70, 71, 81]).

We focus on a special type of curves: oriented curves admitting a parametrization from a compact real interval I to $\mathbb{R}^n$. A parametrization of a curve is a continuous map from a compact real interval I to $\mathbb{R}^n$. There always exists an increasing diffeomorphism from the compact interval I to the segment $[0,1]$, so we can consider I to be $[0,1]$ without loss of generality. Two parametrizations are equivalent if they are different by an increasing diffeomorphism. Two equivalent parametrizations have the same image, but the converse is not true. In order to overcome this problem, we consider the set of curves whose parametrizations are embeddings. Then, the set of curves $\mathfrak{C}$ is identified by the quotient of the embedding space over the increasing diffeomorphism group

$$\mathfrak{C} = \mathrm{Emb}\left([0,1],\mathbb{R}^2\right)/\mathrm{Diff}^+\left([0,1]\right).$$

The difficulty to solve the optimization on the set of curves is that the set of curves is an infinite-dimensional manifold and a curve has infinitely many parametrizations (see more detail in Subsection 2.4.1).

We already have many methods to solve optimization problems such as Simplex

algorithm of George Dantzig, Quantum optimization algorithms, Newton's method, Interior point methods, Coordinate descent methods, Conjugate gradient methods, Ellipsoid method, Conditional gradient method (Frank–Wolfe), Quasi-Newton methods, Interpolation methods, Pattern search methods, etc.

In order to use these methods on the set of curves, we need to define a distance on the set of curves. Usually, just as we do, curves are given by parametrizations. This is not obvious to define a distance between curves given by their parametrizations since the distance must not depend on the chosen parametrizations. There are mainly two ways to define distance between curves. The first way, the elastic distance between curves is defined by the minimal energy required to transform one curve into the other ([51, 63, 95, 96]). The second way, the geodesic distance between curves is defined through geodesics [8, 9, 17, 19, 24, 54, 69]. But those distances are computationally and conceptually hard to handle. Here we propose a description of the set of curves through normal forms. This allows us to define a distance between normal forms giving distance between curves independently from the chosen parametrizations.

The core idea is that two embeddings of the same curve are deduced one from the other by an increasing diffeomorphism. It is to say that we have an action of the increasing diffeomorphism group on the space of embeddings. Two embeddings are equivalent if they are different by an increasing diffeomorphism. From this idea, we construct (in Section 3.2) a normalization on the space of embeddings $\mathrm{Emb}([0,1],\mathbb{R}^n)$ with respect to the equivalent relation by the action of $\mathrm{Diff}^+([0,1])$ as follows

$$\begin{aligned} \mathfrak{N} : \mathrm{Emb}([0,1],\mathbb{R}^n) &\to \mathrm{Emb}([0,1],\mathbb{R}^n) \\ \gamma &\mapsto \mathfrak{N}(\gamma) = \gamma \circ l_\gamma^{-1} \circ k_\gamma, \end{aligned} \tag{1.1}$$

where

- $k_\gamma : [0,1] \to [0, L_\gamma], k_\gamma(v) = v.L_\gamma$ with $L_\gamma = \int_0^1 \|\dot\gamma(s)\|_2 \, ds$ is the length of γ.
- $l_\gamma : [0,1] \to [0, L_\gamma], l_\gamma(v) = \int_0^v \|\dot\gamma(s)\|_2 \, ds$ is the arc length of γ.

A curve is represented by the normal form of its parametrizarions. We identify the set of curves with the set of normal forms

$$\mathfrak{C} \equiv \mathfrak{N}\left(\mathrm{Emb}([0,1],\mathbb{R}^n)\right).$$

Then we can consider the map $\mathfrak{N}$ as follows

$$\begin{aligned}\mathfrak{N} : \mathrm{Emb}\left([0,1],\mathbb{R}^n\right) &\to \mathfrak{C} \\ \gamma &\mapsto \mathfrak{N}(\gamma).\end{aligned} \tag{1.2}$$

We define a distance between curves by using their normal forms. Doing so, we can define a distance between curves which is independent of the chosen parametrizations.

$$\begin{aligned}d^{\mathfrak{N}} &: \mathfrak{C} \times \mathfrak{C} \to \mathbb{R}^+ \\ (\mathfrak{N}(\gamma),\mathfrak{N}(\beta)) &\mapsto d^{\mathfrak{N}}\left(\mathfrak{N}(\gamma),\mathfrak{N}(\beta)\right) := \int_0^1 \|\mathfrak{N}(\gamma)(t) - \mathfrak{N}(\beta)(t)\| dt,\end{aligned}$$

where $\|\cdot\|$ is the Euclidean norm on $\mathbb{R}^n$ and $\mathfrak{N}(\gamma), \mathfrak{N}(\beta)$ are normal forms in $\mathfrak{C}$ (see Section 3.3). This distance is a distance between curves in the geometric meaning. From this distance we research topologies and differential structures on the set of curves.

The set of curves $\mathfrak{C}$ is a manifold by itself and $d^{\mathfrak{N}}$ is a distance on $\mathfrak{C}$, so the set of curves $\mathfrak{C}$ has the topology induced by the distance $d^{\mathfrak{N}}$. The set of curves $\mathfrak{C}$ is also a quotient of the right group action of $\mathrm{Diff}^+\left([0,1]\right)$ on the space $\mathrm{Emb}\left([0,1],\mathbb{R}^n\right)$, thus we have the quotient topology on the set of curves $\mathfrak{C}$. Furthermore, the set of curves $\mathfrak{C}$ is a submanifold of the space $\mathrm{Emb}\left([0,1],\mathbb{R}^n\right)$, so $\mathfrak{C}$ has the induced topology inherited from the classical topology of $\mathrm{Emb}\left([0,1],\mathbb{R}^n\right)$. In Section 3.4, we will compare the topologies on the set of curves $\mathfrak{C}$.

The maps $\mathfrak{N}$ is a map between two differential manifolds. Naturally, we check the map $\mathfrak{N}$ is a differential map. Then, for any $\gamma \in \mathrm{Emb}\left([0,1],\mathbb{R}^n\right)$, the differential of the function $\mathfrak{N}$ at γ, noted $D\mathfrak{N}(\gamma)$, is defined as follows

$$\begin{aligned}D\mathfrak{N}(\gamma) : T_\gamma \mathrm{Emb}\left([0,1],\mathbb{R}^n\right) &\to T_{\mathfrak{N}(\gamma)}\mathfrak{C} \\ \vec{u} = \partial_t f_0 &\mapsto D\mathfrak{N}(\gamma)(\vec{u}) := \lim_{t\to 0} \frac{\mathfrak{N}(f_t) - \mathfrak{N}(f_0)}{t}\end{aligned} \tag{1.3}$$

(see Definition 3.20 in Subsection 3.6.3). The function $D\mathfrak{N}(\gamma)$ is a surjective function from $T_\gamma \mathrm{Emb}\left([0,1],\mathbb{R}^n\right)$ to $T_{\mathfrak{N}(\gamma)}\mathfrak{C}$.

We give everything to do differential and variational calculus on the set of curves. But this is an infinite-dimensional manifold. Really hard to use so we use some finite-dimensional subspaces to approximate curves.

Bézier curves and piecewise Bézier curves are used to make approximations

in the space of continuous curves. The space of Bézier curves and the space of piecewise Bézier curves are finite-dimensional vector spaces. Piecewise uniform cubic Bézier curves are most common in practice. In order to solve optimal problems on the set of curves, we will use piecewise uniform cubic Bézier curves to find approximations of optimal solutions. So, we focus on piecewise uniform cubic Bézier curves.

In Subsection 4.2.2, we define a norm $\|\cdot\|_p^{B_D}$ on the space B_D of Bézier curves of degree D and a norm $\|\cdot\|_p^{B_{N,D}}$ on the space $B_{N,D}$ of uniform N-piece Bézier curves of degree D. The norms $\|\cdot\|_p^{B_D}$ and $\|\cdot\|_p^{B_{N,D}}$ are determined through control points.

The space $B_{N,3}$ of uniform N-piece cubic Bézier curves is a subspace of the space $C^0([0,1],\mathbb{R}^n)$, then $B_{N,3}$ inherits the L_p norm, $1 \leq p \leq \infty$. The equivalence constants for the norm $\|\cdot\|_p^{B_{N,3}}$ and the L_p norm on the space $B_{N,3}$ are studied in Subsection 4.2.3. This is the core idea of Algorithm 2 on page 86 in Chapter 5 using piecewise uniform cubic Bézier curves.

A Bézier curve of degree D can be written as a Bézier curve of degree $D+1$. Then we have more control points in order to give additional freedom for curve design. In Subsection 4.2.4, we will find the equivalence constants for the norm $\|\cdot\|_p^{B_{N,D}}$ and the norm $\|\cdot\|_p^{B_{N,D+1}}$ on the space $B_{N,D}$ of uniform N-piece Bézier curves of degree D.

A uniform N-piece cubic Bézier curve can be split to become a uniform $2N$-piece cubic Bézier curve. This approach creates extra control points in order to give additional freedom for curve design and avoids increasing the degree of the curve. Splitting piecewise cubic Bézier curves plays an important role in Algorithm 2 on page 86 in Chapter 5 using piecewise uniform cubic Bézier curves. So, in Subsection 4.2.4, we will investigate the equivalence constants for the norm $\|\cdot\|_p^{B_{2N,3}}$ and the norm $\|\cdot\|_p^{B_{N,3}}$ on the space $B_{N,3}$.

In Chapter 5, we apply piecewise uniform cubic Bézier curves to trajectory optimization problems, autonomous ordinary differential equations and control of autonomous ordinary differential equations.

Trajectory optimization problems appear in many different domains as robotic ([16, 36, 37, 75]), astrophysics ([6, 76, 92, 94]) and the core of motion planning which is known to be a very difficult problem ([18, 35, 37, 74, 88]). We will propose an algorithm using piecewise uniform cubic Bézier curves to approximate optimal trajectories in trajectory optimization problems (see Section 5.1).

An autonomous ordinary differential equation is a system of ordinary differential equations which does not explicitly depend on the independent variable ([45, 62, 66, 90, 91]). When the variable is time, they are also called time-invariant

systems. Many laws in physics, where the independent variable is usually assumed to be time, are expressed as autonomous ordinary differential equations because it is assumed the laws of nature which hold now are identical to those for any point in the past or future. In Section 5.3, we will apply our method to approximate solution orbits of autonomous ordinary differential equations. In order to show the efficiency of our method, we are going to compare our method and some classical methods in Subsection 5.3.4.

Our method can be applied to control of autonomous ordinary differential equations. In Section 5.5, we will present some examples of control of autonomous ordinary differential equations.

Introduction français

L'optimisation sur l'ensemble des courbes est un problème omniprésent qui a une longue histoire dans la littérature scientifique. Son importance est due au fait que, l'optimisation sur l'ensemble des courbes apparaît dans de nombreux domaines d'applications et pas seulement en mathématiques. Par exemple, l'optimisation des trajectoires a des applications dans l'industrie, la robotique, la marche, la planification de mouvement et l'aérospatiale. L'optimisation de la forme plane peut être interprétée comme un cas particulier d'optimisation de courbes et il se retrouve dans de nombreux problèmes de conception mécanique, l'industrie aérospatiale, la construction automobile, hydraulique, l'océanographie.

Nous nous concentrons sur un type particulier de courbes: courbes orientées admettant une paramétrisation à partir d'un intervalle réel compact I to $\mathbb{R}^n$. Un paramétrage. Une courbe est représenté comme image d'une fonction continue définie sur un intervalle réel compact I à valeur dans $\mathbb{R}^n$. Il existe toujours un difféomorphisme croissant entre I et le segment $[0,1]$. Nous pouvons donc considérer que I est $[0,1]$ sans perte de généralité. Deux paramétrisations sont équivalentes si on obtient l'une de m'autre par composition avec un difféomorphisme croissant. Deux paramétrisations équivalentes ont la même image, mais l'inverse n'est pas vrai. Afin de surmonter ce problème, nous considérons l'ensemble des courbes dont les paramétrisations sont des plongements. Ainsi, l'ensemble des courbes $\mathfrak{C}$ est identifié par le quotient de l'espace de plongements sur le groupe des difféomorphismes croissants

$$\mathfrak{C} = \mathrm{Emb}\left([0,1], \mathbb{R}^2\right) / \mathrm{Diff}^+\left([0,1]\right).$$

Une difficulté pour résoudre u problème d'optimisation sur l'ensemble des courbes est que l'ensemble des courbes est une variété de dimension infinie et qu'une courbe a une infinité de paramétrisations.

Nous avons déjà de nombreuses méthodes pour résoudre des problèmes d'optimisation tels que l'algorithme du simplexe, l'algorithmes d'optimisation quantique, la méthode de Newton, les méthodes de points intérieurs, les méthodes de descente, la méthode du gradient conjugué, la méthode de l'ellipsoïde, l' algorithme de Frank-Wolfe, la méthode quasi-Newton, les méthodes d'interpolation, les méthodes de recherche directe, etc.

Afin d'utiliser ces méthodes sur l'ensemble des courbes, nous devons définir une distance sur l'ensemble des courbes. Habituellement, comme nous le faisons, les courbes sont données par paramétrisation. Il n'est pas évident de définir

une distance entre courbes donnée par leurs paramétrisations puisque la distance ne doit pas dépendre des paramétrisations choisies. Il existe principalement deux façons classiques de définir la distance entre les courbes. La première, la distance élastique entre les courbes est définie par l'énergie minimale requise pour transformer une courbe en une autre. La deuxième, la distance géodésique entre les courbes est définie par la géodésique. Mais ces distances sont algorithmiquement et conceptuellement difficile à gérer. Nous proposons ici une description de l'ensemble des courbes à travers des formes normales. Cela nous permet de définir une distance entre les formes normales donnant une distance entre les courbes indépendamment des paramétrisation choisies.

L'idée centrale est que deux plongements de la même courbe se déduisent l'une de l'autre par un difféomorphisme croissant. C'est dire que nous avons une action du groupe de difféomorphisme croissant sur l'espace de plongements et que deux plongements sont équivalent si et seulement si ils définisssent la même courbe. Suivant cette idée, nous construisons (dans la section 3.2) une normalisation sur l'espace de plongements $\mathrm{Emb}([0,1],\mathbb{R}^2)$ par rapport à la relation équivalente par l'action de $\mathrm{Diff}^+([0,1])$ comme suit

$$\begin{aligned} \mathfrak{N} : \mathrm{Emb}([0,1],\mathbb{R}^n) &\to \mathrm{Emb}([0,1],\mathbb{R}^n) \\ \gamma &\mapsto \mathfrak{N}(\gamma) = \gamma \circ l_\gamma^{-1} \circ k_\gamma, \end{aligned} \tag{1.4}$$

En posant :

- $k_\gamma : [0,1] \to [0, L_\gamma], k_\gamma(v) = v.L_\gamma$ avec $L_\gamma = \int_0^1 \|\dot\gamma(s)\|_2 \, ds$ est la longueur de γ.
- $l_\gamma : [0,1] \to [0, L_\gamma], l_\gamma(v) = \int_0^v \|\dot\gamma(s)\|_2 \, ds$ est la longueur d'un arc γ.

Une courbe est représentée par la forme normale de sa paramétrisation. On identifie l'ensemble des courbes avec l'ensemble des formes normales

$$\mathfrak{C} \equiv \mathfrak{N}\left(\mathrm{Emb}([0,1],\mathbb{R}^n)\right).$$

Ensuite, nous considérons la fonction $\mathfrak{N}$ comme suit

$$\begin{aligned} \mathfrak{N} : \mathrm{Emb}([0,1],\mathbb{R}^n) &\to \mathfrak{C} \\ \gamma &\mapsto \mathfrak{N}(\gamma). \end{aligned} \tag{1.5}$$

Nous définissons une distance entre les courbes en utilisant les formes

normales de leurs paramétrisations. La distance obtenue est indépendante de paramétrisations choisies au départ pour représenter les courbes.

$$d^{\mathfrak{N}} : \mathfrak{C} \times \mathfrak{C} \to \mathbb{R}^+$$
$$(\mathfrak{N}(\gamma), \mathfrak{N}(\beta)) \mapsto d^{\mathfrak{N}}(\mathfrak{N}(\gamma), \mathfrak{N}(\beta)) := \int_0^1 \|\mathfrak{N}(\gamma)(t) - \mathfrak{N}(\beta)(t)\| dt,$$

où $\|\cdot\|$ est la norme euclidienne sur $\mathbb{R}^n$ et $\mathfrak{N}(\gamma)$, $\mathfrak{N}(\beta)$ sont des formes normales dans $\mathfrak{C}$ (voir Section 3.3). Cette distance est une distance entre des courbes dans le sens géométrique. Nous nous servons de cette distance pour étudier les propriťés topologiques et différentielles de l'espace des courbes.

L'ensemble des courbes est une variété intrinsèque et $d^{\mathfrak{N}}$ est une distance sur $\mathfrak{C}$, donc l'ensemble des courbes $\mathfrak{C}$ admet une topologie induite par la distance $d^{\mathfrak{N}}$. L'ensemble des courbes $\mathfrak{C}$ est aussi un quotient de l'action à droite d'un groupe $\mathrm{Diff}^+([0,1])$ sur l'espace $\mathrm{Emb}([0,1], \mathbb{R}^n)$, ainsi nous avons une topologie quotient sur l'ensemble des courbes $\mathfrak{C}$. De plus, l'ensemble des courbes $\mathfrak{C}$ est une sous-variété de l'espace $\mathrm{Emb}([0,1], \mathbb{R}^n)$, alors $\mathfrak{C}$ a la topologie induite de celle de $\mathrm{Emb}([0,1], \mathbb{R}^n)$. Dans Section 3.4, nous comparons ces topologies sur l'ensemble des courbes $\mathfrak{C}$.

La fonction $\mathfrak{N}$ est une application entre variétés différentielles. Naturellement, nous vérifions la fonction N est une fonction différentielle. Ensuite, pour tout $\gamma \in \mathrm{Emb}([0,1], \mathbb{R}^n)$, le différentiel de la fonction $\mathfrak{N}$ en γ, noté $D\mathfrak{N}(\gamma)$, est défini comme suit

$$\begin{aligned} D\mathfrak{N}(\gamma) : T_\gamma \mathrm{Emb}([0,1], \mathbb{R}^n) &\to T_{\mathfrak{N}(\gamma)}\mathfrak{C} \\ \vec{u} = \partial_t f_0 &\mapsto D\mathfrak{N}(\gamma)(\vec{u}) := \lim_{t \to 0} \frac{\mathfrak{N}(f_t) - \mathfrak{N}(f_0)}{t} \end{aligned} \tag{1.6}$$

(voir Définition 3.20 dans Sous-section 3.6.3). La fonction $D\mathfrak{N}(\gamma)$ est une fonction surjective de $T_\gamma \mathrm{Emb}([0,1], \mathbb{R}^n)$ à $T_{\mathfrak{N}(\gamma)}\mathfrak{C}$.

Nous developpons les outils nécessaires pour faire du calcul différentiel et variationnel sur l'ensemble des courbes. Mais $\mathfrak{C}$ est une variété de dimension infinie, ce qui rend le calcul explicite très difficile. Nous explorons alors l'idée d'étudier de faire des approximation dans des sous-espaces de dimensions finies.

Les courbes de Bézier et courbes de Bézier par morceaux sont utilisées pour faire des approximations dans l'espace des courbes continues. Ces espaces sont des espaces vectoriels de dimension finie. Les courbes de Bézier cubiques uniformes par morceaux sont les plus couramment utilisés en pratique. Afin de résoudre des

problèmes d'optimisation sur l'ensemble des courbes, nous utiliserons des courbes de Bézier cubiques uniformes par morceaux pour trouver des approximations de solutions optimales. Nous nous concentrons alors sur les courbes de Bézier par morceaux uniformes de degré 3.

Dans Sous-section 4.2.2, nous définissons une norme $\|\cdot\|_p^{B_D}$ sur l'espace B_D des courbes de Bézier de degré D et une norme $\|\cdot\|_p^{B_{N,D}}$ sur l'espace $B_{N,D}$ des N-pièce uniformes courbes de Bézier de degré D. Les normes $\|\cdot\|_p^{B_D}$ et $\|\cdot\|_p^{B_{N,D}}$ sont déterminées uniquement par des points de contrôle, ce qui les rend facile à utiliser en pratique.

L'espace $B_{N,3}$ des N-pièce uniformes courbes de Bézier cubiques est un sous-espace de l'espace $C^0([0,1],\mathbb{R}^n)$, alors $B_{N,3}$ hérite de la norme L_p, $1 \leq p \leq \infty$. Les constantes d'équivalence pour la norme $\|\cdot\|_p^{B_{N,3}}$ et la norme L_p sur l'espace $B_{N,3}$ sont étudiées à la sous-section 4.2.3. C'est l'idée principale de Algorithme 2, à la page 86 du Chapitre 5, qui utilise des courbes de Bézier cubiques uniformes par morceaux.

Une courbe de Bézier de degré D peut s'écrire comme une courbe de Bézier de degré $D+1$. Ceci permet de rajouter des points de contrôle afin de donner une liberté supplémentaire pour la conception des courbes. Dans Sous-section 4.2.4, nous allons aprocher les constantes d'équivalence pour la norme $\|\cdot\|_p^{B_{N,D}}$ et la norme $\|\cdot\|_p^{B_{N,D+1}}$ sur l'espace $B_{N,D}$ des N-pièce uniformes courbes de Bézier de degré D.

Une courbes de Bézier uniforme cubique ayant N morceaux peut être divisée pour en obtenir une ayant $2N$ morceaux cubiques. Cette approche crée des points de contrôle supplémentaires afin de donner une liberté supplémentaire à la conception de la courbe et évite d'augmenter le degré de la courbe. La division de courbes de Bézier cubiques par morceaux joue un rôle important dans Algorithme 2 dans page 86, au Chapitre 5, en utilisant des courbes de Bézier cubiques uniformes par morceaux. Donc, dans Sous-section 4.2.4, nous étudierons les constantes d'équivalence pour la norme $\|\cdot\|_p^{B_{2N,3}}$ et la norme $\|\cdot\|_p^{B_{N,3}}$ sur l'espace $B_{N,3}$.

Dans Chapitre 5, nous utilisons des courbes de Bézier cubiques uniformes par morceaux aux problèmes d'optimisation de trajectoire, aux équations différentielles ordinaires autonomes et au contrôle d'équations différentielles ordinaires autonomes.

Les problèmes d'optimisation de trajectoire apparaissent dans de nombreux domaines différents sous forme de robotique, astrophysique et le noyau de la planification de mouvement qui est connu pour être un problème très difficile. Nous proposerons un algorithme utilisant des courbes de Bézier cubiques uniformes

par morceaux pour approcher des trajectoires optimales dans des problèmes d'optimisation de trajectoire (voir Section 5.1).

De nombreuses lois de la physique sont exprimées sous forme d'équations différentielles ordinaires autonomes. Dans Section 5.3, nous appliquerons notre méthode pour approcher les orbites de solution d'équations différentielles ordinaires autonomes. Afin de montrer l'efficacité de notre méthode, nous comparons notre méthode et certaines méthodes classiques dans Sous-section 5.3.3.

Notre méthode peut être appliquée au contrôle d'équations différentielles ordinaires autonomes. Dans Section 5.5, nous présenterons quelques exemples d'application de notre approche à des problèmes de contrôle d'équations différentielles ordinaires autonomes.

Chapter 2

Background

In this chapter, we introduce the mathematical background on normalization, topology, differential geometry, geometry, curves and Bézier curves. These tools will be used in the next chapter. The normalization is related to group action and rewriting. We use this to define a distance between curves and study topologies and differential structures on the set of curves. In Chapter 4, we study the space of Bézier curves. We use piecewise uniform cubic Bézier curves to do some applications in Chapter 5.

2.1 Normalizations

Let S be a set and let R be an equivalent relation on S. Naturally we have the quotient set S/R which is the set of equivalence classes. A normalization is a surjective map

$$N : S \to S/R$$

such that $N(x) = N(y)$ if and only if xRy.

We denote $\mathrm{Diff}^+([0,1])$ be the group of increasing diffeomorphisms from $[0,1]$ to itself and $\mathrm{Emb}([0,1],\mathbb{R}^n)$ be the space of embeddings from $[0,1]$ to $\mathbb{R}^n$. The increasing diffeomorphism group $\mathrm{Diff}^+([0,1])$ acts on the space of embeddings $\mathrm{Emb}([0,1],\mathbb{R}^n)$ on the right. Two embeddings γ_1, γ_2 are equivalent if there exists $\delta \in \mathrm{Diff}^+([0,1])$ such that $\gamma_1 = \gamma_2 \circ \delta$. Then we consider the quotient $\mathrm{Emb}([0,1],\mathbb{R}^n)/\mathrm{Diff}^+([0,1])$. In this thesis, we identify the set of curves with the quotient $\mathrm{Emb}([0,1],\mathbb{R}^n)/\mathrm{Diff}^+([0,1])$. The main idea in Chapter 3 is to give normal forms of curves.

We go into the details of the definition of a normalization and examples.

2.1.1 Definitions

We consider S to be a set and R be an equivalent relation on S. We want to have a way to represent the quotient set S/R. Since elements of S/R are equivalence classes, the idea is to be able to associate each class with a special element in the class: the normal form of all elements of the class. Since each class is represented by an element of the class, the quotient set S/R is considered as a subset of S. Generally, a normal form system is given by using a map $N : S \to S$ such that is $xRy \Leftrightarrow N(x) = N(y)$. Then we identify S/R with $N(S)$.

Definition 2.1. ([47, 60, 80]) A normalization with respect to an equivalence relation R on a set S is a mapping $c : S \to S$ such that for all $s, s_1, s_2 \in S$:

1. $c(s) = c(c(s))$ (idempotence),

2. $c(s_1) = c(s_2)$ if and only if $s_1 \ R \ s_2$ (decisiveness) and

3. $s \ R \ c(s)$ (representativeness).

The element $c(s)$ is called the normal form of s.

The property 3 is redundant, it follows by applying 2 to 1.

In practical terms, one wants to be able to compute the normal forms. There is also a practical, algorithmic question to consider: how to pass from a given object s in S to its normal form s^*? If c is a morphism and S/R has a structure, then it is possible to operate directly on the equivalence classes. For example, in modular arithmetic, the normal form for a residue class is usually taken as the least non-negative integer in it. Operations on classes are carried out by combining these representatives and then reducing the result to its least non-negative residue. The uniqueness requirement is sometimes relaxed, allowing the forms to be unique up to some finer equivalence relation, like allowing reordering of terms (if there is no natural ordering on terms).

A normal form may simply be a convention, or a deep theorem. For example, polynomials are conventionally written with the terms in decreasing powers: it is more usual to write $x^2 + x + 30$ rather than $x + 30 + x^2$, although the two forms define the same polynomial. In contrast, the existence of Jordan normal form for a matrix is a deep theorem.

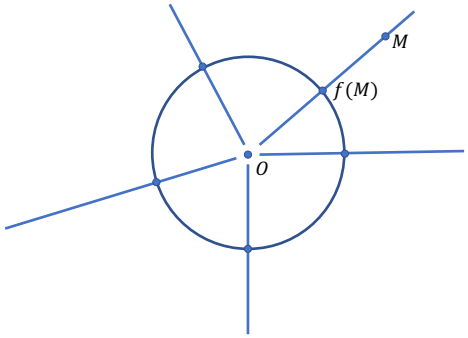

Fig. 2.1: The normalization on the set $\mathbb{R}^2\backslash\{(0,0)\}$.

2.1.2 Examples

The normalization on the set $\mathbb{R}^2\backslash\{(0,0)\}$

We consider the set $\mathbb{R}^2\backslash\{(0,0)\}$. Two points M, N in $\mathbb{R}^2\backslash\{(0,0)\}$ are equivalent if there exists $\lambda \in \mathbb{R}^+\backslash\{0\}$ such that $M = \lambda N$.

The normalization f on $\mathbb{R}^2\backslash\{(0,0)\}$ is defined as follows

$$\begin{aligned} f : \mathbb{R}^2\backslash\{(0,0)\} &\to \mathbb{R}^2\backslash\{(0,0)\} \\ M &\mapsto f(M) := \frac{M}{\|OM\|}, \end{aligned}$$

where $\|\cdot\|$ is the Euclidean norm on $\mathbb{R}^2$.

The normalization f satisfies

1. $f(M) = f(f(M))$ (idempotence),

2. $f(M) = f(N)$ if and only if M is equivalent to N (decisiveness)

for all $M, N \in \mathbb{R}^2\backslash\{(0,0)\}$.

From the equivalent relation on $\mathbb{R}^2\backslash\{(0,0)\}$, each equivalence class is a semi-line which starts the origin. A semi-line which starts the origin intersects the unit circle at the unique point. With a point on the unit circle, there is a semi-line which starts the origin and goes through the point. So, the set of equivalence classes is isomorphic to the unit circle. An equivalence class is presented by a point on the unit circle.

Normal matrices over the complex numbers

A complex square matrix A is normal if

$$A^*A = AA^*,$$

where A^* is the conjugate transpose of A. That is, a matrix is normal if it commutes with its conjugate transpose.

Proposition 2.2. ([11, 49, 50]) A matrix A is normal if and only if there exists a diagonal matrix Λ and a unitary matrix U such that $A = U\Lambda U^*$.

Matrix A is equivalent to matrix B if $A = U^*BU$ for some unitary matrix U. We set $\mathcal{M}$ be the normal matrices over the complex numbers. The normalization f on $\mathcal{M}$ as follows

$$\begin{aligned} f : \mathcal{M} &\to \mathcal{M} \\ A &\mapsto \Lambda_A, \end{aligned}$$

where Λ_A is the diagonal matrix which is unitarily similar to A.

The normalization f satisfies

1. $f(A) = f(f(A))$ (idempotence),
2. $f(A) = f(B)$ if and only if A is equivalent to matrix B (decisiveness)

for all $A, B \in \mathcal{M}$.

From the equivalent relation on the set $\mathcal{M}$, for each $A \in \mathcal{M}$, we have the equivalence class

$$\overline{A} := \{U^*AU |\ U \text{ is a unitary matrix } \}.$$

An equivalence class $\overline{A}$ has the unique diagonal matrix Λ_A. Another way, from a diagonal matrix Λ, we have the unique equivalent relation $\overline{\Lambda}$. So, the set of equivalence classes on $\mathcal{M}$ is isomorphic to the set of diagonal matrices. An equivalence class on $\mathcal{M}$ is presented by a diagonal matrix.

Matrices over the complex numbers

We consider the set $\mathcal{X}$ of matrices over the complex numbers. On X we consider an equivalence relation: Matrix A is equivalent to matrix B if $A = UBV^*$ for some unitary matrices U and V.

Theorem 2.3. ([40, 42]) (Singular-value decomposition) Suppose M is a $m \times n$ matrix whose entries come from the field K, which is either the field of real numbers or the field of complex numbers. Then there exists a factorization, called a singular value decomposition of M, of the form

$$M = U\Sigma V^*,$$

where

- U is an $m \times m$ unitary matrix over K (if $K = \mathbb{R}$, unitary matrices are orthogonal matrices),
- Σ is a diagonal m $\times$ n matrix with non-negative real numbers on the diagonal,
- V is an $n \times n$ unitary matrix over K and
- V^* is the conjugate transpose of V.

The diagonal entries σ_i of Σ are known as the singular values of M. A common convention is to list the singular values in descending order. In this case, the diagonal matrix, Σ, is uniquely determined by M (though not the matrices U and V).

The normalization h on $\mathcal{X}$ as follows

$$\begin{aligned} h : \mathcal{X} &\to \mathcal{X} \\ M &\mapsto \Sigma_M, \end{aligned}$$

where Σ_M is a diagonal matrix which is is uniquely determined by M.

The normalization h satisfies

1. $h(A) = h(h(A))$ (idempotence),
2. $h(A) = h(B)$ if and only if A is equivalent to matrix B (decisiveness)

for all $A, B \in \mathcal{X}$.

From the equivalent relation on the set $\mathcal{X}$, for each $A \in \mathcal{X}$, we have the equivalence class

$$\overline{A} := \{UAV^* |\ U, V \text{ are unitary matrices } \}.$$

An equivalence class $\overline{A}$ has the unique diagonal matrix Σ_A. Another way, from a diagonal matrix Σ, we have unique equivalent relation $\overline{\Sigma}$. So, the set of equivalence

classes on $\mathcal{X}$ is isomorphic to the set of diagonal matrices. An equivalence class on $\mathcal{X}$ is presented by a diagonal matrix.

2.2 Topologies

Let S be a topological space, R be an equivalent relation on S and $N : S \to S/R$ be a normalization. We have two types of topology which we can consider on S/R : the quotient topology (the one for which N is continuous) and the topology which is induced from a distance on S/R. We will focus on these two types of topology. The aim of this section is to recall definitions of topologies and continuous functions.

2.2.1 Topological spaces

Definition 2.4. ([25, 32, 52]) A topological space is a pair (X, τ) consisting of a set X and a family τ of its subsets which is subject to the following conditions:

1. $\emptyset \in \tau, X \in \tau$.
2. If $U_1 \in \tau$ and $U_2 \in \tau$, then $U_1 \cap U_2 \in \tau$.
3. If $U_s \in \tau$ for every $s \in S$, where S is an arbitrary set, then $\bigcup_{s \in S} U_s \in \tau$.

The set X will be called a space, its elements are points of the space and subsets belonging to the family τ are open sets in the space. The family τ is called a topology on the set X.

A subset of X is said to be closed if its complement is in τ (i.e., its complement is open). A subset of X may be open, closed, both (clopen set), or neither. The empty set and X itself are always both closed and open.

Example 2.5. (Finite complement topology) Define τ to be the collection of all subsets U of X such that $X \setminus U$ either is finite or X itself. Then τ defines a topology on X, called finite complement topology of X.

Once we define a structure on a set, often we try to understand what the minimum data you need to specify the structure. In many cases, this minimum data is called a basis and we say that the basis generates the structure.

Definition 2.6. ([25, 32, 52]) Let (X, τ) be a topological space. A family $\mathfrak{B} \subset \tau$ is called a base of the topological space (X, τ) if:

1. For every $x \in X$, there is an element B in $\mathfrak{B}$ such that $x \in B$.
2. If $x \in B_1 \cap B_2$ where B_1, B_2 are in $\mathfrak{B}$, then there is B_3 in $\mathfrak{B}$ such that $x \in B_3 \subset B_1 \cap B_2$.

Example 2.7. (Standard Topology of $\mathbb{R}$) Let $\mathbb{R}$ be the set of all real numbers. Let $\mathfrak{B}$ be the collection of all open intervals:

$$(a, b) := \{x \in \mathbb{R} |\ a < x < b\}$$

Then $\mathbb{R}$ is a basis of a topology and the topology generated by $\mathbb{R}$ is called the standard topology of $\mathbb{R}$.

Definition 2.8. ([25, 32, 52]) Let τ_1, τ_2 be two topologies for a set X. We say τ_2 is thinner than τ_1 or τ_1 is coarser than τ_2 if $\tau_1 \subset \tau_2$. The intuition for this notion is "(X, τ_2) has more open subsets to separate two points in X than $(X; \tau_1)$".

2.2.2 Induced topology

A subset Y of a topological space X has a naturally topology induced by the topology of X, called the induced topology.

Definition 2.9. ([25, 32, 52]) Let $(X; \tau)$ be a topological space. Let Y be a subset of X. The collection

$$\tau_Y := \{Y \cap U \mid U \in \tau\}$$

is a topology on Y, called the induced topology.

2.2.3 Hausdorff Spaces, Continuous Functions

Definition 2.10. ([25, 32, 52]) A topological space $(X; \tau)$ is called a Hausdorff space if

$$\forall x, y \in X \text{ such that } x \neq y,\ \exists U_x, U_y \in \tau \text{ such that } x \in U_x, y \in U_y \text{ and } U_x \cap U_y = \emptyset$$

i.e., for every pair of distinct points x, y in X, there are disjoint neighbourhoods U_x and U_y of x and y respectively.

Example 2.11. $\mathbb{R}^n$ with the standard topology is a Hausdorff space.

Definition 2.12. ([25, 32, 52]) Let $\{x_n | n \in \mathbb{N}\}$ be a sequence of points in a topological space. The sequence $\{x_n | n \in \mathbb{N}\}$ converges to a point $x \in X$ if, for

every neighborhood U of x, there is a positive integer $N \in \mathbb{N}$ such that $x_n \in U$ for all $n \geq N$.

Continuity is a topological notion.

Definition 2.13. ([25, 32, 52]) Let X, Y be topological spaces. A function $f : X \to Y$ is continuous if $f^{-1}(U)$ is open in X for all open sets $U \in Y$.

Proposition 2.14. ([25, 32, 52]) A function $f : X \to Y$ is continuous if and only if $f^{-1}(V)$ is closed in X for all closed sets $V \in Y$.

2.2.4 Quotient topology

Let (X, τ) be a topological space, and let $\sim$ be an equivalence relation on X. The quotient space, $Y = X/\sim$ is defined to be the set of equivalence classes of elements of X

$$Y = \{[x] : x \in X\} = \{\{v \in X : v \sim x\} : x \in X\},$$

equipped with the topology where the open sets are defined to be those sets of equivalence classes whose unions are open sets in X

$$\tau_Y = \left\{ U \in Y : \bigcup U = \bigcup_{[a] \in U} [a] \in \tau_X \right\}.$$

The topology τ_Y is called a quotient topology on the quotient space $Y = X/\sim$. One can see more detail in ([25, 32, 52]).

From the definition, if $N : S \to S/R$ is a normalization, then N is continuous for the quotient topology.

2.3 Differential Geometry

This section is devoted to the needed background of differential geometry.

2.3.1 Finite dimensional manifolds

Definitions

A differential manifold is a set where each point has a neighborhood diffeomorphic to an open subset of $\mathbb{R}^d$ and with compatibility condition between two neighborhoods.

Definition 2.15. ([59, 93, 97]) Let M be a topological Hausdorff space. A d-dimensional local chart on M is a pair (U, Φ) where U is an open subset of M and Φ a homeomorphism between U and some open subset of $\mathbb{R}^d$.

Two d-dimensional local charts, (U_1, Φ_1) and (U_2, Φ_2) are C^∞-compatible if either U_1 and U_2 do not overlap, or the function $\Phi_1 \circ \Phi_2^{-1}$ is a C^∞-diffeomorphism between $\Phi_2(U_2 \cap U_1)$ and $\Phi_1(U_2 \cap U_1)$.

A d-dimensional atlas on M is a family of pairwise compatible local charts $((U_i, \Phi_i), i \in I)$, such that $M = \bigcup_i U_i$. Two atlases on M are equivalents if their union is also an atlas, i.e., if every local chart of the first one is compatible with every local chart of the second one.

A Hausdorff space with a d-dimensional atlas is called a d-dimensional (C^∞) differential manifold.

If M is a manifold, a local chart on M will always be assumed to be compatible with the atlas on M. If M and N are two manifolds, their product $M \times N$ is also a manifold; if (U, Φ) is a chart on M, (V, Ψ) a chart on N, $(U \times V, (\Phi, \Psi))$ is a chart on $M \times N$, and one shows easily that one can form an atlas for $M \times N$ from cross products of two atlases of M and N.

When a local chart (U, Φ) is given, the coordinate functions $x_1, ..., x_d$ are defined by $\Phi(p) = (x_1(p), ..., x_d(p))$ for $p \in U$. Formally, x_i is a function from U to $\mathbb{R}$. However, when a point p is given, one generally refers to $x_i = x_i(p) \in \mathbb{R}$ as the ith coordinate of p in the chart (U, Φ).

We now consider functions on manifolds.

Definition 2.16. ([59, 93, 97]) A function $\psi : M \to \mathbb{R}$ is C^∞ if, for every local chart (U, Φ) on M, the function $\psi \circ \Phi^{-1} : \Phi(U) \subset \mathbb{R}^d \to \mathbb{R}$, is C^∞ in the usual sense. The function $\psi \circ \Phi^{-1}$ is called the interpretation of ψ in (U, Φ).

From the compatibility condition, if this property is true for an atlas, it is true for all charts compatible with it. The set of C^∞ functions on M is denoted $C^\infty(M)$. If U is open in M, the set $C^\infty(U)$ contains functions defined on U which can be interpreted as C^∞ functions of the coordinates for all local charts of M which are contained in U.

The tangent space

We fix, in this section, a differential manifold, denoted M, of dimension d.

Suppose that M is a C^k manifold ($k \geq 1$) and that $x \in M$. Pick a coordinate chart $\varphi : U \to \mathbb{R}^n$, where U is an open subset of M containing x. Suppose further

that two curves $\gamma_1, \gamma_2 : (-\epsilon, \epsilon) \to M$ with $\gamma_1(0) = x = \gamma_2(0)$ are given such that both $\varphi \circ \gamma_1, \varphi \circ \gamma_2 : (-\epsilon, \epsilon) \to \mathbb{R}^n$ are differentiable in the ordinary sense (we call these differentiable curves initialized at x). Then γ_1 and γ_2 are said to be equivalent at 0 if and only if the derivatives of $\varphi \circ \gamma_1$ and $\varphi \circ \gamma_2$ at 0 coincide. This defines an equivalence relation on the set of all differentiable curves initialized at x, and equivalence classes of such curves are known as tangent vectors of M at x. The equivalence class of any such curve γ is denoted by $\gamma'(0)$. The tangent space of M at x, denoted by T_xM, is then defined as the set of all tangent vectors at x; it does not depend on the choice of coordinate chart $\varphi : U \to \mathbb{R}^n$.

To define vector-space operations on T_xM, we use a chart $\varphi : U \to \mathbb{R}^n$ and define a map $d\varphi_x : T_xM \to \mathbb{R}^n$ by $d\varphi_x(\gamma'(0)) := \dfrac{d}{dt}\left[(\varphi \circ \gamma)(t)\right]|_{t=0}$.

Proposition 2.17. ([55, 56, 59, 82–86, 97]) For all $p \in M$, the tangent space T_pM is an d-dimensional vector space.

Maps Between Two Manifolds

Definition 2.18. ([59, 93, 97]) Let M and N be two differentiable manifolds. A map $\Phi : M \to N$ has class C^∞ (or smooth or differentiable) if and only if, for all $\varphi \in C^\infty(N)$, one has $\varphi \circ \Phi \in C^\infty(M)$.

Definition 2.19. ([59, 93, 97]) Let a differentiable map $\varphi : M \to N$ between differentiable manifolds and $x \in M$. The derivative of the φ at x between their corresponding tangent spaces

$$D\varphi_x : T_xM \to T_{\varphi(x)}N$$

is defined by: for all $\vec{u} \in T_xM$,

$$D\varphi_x(\vec{u}) := (\varphi \circ \gamma)'(0)$$

where $\gamma : (-\epsilon, \epsilon)$ is a curve which satisfies $\gamma(0) = x$ and $\gamma'(0) = \vec{u}$.

An important result regarding the derivative map is the following

Theorem 2.20. ([55, 56, 59, 82–86, 97]) If $\varphi : M \to N$ is a local diffeomorphism at x in M, then $D\varphi_x : T_xM \to T_{\varphi(x)}N$ is a linear isomorphism. Conversely, if $D\varphi_x$ is an isomorphism, then there is an open neighborhood U of x such that φ maps U diffeomorphically onto its image.

Theorem 2.21. ([55, 59, 61, 82, 83, 85]) Let $\varphi : M \to N$ be a differentiable map between differentiable manifolds and let $x \in M$. Then the derivative of the φ at x

$$D\varphi_x : T_xM \to T_{\varphi(x)}N$$

is linear.

Immersions and embeddings

Definition 2.22. ([1, 68, 78]) Let M and N be smooth manifolds and $f : M \to N$ be a smooth map. Then f is called an immersion if its derivative is everywhere injective.

Definition 2.23. ([1, 68, 78]) Let M and N be smooth manifolds and $f : M \to N$ be a smooth map. Then f is called an embedding (or a smooth embedding) if it is an injective immersion which is an embedding in the topological sense mentioned above (i.e., homeomorphism onto its image).

Theorem 2.24. ([1, 68, 78]) If $f : M \to N$ is an injective immersion, and M is compact, then f is an embedding.

2.3.2 Infinite dimensional manifolds

This section is devoted to the foundations of infinite dimensional manifolds. We treat here only manifolds described by charts onto open subsets of convenient vector spaces.

A chart (U, u) on a set M is a bijection $u : U \to u(U) \subseteq E_U$ from a subset $U \subseteq M$ onto an open subset of a convenient vector space E_U.
For two charts (U_α, u_α) and (U_β, u_β) on M the mapping $u_{\alpha\beta} := u_\alpha \circ u_\beta : u_\beta(U_{\alpha\beta}) \to u_\alpha(U_{\alpha\beta})$ for $\alpha, \beta \in A$ is called the chart changing, where $U_{\alpha\beta} := U_\alpha \cap U_\beta$. A family $(U_\alpha, u_\alpha)_{\alpha\in A}$ of charts on M is called an atlas for M, if the U_α form a cover of M and all chart changings $u_{\alpha\beta}$ are defined on open subsets.
An atlas $(U_\alpha, u_\alpha)_{\alpha\in A}$ for M is said to be a $C^\infty-$atlas, if all chart changing $u_{\alpha\beta} : u_\beta(U_{\alpha\beta}) \to u_\alpha(U_{\alpha\beta})$ are smooth. Two $C^\infty-$atlas are called $C^\infty-$equivalent, if their union is again a $C^\infty-$atlas for M. An equivalence class of $C^\infty-$atlas is sometimes called a $C^\infty-$structure on M. The union of all atlas in an equivalence class is again an atlas, the maximal atlas for this $C^\infty-$structure. A $C^\infty-$manifold M is a set together with a $C^\infty-$structure on it.

A mapping $f : M \to N$ between manifolds is called smooth if for each $x \in M$ and each chart (V, v) on N with $f(x) \in N$ there is a chart (U, u) on M with $x \in U, f(U) \subseteq V$, such that $v \circ f \circ u^{-1}$ is smooth.
We will denote by $C^\infty(M, N)$ the space of all $C^\infty-$mappings from M to N.
A smooth mapping $f : M \to N$ is called a diffeomorphism if f is bijective and its inverse is also smooth. Two manifolds are called diffeomorphic if there exists a diffeomorphism between them.

The natural topology on a manifold M is the identification topology with respect to some (smooth) atlas $(u_\alpha : M \supseteq U_\alpha \to u_\alpha(U_\alpha) \subseteq E_\alpha)$, where a subset $W \subseteq M$ is open if and only if $u_\alpha(U_\alpha \cap W)$ is $C^\infty-$open in E_α for all α. This topology depends only on the structure since diffeomorphisms are homeomorphisms for the $C^\infty-$topologies.

One can see more detail in [57, 68].

2.4 Geometry and Bézier curves

In this section, we remind about the set of curves, parametrization of a curve and arc length. These definitions, notations are used a lot in this thesis. We also introduce Bézier curve. We will research the space of Bézier curve in chapter 4 and use it to do some applications in chapter 5.

2.4.1 Geometry

Parametrized curve

Definition 2.25. ([28, 97]) A parametrization of a curve is a map $\gamma : [a, b] \to \mathbb{R}^n$, where $I = [a, b]$ is an interval.

The image of the parametrization is called a parametrized curve in $\mathbb{R}^n$.

The curve is closed if its starting point is also its ending point.

A curve is a Jordan curve if it is closed and it has no self-intersection.

The curve is piecewise if its parametrization is continuous and C^1 everywhere except in a finite number of points.

Definition 2.26. ([28, 97]) A C^1 curve is a regular curve if its parametrization $\gamma : I \to \mathbb{R}^n$ satisfies $\dot{\gamma}(u) \neq 0$ for all $u \in I$. If γ is only piecewise C^1, we extend the definition by requiring that all left and right derivatives of its parametrization are non-vanishing.

Notation 2.27. We denoted $\mathfrak{C}$ be the set of parametrized curves and we often omit the word parametrized.

Geometric Equivalence

Definition 2.28. ([28, 30, 97]) Let $\gamma : I \to \mathbb{R}^n$ be a parametrization, where I is a compact interval. A change of parameter for γ is a function $\delta : I' \to I$ such that:

1. I' is a compact interval;

2. δ is increasing (strictly) and is a diffeomorphism.

The new parametrization $\tilde{\gamma} = \gamma \circ \delta$ is called a reparametrization of γ. The images $\gamma(I)$ and $\tilde{\gamma}(I')$ coincide.

(Can sua doan nay)

Notation 2.29. ([97, chapter 1, p. 2]) Let $\gamma \in C^0([0,1], \mathbb{R}^n)$ be a parametrization, and let $\delta \in \text{Diff}^+([0,1])$ be an increasing diffeomorphism of $[0,1]$. The map $\gamma \circ \delta$ is called a reparameterization of γ.

Notation 2.30. ([2, p. 86], [41, p. 763]) A diffeomorphisms $\delta : [0,1] \to [0,1]$ is called *increasing* when the derivative is always positive on $[0,1]$.

The set of increasing diffeomorphisms on $[0,1]$ is denoted $\text{Diff}^+([0,1])$.

Remark 2.31. There always exists an increasing diffeomorphism from the compact interval I to the segment $[0,1]$, so we can consider I to be $[0,1]$ without loss of generality.

Notation 2.32. We denote $\text{Diff}^+([0,1])$ be the set of increasing diffeomorphisms from $[0,1]$ to itself.

A curve has a parametrization γ, then $\gamma \circ \delta, \forall \delta \in \text{Diff}^+([0,1])$ is also a parametrization of the curve. So, a parametrized curve has infinitely many parametrizations.

Definition 2.33. ([28, 30, 97]) Two parametrizations γ_1, γ_2 are equivalent if there exists $\delta \in \text{Diff}^+([0,1])$ such that $\gamma_1 = \gamma_2 \circ \delta$.

This relation is an equivalent relation. Two equivalent parametrizations define the same curve. Note that the converse is not true. Two parametrizations have the same image, they are not necessarily equivalent. For example, the parametrization $\gamma(t) = (2t, 0), t \in [0, 1/2]$ and $\gamma(t) = (2 - 2t, 0), t \in [1/2, 1]$ has same image with

$\tilde{\gamma}(t) = (t, 0), t \in [0, 1]$ but they are not equivalent, since we have required the change of parameter to be increasing (changes of orientation are not allowed).

In order to overcome this problem, we consider the space of parametrizations those are embeddings.

Notation 2.34. We denote $\mathrm{Emb}([0, 1], \mathbb{R}^n)$ be the space of embeddings from $[0, 1]$ to $\mathbb{R}^n$.

From this section, we always consider a curve is a parametrized curve and its parametrization is an embedding from $[0, 1]$ to $\mathbb{R}^n$. The space of embeddings $\mathrm{Emb}([0, 1], \mathbb{R}^n)$ have many useful properties.

Proposition 2.35. ([46, 57, 68]) The space $\mathrm{Emb}([0, 1], \mathbb{R}^n)$ is a Fréchet manifold.

Proposition 2.36. ([1, 68, 78]) If two embeddings have the same image and the same starting point, then two embeddings are equivalent.

Therefore we identify the set of curves with the quotient

$$\mathfrak{C} = \mathrm{Emb}([0, 1], \mathbb{R}^n) / \mathrm{Diff}^+([0, 1]).$$

We have the important property about the set of curves.

Proposition 2.37. ([12, 20, 67, 68]) The quotient $\mathfrak{C} := \mathrm{Emb}([0, 1], \mathbb{R}^n) / \mathrm{Diff}^+([0, 1])$ is a smooth Hausdorff manifold.

Arc Length

We recall that a curve is an image of an embedding. A parametrization of a curve is an embedding from $[0, 1]$ to $\mathbb{R}^n$.

Definition 2.38. ([89, 97]) Let $\overline{\gamma}$ be a curve and let $\gamma \in \mathrm{Emb}([0, 1], \mathbb{R}^n)$ be a parametrization of $\overline{\gamma}$. Its length $L_{\overline{\gamma}}$ is defined by

$$L_{\overline{\gamma}} = \int_0^1 \|\dot{\gamma}(t)\|_2 dt.$$

The function $l_\gamma : [0, 1] \to [0, L_m]$ defined by

$$l_\gamma(u) = \int_0^u \|\dot{\gamma}(t)\|_2 dt$$

is called the arc length of the curve (it is the length of the arc between $\gamma(a)$ and $\gamma(u)$).

We have the important properties:

Proposition 2.39. ([7, 53, 89, 97]) The length of a curve does not depend on reparametrization.

Proposition 2.40. ([7, 53, 89, 97]) Let $\overline{\gamma}$ be a curve and let $\gamma \in \mathrm{Emb}([0,1], \mathbb{R}^n)$ be a parametrization of $\overline{\gamma}$. The function l_γ is an increasing diffeomorphism form $[0,1]$ to $[0, L_{\overline{\gamma}}]$.

2.4.2 Bézier curves

The Bézier curve was widely publicized in 1962 by the French engineer Pierre Bézier. The set of all Bézier curves of degree D is a finite dimensional vector space. Each Bézier curve just depends on a finite number of control points and it lies on convex hull of these control points. The Bézier curves space is used to make the approximation in the space of continuous curves.

Definition 2.41. ([38, 44, 72]) (Explicit definition) Let $\mathbf{P} = \{P_0, \ldots, P_D\}$ be a set of distinct points $P_i \in \mathbb{R}^n, \forall i = 0, \ldots, D$. The Bézier curve associated to the set $\mathbf{P}$ define as follows

$$B([P_0, \ldots, P_D], t) := \sum_{i=0}^{D} P_i b_{i,D}(t), \quad t \in [0,1], \tag{2.1}$$

where $b_{i,D}(t)$, $i = 0, \ldots, D$, represents the Bernstein polynomial which is given by

$$b_{i,D}(t) = \binom{D}{i} t^i (1-t)^{D-i}.$$

Definition 2.42. ([38, 44, 72]) (Recursive definition) Let $\mathbf{P} = \{P_0, \ldots, P_D\}$ be a set of distinct points $P_i \in \mathbb{R}^n, \forall i = 0, \ldots, D$. The Bézier curve associated to the set $\mathbf{P}$ is

$$B([P_0, \ldots, P_D], t) := \begin{cases} P_0 & \text{if } D = 0 \\ (1-t)B([P_0, \ldots, P_{D-1}], t) + tB([P_1, \ldots, P_D], t) & \text{if } D \geq 1. \end{cases}$$

Definition 4.9 and Definition 2.42 are equivalent.

Remark 2.43. From (4.1), the Bézier curve lies inside the convex hull of its control points.

From Definition 4.9, all Bézier curves are polynomial curves. Conversely, from properties of Bernstein polynomials, all polynomial curves are also Bézier curves.

Theorem 2.44. ([13, 38, 43, 44, 72]) Let Γ be a continuous curve on the interval $[0,1]$. There exists a sequence of Bézier curves $\{\Gamma_n\}$ which tends uniformly to Γ.

Definition 2.45. ([38, 44, 72]) Let $\mathbf{P} = \{P_0, \ldots, P_D, \ldots, P_{DN}\}$ be a set of distinct points $P_i \in \mathbb{R}^n, \forall i = 0, \ldots, DN-1$. An N-piece Bézier curve $\Gamma : [0,1] \to \mathbb{R}^n$ associated to the set $\mathbf{P} = \{P_0, \ldots, P_D, \ldots, P_{DN}\}$ is formed by N Bézier curves $B([P_{jD}, \ldots, P_{jD+D}], t)$ which is a Bézier curve of degree D associated to $D+1$ points $P_{jD}, \ldots, P_{jD+D}, j = 0, \ldots, N-1$.

$$\Gamma(t) = B([P_{jD}, \ldots, P_{jD+D}], Nt - j) \text{ if } t \in \left[\frac{j}{N}, \frac{j+1}{N}\right], \quad t \in [0,1].$$

Theorem 2.46. ([13, 38, 43, 44, 72]) Let Γ be a continuous curve on the interval $[0,1]$. There exists a sequence of N-piece Bézier curves $\{\Gamma_N\}$ which tends uniformly to Γ.

Chapter 3

Normal forms of parametrized curves and the distance between curves

We consider oriented curves, i.e., each curve has a starting point and an end point. This is not the case in the literature on distance on the space of curves since they often consider closed curves without consideration of the orientation. That fact can explain that the simple ideas presented here can not be found in current literatures. We note that we consider only parametrized curves and parametrizations of curves are embeddings.

The set of curves is an infinite-dimensional manifold and a curve has infinitely many parametrizations. In order to define a distance between curves, we need to find a distance which is independent in the chosen parametrizations. The distance between curves is often calculate by geodesic distance ([8, 9, 17, 19, 24, 54, 69]) or elastic distance ([51, 63, 95, 96]). But those distances are difficult to compute. We determine a special parametrization of each curve. This parametrization is called the normal form of the curve. Each curve is presented by a normal form, so we identify the set of curves with the set of normal forms. Using normal forms of curves, we can define a distance between curves. From the distance between curves, we can research topologies and differential structures on the set of curves.

3.1 The set of curves

The goal here is to explain that we can restrict our work to the study of parametrizations from $[0, 1]$ to $\mathbb{R}^n$ and define the set of curves as a quotient space.

A curve is an image of a compact interval by an embedding. The set of curves is denoted by $\mathfrak{C}$. A parametrization of a curve is a function from a compact interval I to $\mathbb{R}^n$. There always exists an isomorphism from the compact interval I to the segment $[0,1]$, so we consider I to be $[0,1]$ without loss of generality. In this chapter, a parametrization is an embedding from $[0,1]$ to $\mathbb{R}^n$. We denote the set of embeddings from $[0,1]$ to $\mathbb{R}^n$ by $\mathrm{Emb}\left([0,1],\mathbb{R}^n\right)$. In order to reparametrize, we consider $\mathrm{Diff}^+\left([0,1]\right)$ being the set of increasing diffeomorphism from $[0,1]$ to $[0,1]$. If γ is a parametrization, $\gamma\circ\delta$ is also a parametrization of the same curve for all $\delta\in\mathrm{Diff}^+\left([0,1]\right)$. The group $\mathrm{Diff}^+\left([0,1]\right)$ acts on $\mathrm{Emb}\left([0,1],\mathbb{R}^n\right)$ on the right. Each curve is presented by a class $[\gamma]:=\left\{\gamma\circ\delta|\ \ \delta\in\mathrm{Diff}^+\left([0,1]\right)\right\}$ in the quotient $\mathrm{Emb}\left([0,1],\mathbb{R}^n\right)/\mathrm{Diff}^+\left([0,1]\right)$. So,

$$\mathfrak{C}:=\mathrm{Emb}\left([0,1],\mathbb{R}^n\right)/\mathrm{Diff}^+\left([0,1]\right).$$

In all the reminder of this thesis, we will refer to $\mathfrak{C}$ as the set of curves.

3.2 The normalization on Emb $([0,1],\mathbb{R}^n)$

A curve has infinitely many parametrizations. We want to determine a normal form of each curve. From the idea that two parametrizations of a curve are equivalent and the length of a curve does not depend on the reparametrization, we construct a normalization on $\mathrm{Emb}\left([0,1],\mathbb{R}^n\right)$ for the action of $\mathrm{Diff}^+\left([0,1]\right)$.

The group $\mathrm{Diff}^+\left([0,1]\right)$ acts on $\mathrm{Emb}\left([0,1],\mathbb{R}^n\right)$ on the right. The associated equivalence relation is defined as follows:

Definition 3.1. Two embeddings $\gamma_1,\gamma_2\in\mathrm{Emb}\left([0,1],\mathbb{R}^n\right)$ are equivalent if there exists $\delta\in\mathrm{Diff}^+\left([0,1]\right)$ such that $\gamma_1=\gamma_2\circ\delta$.

Let us consider the following map from $\mathrm{Emb}\left([0,1],\mathbb{R}^n\right)$ into itself.

Definition 3.2. We define the map $\mathfrak{N}$ as follows

$$\begin{aligned}\mathfrak{N}:\mathrm{Emb}\left([0,1],\mathbb{R}^n\right)&\to\mathrm{Emb}\left([0,1],\mathbb{R}^n\right)\\ \gamma&\mapsto\mathfrak{N}(\gamma)=\gamma\circ l_\gamma^{-1}\circ k_\gamma,\end{aligned}\tag{3.1}$$

where

- $k_\gamma:[0,1]\to[0,L_\gamma]$, $k_\gamma(v)=v.L_\gamma$ with $L_\gamma=\int_0^1\|\dot\gamma(s)\|_2 ds$ is the length of γ.

- $l_\gamma : [0,1] \to [0, L_\gamma]$, $l_\gamma(v) = \int_0^v \|\dot{\gamma}(s)\|_2 ds$ is the arc length of γ.

It is clear that l_γ^{-1} and k_γ are smooth functions and their derivatives are positive. Since $l_\gamma^{-1} \circ k_\gamma$ goes from $[0,1]$ to $[0,1]$, the map $l_\gamma^{-1} \circ k_\gamma \in \mathrm{Diff}^+([0,1])$. Thus $\mathfrak{N}$ is a map from $\mathrm{Emb}([0,1], \mathbb{R}^n)$ into itself.

We will show that the map $\mathfrak{N}$ is a normalization on $\mathrm{Emb}([0,1], \mathbb{R}^n)$ with respect to the action of $\mathrm{Diff}^+([0,1])$ on $\mathrm{Emb}([0,1], \mathbb{R}^n)$.

Proposition 3.3. For any $\gamma \in \mathrm{Emb}([0,1], \mathbb{R}^n)$, we have $\mathfrak{N}(\gamma) = \mathfrak{N}(\mathfrak{N}(\gamma))$.

Proof. Let $t \in [0,1]$. From the definition of $\mathfrak{N}$, it is easy to see that the point $v \in [0,1]$ satisfying $\int_0^v \|\dot{\gamma}(s)\|_2 ds = tL_\gamma$ will hold the following formula

$$\mathfrak{N}(\gamma)(t) = \gamma(v).$$

By the same reasoning, we also have

$$\mathfrak{N}(\mathfrak{N}(\gamma))(t) = \mathfrak{N}(\gamma)(u) = \gamma\left((l_\gamma^{-1} \circ k_\gamma)(u)\right)$$

for some $u \in [0,1]$ and $\int_0^u \left\|(\mathfrak{N}(\gamma))'(s)\right\|_2 ds = tL_{\mathfrak{N}(\gamma)}$.
Because $\mathfrak{N}(\gamma) = \gamma \circ l_\gamma^{-1} \circ k_\gamma$ and $l_\gamma^{-1} \circ k_\gamma \in \mathrm{Diff}^+([0,1])$,

$$\begin{aligned}\int_0^u \left\|(\mathfrak{N}(\gamma))'(s)\right\|_2 ds &= \int_0^u \left\|\gamma'\left((l_\gamma^{-1} \circ k_\gamma)(s)\right)\right\|_2 \left(l_\gamma^{-1} \circ k_\gamma\right)'(s) ds \\ &= \int_0^{(l_\gamma^{-1} \circ k_\gamma)(u)} \|\dot{\gamma}(s)\|_2 ds\end{aligned}$$

and $L_{\mathfrak{N}(\gamma)} = L_\gamma$. Then

$$\mathfrak{N}(\mathfrak{N}(\gamma))(t) = \gamma\left((l_\gamma^{-1} \circ k_\gamma)(u)\right),$$

where $u \in [0,1]$ and

$$\int_0^{(l_\gamma^{-1} \circ k_\gamma)(u)} \|\dot{\gamma}(s)\|_2 ds = tL_\gamma = \int_0^v \|\dot{\gamma}(s)\|_2 ds.$$

Hence we have $(l_\gamma^{-1} \circ k_\gamma)(u) = v$ and $\mathfrak{N}(\mathfrak{N}(\gamma))(t) = \gamma(v) = \mathfrak{N}(\gamma)(t)$. This means

that

$$\mathfrak{N}(\gamma)(t) = \mathfrak{N}\left(\mathfrak{N}(\gamma)\right)(t), \forall t \in [0,1].$$

□

Proposition 3.4. Let $\gamma,\ \beta \in \mathrm{Emb}\left([0,1],\mathbb{R}^n\right)$. Then $\mathfrak{N}(\gamma) = \mathfrak{N}(\beta)$ if and only if γ is equivalent to β.

Proof. If $\mathfrak{N}(\gamma) = \mathfrak{N}(\beta)$, we have $\gamma \circ l_\gamma^{-1} \circ k_\gamma = \beta \circ l_\beta^{-1} \circ k_\beta$. So,

$$\gamma = \beta \circ l_\beta^{-1} \circ k_\beta \circ \left(l_\gamma^{-1} \circ k_\gamma\right)^{-1} = \beta \circ \left(l_\beta^{-1} \circ k_\beta \circ \left(l_\gamma^{-1} \circ k_\gamma\right)^{-1}\right).$$

Since $l_\gamma^{-1} \circ k_\gamma \in \mathrm{Diff}^+\left([0,1]\right)$ and $l_\beta^{-1} \circ k_\beta \in \mathrm{Diff}^+\left([0,1]\right)$, $l_\beta^{-1} \circ k_\beta \circ \left(l_\gamma^{-1} \circ k_\gamma\right)^{-1} \in \mathrm{Diff}^+\left([0,1]\right)$. This means that γ is equivalent to β.

If γ is equivalent to β, then $\gamma = \beta \circ \delta$ for some $\delta \in \mathrm{Diff}^+\left([0,1]\right)$. Let $t \in [0,1]$. From the definition of $\mathfrak{N}$, it is easy to see that the point $u \in [0,1]$ satisfying $\int_0^u \|\dot{\beta}(s)\|_2 ds = tL_\beta$ will hold the following formula

$$\mathfrak{N}(\beta)(t) = \beta(u).$$

By the same reasoning, for $v \in [0,1]$ such that $\int_0^v \|\dot{\gamma}(s)\|_2 ds = tL_\gamma$, we also have

$$\mathfrak{N}(\gamma)(t) = \gamma(v) = \beta\left(\delta(v)\right).$$

Because $\gamma = \beta \circ \delta$,

$$\int_0^v \|\dot{\gamma}(s)\|_2 \, ds = \int_0^v \|\beta'\left(\delta(s)\right)\|_2 \, \delta'(s) ds = \int_0^{\delta(v)} \left\|\dot{\beta}(s)\right\|_2 ds$$

and $L_\beta = L_\gamma$. Thus $u = \delta(v)$ and $\mathfrak{N}(\beta)(t) = \beta\left(\delta(v)\right) = \mathfrak{N}(\gamma)(t)$. Therefore

$$\mathfrak{N}(\beta)(t) = \mathfrak{N}(\gamma)(t), \forall t \in [0,1].$$

□

From the two above propositions, we have the following theorem.

Theorem 3.5. The map $\mathfrak{N}$ is a normalization on $\mathrm{Emb}\left([0,1],\mathbb{R}^n\right)$ with respect to the action of $\mathrm{Diff}^+\left([0,1]\right)$ on $\mathrm{Emb}\left([0,1],\mathbb{R}^n\right)$.

Two equivalent embeddings have the same normal form. So, each equivalence class on $\mathfrak{C}$ is presented by a normal form. We identify the set of curves with the set of normal forms

$$\mathfrak{C} \equiv \mathfrak{N}\left(\mathrm{Emb}\left([0,1],\mathbb{R}^2\right)\right).$$

Therefore we can consider the map $\mathfrak{N}$ as follows

$$\begin{aligned} \mathfrak{N} : \mathrm{Emb}\left([0,1],\mathbb{R}^n\right) &\to \mathfrak{C} \subset \mathrm{Emb}\left([0,1],\mathbb{R}^n\right) \\ \gamma &\mapsto \mathfrak{N}(\gamma). \end{aligned} \tag{3.2}$$

Thanks to the map $\mathfrak{N}$ we will be able to consider $\mathfrak{C}$ as a submanifold of $\mathrm{Emb}\left([0,1],\mathbb{R}^n\right)$.

3.3 The distance between curves

A curve is represented by a normal form. In order to define a distance between curves, we will use the normal forms of those curves. Doing so, we can define a distance between curves which is independent of the chosen parametrizations. It is to say that, it is a distance between curves in the geometric meaning.

Definition 3.6. The function $d^{\mathfrak{N}}$ is defined as follows

$$\begin{aligned} d^{\mathfrak{N}} &: \mathfrak{C} \times \mathfrak{C} \to \mathbb{R}^+ \\ (\mathfrak{N}(\gamma), \mathfrak{N}(\beta)) &\mapsto d^{\mathfrak{N}}\left(\mathfrak{N}(\gamma), \mathfrak{N}(\beta)\right) := \int_0^1 \|\mathfrak{N}(\gamma)(t) - \mathfrak{N}(\beta)(t)\|\, dt, \end{aligned}$$

where $\|\cdot\|$ is the Euclidean norm on $\mathbb{R}^n$ and $\mathfrak{N}(\gamma), \mathfrak{N}(\beta)$ are normal forms in $\mathfrak{C}$.

Proposition 3.7. The function $d^{\mathfrak{N}}$ is a distance on the set of curves $\mathfrak{C}$.

From properties of the Euclidean norm on $\mathbb{R}^n$ and the integral, it is clear that $d^{\mathfrak{N}}$ satisfies all conditions of a distance. Since $\mathfrak{N}$ is a normalization on $\mathrm{Emb}\left([0,1],\mathbb{R}^n\right)$ with respect to the equivalence relation associated the right action of $\mathrm{Diff}^+\left([0,1]\right)$, we have the following property.

Proposition 3.8. The distance $d^{\mathfrak{N}}$ does not depend on the chosen parametrizations.

Remark 3.9. This distance is called the normal form distance or the distance through normal forms.

Using this distance between curves, we study topologies and differential structures on the set of curves.

3.4 Topologies on the set of curves $\mathfrak{C}$

The set of curves $\mathfrak{C}$ is a manifold by itself and $d^{\mathfrak{N}}$ is a distance on $\mathfrak{C}$, so the set of curves $\mathfrak{C}$ has the topology induced by the distance $d^{\mathfrak{N}}$. The set of curves $\mathfrak{C}$ is also a quotient of the right group action of $\mathrm{Diff}^{+}([0,1])$ on the space $\mathrm{Emb}([0,1],\mathbb{R}^n)$, thus we have the quotient topology on the set of curves $\mathfrak{C}$. Furthermore, the set of curves $\mathfrak{C}$ is a submanifold of the space $\mathrm{Emb}([0,1],\mathbb{R}^n)$, so $\mathfrak{C}$ has the induced topology inherited from the classical topology of $\mathrm{Emb}([0,1],\mathbb{R}^n)$. In Section 3.2, we will compare the topologies on the set of curves $\mathfrak{C}$.

We note that on the space $\mathrm{Emb}([0,1],\mathbb{R}^n)$, we consider the classical topology which is induced by the classical distance

$$d(\alpha,\beta)=\int_0^1 \|\alpha(t)-\beta(t)\|dt,$$

where $\|\cdot\|$ is the Euclidean norm on $\mathbb{R}^n$ and $\alpha,\beta\in\mathrm{Emb}([0,1],\mathbb{R}^n)$.

We first compare the topology induced by the distance $d^{\mathfrak{N}}$ and the quotient topology on the set of curves $\mathfrak{C}$. The following lemmas is used to the comparison of the topologies.

Lemma 3.10. On the set of curves $\mathfrak{C}$, the topology induced by the distance $d^{\mathfrak{N}}$ is not a subset of the quotient topology.

Proof. We will show that there exists an open set in $\mathfrak{C}$ for the topology induced by the distance $d^{\mathfrak{N}}$ such that it is not an open set in $\mathfrak{C}$ for the quotient topology.

Let $\gamma(s)=(s,0), s\in[0,1]$ be an embedding. We have $\mathfrak{N}(\gamma)\in\mathfrak{C}$ and an open ball $B(\mathfrak{N}(\gamma),\frac{1}{32}):=\left\{\mathfrak{N}(\psi)\in\mathfrak{C}: d^{\mathfrak{N}}(\mathfrak{N}(\gamma),\mathfrak{N}(\psi))<\frac{1}{32},\right\}\subset\mathfrak{C}$ in $\mathfrak{C}$ for the topology induced by the distance $d^{\mathfrak{N}}$. We will prove that $B(\mathfrak{N}(\gamma),\frac{1}{32})$ is not an open set in $\mathfrak{C}$ for the quotient topology. This means we show that $\mathfrak{N}^{-1}\left(B(\mathfrak{N}(\gamma),\frac{1}{32})\right)$ is not an open set in $\mathrm{Emb}([0,1],\mathbb{R}^n)$ for the classical topology.

It is clear that $\gamma\in\mathfrak{N}^{-1}\left(B(\mathfrak{N}(\gamma),\frac{1}{32})\right)$. We consider a sequence $\{\gamma_n\}\subset\mathrm{Emb}([0,1],\mathbb{R}^n)$ as follows

$$\gamma_n(s)=\begin{cases}(s,0) & \text{if } s\in[0,1-1/n],\\ \left(1-\frac{1}{n},(n-1)s+(2-n-\frac{1}{n})\right) & \text{if } s\in\left[1-\frac{1}{n},1\right].\end{cases}$$

We have the normal form of γ_n as follows

$$\mathfrak{N}(\gamma_n)(s) = \begin{cases} \left(s(2-\frac{2}{n}), 0\right) & \text{if } s \in \left[0, \frac{1}{2}\right], \\ \left(1-\frac{1}{n}, s(2-\frac{2}{n}-1+\frac{1}{n})\right) & \text{if } s \in \left[\frac{1}{2}, 1\right] \end{cases}$$

and the normal form of γ as follows

$$\mathfrak{N}(\gamma)(s) \equiv \gamma(s) = (s, 0), s \in [0, 1].$$

We have $d(\gamma_n, \gamma) \to 0$ as $n \to \infty$. So, if $\mathfrak{N}^{-1}\left(B(\mathfrak{N}(\gamma), \frac{1}{32})\right)$ is an open set then $\gamma_n \in \mathfrak{N}^{-1}\left(B(\mathfrak{N}(\gamma), \frac{1}{32})\right)$ for all n large enough.

However,

$$\begin{aligned} d^{\mathfrak{N}}(\mathfrak{N}(\gamma), \mathfrak{N}(\gamma_n)) =& \int_0^1 \|\mathfrak{N}(\gamma_n)(s) - \mathfrak{N}(\gamma)(s)\| \, ds \\ \geq& \int_{1/4}^{1/2} \|\mathfrak{N}(\gamma_n)(s) - \mathfrak{N}(\gamma)(s)\| \, ds = \int_{1/4}^{1/2} \left|s - \frac{2s}{n}\right| ds \\ =& \frac{3}{32} - \frac{1}{2n}. \end{aligned}$$

This implies that for all n large enough, $d^{\mathfrak{N}}(\mathfrak{N}(\gamma), \mathfrak{N}(\gamma_n)) \geq \frac{3}{32} - \frac{1}{2n} > \frac{1}{32}$ and $\mathfrak{N}(\gamma_n) \notin B(\mathfrak{N}(\gamma), \frac{1}{32})$. Then $\mathfrak{N}^{-1}(\mathfrak{N}(\gamma_n)) \ni \gamma_n \notin \mathfrak{N}^{-1}\left(B(\mathfrak{N}(\gamma), \frac{1}{32})\right)$ for all n large enough.

Therefore $\mathfrak{N}^{-1}\left(B(\mathfrak{N}(\gamma), \frac{1}{32})\right)$ is not an open set in $\mathrm{Emb}\left([0, 1], \mathbb{R}^n\right)$ for the classical topology. □

Lemma 3.11. On the set of curves $\mathfrak{C}$, the quotient topology is a subset of the topology induced by the distance $d^{\mathfrak{N}}$.

Proof. Let U be an open set in $\mathfrak{C}$ for the quotient topology. We show that U is also an open set in $\mathfrak{C}$ for the topology induced by the distance $d^{\mathfrak{N}}$.

If U is not an open set in $\mathfrak{C}$ for the topology induced by the distance $d^{\mathfrak{N}}$, then there exists an element $\mathfrak{N}(\gamma) \in U$ such that for every $r > 0$, we have

$$B\left(\mathfrak{N}(\gamma), r\right) := \left\{\mathfrak{N}(\psi) \in \mathfrak{C} : d^{\mathfrak{N}}\left(\mathfrak{N}(\gamma), \mathfrak{N}(\psi)\right) < r\right\} \not\subset U.$$

This means that there exists a sequence $\{\mathfrak{N}(\gamma_n)\} \subset \mathfrak{C}$ such that

$$\mathfrak{N}(\gamma_n) \notin U, \forall n \text{ and } d^{\mathfrak{N}}\left(\mathfrak{N}(\gamma_n), \mathfrak{N}(\gamma)\right) < \frac{1}{n}.$$

We consider the sequence $\{\mathfrak{N}(\gamma_n)\} \subset \mathrm{Emb}([0,1],\mathbb{R}^n)$. We have $d(\mathfrak{N}(\gamma_n),\mathfrak{N}(\gamma)) = d^{\mathfrak{N}}(\mathfrak{N}(\gamma_n),\mathfrak{N}(\gamma)) < \dfrac{1}{n}$. This means $\mathfrak{N}(\gamma_n) \to \mathfrak{N}(\gamma)$ as $n \to \infty$. It is clear that $\mathfrak{N}(\gamma) \in \mathfrak{N}^{-1}(\mathfrak{N}(\gamma))$ and $\mathfrak{N}^{-1}(U)$ is an open set in $\mathrm{Emb}([0,1],\mathbb{R}^n)$ for the classical topology. Because $\mathfrak{N}(\gamma_n) \to \mathfrak{N}(\gamma)$ as $n \to \infty$, there exists N such that

$$\mathfrak{N}(\gamma_n) \in \mathfrak{N}^{-1}(U), \forall n > N.$$

Therefore $\mathfrak{N}(\mathfrak{N}(\gamma_n)) \equiv \mathfrak{N}(\gamma_n) \in U$ for all $n > N$. This contradicts $\mathfrak{N}(\gamma_n) \notin U$ for all n. So, U is also an open set in $\mathfrak{C}$ for the topology induced by the distance $d^{\mathfrak{N}}$. □

Combining the two above lemmas, we have the following proposition.

Proposition 3.12. On the set of curves $\mathfrak{C}$, the topology induced by the distance $d^{\mathfrak{N}}$ is strictly thinner than the quotient topology.

Consequently, the topology induced by the distance $d^{\mathfrak{N}}$ brings more information than the quotient topology. We next compare the induced topology and the quotient topology on the set of curves $\mathfrak{C}$.

Proposition 3.13. On the set of curves $\mathfrak{C}$, the induced topology is strictly thinner than the quotient topology.

Proof. Let U be an open set in $\mathfrak{C}$ for the quotient topology. By the definition of the quotient topology, we have $\mathfrak{N}^{-1}(U)$ is an open set in $\mathrm{Emb}([0,1],\mathbb{R}^n)$ for the classical topology. And by the definition of the map $\mathfrak{N}$, we have $U \subset \mathfrak{N}^{-1}(U)$. Hence U is an open set in $\mathfrak{C}$ for the induced topology since $U = U \cap \mathfrak{N}^{-1}(U)$ and $\mathfrak{N}^{-1}(U)$ is an open set in $\mathrm{Emb}([0,1],\mathbb{R}^n)$ for the classical topology. This means that the quotient topology is a subset of the induced topology.

The opposite is not true. We will show that there exists an open set in $\mathfrak{C}$ for the induced topology but it is not an open set in $\mathfrak{C}$ for the quotient topology. We consider $\gamma(s) \equiv \mathfrak{N}(\gamma_0) = (s,0), s \in [0,1]$ and the set $A = \mathfrak{C} \cap B(\gamma, \frac{1}{32})$, where

$$B(\mathfrak{N}(\gamma_0),\epsilon) := \Big\{\gamma \in \mathrm{Emb}([0,1],\mathbb{R}^n) : d(\gamma,\mathfrak{N}(\gamma)) < \epsilon\Big\} \subset \mathrm{Emb}([0,1],\mathbb{R}^n).$$

It is clear that A is an open set in $\mathfrak{C}$ for the induced topology. We prove that $\mathfrak{N}^{-1}(A)$ is not an open set in $\mathrm{Emb}([0,1],\mathbb{R}^n)$ for the classical topology. Let a sequence $\{\gamma_n\} \subset \mathrm{Emb}([0,1],\mathbb{R}^n)$ as follows

$$\gamma_n(s) = \begin{cases} (s,0) & \text{if } s \in [0, 1-1/n], \\ \big(1-\frac{1}{n}, (n-1)s + (2-n-\frac{1}{n})\big) & \text{if } s \in \big[1-\frac{1}{n}, 1\big]. \end{cases}$$

We have the normal form of γ_n as follows

$$\mathfrak{N}(\gamma_n)(s) = \begin{cases} \big(s(2-\frac{2}{n}), 0\big) & \text{if } s \in \big[0, \frac{1}{2}\big], \\ \big(1-\frac{1}{n}, s(2-\frac{2}{n}-1+\frac{1}{n})\big) & \text{if } s \in \big[\frac{1}{2}, 1\big] \end{cases}$$

and the normal form of γ as follows

$$\mathfrak{N}(\gamma)(s) \equiv \gamma(s) = (s, 0), s \in [0, 1].$$

Thus

$$\begin{aligned} d^{\mathfrak{N}}(\mathfrak{N}(\gamma), \mathfrak{N}(\gamma_n)) &= \int_0^1 \|\mathfrak{N}(\gamma_n)(s) - \mathfrak{N}(\gamma)(s)\| \, ds \\ &\geq \int_{1/4}^{1/2} \|\mathfrak{N}(\gamma_n)(s) - \mathfrak{N}(\gamma)(s)\| \, ds = \int_{1/4}^{1/2} \Big|s - \frac{2s}{n}\Big| ds \\ &= \frac{3}{32} - \frac{1}{2n}. \end{aligned}$$

We have $d(\gamma_n, \gamma) \to 0$ as $n \to \infty$. But for n large enough, $d^{\mathfrak{N}}(\mathfrak{N}(\gamma), \mathfrak{N}(\gamma_n)) \geq \frac{3}{32} - \frac{1}{2n} > \frac{1}{32}$ and $\mathfrak{N}(\gamma_n) \notin B(\mathfrak{N}(\gamma), \frac{1}{32})$. Then, there exists a sequence $\{\gamma_n\}$ such that $\gamma_n \to \gamma \in \mathfrak{N}^{-1}(A)$ but $\{\gamma_n\} \not\subset \mathfrak{N}^{-1}(A)$. This means that $\mathfrak{N}^{-1}(A)$ is not an open set in $\mathrm{Emb}\,([0,1], \mathbb{R}^n)$ for the classical topology.

□

Then, the induced topology brings more information than the quotient topology. Finally, we study the relation between the induced topology and the topology induced by the distance $d^{\mathfrak{N}}$ on the set of curves $\mathfrak{C}$.

Proposition 3.14. On the set of curves $\mathfrak{C}$, the induced topology equals the topology induced by the distance $d^{\mathfrak{N}}$.

Proof. Let A be an open set in $\mathfrak{C}$ for the induced topology. We show that A is an open set in $\mathfrak{C}$ for the topology induced by the distance $d^{\mathfrak{N}}$. By the definition of the induced topology, there exists an open set U in $\mathrm{Emb}\,([0,1], \mathbb{R}^n)$ for the classical topology such that $A = \mathfrak{C} \cap U$. For any $\mathfrak{N}(\gamma_0) \in A$, there is an open ball

$$B(\mathfrak{N}(\gamma_0), \epsilon) := \Big\{\gamma \in \mathrm{Emb}\,([0,1], \mathbb{R}^n) : d(\gamma, \mathfrak{N}(\gamma)) < \epsilon\Big\} \subset \mathrm{Emb}\,([0,1], \mathbb{R}^n)$$

in $\mathrm{Emb}\,([0,1], \mathbb{R}^n)$ for the classical topology such that $B(\mathfrak{N}(\gamma_0), \epsilon) \subset U$. We

consider an open ball in $\mathfrak{C}$ for the topology induced by the distance $d^{\mathfrak{N}}$ as follows

$$B_{\mathfrak{N}}(\mathfrak{N}(\gamma_0), \epsilon) := \left\{ \mathfrak{N}(\gamma) \in \mathfrak{C} : d^{\mathfrak{N}}(\mathfrak{N}(\gamma_0), \mathfrak{N}(\gamma)) < \epsilon \right\} \subset \mathfrak{C}.$$

It is easy to see that $B_{\mathfrak{N}}(\mathfrak{N}(\gamma_0), \epsilon) \subset B(\mathfrak{N}(\gamma_0), \epsilon)$. So, $\mathfrak{N}(\gamma_0) \in B_{\mathfrak{N}}(\mathfrak{N}(\gamma_0), \epsilon) \subset \mathfrak{C} \cap U = A$. This means that there exists the open set $B_{\mathfrak{N}}(\mathfrak{N}(\gamma_0), \epsilon)$ in $\mathfrak{C}$ for the topology induced by the distance $d^{\mathfrak{N}}$ such that $\mathfrak{N}(\gamma_0) \in B_{\mathfrak{N}}(\mathfrak{N}(\gamma_0), \epsilon) \subset A$. Then A is an open set in $\mathfrak{C}$ for the topology induced by the distance $d^{\mathfrak{N}}$.

Let A be an open set in $\mathfrak{C}$ for the topology induced by the distance $d^{\mathfrak{N}}$. We show that A is an open set in $\mathfrak{C}$ for the induced topology. For any $\mathfrak{N}(\gamma_0) \in A$, there exists an open ball

$$B_{\mathfrak{N}}(\mathfrak{N}(\gamma_0), \epsilon) := \left\{ \mathfrak{N}(\gamma) \in \mathfrak{C} : d^{\mathfrak{N}}(\mathfrak{N}(\gamma_0), \mathfrak{N}(\gamma)) < \epsilon \right\} \subset \mathfrak{C}$$

in $\mathfrak{C}$ for the classical topology such that $\mathfrak{N}(\gamma_0) \in B_{\mathfrak{N}}(\mathfrak{N}(\gamma_0), \epsilon) \subset A$. We consider an open ball in $\mathrm{Emb}([0,1], \mathbb{R}^n)$ for the classical topology as follows

$$B(\mathfrak{N}(\gamma_0), \epsilon) := \left\{ \gamma \in \mathrm{Emb}([0,1], \mathbb{R}^n) : d(\gamma, \mathfrak{N}(\gamma)) < \epsilon \right\} \subset \mathrm{Emb}([0,1], \mathbb{R}^n).$$

It is clear that $B_{\mathfrak{N}}(\mathfrak{N}(\gamma_0), \epsilon) = \mathfrak{C} \cap B(\mathfrak{N}(\gamma_0), \epsilon)$. This means that there exists the open set $\mathfrak{C} \cap B(\mathfrak{N}(\gamma_0), \epsilon)$ in $\mathfrak{C}$ for the induced topology such that $\mathfrak{N}(\gamma_0) \in \mathfrak{C} \cap B(\mathfrak{N}(\gamma_0), \epsilon) \subset A$. Then A is an open set in $\mathfrak{C}$ for the induced topology.

□

3.5 Continuous functions

From the topologies on the set of curves $\mathfrak{C}$, we study the continuity of functions on the set of curves $\mathfrak{C}$.

Let X be a topological space. Continuous maps from $\mathfrak{C} \to X$ will come from continuous maps from $\mathrm{Emb}([0,1], \mathbb{R}^n) \to X$ being invariant under the action of $\mathrm{Diff}^+([0,1])$.

Definition 3.15. Let X be a topological space. A function $f : \mathrm{Emb}([0,1], \mathbb{R}^n) \to X$ is called compatible with the action of $\mathrm{Diff}^+([0,1])$ if $\mathfrak{N}(\gamma_1) = \mathfrak{N}(\gamma_2)$ implies $f(\gamma_1) = f(\gamma_2)$.

Proposition 3.16. Let X be a topological space. Let $f : \mathrm{Emb}([0,1], \mathbb{R}^n) \to X$ be a function such that f is continuous for a classical topology on $\mathrm{Emb}([0,1], \mathbb{R}^n)$

and f is compatible with the action of $\mathrm{Diff}^+([0,1])$. Then there exists a continuous function $\bar{f}: \mathfrak{C} \to X$ for the quotient topology such that

$$\bar{f}(\mathfrak{N}(\gamma)) = f(\gamma), \forall \gamma \in \mathrm{Emb}([0,1], \mathbb{R}^n).$$

Proof. We define $\bar{f}$ as follows

$$\begin{aligned} &\bar{f}: \mathfrak{C} \to X \\ &\mathfrak{N}(\gamma) \mapsto \bar{f}(\mathfrak{N}(\gamma)) := f(\gamma). \end{aligned} \tag{3.3}$$

Since f is compatible with the action of $\mathrm{Diff}^+([0,1])$, $\bar{f}$ is well definited on $\mathfrak{C}$. We prove that $\bar{f}$ is a continuous function.

Let U be an open set on X. We show that $\bar{f}^{-1}(U) = \left\{\mathfrak{N}(\gamma) \in \mathfrak{C} | \bar{f}(\mathfrak{N}(\gamma)) = f(\gamma) \in U\right\}$ is an open set on $\mathfrak{C}$ for the quotient topology. By the definition of the quotient topology, we need to show that $\mathfrak{N}^{-1}\left(\bar{f}^{-1}(U)\right)$ is an open set on $\mathrm{Emb}([0,1], \mathbb{R}^n)$.

The function f is a continuous function and U is an open set on X, hence the set $f^{-1}(U)$ is an open set on $\mathrm{Emb}([0,1], \mathbb{R}^n)$. We will prove that $\mathfrak{N}^{-1}\left(\bar{f}^{-1}(U)\right)$ equals $f^{-1}(U)$.

Let γ be an element in $\mathfrak{N}^{-1}\left(\bar{f}^{-1}(U)\right)$. We have $\mathfrak{N}(\gamma) \in \bar{f}^{-1}(U)$. Clearly, $f(\gamma) = \bar{f}(\mathfrak{N}(\gamma)) \in U$. So,

$$\gamma \in f^{-1}(U), \forall \gamma \in \mathfrak{N}^{-1}\left(\bar{f}^{-1}(U)\right).$$

Equivalently, $\mathfrak{N}^{-1}\left(\bar{f}^{-1}(U)\right) \subset f^{-1}(U)$.

Let γ be an element in $f^{-1}(U)$. We have $\bar{f}(\mathfrak{N}(\gamma)) = f(\gamma) \in U$. Clearly, $\mathfrak{N}(\gamma) \in \bar{f}^{-1}(U)$. So,

$$\gamma \in \mathfrak{N}^{-1}(\mathfrak{N}(\gamma)) \subset \mathfrak{N}^{-1}\left(\bar{f}^{-1}(U)\right), \forall \gamma \in f^{-1}(U).$$

Equivalently, $f^{-1}(U) \subset \mathfrak{N}^{-1}\left(\bar{f}^{-1}(U)\right)$.

Thus $\mathfrak{N}^{-1}\left(\bar{f}^{-1}(U)\right)$ equals $f^{-1}(U)$. This means that $\bar{f}^{-1}(U)$ is an open set on $\mathfrak{C}$ for the quotient topology. Therefore $\bar{f}$ is a continuous function for the quotient topology and it is clear that

$$\bar{f}(\mathfrak{N}(\gamma)) = f(\gamma), \forall \gamma \in \mathrm{Emb}([0,1], \mathbb{R}^n).$$

□

3.6 The tangent space

We want to understand differential structures of the set of curves $\mathfrak{C}$ in order to be able to do variational calculus. Then in this section, we show the existence of the differential of the map $\mathfrak{N}$ going from the tangent space of the embedding space to the tangent space of the set of curves. Hence we research the tangent space of the set of curves.

We first define the tangent space of $\mathrm{Emb}([0,1],\mathbb{R}^n)$ and the tangent space of the set of curves $\mathfrak{C}$. We show that for $\gamma \in \mathrm{Emb}([0,1],\mathbb{R}^n)$, there exists the differential of $\mathfrak{N}$ at γ

$$D\mathfrak{N}(\gamma) : T_\gamma \mathrm{Emb}([0,1],\mathbb{R}^n) \to T_{\mathfrak{N}(\gamma)}\mathfrak{C}.$$

Furthermore, for any $\gamma \in \mathrm{Emb}([0,1],\mathbb{R}^n)$, we will construct a group H acting on $T_\gamma \mathrm{Emb}([0,1],\mathbb{R}^n)$ on the right such that $T_\gamma \mathrm{Emb}/H$ is isomorphic to $T_{\mathfrak{N}(\gamma)}\mathfrak{C}$.

3.6.1 Definition of the tangent space of Emb $([0,1],\mathbb{R}^n)$

At each $\gamma \in \mathrm{Emb}([0,1],\mathbb{R}^n)$, the tangent space $T_\gamma \mathrm{Emb}([0,1],\mathbb{R}^n)$ is defined as follows:

Let $f : t \in (-\epsilon,\epsilon) \mapsto f_t \in \mathrm{Emb}([0,1],\mathbb{R}^n)$ be a smooth function such that $f_0 = \gamma$. The derivative of f at $t = 0$ is defined by

$$\partial_t f_0 := \partial_t f_t\Big|_{t=0} = \lim_{t\to 0} \frac{f_t - f_0}{t}.$$

Two smooth functions $f : t \in (-\epsilon,\epsilon) \mapsto f_t \in \mathrm{Emb}([0,1],\mathbb{R}^n)$ and $g : t \in (-\epsilon,\epsilon) \mapsto g_t \in \mathrm{Emb}([0,1],\mathbb{R}^n)$ such that $f_0 = g_0 = \gamma$ are said to be equivalent at $t = 0$ if and only if the derivatives $\partial_t f_0$, $\partial_t g_0$ coincide. This defines an equivalence relation on the set of all smooth functions initialized at γ, and equivalence classes of such curves are known as tangent vectors of $\mathrm{Emb}([0,1],\mathbb{R}^n)$ at γ. The equivalence class of any such function f is denoted by $\partial_t f_0$. The tangent space of $\mathrm{Emb}([0,1],\mathbb{R}^n)$ at γ, denoted by $T_\gamma \mathrm{Emb}([0,1],\mathbb{R}^n)$, is then defined as the set of all tangent vectors at γ.

$C^1([0,1],\mathbb{R}^n)$ is an affine space with $C^1([0,1],\mathbb{R}^n)$ as the underlying vector space. So, to each $\gamma \in C^1([0,1],\mathbb{R}^n)$ we have $T_\gamma C^1([0,1],\mathbb{R}^n) = C^1([0,1],\mathbb{R}^n)$. Furthermore, $\mathrm{Emb}([0,1],\mathbb{R}^n)$ is a dense open subset in $C^1([0,1],\mathbb{R}^n)$ ([22, 31, 57, 68]). In a way that for every $\gamma \in \mathrm{Emb}([0,1],\mathbb{R}^n)$ we have $T_\gamma \mathrm{Emb}([0,1],\mathbb{R}^n) =$

$T_\gamma C^1([0,1],\mathbb{R}^n)$. Then for any $\gamma \in \mathrm{Emb}([0,1],\mathbb{R}^n)$ we have

$$T_\gamma \mathrm{Emb}([0,1],\mathbb{R}^n) = C^1([0,1],\mathbb{R}^n).$$

3.6.2 Definition of the tangent space of the set of curves $\mathfrak{C}$

At each $\mathfrak{N}(\gamma) \in \mathfrak{C}$, the tangent space $T_{\mathfrak{N}(\gamma)}\mathfrak{C}$ is defined as follows:

Let $\hat{f} : t \in (-\epsilon,\epsilon) \mapsto \hat{f}_t \in \mathfrak{C}$ be a smooth function such that $\hat{f}_0 = \mathfrak{N}(\gamma)$. The derivative of $\hat{f}$ at $t = 0$ is defined by

$$\partial_t \hat{f}_0 := \partial_t \hat{f}_t\Big|_{t=0} = \lim_{t\to 0} \frac{\hat{f}_t - \hat{f}_0}{t}.$$

Two smooth functions $\hat{f} : t \in (-\epsilon,\epsilon) \mapsto \hat{f}_t \in \mathfrak{C}$ and $\hat{g} : t \in (-\epsilon,\epsilon) \mapsto \hat{g}_t \in \mathfrak{C}$ such that $\hat{f}_0 = \hat{g}_0 = \mathfrak{N}(\gamma)$ are said to be equivalent at $t = 0$ if and only if the derivatives $\partial_t \hat{f}_0$, $\partial_t \hat{g}_0$ coincide. This defines an equivalence relation on the set of all smooth functions initialized at $\mathfrak{N}(\gamma)$, and equivalence classes of such curves are known as tangent vectors of $\mathfrak{C}$ at $\mathfrak{N}(\gamma)$. The equivalence class of any such function $\hat{f}$ is denoted by $\partial_t \hat{f}_0$. The tangent space of $\mathfrak{C}$ at $\mathfrak{N}(\gamma)$, denoted by $T_{\mathfrak{N}(\gamma)}\mathfrak{C}$, is then defined as the set of all tangent vectors at $\mathfrak{N}(\gamma)$.

3.6.3 The differential of the map $\mathfrak{N}$

In this subsection, we show that for $\gamma \in \mathrm{Emb}([0,1],\mathbb{R}^n)$, there exists the differential of $\mathfrak{N}$ at γ going from the tangent space of $\mathrm{Emb}([0,1],\mathbb{R}^n)$ at γ to the tangent space of $\mathfrak{C}$ at $\mathfrak{N}(\gamma)$.

Firstly, we remark that for any $\gamma \in \mathrm{Emb}([0,1],\mathbb{R}^n)$ we have $\mathfrak{N}(\gamma) = \gamma \circ l_\gamma^{-1} \circ k_\gamma \in \mathrm{Emb}([0,1],\mathbb{R}^n)$. Then the map $\mathfrak{N} : \mathrm{Emb}([0,1],\mathbb{R}^n) \to \mathfrak{C}$ is an embedding. So, the limits and everything take place in $\mathrm{Emb}([0,1],\mathbb{R}^n)$.

In order to show the differential of the map $\mathfrak{N}$, we need some lemmas as follows:

Lemma 3.17. Let $f, g : [0,1] \to \mathbb{R}^n$ be two continuous functions such that $f(v) \neq 0_{\mathbb{R}^n}$ for every $v \in [0,1]$. The following holds

$$\lim_{t\to 0} \frac{\int_0^1 \|f(v) + tg(v)\|_2 \, dv - \int_0^1 \|f(v)\|_2 \, dv}{t} = \int_0^1 \frac{\langle f(v), g(v)\rangle}{\|f(v)\|_2} dv.$$

From the properties of the inner product and the integral, we can easily prove this lemma. Using this lemma, we have the following lemma.

Lemma 3.18. Let $\epsilon > 0$ and $f : t \in (-\epsilon, \epsilon) \mapsto f_t \in \mathrm{Emb}([0,1], \mathbb{R}^n)$ be a smooth function. Then for any $v \in [0,1]$ we have

$$\lim_{t\to 0} \frac{k_{f_t}(v) - k_{f_0}(v)}{t} = v \int_0^1 \frac{\langle \partial_v f_0(v), \partial_{tv} f_0(v) \rangle}{\|\partial_v f_0(v)\|_2} dv.$$

Proof. Let $v \in [0,1]$. Because f is smooth and using Taylor's theorem ([23, chapter 5, p. 111]) for f at $t = 0$, we have

$$f_t = f_0 + t\partial_t f_0 + \frac{t^2}{2}\partial_{tt} f_c \tag{3.4}$$

for some real number c between 0 and t. Since f is smooth and $f_t, f_0, f_c \in \mathrm{Emb}([0,1], \mathbb{R}^n)$, we can take the derivative of the functions in (3.4) with respect to the variable v and obtain

$$\partial_v f_t(v) = \partial_v f_0(v) + t\partial_{tv} f_0(v) + \frac{t^2}{2}\partial_{ttv} f_c(v)$$

for some real number c between 0 and t. Then we have

$$\begin{aligned}
&\lim_{t\to 0} \frac{k_{f_t}(v) - k_{f_0}(v)}{t} \\
=&\lim_{t\to 0} \frac{vL_{f_t} - vL_{f_0}}{t} = v \lim_{t\to 0} \frac{\int_0^1 \|\partial_v f_t(v)\|_2 \, dv - \int_0^1 \|\partial_v f_0(v)\|_2 \, dv}{t} \\
=&v \lim_{t\to 0} \frac{\int_0^1 \|\partial_v f_0(v) + t\partial_{tv} f_0(v) + \frac{t^2}{2}\partial_{ttv} f_c(v)\|_2 dv - \int_0^1 \|\partial_v f_0(v)\|_2 \, dv}{t} \\
=&v \lim_{t\to 0} \frac{\int_0^1 \|\partial_v f_0(v) + t\partial_{tv} f_0(v)\|_2 dv - \int_0^1 \|\partial_v f_0(v)\|_2 \, dv}{t} \\
&+ v \lim_{\substack{t\to 0 \\ t\in[-\frac{\epsilon}{2}, \frac{\epsilon}{2}]}} \frac{t^2}{2t} \int_0^1 \Big\langle 2\partial_v f_0(v) + 2t\partial_{tv} f_0(v) + \frac{t^2}{2}\partial_{ttv} f_c(v), \partial_{ttv} f_c(v) \Big\rangle dv.
\end{aligned}$$

Since f is smooth on $(-\epsilon, \epsilon) \times [0,1]$, the functions $\partial_v f$, $\partial_{tv} f$ and $\partial_{ttv} f$ are bounded on the compact set $[-\frac{\epsilon}{2}, \frac{\epsilon}{2}] \times [0,1]$. Thus

$$\lim_{t\to 0} \frac{k_{f_t}(v) - k_{f_0}(v)}{t} = v \lim_{t\to 0} \frac{\int_0^1 \|\partial_v f_0(v) + t\partial_{tv} f_0(v)\|_2 dv - \int_0^1 \|\partial_v f_0(v)\|_2 \, dv}{t}.$$

Because f_0 is an embedding, $\partial_v f_0(v) \neq O_{\mathbb{R}^n}$ for all $v \in [0,1]$. Applying Lemma 3.17, we get

$$\lim_{t\to 0} \frac{k_{f_t}(v) - k_{f_0}(v)}{t} = v \int_0^1 \frac{\langle \partial_v f_0(v), \partial_{tv} f_0(v)\rangle}{\|\partial_v f_0(v)\|_2} dv.$$

□

The following lemma states the differential of the map l_γ^{-1}.

Lemma 3.19. For any $\gamma \in \mathrm{Emb}([0,1],\mathbb{R}^n)$, the function

$$l_\gamma(v) = \int_0^v \|\dot\gamma(s)\|_2 \, ds$$

has an inverse function $(l_\gamma)^{-1}$ which is continuously differentiable.

Proof. It is clear that l_γ is continuously differentiable. Since γ is an embedding, $\dot\gamma(s) \neq O_{\mathbb{R}^n}$, $\forall s \in [0,1]$. So $\|\dot\gamma(s)\|_2 > 0$, $\forall s \in [0,1]$. Applying Inverse mapping theorem ([58, chapter 17, p. 418]), the function l_γ has an inverse function $(l_\gamma)^{-1}$ which is continuously differentiable. □

Using the above lemmas, we define the differential of the normalization $\mathfrak{N}$ as follows:

Definition 3.20. Let $\gamma \in \mathrm{Emb}([0,1],\mathbb{R}^n)$. For any $\vec u \in T_\gamma \mathrm{Emb}([0,1],\mathbb{R}^n)$, let $f : t \in (-\epsilon,\epsilon) \mapsto f_t \in \mathrm{Emb}([0,1],\mathbb{R}^n)$ be a smooth function such that $f_0 = \gamma$ and $\partial_t f_0 = \vec u$. We define the function $D\mathfrak{N}(\gamma)$ as follows

$$D\mathfrak{N}(\gamma) : T_\gamma \mathrm{Emb}([0,1],\mathbb{R}^n) \to T_{\mathfrak{N}(\gamma)}\mathfrak{C}$$
$$\vec u = \partial_t f_0 \mapsto D\mathfrak{N}(\gamma)(\vec u) := \frac{d}{dt}\Big(\mathfrak{N}(f_t)\Big)\Big|_{t=0} = \lim_{t\to 0} \frac{\mathfrak{N}(f_t) - \mathfrak{N}(f_0)}{t}. \tag{3.5}$$

The function $D\mathfrak{N}(\gamma)$ is called the differential of $\mathfrak{N}$ at γ.

We show that $\frac{d}{dt}\Big(\mathfrak{N}(f_t)\Big)\Big|_{t=0}$ exists and $\frac{d}{dt}\Big(\mathfrak{N}(f_t)\Big)\Big|_{t=0}$ does not depend on the chosen function f. So, we will find the formula of the differential of $\mathfrak{N}$ at γ.

We propose two ways to compute the formula of the differential of $\mathfrak{N}$ at γ using two different methods and check that those give the same result.

First way: we use the derivative of a composite function and compute $\frac{d}{dt}\left(z_{f_t}(v)\right)\Big|_{t=0} = \frac{d}{dt}\left((l_{f_t}^{-1} \circ k_{f_t})(v)\right)\Big|_{t=0}$ by using $l_{f_t} \circ z_{f_t} = k_{f_t}$.

We set $z_\gamma := l_\gamma^{-1} \circ k_\gamma : [0,1] \to [0,1]$. For $v \in [0,1]$, we have

$$\begin{aligned}\frac{d}{dt}\Big(\mathfrak{N}(f_t)(v)\Big)\Big|_{t=0} =& \frac{d}{dt}\Big((f_t \circ l_{f_t}^{-1} \circ k_{f_t})(v)\Big)\Big|_{t=0} = \frac{d}{dt} f_t\Big(z_{f_t}(v)\Big)\Big|_{t=0} \\ =& \partial_t f_t\Big(z_{f_t}(v)\Big)\Big|_{t=0} + \partial_z f_t\Big(z_{f_t}(v)\Big)\Big|_{t=0} . \frac{d}{dt}\left(z_{f_t}(v)\right)\Big|_{t=0} \\ =& \partial_t f_0\Big(z_{f_0}(v)\Big) + \partial_z f_0\Big(z_{f_0}(v)\Big) . \frac{d}{dt}\left(z_{f_t}(v)\right)\Big|_{t=0} \\ =& \vec{u}(z_\gamma(v)) + \dot{\gamma}(z_\gamma(v)) . \frac{d}{dt}\left(z_{f_t}(v)\right)\Big|_{t=0} .\end{aligned}$$

From Lemma 3.18, we have

$$\begin{aligned}\frac{d}{dt} k_{f_t}(v)\Big|_{t=0} =& \lim_{t\to 0} \frac{v\int_0^1 \|\partial_v f_t(s)\|_2 ds - v\int_0^1 \|\partial_v f_0(s)\|_2 ds}{t} = v\int_0^1 \frac{\langle \partial_v f_0(s), \partial_{tv} f_0(s)\rangle}{\|\partial_v f_0(s)\|_2} ds \\ =& v . \int_0^1 \frac{\langle \dot{\gamma}(s), \dot{\vec{u}}(s)\rangle}{\|\dot{\gamma}(s)\|_2} ds.\end{aligned}$$

Furthermore,

$$l_{f_t} \circ z_{f_t} = k_{f_t}.$$

Then, for $v \in [0,1]$, we have

$$\begin{aligned}\frac{d}{dt} k_{f_t}(v) =& \frac{d}{dt}(l_{f_t} \circ z_{f_t})(v) = \frac{d}{dt} l_{f_t}\Big(z_{f_t}(v)\Big) = \frac{d}{dt}\int_0^{z_{f_t}(v)} \|\partial_v f_t(s)\|_2 ds \\ =& \int_0^{z_{f_t}(v)} \frac{d}{dt}\|\partial_v f_t(s)\|_2 ds + \|\partial_v f_t(z_{f_t}(v))\|_2 . \frac{d}{dt} z_{f_t}(v) \\ =& \int_0^{z_{f_t}(v)} \frac{\langle \partial_v f_t(s), \partial_{tv} f_t(s)\rangle}{\|\partial_v f_t(s)\|_2} ds + \|\partial_v f_t(z_{f_t}(v))\|_2 . \frac{d}{dt} z_{f_t}(v)\end{aligned}$$

So,

$$\frac{d}{dt} z_{f_t}(v) = \frac{1}{\|\partial_v f_t(z_{f_t}(v))\|_2}\left(\frac{d}{dt} k_{f_t}(v) - \int_0^{z_{f_t}(v)} \frac{\langle \partial_v f_t(s), \partial_{tv} f_t(s)\rangle}{\|\partial_v f_t(s)\|_2} ds\right)$$

$$\Rightarrow \frac{d}{dt}z_{f_t}(v)\Big|_{t=0} = \frac{1}{\|\partial_v f_0(z_{f_0}(v))\|_2}\left(\frac{d}{dt}k_{f_t}(v)\Big|_{t=0} - \int_0^{z_{f_0}(v)} \frac{\langle \partial_v f_0(s), \partial_{tv} f_0(s)\rangle}{\|\partial_v f_0(s)\|_2} ds\right)$$

$$= \frac{1}{\|\dot\gamma(z_\gamma(v))\|_2}\left(v.\int_0^1 \frac{\langle \dot\gamma(s), \dot{\vec{u}}(s)\rangle}{\|\dot\gamma(s)\|_2} ds - \int_0^{z_\gamma(v)} \frac{\langle \dot\gamma(s), \dot{\vec{u}}(s)\rangle}{\|\dot\gamma(s)\|_2} ds\right).$$

Then

$$\frac{d}{dt}\Big(\mathfrak{N}(f_t)(v)\Big)\Big|_{t=0} = \vec{u}(z_\gamma(v)) + \dot\gamma(z_\gamma(v)).\frac{d}{dt}\left(z_{f_t}(v)\right)\Big|_{t=0}$$

$$= \vec{u}(z_\gamma(v)) + \frac{\dot\gamma(z_\gamma(v))}{\|\dot\gamma(z_\gamma(v))\|_2}\left(v.\int_0^1 \frac{\langle \dot\gamma(s), \dot{\vec{u}}(s)\rangle}{\|\dot\gamma(s)\|_2} ds - \int_0^{z_\gamma(v)} \frac{\langle \dot\gamma(s), \dot{\vec{u}}(s)\rangle}{\|\dot\gamma(s)\|_2} ds\right),$$

where $z_\gamma(v) = (l_\gamma^{-1} \circ k_\gamma)(v)$.
So, for $v \in [0,1]$, we have

$$\boxed{\frac{d}{dt}\Big(\mathfrak{N}(f_t)(v)\Big)\Big|_{t=0} = \vec{u}(z_\gamma(v)) + \frac{\dot\gamma(z_\gamma(v))}{\|\dot\gamma(z_\gamma(v))\|_2}\left(v.\int_0^1 \frac{\langle \dot\gamma(s), \dot{\vec{u}}(s)\rangle}{\|\dot\gamma(s)\|_2} ds - \int_0^{z_\gamma(v)} \frac{\langle \dot\gamma(s), \dot{\vec{u}}(s)\rangle}{\|\dot\gamma(s)\|_2} ds\right),}$$

where $z_\gamma(v) = (l_\gamma^{-1} \circ k_\gamma)(v)$.

Second way: we compute $\frac{d}{dt}\left(z_{f_t}(v)\right)\Big|_{t=0} = \frac{d}{dt}\left((l_{f_t}^{-1} \circ k_{f_t})(v)\right)\Big|_{t=0}$ directly.

We set $z_\gamma := l_\gamma^{-1} \circ k_\gamma : [0,1] \to [0,1]$. For $v \in [0,1]$, we have

$$\frac{d}{dt}\Big(\mathfrak{N}(f_t)(v)\Big)\Big|_{t=0} = \frac{d}{dt}\Big((f_t \circ l_{f_t}^{-1} \circ k_{f_t})(v)\Big)\Big|_{t=0} = \frac{d}{dt} f_t\Big(z_{f_t}(v)\Big)\Big|_{t=0}$$

$$= \partial_t f_t\Big(z_{f_t}(v)\Big)\Big|_{t=0} + \partial_z f_t\Big(z_{f_t}(v)\Big)\Big|_{t=0}.\frac{d}{dt}\left(z_{f_t}(v)\right)\Big|_{t=0}$$

$$= \partial_t f_0\Big(z_{f_0}(v)\Big) + \partial_z f_0\Big(z_{f_0}(v)\Big).\frac{d}{dt}\left(z_{f_t}(v)\right)\Big|_{t=0}$$

$$= \vec{u}(z_\gamma(v)) + \dot\gamma(z_\gamma(v)).\frac{d}{dt}\left(z_{f_t}(v)\right)\Big|_{t=0}.$$

We will compute $\frac{d}{dt}\left(z_{f_t}(v)\right)\Big|_{t=0} = \frac{d}{dt}\left((l_{f_t}^{-1} \circ k_{f_t})(v)\right)\Big|_{t=0}$ directly. Suppose that

$$t_0 = (l_{f_0}^{-1} \circ k_{f_0})(v) \text{ and } t_1 = (l_{f_t}^{-1} \circ k_{f_t})(v).$$

Then,

$$\int_0^{t_0} \|\partial_v f_0(s)\|_2 ds = v \int_0^1 \|\partial_v f_0(s)\|_2 ds \tag{3.6}$$

and

$$\int_0^{t_1} \|\partial_v f_t(s)\|_2 ds = v \int_0^1 \|\partial_v f_t(s)\|_2 ds. \tag{3.7}$$

We have that $f_t(s) = f(t,s)$, hence

$$\begin{aligned}\partial_v f_t(s) =& \partial_v f(t,s) = \partial_v f(0,s) + \partial_{tv} f(0,s)t + O(t)\\ =& \partial_v f_0(s) + \partial_{tv} f_0(s)t + O(t)\\ =& \partial_v f_0(s) + g(t,s).\end{aligned}$$

So,

$$\begin{aligned}\int_0^1 \|\partial_v f_t(s)\|_2 ds &= \int_0^1 \|\partial_v f_0(s) + g(t,s)\|_2 ds\\ &= \int_0^1 \left(\|\partial_v f_0(s)\|_2 + \frac{2\langle \partial_v f_0(s), g(t,s)\rangle + \|g(t,s)\|_2^2}{\|\partial_v f_0(s) + g(t,s)\|_2 + \|g(t,s)\|_2} \right) ds\end{aligned} \tag{3.8}$$

and

$$\begin{aligned}\int_0^{t_1} \|\partial_v f_t(s)\|_2 ds &= \int_0^{t_1} \|\partial_v f_0(s) + g(t,s)\|_2 ds\\ &= \int_0^{t_1} \left(\|\partial_v f_0(s)\|_2 + \frac{2\langle \partial_v f_0(s), g(t,s)\rangle + \|g(t,s)\|_2^2}{\|\partial_v f_0(s) + g(t,s)\|_2 + \|g(t,s)\|_2} \right) ds\end{aligned} \tag{3.9}$$

Combining (3.7), (3.8) and (3.9), we have that

$$\begin{aligned}v \int_0^1 &\left(\|\partial_v f_0(s)\|_2 + \frac{2\langle \partial_v f_0(s), g(t,s)\rangle + \|g(t,s)\|_2^2}{\|\partial_v f_0(s) + g(t,s)\|_2 + + \|g(t,s)\|_2} \right) ds\\ = \int_0^{t_1} &\left(\|\partial_v f_0(s)\|_2 + \frac{2\langle \partial_v f_0(s), g(t,s)\rangle + \|g(t,s)\|_2^2}{\|\partial_v f_0(s) + g(t,s)\|_2 + + \|g(t,s)\|_2} \right) ds.\end{aligned}$$

Since $\int_0^{t_0} \|\partial_v f_0(s)\|_2 ds = v \int_0^1 \|\partial_v f_0(s)\|_2 ds$, we get

$$\int_0^{t_0} \|\partial_v f_0(s)\|_2 ds + v \int_0^1 \frac{2\langle \partial_v f_0(s), g(t,s)\rangle + \|g(t,s)\|_2^2}{\|\partial_v f_0(s) + g(t,s)\|_{2+} + \|g(t,s)\|_2} ds$$
$$= \int_0^{t_1} \left(\|\partial_v f_0(s)\|_{2+} \frac{2\langle \partial_v f_0(s), g(t,s)\rangle + \|g(t,s)\|_2^2}{\|\partial_v f_0(s) + g(t,s)\|_{2+} + \|g(t,s)\|_2} \right) ds.$$

Hence

$$\int_{t_0}^{t_1} \|\partial_v f_0(s)\|_2 ds$$
$$= v \int_0^1 \frac{2\langle \partial_v f_0(s), g(t,s)\rangle + \|g(t,s)\|_2^2}{\|\partial_v f_0(s) + g(t,s)\|_{2+} + \|g(t,s)\|_2} ds - \int_0^{t_1} \frac{2\langle \partial_v f_0(s), g(t,s)\rangle + \|g(t,s)\|_2^2}{\|\partial_v f_0(s) + g(t,s)\|_{2+} + \|g(t,s)\|_2} ds.$$

Dividing both side by t and passing to the limit as $t \to 0$, we obtain

$$\lim_{t\to 0} \frac{1}{t} \int_{t_0}^{t_1} \|\partial_v f_0(s)\|_2 ds = v \int_0^1 \frac{\langle \partial_v f_0(s), \partial_{tv} f_0(s)\rangle}{\|\partial_v f_0(s)\|_2} ds - \int_0^{t_0} \frac{\langle \partial_v f_0(s), \partial_{tv} f_0(s)\rangle}{\|\partial_v f_0(s)\|_2} ds.$$

On the other hand, we have that

$$\lim_{t\to 0} \frac{1}{t} \int_{t_0}^{t_1} \|\partial_v f_0(s)\|_2 ds = \|\partial_v f_0(t_0)\|_2 . \lim_{t\to 0} \frac{t_1 - t_0}{t}.$$

Hence, we obtain that

$$\lim_{t\to 0} \frac{t_1 - t_0}{t} = \frac{1}{\|\partial_v f_0(t_0)\|_2} \left(v \int_0^1 \frac{\langle \partial_v f_0(s), \partial_{tv} f_0(s)\rangle}{\|\partial_v f_0(s)\|_2} ds - \int_0^{t_0} \frac{\langle \partial_v f_0(s), \partial_{tv} f_0(s)\rangle}{\|\partial_v f_0(s)\|_2} ds \right)$$
$$\Rightarrow \frac{d}{dt} \left((l_{f_t}^{-1} \circ k_{f_t})(v) \right) \Big|_{t=0} = \frac{1}{\|\partial_v f_0(t_0)\|_2} \left(v \int_0^1 \frac{\langle \partial_v f_0(s), \partial_{tv} f_0(s)\rangle}{\|\partial_v f_0(s)\|_2} ds \right.$$
$$\left. - \int_0^{t_0} \frac{\langle \partial_v f_0(s), \partial_{tv} f_0(s)\rangle}{\|\partial_v f_0(s)\|_2} ds \right).$$

Then,

$$\begin{aligned}\frac{d}{dt}\Big(\mathfrak{N}(f_t)(v)\Big)\Big|_{t=0} =&\vec{u}(z_\gamma(v)) + \dot{\gamma}(z_\gamma(v)).\frac{d}{dt}\left(z_{f_t}(v)\right)\Big|_{t=0}\\ =&\vec{u}(z_\gamma(v)) + \dot{\gamma}(z_\gamma(v)).\frac{d}{dt}\left((l_{f_t}^{-1}\circ k_{f_t})(v)\right)\Big|_{t=0}\\ =&\vec{u}(z_\gamma(v)) + \frac{\dot{\gamma}(z_\gamma(v))}{\|\partial_v f_0(t_0)\|_2}\left(v\int_0^1 \frac{\langle\partial_v f_0(s), \partial_{tv} f_0(s)\rangle}{\|\partial_v f_0(s)\|_2}ds\right.\\ &\left.-\int_0^{t_0}\frac{\langle\partial_v f_0(s), \partial_{tv} f_0(s)\rangle}{\|\partial_v f_0(s)\|_2}ds\right)\\ =&\vec{u}(t_0) + \frac{\dot{\gamma}(t_0)}{\|\dot{\gamma}(t_0)\|_2}\left(v.\int_0^1 \frac{\langle\dot{\gamma}(s), \dot{\vec{u}}(s)\rangle}{\|\dot{\gamma}(s)\|_2}ds - \int_0^{t_0}\frac{\langle\dot{\gamma}(s), \dot{\vec{u}}(s)\rangle}{\|\dot{\gamma}(s)\|_2}ds\right),\end{aligned}$$

where $t_0 = z_\gamma(v) = (l_\gamma^{-1}\circ k_\gamma)(v)$.

So, for $v \in [0,1]$, we have

$$\boxed{\frac{d}{dt}\Big(\mathfrak{N}(f_t)(v)\Big)\Big|_{t=0} = \vec{u}(t_0) + \frac{\dot{\gamma}(t_0)}{\|\dot{\gamma}(t_0)\|_2}\left(v.\int_0^1 \frac{\langle\dot{\gamma}(s), \dot{\vec{u}}(s)\rangle}{\|\dot{\gamma}(s)\|_2}ds - \int_0^{t_0}\frac{\langle\dot{\gamma}(s), \dot{\vec{u}}(s)\rangle}{\|\dot{\gamma}(s)\|_2}ds\right),}$$

where $t_0 = (l_\gamma^{-1}\circ k_\gamma)(v)$.

We observe that $\frac{d}{dt}\Big(\mathfrak{N}(f_t)\Big)\Big|_{t=0}$ just depends on γ and $\vec{u}$. Then the function $D\mathfrak{N}(\gamma) : T_\gamma \mathrm{Emb}([0,1],\mathbb{R}^n) \to T_{\mathfrak{N}(\gamma)}\mathfrak{C}$ is well defined.

Remark 3.21. The definition does not depend on the chosen f.

It is easy to see that the function $D\mathfrak{N}(\gamma) : T_\gamma \mathrm{Emb}([0,1],\mathbb{R}^n) \to T_{\mathfrak{N}(\gamma)}\mathfrak{C}$ is a linear map. We next consider how the action of $\mathrm{Diff}^+([0,1])$ goes to the differential of the map $\mathfrak{N}$.

Proposition 3.22. Let $\gamma \in \mathrm{Emb}([0,1],\mathbb{R}^n)$ and $\delta \in \mathrm{Diff}^+([0,1])$. For any smooth function $f : t \in (-\epsilon,\epsilon) \mapsto f_t \in \mathrm{Emb}([0,1],\mathbb{R}^n)$ such that $f_0 = \gamma$, then

$$D\mathfrak{N}(\gamma)\left(\partial_t f_0\right) = D\mathfrak{N}(\gamma\circ\delta)\Big(\partial_t(f_0\circ\delta)\Big).$$

Proof. We have $\mathfrak{N}(f_0\circ\delta) = \mathfrak{N}(f_0) = \mathfrak{N}(\gamma)$ and $\mathfrak{N}(f_t\circ\delta) = \mathfrak{N}(f_t)$ for every $t \in (-\epsilon,\epsilon)$. Then $D\mathfrak{N}(\gamma)\left(\partial_t f_0\right) = D\mathfrak{N}(\gamma\circ\delta)(\partial_t(f_0\circ\delta))$. □

The following proposition presents the images of the differentials of the map $\mathfrak{N}$ at two equivalent embeddings.

Proposition 3.23. If two embeddings α, β are equivalent, then the image of $D\mathfrak{N}(\alpha)$ and the image of $D\mathfrak{N}(\beta)$ are the same.

Proof. We first show that $D\mathfrak{N}(\alpha)\left(T_\alpha \mathrm{Emb}\left([0,1],\mathbb{R}^n\right)\right) \subseteq D\mathfrak{N}(\beta)\left(T_\beta \mathrm{Emb}\left([0,1],\mathbb{R}^n\right)\right)$. For any $\vec{u} \in T_\alpha \mathrm{Emb}\left([0,1],\mathbb{R}^n\right)$, there exists a smooth function $f : t \in (-\epsilon,\epsilon) \mapsto f_t \in \mathrm{Emb}\left([0,1],\mathbb{R}^n\right)$ such that $f_0 = \alpha$ and $\partial_t f_0 = \vec{u}$. Because α, β are equivalent, there exists $\delta \in \mathrm{Diff}^+\left([0,1]\right)$ such that $\alpha = \beta \circ \delta$. We consider the function

$$\begin{aligned} g : (-\epsilon,\epsilon) &\to \mathrm{Emb}\left([0,1],\mathbb{R}^n\right) \\ t &\mapsto g_t := f_t \circ \delta. \end{aligned}$$

It is easy to check that $g_0 = \alpha\circ\delta = \beta$ and g is smooth. So $\partial_t g_0 \in T_\beta \mathrm{Emb}\left([0,1],\mathbb{R}^n\right)$. Using Proposition 3.22, we have

$$D\mathfrak{N}(\alpha)\left(\partial_t f_0\right) = D\mathfrak{N}(\alpha\circ\delta)\Big(\left(\partial_t (f_0\circ\delta)\right)\Big) = D\mathfrak{N}(\beta)\left(\partial_t g_0\right).$$

Then

$$D\mathfrak{N}(\alpha)\left(\vec{u}\right) = D\mathfrak{N}(\beta)\left(\partial_t g_0\right) \in D\mathfrak{N}(\beta)\left(T_\beta \mathrm{Emb}\left([0,1],\mathbb{R}^n\right)\right).$$

This means that $D\mathfrak{N}(\alpha)\left(T_\alpha \mathrm{Emb}\left([0,1],\mathbb{R}^n\right)\right) \subseteq D\mathfrak{N}(\beta)\left(T_\beta \mathrm{Emb}\left([0,1],\mathbb{R}^n\right)\right)$.

Similarly, we have $D\mathfrak{N}(\beta)\left(T_\beta \mathrm{Emb}\left([0,1],\mathbb{R}^n\right)\right) \subseteq D\mathfrak{N}(\alpha)\left(T_\alpha \mathrm{Emb}\left([0,1],\mathbb{R}^n\right)\right)$. □

The following proposition states that the differential of $\mathfrak{N}$ at an embedding is a surjection.

Proposition 3.24. For $\gamma \in \mathrm{Emb}\left([0,1],\mathbb{R}^n\right)$, the function $D\mathfrak{N}(\gamma) : T_\gamma \mathrm{Emb}\left([0,1],\mathbb{R}^n\right) \to T_{\mathfrak{N}(\gamma)}\mathfrak{C}$ is surjective.

Proof. For any $\hat{u} \in T_{\mathfrak{N}(\gamma)}\mathfrak{C}$, there exists a smooth function $\hat{f} : t \in (-\epsilon,\epsilon) \mapsto \hat{f}_t \in \mathfrak{C}$ such that $\hat{f}_0 = \mathfrak{N}(\gamma)$ and $\partial_t \hat{f}_0 = \hat{u}$. Because $\mathfrak{C} \subset \mathrm{Emb}\left([0,1],\mathbb{R}^n\right)$ and there exists $\delta \in \mathrm{Diff}^+\left([0,1]\right)$ such that $\mathfrak{N}(\gamma)\circ\delta = \gamma$, we consider

$$\begin{aligned} f : (-\epsilon,\epsilon) &\to \mathrm{Emb}\left([0,1],\mathbb{R}^n\right) \\ t &\mapsto f_t := \hat{f}_t \circ \delta. \end{aligned}$$

It is easy to check that f is a smooth function and $f_0 = \gamma$. Then

$$\partial_t f_0 \in T_\gamma \mathrm{Emb}\left([0,1],\mathbb{R}^n\right).$$

We have $\mathfrak{N}(f_0) = \mathfrak{N}(\gamma)$ and $\mathfrak{N}(f_t) = \mathfrak{N}(\hat{f}_t \circ \delta) = \hat{f}_t$ for every $t \in (-\epsilon, \epsilon)$. So

$$D\mathfrak{N}(\gamma)(\partial_t f_0) = \partial_t \hat{f}_0 = \hat{u}.$$

Therefore the function $D\mathfrak{N}(\gamma)$ is surjective. □

Chapter 4

The space of N-piece cubic Bézier curves

Just as rationals give a way to approximate real numbers, Bézier curves and piecewise Bézier curves are used to approximate continuous curves. Piecewise uniform cubic Bézier curves are most common in practice. We will make special emphasis on the space $B_{N,3}$ of uniform N-piece cubic Bézier curves. For convenience, we sometimes drop "uniform".

In this chapter, we define a new norm $\|\cdot\|_p^{B_D}$ on the space B_D of Bézier curves of degree D and a new norm $\|\cdot\|_p^{B_{N,D}}$ on the space $B_{N,D}$ of uniform N-piece Bézier curves of degree D. The norms $\|\cdot\|_p^{B_D}$ and $\|\cdot\|_p^{B_{N,D}}$ are determined through control points. This chapter deals with the equivalence constants for the norm $\|\cdot\|_p^{B_{N,3}}$ and the L_p norm on the space $B_{N,3}$. This is the core idea of Algorithm 2 on page 86 in Chapter 5 using piecewise uniform cubic Bézier curves.

Theorem 4.1. Let $p \in [1, \infty[\cup\{\infty\}$. For any $\Gamma \in B_{N,3}$, we have

$$\|\Gamma\|_{L_p} \leq \|\Gamma\|_p^{B_{N,3}} \leq 2^{10} \|\Gamma\|_{L_p}.$$

A Bézier curve of degree D can be written as a Bézier curve of degree $D+1$. Then we have more control points in order to give additional freedom for curve design. We will study the equivalence constants for the norm $\|\cdot\|_p^{B_{N,D}}$ and the norm $\|\cdot\|_p^{B_{N,D+1}}$ on the space $B_{N,D}$.

Theorem 4.2. Let $p \in [1, \infty[\cup\{\infty\}$. For all $\Gamma \in B_{N,D}$, we have

$$\frac{1}{2(D+1)} \|\Gamma\|_p^{B_{N,D}} \leq \|\Gamma\|_p^{B_{N,D+1}} \leq 2\|\Gamma\|_p^{B_{N,D}}.$$

A uniform N-piece cubic Bézier curve can be split to become a uniform $2N$-piece cubic Bézier curve. This approach creates extra control points in order to give additional freedom for curve design and avoids increasing the degree of the curve. Splitting piecewise cubic Bézier curves plays an important role in Algorithm 2 on page 86 in Chapter 5 using piecewise uniform cubic Bézier curves. So, we investigate the equivalence constants for the norm $\|\cdot\|_p^{B_{2N,3}}$ and the norm $\|\cdot\|_p^{B_{N,3}}$ on the space $B_{N,3}$.

Theorem 4.3. Let $p \in [1, \infty[\cup \infty$. For any $\Gamma \in B_{N,3}$, we have

$$\min\left\{\frac{1}{24^{1/p}}, \frac{1}{4}\right\}\|\Gamma\|_p^{B_{N,3}} \leq \|\Gamma\|_p^{B_{2N,3}} \leq 3^{1/p}\ \|\Gamma\|_p^{B_{N,3}}.$$

4.1 Norms on the space of parametrizations

In this section, we recall the L_p norm and define a norm $\|\cdot\|_*$ on the space of parametrizations. The norm $\|\cdot\|_*$ is invariant under any change of parametrization and convenient for computations.

4.1.1 The space of parametrizations

A *parametrization* of a curve is a map from the parameter interval $[0, 1]$ to $\mathbb{R}^n$. The image of a parametrization is called a *curve*. A parametrization contains more information about a curve than its image. It tells us, for example, how fast we go along a curve. Let us first fix some notations and definitions:

Notation 4.4. ([34, chapter 1, p. 3]) $C^0([0, 1], \mathbb{R}^n)$ is the set of continuous parametrizations on $[0, 1]$.

The set $C^0([0, 1], \mathbb{R}^n)$ is a vector space over $\mathbb{R}$. Since the segment $[0, 1]$ is compact and each parametrization in the vector space $C^0([0, 1], \mathbb{R}^n)$ is continuous, every parametrization in $C^0([0, 1], \mathbb{R}^n)$ is integrable on $[0, 1]$. Hence, one can define norms and distances on $C^0([0, 1], \mathbb{R}^n)$ using integrals.

4.1.2 L_p norm on the space of parametrizations

On the space $C^0([0,1],\mathbb{R}^n)$, we have the L_p norm ([14, chapter 4], [34, chapter 1]) as follows

$$\|\cdot\|_{L_p}\colon C^0([0,1],\mathbb{R}^n)\to\mathbb{R}$$
$$\alpha\mapsto\|\alpha\|_{L_p}:=\begin{cases}\Big(\int\limits_0^1\|\alpha(t)\|_p^p dt\Big)^{1/p} & \text{if } p\in[1,\infty[\\ \max\limits_{t\in[0,1]}\|\alpha(t)\|_\infty & \text{if } p=\infty,\end{cases}$$

where $\|\cdot\|_p$ is the p-norm on $\mathbb{R}^n$.

We associate to $\|\cdot\|_{L_p}$ a distance d_{L_p} on $C^0([0,1],\mathbb{R}^n)$ defined as usual

$$d_{L_p}(\alpha,\beta):=\|\alpha-\beta\|_{L_p}.$$

4.1.3 Invariance of $\|\cdot\|_*$ under $\mathrm{Diff}^+([0,1])$ action

We want a norm which is independent of the reparametrization and easy to compute.

Notation 4.5. We denote by $C^1([0,1],\mathbb{R}^n)$ the vector space of continuously differentiable parametrizations on $[0,1]$.

Definition 4.6. On the vector space $C^1([0,1],\mathbb{R}^n)$, we define a function $\|\cdot\|_*$: $C^1([0,1],\mathbb{R}^n)\to\mathbb{R}$ as follows

$$\|\alpha\|_*:=\int\limits_0^1\|\alpha'(t)\|_1 dt+\|\alpha(0)\|_1,$$

where $\|\cdot\|_1$ is the 1-norm on $\mathbb{R}^n$.

From the properties of the norm $\|\cdot\|_1$ on $\mathbb{R}^n$, it is easily seen that $\|\cdot\|_*$ is a norm on the vector space $C^1([0,1],\mathbb{R}^n)$.

Proposition 4.7. The norm $\|\cdot\|_*$ is invariant under any change of parametrization.

Proof. For any $\alpha\in C^1([0,1],\mathbb{R}^n)$ and $\varphi\in\mathrm{Diff}^+([0,1])$, we have $\varphi(0)=0$ and $\varphi'(t)>0,\forall t\in[0,1]$. Then

$$\|\alpha\circ\varphi\|_*=\int\limits_0^1\|\alpha_i'(\varphi(t))\|_1\varphi'(t)dt+\|\alpha(\varphi(0))\|_1=\int\limits_0^1\|\alpha'(t)\|_1 dt+\|\alpha(0)\|_1=\|\alpha\|_*.$$

□

Notation 4.8. We can use $\|\cdot\|_*$ to compute norms of curves because $\|\cdot\|_*$ does not depend on the chosen parametrization.

Since $C^1([0,1],\mathbb{R}^n)$ is a vector space, we have a distance d_* on $C^1([0,1],\mathbb{R}^n)$ defined by $d_*(\alpha,\beta) := \|\alpha-\beta\|_*$.

The distance d_* is not parameterization invariant although $\|\cdot\|_*$ is invariant under any change of parametrization. In practice, we use some finite-dimensional spaces to approximate curves. Next, we consider the space of N-piece cubic Bézier curves.

4.2 Norms on the space of N-piece cubic Bézier curves

The Bernstein polynomials have been known since 1912, but their applicability to graphics was not realized for another half century. The Bézier curve was widely publicized in 1962 by the French engineer Pierre Bézier. The study of these curves was however first developed in 1959 by the mathematician Paul de Casteljau using de Casteljau's algorithm. The space of Bézier curves is used to make approximation in the space of continuous curves. Many books and articles present Bézier curves such as [39, 44, 64, 72, 79].

A continuous curve can be approximated by a Bézier curve but the degree of this Bézier curve may be large. Higher degree curves are computationally more expensive to evaluate. When more complex shapes are needed, low order Bézier curves are patched together, producing a composite Bézier curve. In practice, N-piece cubic Bézier curves are most common. So we concentrate on the space of uniform N-piece cubic Bézier curves.

In this section, we introduce a norm $\|\cdot\|_p^{B_D}$ on B_D and a norm $\|\cdot\|_p^{B_{N,D}}$ on $B_{N,D}$. We will study the equivalence constants for the norm $\|\cdot\|_p^{B_{N,3}}$ and the L_p norm on the space $B_{N,3}$.

A uniform N-piece Bézier curve of degree D can be considered as an N-piece Bézier curve of degree $D+1$. This means that the space $B_{N,D}$ inherits the norm $\|\cdot\|_p^{B_{N,D+1}}$. We look for the equivalence constants for the norm $\|\cdot\|_p^{B_{N,D+1}}$ and the norm $\|\cdot\|_p^{B_{N,D}}$ on the space $B_{N,D}$.

We then present how to split a uniform N-piece cubic Bézier curve to become a uniform $2N$-piece cubic Bézier curve. So, a uniform N-piece cubic Bézier curve

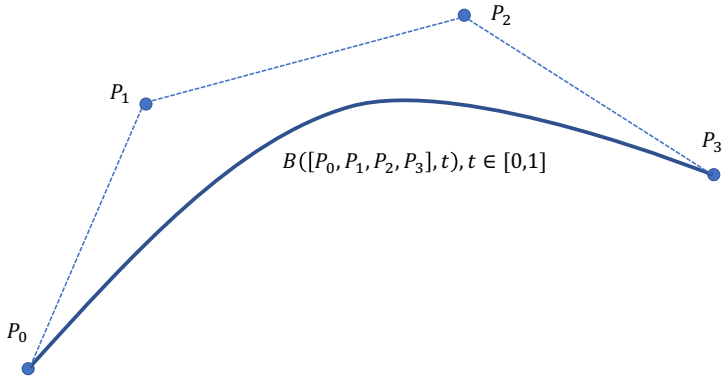

Fig. 4.1: A cubic Bézier curve.

can be considered as a uniform $2N$-piece cubic Bézier curve and the norm $\|\cdot\|_p^{B_{2N,3}}$ is a norm on the space $B_{N,3}$. We also investigate the equivalence constants for the norm $\|\cdot\|_p^{B_{2N,3}}$ and the norm $\|\cdot\|_p^{B_{N,3}}$ on the space $B_{N,3}$.

4.2.1 Bézier curves and N-piece Bézier curves

This subsection presents some definitions and notations of Bézier curves, N-piece Bézier curves.

Definition 4.9. ([64, chapter 6, p. 141]) Let $D \geq 0$ be an integer. Let $\mathbf{P} = \{P_0, \ldots, P_D\} \subset \mathbb{R}^n$. The *Bézier curve of degree D* associated to the set $\mathbf{P}$ is defined as follows

$$B([P_0, \ldots, P_D], t) := \sum_{i=0}^{D} P_i b_{i,D}(t), \quad t \in [0,1], \tag{4.1}$$

where $b_{i,D}(t)$, $i = 0, \ldots, D$, represents the Bernstein polynomial which is given by

$$b_{i,D}(t) = \binom{D}{i} t^i (1-t)^{D-i}.$$

The points $P_0, \ldots, P_D$ are called control points of the Bézier curve.

A uniform N-piece Bézier curve of degree D is a piecewise Bézier curve which has N pieces, each piece is a Bézier curve of degree D and the point at $t = \frac{j}{N}$, $j = 1, \ldots, N-1$, is the connecting point of the pieces. We often drop "uniform". Let us consider the definition of the N-piece Bézier curve of degree D.

Definition 4.10. ([64, chapter 7, p. 169]) Let $D \geq 0$ and $N > 0$ be integers. Let $\mathbf{P} = \{P_0, \ldots, P_{ND}\} \subset \mathbb{R}^n$. The *$N$-piece Bézier curve of degree D* associated to the

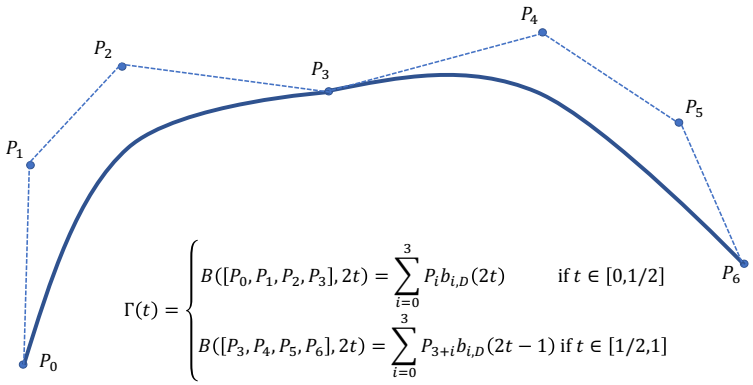

Fig. 4.2: A two-piece cubic Bézier curve.

set $\mathbf{P}$ is formed by

$$\Gamma : [0,1] \to \mathbb{R}^n$$
$$t \mapsto \Gamma(t) = B\left([P_{jD}, \ldots, P_{jD+D}], Nt - j\right) \text{ if } t \in \left[\frac{j}{N}, \frac{j+1}{N}\right].$$

The points $P_0, \ldots, P_{ND}$ are called control points of Γ.

Notation 4.11.

- The symbol B_D denotes the vector space of Bézier curves of degree D.
- The symbol $B_{N,D}$ denotes the vector space of N-piece Bézier curves of degree D.

4.2.2 Norms and distances on B_D, $B_{N,D}$

In this section, we define some norms and distances through control points on the space of Bézier curves of degree D and on the space of N-piece Bézier curves of degree D.

Definition 4.12. Let $\Gamma \in B_D$ be a Bézier curve of degree D defined by

$$\Gamma(t) = \sum_{i=0}^{D} P_i b_{i,D}(t), \quad t \in [0,1],$$

where $P_i \in \mathbb{R}^n, i = 0, \ldots, D$. Let $p \in [1, \infty[\cup \{\infty\}$. We define a function $\|\cdot\|_p^{B_D}$:

$B_D \to \mathbb{R}$ as follows:

$$\|\Gamma\|_p^{B_D} := \begin{cases} \Big(\sum_{i=0}^{D} \|P_i\|_p^p \Big)^{1/p} & \text{if } p \in [1, \infty[\\ \max\limits_{i=0,\dots,D} \{\|P_i\|_\infty\} & \text{if } p = \infty, \end{cases}$$

where $\|\cdot\|_p$ is the p-norm on $\mathbb{R}^n$.

From the properties of the p-norm on $\mathbb{R}^n$ and the Minkowski inequality, it is easily seen that $\|\cdot\|_p^{B_D}$ is a norm on the vector space B_D. In fact, it is a norm on the space $(\mathbb{R}^n)^{D+1}$ of control polygons. We then have an induced distance on B_D by $d_p^{B_D}(\Gamma, \Delta) := \|\Gamma - \Delta\|_p^{B_D}$.

Definition 4.13. Let $\Gamma \in B_{N,D}$ be an N-piece Bézier curve of degree D defined by

$$\Gamma(t) = \begin{cases} \Gamma^{(0)}(Nt) = \sum\limits_{i=0}^{D} P_i b_{i,D}(Nt) & \text{if } t \in \left[0, \dfrac{1}{N}\right], \\ \Gamma^{(j)}(Nt - j) = \sum\limits_{i=0}^{D} P_{jD+i} b_{i,D}(Nt - j) & \text{if } t \in \left[\dfrac{j}{N}, \dfrac{j+1}{N}\right], \\ & j = 1, \dots, N-1, \end{cases}$$

where $P_{jD+i} \in \mathbb{R}^n$, $j = 0, \dots, N-1$, $i = 0, \dots, D$. Let $p \in [1, \infty[\cup \{\infty\}$. We define a function $\|\cdot\|_p^{B_{N,D}}$: $B_{N,D} \to \mathbb{R}$ by:

$$\|\Gamma\|_p^{B_{N,D}} := \begin{cases} \dfrac{1}{N^{1/p}} \left(\sum\limits_{j=0}^{N-1} \left(\|\Gamma^{(j)}\|_p^{B_D} \right)^p \right)^{1/p} & \text{if } p \in [1, \infty[\\ \max\limits_{j=0,\dots,N-1} \left\{ \|\Gamma^{(j)}\|_\infty^{B_D} \right\} & \text{if } p = \infty. \end{cases}$$

From the properties of the norm $\|\cdot\|_p^{B_D}$ on B_D and the Minkowski inequality, it is easy to check that $\|\cdot\|_p^{B_D}$ is a norm on the vector space $B_{N,D}$. Then we have again an induced distance on $B_{N,D}$ defined by $d_p^{B_{N,D}}(\Gamma, \Delta) := \|\Gamma - \Delta\|_p^{B_{N,D}}$.

These norms and these distances can be computed more efficiently than, for example, the L_p- norm.

4.2.3 The equivalence between the norm $\|\cdot\|_p^{B_{N,3}}$ and the norm $\|\cdot\|_{L_p}$ on the space $B_{N,3}$

The space $B_{N,3}$ is a subspace of the space $C^0([0,1], \mathbb{R}^n)$. So, the space $B_{N,D}$ inherits the norm $\|\cdot\|_{L_p}$ from the space $C^0([0,1], \mathbb{R}^n)$. We defined the norm $\|\cdot\|_p^{B_{N,D}}$ through

control points on the space $B_{N,D}$ and this norm is easy to compute. When the degree of Bézier curves is big, the estimation of the constants in the equivalence inequalities between the norm $\|\cdot\|_p^{B_{N,D}}$ and the norm $\|\cdot\|_{L_p}$ seems to be difficult to compute. However, it is common and convenient to approximate continuous curves by N-piece cubic Bézier curves. So, in this subsection, we study the equivalence constants for the norm $\|\cdot\|_p^{B_{N,3}}$ and the norm $\|\cdot\|_{L_p}$ on the space $B_{N,3}$.

Find a constant m such that $m\|\cdot\|_{L_p} \leq \|\cdot\|_p^{B_{N,D}}$ on $B_{N,D}$

Consider $p \in [1, \infty[$. First, we look for a lower bound for the norm $\|\cdot\|_p^{B_D}$ with respect to the norm $\|\cdot\|_{L_p}$ on the space B_D. Using this lower bound, we get a constant m such that $m\|\cdot\|_{L_p} \leq \|\cdot\|_p^{B_{N,D}}$ on the space $B_{N,D}$ of N-piece Bézier curves of degree D.

Lemma 4.14. For every $p \in [1, \infty[$, the following inequality

$$\|\Gamma\|_{L_p} \leq \|\Gamma\|_p^{B_D}$$

holds for any $\Gamma \in B_D$.

Proof. Let $\Gamma \in B_D$ be a Bézier curve of degree D with control points $P_i \in \mathbb{R}^n$, $i = 0, \ldots, D$. So

$$\Gamma(t) = \sum_{i=0}^{D} P_i b_{i,D}(t), \quad t \in [0, 1].$$

We have

$$\|\Gamma\|_{L_p} = \Big(\int_0^1 \Big\| \sum_{i=0}^{D} P_i b_{i,D}(t) \Big\|_p^p dt \Big)^{1/p} \leq \Big(\int_0^1 \Big(\sum_{i=0}^{D} \|P_i\|_p b_{i,D}(t) \Big)^p dt \Big)^{1/p}.$$

Case $p = 1$. We get

$$\sum_{i=0}^{D} \|P_i\|_1 b_{i,D}(t) \leq \sum_{i=0}^{D} \|P_i\|_1 = \Big(\sum_{i=0}^{D} \|P_i\|_1^1 \Big)^{1/1}.$$

Case $p \in]1, \infty[$. Using Holder's inequality, we get

$$\begin{aligned} \sum_{i=0}^{D} \|P_i\|_p b_{i,D}(t) &\leq \Big(\sum_{i=0}^{D} \|P_i\|_p^p \Big)^{1/p} \Big(\sum_{i=0}^{D} (b_{i,D}(t))^{p/(p-1)} \Big)^{(p-1)/p} \\ &\leq \Big(\sum_{i=0}^{D} \|P_i\|_p^p \Big)^{1/p} \Big(\sum_{i=0}^{D} b_{i,D}(t) \Big)^{(p-1)/p} = \Big(\sum_{i=0}^{D} \|P_i\|_p^p \Big)^{1/p}. \end{aligned}$$

Combining the above two cases, we obtain

$$\|\Gamma\|_{L_p} \leq \Big(\int_0^1 \sum_{i=0}^{D} \|P_i\|_p^p dt \Big)^{1/p} = \Big(\sum_{i=0}^{D} \|P_i\|_p^p \Big)^{1/p} = \|\Gamma\|_p^{B_D}.$$

□

We use this lower bound on the space B_D of Bézier curves of degree D to obtain a lower estimate for the norm $\|\cdot\|_p^{B_{N,D}}$ with respect to the norm $\|\cdot\|_{L_p}$ on the space $B_{N,D}$ of N-piece Bézier curves of degree D.

Proposition 4.15. For every $p \in [1, \infty[$, the following inequality

$$\|\Gamma\|_{L_p} \leq \|\Gamma\|_p^{B_{N,D}}$$

holds for any $\Gamma \in B_{N,D}$.

Proof. Let $\Gamma \in B_{N,D}$ be an N-piece Bézier curve of degree D with control points $P_{jD+i} \in \mathbb{R}^n$, $i = 0, \ldots, D$, $j = 0, \ldots, N-1$. So

$$\Gamma(t) = \begin{cases} \Gamma^{(0)}(Nt) = \sum_{i=0}^{D} P_i b_{i,D}(Nt) & \text{if } t \in \Big[0, \frac{1}{N}\Big], \\ \Gamma^{(j)}(Nt-j) = \sum_{i=0}^{D} P_{jD+i} b_{i,D}(Nt-j) & \text{if } t \in \Big[\frac{j}{N}, \frac{j+1}{N}\Big], \\ & \qquad j = 1, \ldots, N-1. \end{cases}$$

We have

$$\begin{aligned} \|\Gamma\|_{L_p} &= \Big(\int_0^1 \|\Gamma(t)\|_p^p dt \Big)^{1/p} = \Big(\sum_{j=0}^{N-1} \int_{\frac{j}{N}}^{\frac{j+1}{N}} \|\Gamma^{(j)}(Nt-j)\|_p^p dt \Big)^{1/p} \\ &= \frac{1}{N^{1/p}} \Big(\sum_{j=0}^{N-1} \int_0^1 \|\Gamma^{(j)}(t)\|_p^p dt \Big)^{1/p}. \end{aligned}$$

Using Lemma 4.14, we get

$$\|\Gamma\|_{L_p} \leq \frac{1}{N^{1/p}} \Big(\sum_{j=0}^{N-1} \Big(\|\Gamma^{(j)}\|_p^{B_D} \Big)^p \Big)^{1/p} = \|\Gamma\|_p^{B_{N,D}}.$$

□

Find a constant m such that $m\|\cdot\|_{L_\infty} \leq \|\cdot\|_\infty^{B_{N,D}}$ on $B_{N,D}$

We find a lower bound for the norm $\|\cdot\|_\infty^{B_D}$ with respect to the norm $\|\cdot\|_{L_\infty}$ on the space B_D. Using this, we obtain as before a constant m such that $m\|\cdot\|_{L_\infty} \leq \|\cdot\|_\infty^{B_{N,D}}$ on the space $B_{N,D}$ of N-piece Bézier curves of degree D.

Lemma 4.16. For any $\Gamma \in B_D$, we have

$$\|\Gamma\|_{L_\infty} \leq \|\Gamma\|_\infty^{B_D}.$$

Proof. Let $\Gamma \in B_D$ be a Bézier curve of degree D with control points $P_i \in \mathbb{R}^n$, $i = 0, \ldots, D$. So

$$\Gamma(t) = \sum_{i=0}^{D} P_i b_{i,D}(t), \quad t \in [0,1].$$

We have

$$\Big\| \sum_{i=0}^{D} P_i b_{i,D}(t) \Big\|_{L_\infty} \leq \sum_{i=0}^{D} \|P_i\|_\infty b_{i,D}(t) \leq \Big(\sum_{i=0}^{D} b_{i,D}(t) \Big) \max_{i=0,\ldots,D} \|P_i\|_\infty = \max_{i=0,\ldots,D} \|P_i\|_\infty.$$

Thus

$$\|\Gamma\|_{L_\infty} \leq \|\Gamma\|_\infty^{B_D}.$$

□

Proposition 4.17. For any $\Gamma \in B_{N,D}$, we have

$$\|\Gamma\|_{L_\infty} \leq \|\Gamma\|_\infty^{B_{N,D}}.$$

Proof. Let $\Gamma \in B_{N,D}$ be an N-piece Bézier curve of degree D with control points $P_{jD+i} \in \mathbb{R}^n$, $i = 0, \ldots, D$, $j = 0, \ldots, N-1$. So

$$\Gamma(t) = \begin{cases} \Gamma^{(0)}(Nt) = \sum\limits_{i=0}^{D} P_i b_{i,D}(Nt) & \text{if } t \in \Big[0, \dfrac{1}{N}\Big], \\ \Gamma^{(j)}(Nt-j) = \sum\limits_{i=0}^{D} P_{jD+i} b_{i,D}(Nt-j) & \text{if } t \in \Big[\dfrac{j}{N}, \dfrac{j+1}{N}\Big], \\ & \qquad j = 1, \ldots, N-1. \end{cases}$$

We have

$$\begin{aligned}\|\Gamma\|_{L_\infty} &= \max_{t\in[0,1]}\|\Gamma(t)\|_\infty = \max_{j=0,\dots,N-1}\max_{t\in[\frac{j}{N},\frac{j+1}{N}]}\|\Gamma^{(j)}(Nt-j)\|_\infty \\ &= \max_{j=0,\dots,N-1}\max_{t\in[0,1]}\|\Gamma^{(j)}(t)\|_\infty.\end{aligned}$$

Using Lemma 4.16, we get

$$\|\Gamma\|_{L_\infty} \leq \max_{j=0,\dots,N-1}\|\Gamma\|_\infty^{B_D} = \|\Gamma\|_\infty^{B_{N,D}}.$$

□

Consequently, for $p \in [1,\infty[\cup\{\infty\}$, we obtained a constant m such that $m\|\cdot\|_{L_p} \leq \|\cdot\|_p^{B_{N,D}}$ on the space $B_{N,D}$. The above propositions can be applied to the space $B_{N,3}$ of N-piece *cubic* Bézier curves

Find a constant M such that $\|\cdot\|_p^{B_{N,3}} \leq M\|\cdot\|_{L_p}$ on $B_{N,3}$

Consider $p \in [1,\infty[$. When the degree of Bézier curves is greater than 3, it seems to be difficult to find a constant M such that $\|\cdot\|_p^{B_{N,D}} \leq M\|\cdot\|_{L_p}$ on the space $B_{N,D}$ of N-piece Bézier curves of degree D. So, we consider the space $B_{N,3}$ of N-piece *cubic* Bézier curves.

We first estimate the cubic Bézier curves. This is the core idea to look for a constant M such that $\|\cdot\|_p^{B_{N,3}} \leq M\|\cdot\|_{L_p}$ on the space $B_{N,3}$ of N-piece *cubic* Bézier curves.

Lemma 4.18. Let $p \in [1,\infty[$. For any $P_0, P_1, P_2, P_3 \in \mathbb{R}^n$, we have

$$\int_0^1 \Big\| \sum_{i=0}^3 P_i b_{i,D}(t)\Big\|_p^p dt \geq \frac{1}{2^{10p}}\Big(\sum_{i=0}^3 \|P_i\|_p^p\Big).$$

Proof. We consider $\max\Big\{\|P_0\|_p, \frac{1}{3}\|P_1\|_p, \frac{1}{3}\|P_2\|_p, \|P_3\|_p\Big\}$.

- Case 1: $\|P_0\|_p = \max\Big\{\|P_0\|_p, \frac{1}{3}\|P_1\|_p, \frac{1}{3}\|P_2\|_p, \|P_3\|_p\Big\}$.

We consider the interval $\Big[0, \frac{1}{16}\Big]$. For any $t \in \Big[0, \frac{1}{16}\Big]$, we have

$$\begin{aligned}
&\|P_0(1-t)^3\|_p \geq \Big(1-\frac{1}{16}\Big)^3\|P_0\|_p = \frac{15^3}{16^3}\|P_0\|_p.\\
&\|P_1 3t(1-t)^2\|_p \leq 3\frac{1}{16}\Big(1-\frac{1}{16}\Big)^2\|P_1\|_p \leq 3\|P_0\|_p\frac{3.15^2}{16^3} = \frac{9.15^2}{16^3}\|P_0\|_p\\
&\|P_2 3t^2(1-t)\|_p \leq 3\Big(\frac{1}{16}\Big)^2\Big(1-\frac{1}{16}\Big)\|P_2\|_p \leq 3\|P_0\|_p\frac{3.15}{16^3} = \frac{9.15}{16^3}\|P_0\|_p\\
&\|P_3 t^3\|_p \leq \frac{1}{16^3}\|P_3\|_p \leq \frac{1}{16^3}\|P_0\|_p.
\end{aligned}$$

So, for any $t \in \Big[0, \frac{1}{8}\Big]$, we have

$$\begin{aligned}
&\Big\|\sum_{i=0}^{3} P_i b_{i,D}(t)\Big\|_p\\
&\quad\geq \|P_0(1-t)^3\|_p - \|P_1 3t(1-t)^2\|_p - \|P_2 3t^2(1-t)\|_p - \|P_3 t^3\|_p\\
&\quad\geq \frac{15^3}{16^3}\|P_0\|_p - \frac{9.15^2}{16^3}\|P_0\|_p - \frac{9.15}{16^3}\|P_0\|_p - \frac{1}{16^3}\|P_0\|_p = \frac{1214}{4096}\|P_0\|_p.
\end{aligned}$$

Then

$$\begin{aligned}
\int_0^1 \Big\|\sum_{i=0}^{3} P_i b_{i,D}(t)\Big\|_p^p dt &\geq \int_0^{\frac{1}{16}} \Big\|\sum_{i=0}^{3} P_i b_{i,D}(t)\Big\|_p^p dt \geq \int_0^{\frac{1}{16}} \left(\frac{1214}{4096}\right)^p \|P_0\|_p^p dt\\
&\geq \frac{1}{16}\left(\frac{1214}{4096}\right)^p \frac{1}{2+2.3^p}\Big(\sum_{i=0}^{3}\|P_0\|_p^p\Big) \geq \frac{1}{2^{10p}}\Big(\sum_{i=0}^{3}\|P_0\|_p^p\Big).
\end{aligned}$$

- Case 2: $\frac{1}{3}\|P_1\|_p = \max\Big\{\|P_0\|_p, \frac{1}{3}\|P_1\|_p, \frac{1}{3}\|P_2\|_p, \|P_3\|_p\Big\}$.
  We consider the interval $\Big[\frac{7}{32}, \frac{9}{32}\Big]$. For any $t \in \Big[\frac{7}{32}, \frac{9}{32}\Big]$, we have

$$\begin{aligned}
&\|P_1 3t(1-t)^2\|_p \geq 3\frac{7}{32}\Big(1-\frac{7}{32}\Big)^2 = \frac{3.7.25^2}{32^3}\|P_1\|_p\\
&\|P_0(1-t)^3\|_p \leq \Big(1-\frac{7}{32}\Big)^3\|P_0\|_p \leq \frac{25^3}{32^3}\frac{1}{3}\|P_1\|_p = \frac{25^3}{3.32^3}\|P_1\|_p\\
&\|P_2 3t^2(1-t)\|_p \leq 3\Big(\frac{9}{32}\Big)^2\Big(1-\frac{9}{32}\Big)\|P_2\|_p \leq \frac{3.9^2.23}{32^3}\|P_1\|_p\\
&\|P_3 t^3\|_p \leq \frac{9^3}{32^3}\|P_3\|_p \leq \frac{1}{3}\|P_1\|_p\frac{9^3}{32^3} = \frac{9^3}{3.32^3}\|P_1\|_p.
\end{aligned}$$

So, for any $t \in \Big[\frac{7}{32}, \frac{9}{32}\Big]$, we have

$$\begin{aligned}
&\Big\| \sum_{i=0}^{3} P_i b_{i,D}(t) \Big\|_p \\
&\quad \geq \|P_1 3t(1-t)^2\|_p - \|P_0(1-t)^3\|_p - \|P_2 3t^2(1-t)\|_p - \|P_3 t^3\|_p \\
&\quad \geq \frac{3.7.25^2}{32^3}\|P_1\|_p - \frac{25^3}{3.32^3}\|P_1\|_p - \frac{3.9^2.23}{32^3}\|P_1\|_p - \frac{9^3}{3.32^3}\|P_1\|_p = \frac{6254}{98304}\|P_1\|_p.
\end{aligned}$$

Then

$$\begin{aligned}
\int_0^1 \Big\| \sum_{i=0}^{3} P_i b_{i,D}(t) \Big\|_p^p dt &\geq \int_{\frac{7}{32}}^{\frac{9}{32}} \Big\| \sum_{i=0}^{3} a_i b_{i,D}(t) \Big\|_p^p dt \geq \int_{\frac{7}{32}}^{\frac{9}{32}} \left(\frac{6254}{98304}\right)^p \|P_1\|_p^p dt \\
&\geq \frac{1}{16}\left(\frac{6254}{98304}\right)^p \frac{1}{2 + 2.3^{-p}} \Big(\sum_{i=0}^{3} \|P_i\|_p^p \Big) \\
&\geq \frac{1}{2^{10p}} \Big(\sum_{i=0}^{3} \|P_i\|_p^p \Big).
\end{aligned}$$

- Case 3: $\frac{1}{3}\|P_2\|_p = \max\Big\{\|P_0\|_p, \frac{1}{3}\|P_1\|_p, \frac{1}{3}\|P_2\|_p, \|P_3\|_p\Big\}$. Case 3 becomes Case 2 when we make the substitution $s = 1 - t$.
- Case 4: $\|P_3\|_p = \max\Big\{\|P_0\|_p, \frac{1}{3}\|P_1\|_p, \frac{1}{3}\|P_2\|_p, \|P_3\|_p\Big\}$. Case 4 becomes Case 1 when we make the substitution $s = 1 - t$.

Combining the above four cases, we get

$$\int_0^1 \Big\| \sum_{i=0}^{3} P_i b_{i,D}(t) \Big\|_p^p dt \geq \frac{1}{2^{10p}} \Big(\sum_{i=0}^{3} \|P_i\|_p^p \Big).$$

□

We use the above lemma to find a constant M such that $\|\cdot\|_p^{B_{N,3}} \leq M\|\cdot\|_{L_p}$ on the space $B_{N,3}$ of N-piece cubic Bézier curves.

Proposition 4.19. Let $p \in [1, \infty[$. Then for any $\Gamma \in B_{N,3}$, we have

$$\|\Gamma\|_p^{B_{N,3}} \leq 2^{10}\|\Gamma\|_{L_p}.$$

Proof. Let $\Gamma \in B_{N,3}$ be an N-piece cubic Bézier curve with control points $P_{j3+i} \in$

$\mathbb{R}^n$, $i = 0, \ldots, 3$, $j = 0, \ldots, N-1$. So

$$\Gamma(t) = \begin{cases} \Gamma^{(0)}(Nt) = \sum_{i=0}^{3} P_i b_{i,3}(Nt) & \text{if } t \in \Big[0, \frac{1}{N}\Big], \\ \Gamma^{(j)}(Nt-j) = \sum_{i=0}^{3} P_{j3+i} b_{i,3}(Nt-j) & \text{if } t \in \Big[\frac{j}{N}, \frac{j+1}{N}\Big], \\ & j = 1, \ldots, N-1. \end{cases}$$

We have

$$\begin{aligned} \|\Gamma\|_{L_p} &= \Big(\int_0^1 \|\Gamma(t)\|_p^p dt \Big)^{1/p} = \Big(\sum_{j=0}^{N-1} \int_{\frac{j}{N}}^{\frac{j+1}{N}} \Big\| \sum_{i=0}^{3} P_{j3+i} b_{i,3}(Nt-j) \Big\|_p^p dt \Big)^{1/p} \\ &= \frac{1}{N^{1/p}} \Big(\sum_{j=0}^{N-1} \int_0^1 \Big\| \sum_{i=0}^{3} P_{j3+i} b_{i,3}(t) \Big\|_p^p dt \Big)^{1/p}. \end{aligned}$$

Using Lemma 4.18, we obtain

$$\|\Gamma\|_{L_p} \geq \frac{1}{N^{1/p}} \Big(\sum_{j=0}^{N-1} \frac{1}{2^{10p}} \Big(\sum_{i=0}^{3} \|P_{j3+i}\|_p^p \Big) \Big)^{1/p} \geq \frac{1}{2^{10}} \|\Gamma\|_p^{B_{N,3}}.$$

□

Find a constant M such that $\|\cdot\|_\infty^{B_{N,3}} \leq M\|\cdot\|_{L_\infty}$ on the space $B_{N,3}$

We first consider the maximum of cubic Bézier curves. From this, we obtain a constant M such that $\|\cdot\|_\infty^{B_{N,3}} \leq M\|\cdot\|_{L_\infty}$ on the space $B_{N,3}$ of N-piece cubic Bézier curves.

Lemma 4.20. For any $P_0, P_1, P_2, P_3 \in \mathbb{R}^n$, we have

$$\max_{t\in[0,1]} \Big\| \sum_{i=0}^{3} P_i b_{i,D}(t) \Big\|_\infty \geq \frac{13}{96} \max_{i=0,\ldots,3} \|P_i\|_\infty.$$

Proof. We consider $\max\Big\{\|P_0\|_\infty, \frac{1}{3}\|P_1\|_\infty, \frac{1}{3}\|P_2\|_\infty, \|P_3\|_\infty\Big\}$.

- Case 1: $\|P_0\|_\infty = \max\Big\{\|P_0\|_\infty, \frac{1}{3}\|P_1\|_\infty, \frac{1}{3}\|P_2\|_\infty, \|P_3\|_\infty\Big\}$.

We consider at $t = 0$. We have

$$\Big\| \sum_{i=0}^{3} P_i b_{i,D}(0) \Big\|_\infty = \|P_0\|_\infty$$
$$\Rightarrow \max_{t\in[0,1]} \Big\| \sum_{i=0}^{3} P_i b_{i,D}(0) \Big\|_\infty \geq \|P_0\|_\infty = \max_{i=0,\dots,3} \|P_i\|_\infty.$$

- Case 2: $\frac{1}{2}\|P_1\|_\infty = \max\Big\{\|P_0\|_\infty, \frac{1}{3}\|P_1\|_\infty, \frac{1}{3}\|P_2\|_\infty, \|P_3\|_\infty\Big\}$.

  We consider at $t = \frac{1}{4}$. We have

$$\begin{aligned}\Big\| \sum_{i=0}^{3} P_i b_{i,D}\Big(\frac{1}{4}\Big) \Big\|_\infty &\geq \frac{27}{64}\|P_1\|_\infty - \frac{27}{64}\|P_0\|_\infty - \frac{9}{64}\|P_2\|_\infty - \frac{1}{64}\|P_3\|_\infty \\ &\geq \frac{27}{64}\|P_1\|_\infty - \frac{9}{64}\|P_1\|_\infty - \frac{9}{64}\|P_1\|_\infty - \frac{1}{192}\|P_1\|_\infty \\ &= \frac{13}{96}\|P_1\|_\infty.\end{aligned}$$

  Thus

$$\max_{t\in[0,1]} \Big\| \sum_{i=0}^{3} a_i b_{i,D}(t) \Big\|_\infty \geq \frac{13}{96} \max_{i=0,\dots,3} \|a_i\|_\infty.$$

- Case 3: $\frac{1}{3}|\|P_2\|_\infty = \max\Big\{\|P_0\|_\infty, \frac{1}{3}\|P_1\|_\infty, \frac{1}{3}\|P_2\|_\infty, \|P_3\|_\infty\Big\}$. This case is similar to Case 2.
- Case 4: $\|P_3\|_\infty = \max\Big\{\|P_0\|_\infty, \frac{1}{3}\|P_1\|_\infty, \frac{1}{3}\|P_2\|_\infty, \|P_3\|_\infty\Big\}$. This case is similar to Case 1.

Combining the above four cases, we obtain

$$\max_{t\in[0,1]} \Big\| \sum_{i=0}^{3} P_i b_{i,D}(t) \Big\|_\infty \geq \frac{13}{96} \max_{i=0,\dots,3} \|P_i\|_\infty.$$

□

From the above lemma, we have the following proposition on the space $B_{N,3}$ of N-piece cubic Bézier curves.

Proposition 4.21. For any $\Gamma \in B_{N,3}$, we have

$$\|\Gamma\|_\infty^{B_{N,3}} \leq \frac{96}{13} \|\Gamma\|_{L_\infty}.$$

Proof. Let $\Gamma \in B_{N,3}$ be an N-piece cubic Bézier curve with control points $P_{j3+i} \in \mathbb{R}^n$, $i = 0, \ldots, 3$, $j = 0, \ldots, N-1$. So

$$\Gamma(t) = \begin{cases} \Gamma^{(0)}(Nt) = \sum_{i=0}^{3} P_i b_{i,3}(Nt) & \text{if } t \in \left[0, \frac{1}{N}\right], \\ \Gamma^{(j)}(Nt-j) = \sum_{i=0}^{3} P_{j3+i} b_{i,D}(Nt-j) & \text{if } t \in \left[\frac{j}{N}, \frac{j+1}{N}\right], \\ & j = 1, \ldots, N-1. \end{cases}$$

We have

$$\begin{aligned} \|\Gamma\|_{L_\infty} &= \max_{t\in[0,1]} \|\Gamma(t)\|_\infty = \max_{j=0,\ldots,N-1} \max_{t\in[\frac{j}{N}, \frac{j+1}{N}]} \left\| \sum_{i=0}^{3} P_{j3+i} b_{i,3}(Nt-j) \right\|_\infty \\ &= \max_{j=0,\ldots,N-1} \max_{t\in[0,1]} \left\| \sum_{i=0}^{3} P_{j3+i} b_{i,3}(t) \right\|_\infty . \end{aligned}$$

Using Lemma 4.20, we get

$$\|\Gamma\|_{L_\infty} \geq \max_{j=0,\ldots,N-1} \frac{13}{96} \max_{i=0,\ldots,3} \|P_{j3+i}\|_\infty = \frac{13}{96} \|\Gamma\|_\infty^{B_{N,3}}.$$

□

Equivalence constants for the norms $\|\cdot\|_p^{B_{N,3}}$ and $\|\cdot\|_{L_p}$ on $B_{N,3}$

Combining the above propositions, we have the equivalence constants for the norm $\|\cdot\|_p^{B_{N,3}}$ and the norm $\|\cdot\|_{L_p}$ on the space $B_{N,3}$ of N-piece cubic Bézier curve as follows.

Theorem 4.1. Let $p \in [1, \infty[\cup \{\infty\}$. For any $\Gamma \in B_{N,3}$, we have

$$\|\Gamma\|_{L_p} \leq \|\Gamma\|_p^{B_{N,3}} \leq 2^{10} \, \|\Gamma\|_{L_p}.$$

Proof. Using Proposition 4.15, Proposition 4.17, Proposition 4.19 and Proposition 4.21, we have the proof of this theorem. □

The equivalence constants does not depend on the number of pieces in piecewise cubic Bézier curves. This theorem plays an important role in Algorithm 2 on page 86 in Chapter 5. From the above theorem, we get the following corollary:

$$d_{L_p}(\Gamma - \Delta) \leq d_p^{B_{N,3}}(\Gamma - \Delta) \leq 2^{10} \, d_{L_p}(\Gamma - \Delta)$$

for any $\Gamma, \Delta \in B_{N,3}$.

4.2.4 The equivalence between the norm $\|\cdot\|_p^{B_{N,D+1}}$ and the norm $\|\cdot\|_p^{B_{N,D}}$ on the space $B_{N,D}$

A Bézier curve of degree D can be considered as a Bézier curve of degree $D+1$. So the space B_D is a subspace of the space B_{D+1} and $\|\cdot\|_p^{B_{D+1}}$ is also a norm on the space B_D. More generally, the space $B_{N,D}$ is a subspace of the space $B_{N,D+1}$ and then $\|\cdot\|_p^{B_{N,D+1}}$ is also a norm on the space $B_{N,D}$. The purpose of this subsection is to study the equivalence constants for the norm $\|\cdot\|_p^{B_{N,D+1}}$ and the norm $\|\cdot\|_p^{B_{N,D}}$ on the space of N-piece Bézier curves of degree D.

For any Bézier curve of degree D,

$$\Gamma(t) = B([P_0, \ldots, P_D], t) = \sum_{i=0}^{D} P_i b_{i,D}(t), \quad t \in [0,1],$$

where $P_i \in \mathbb{R}^n$, $i = 0, \ldots, D$.

We can consider Γ as a Bézier curve of degree $D+1$ as follows

$$\Gamma(t) = B([Q_0, \ldots, Q_{D+1}], t) = \sum_{i=0}^{D+1} Q_i b_{i,D}(t), \quad t \in [0,1],$$

where $Q_i \in \mathbb{R}^n$, $i = 0, \ldots, D+1$, such that

$$Q_i = \begin{cases} P_0 & \text{if } i = 0, \\ \dfrac{i}{D+1} P_{i-1} + \dfrac{D+1-i}{D+1} P_i & \text{if } i = 1, \ldots, D, \\ P_D & \text{if } i = D+1. \end{cases} \tag{4.2}$$

It is clear that

$$\Gamma(t) = B([P_0, \ldots, P_D], t) = B([Q_0, \ldots, Q_{D+1}], t), \forall t \in [0,1].$$

Notation 4.22. For convenience, we denote $P_{-1} = P_{D+1} = O_{\mathbb{R}^n}$.

Then

$$Q_i = \frac{i}{D+1} P_{i-1} + \frac{D+1-i}{D+1} P_i, \quad \forall i = 0, \ldots, D+1.$$

Find a constant M such that $\|\cdot\|_p^{B_{N,D+1}} \leq M\|\cdot\|_p^{B_{N,D}}$ on $B_{N,D}$

Consider $p \in [1, \infty[$. First we estimate an upper bound for the norm $\|\cdot\|_p^{B_{D+1}}$ with respect to the norm $\|\cdot\|_p^{N,B_D}$ on the space B_D. Then we use this estimate to look for a constant M such that $\|\cdot\|_p^{B_{N,D+1}} \leq M\|\cdot\|_p^{B_{N,D}}$ on the space $B_{N,D}$.

Lemma 4.23. Let $p \in [1, \infty[$. Then for all $\Gamma \in B_D$, we have

$$\|\Gamma\|_p^{B_{D+1}} \leq 2\|\Gamma\|_p^{B_D}.$$

Proof. For any $\Gamma \in B_D$, we can assume that

$$\begin{aligned}\Gamma(t) =& B([P_0, \dots, P_D], t) = \sum_{i=0}^{D} P_i b_{i,D}(t), \quad t \in [0,1] \\ =& B([Q_0, \dots, Q_{D+1}], t) = \sum_{i=0}^{D+1} Q_i b_{i,D+1}(t), \quad t \in [0,1],\end{aligned}$$

where $P_i \in \mathbb{R}^n$, $i = 0, \dots, D$, and $Q_i \in \mathbb{R}^n$, $i = 0, \dots, D+1$, such that

$$Q_i = \begin{cases} P_0 & \text{if } i = 0, \\ \dfrac{i}{D+1} P_{i-1} + \dfrac{D+1-i}{D+1} P_i & \text{if } i = 1, \dots, D, \\ P_D & \text{if } i = D+1. \end{cases}$$

We then have

$$\|\Gamma\|_p^{B_{D+1}} = \left(\sum_{i=0}^{D+1} \|Q_i\|_p^p \right)^{1/p} = \left(\sum_{i=0}^{D+1} \left\| \frac{i}{D+1} P_{i-1} + \frac{D+1-i}{D+1} P_i \right\|_p^p \right)^{1/p}.$$

Using the Minkowski inequality, we get

$$\begin{aligned}\|\Gamma\|_p^{B_{D+1}} \leq& \left(\sum_{i=0}^{D+1} \left\| \frac{i}{D+1} P_{i-1} \right\|_p^p \right)^{1/p} + \left(\sum_{i=0}^{D+1} \left\| \frac{D+1-i}{D+1} P_i \right\|_p^p \right)^{1/p} \\ \leq& \left(\sum_{i=0}^{D} \|P_i\|_p^p \right)^{1/p} + \left(\sum_{i=0}^{D} \|P_i\|_p^p \right)^{1/p} = 2\|\Gamma\|_p^{B_D}.\end{aligned}$$

□

Proposition 4.24. Let $p \in [1, \infty[$. Then for all $\Gamma \in B_{N,D}$, we have

$$\|\Gamma\|_p^{B_{N,D+1}} \leq 2\|\Gamma\|_p^{B_{N,D}}.$$

Proof. Let $\Gamma \in B_{N,D}$ be an N-piece Bézier curve of degree D with control points $P_{jD+i} \in \mathbb{R}^n$, $i = 0, \ldots, D$, $j = 0, \ldots, N-1$. So

$$\Gamma(t) = \begin{cases} \Gamma^{(0)}(Nt) = \sum_{i=0}^{D} P_i b_{i,D}(Nt) & \text{if } t \in \left[0, \frac{1}{N}\right], \\ \Gamma^{(j)}(Nt-j) = \sum_{i=0}^{D} P_{jD+i} b_{i,D}(Nt-j) & \text{if } t \in \left[\frac{j}{N}, \frac{j+1}{N}\right], \\ & j = 1, \ldots, N-1. \end{cases}$$

Each piece $\Gamma^{(j)}$ can be considered as a Bézier curve of degree $D+1$. This means that Γ can be considered as an N-piece Bézier curve of degree $D+1$. Using Lemma 4.23, we have

$$\begin{aligned} \|\Gamma\|_p^{B_{N,D+1}} &= \frac{1}{N^{1/p}} \left(\sum_{j=0}^{N-1} \left(\|\Gamma^{(j)}\|_p^{B_{D+1}} \right)^p \right)^{1/p} \\ &\leq \frac{1}{N^{1/p}} \left(\sum_{j=0}^{N-1} \left(2\|\Gamma^{(j)}\|_p^{B_D} \right)^p \right)^{1/p} = 2\|\Gamma\|_p^{B_{N,D}}. \end{aligned}$$

□

Find a constant M such that $\|\cdot\|_\infty^{B_{N,D+1}} \leq M\|\cdot\|_\infty^{B_{N,D}}$ on $B_{N,D}$

Similarly, we look for the upper bound for the norm $\|\cdot\|_\infty^{B_{D+1}}$ with respect to the norm $\|\cdot\|_\infty^{B_D}$ on the space B_D and then we get a constant M such that $\|\cdot\|_\infty^{B_{N,D+1}} \leq M\|\cdot\|_\infty^{B_{N,D}}$ on the space $B_{N,D}$.

Lemma 4.25. For all $\Gamma \in B_D$, we have

$$\|\Gamma\|_\infty^{B_{D+1}} \leq 2\|\Gamma\|_\infty^{B_D}.$$

Proof. For any $\Gamma \in B_D$, we can assume that

$$\begin{aligned} \Gamma(t) &= B([P_0, \ldots, P_D], t) = \sum_{i=0}^{D} P_i b_{i,D}(t), \quad t \in [0,1] \\ &= B([Q_0, \ldots, Q_{D+1}], t) = \sum_{i=0}^{D+1} Q_i b_{i,D+1}(t), \quad t \in [0,1], \end{aligned}$$

where $P_i \in \mathbb{R}^n$, $i = 0, \ldots, D$, and $Q_i \in \mathbb{R}^n$, $i = 0, \ldots, D+1$, such that

$$Q_i = \begin{cases} P_0 & \text{if } i = 0, \\ \dfrac{i}{D+1} P_{i-1} + \dfrac{D+1-i}{D+1} P_i & \text{if } i = 1, \ldots, D, \\ P_D & \text{if } i = D+1. \end{cases}$$

We then have

$$\begin{aligned} \|\Gamma\|_\infty^{B_{D+1}} &= \max_{i=0,\ldots,D+1} \|Q_i\|_\infty = \max_{i=0,\ldots,D+1} \left\| \frac{i}{D+1} P_{i-1} + \frac{D+1-i}{D+1} P_i \right\|_\infty \\ &\leq \max_{i=0,\ldots,D+1} \left\| \frac{i}{D+1} P_{i-1} \right\|_\infty + \max_{i=0,\ldots,D+1} \left\| \frac{D+1-i}{D+1} P_i \right\|_\infty \\ &\leq 2 \max_{i=0,\ldots,D} \|P_i\|_\infty = 2\|\Gamma\|_\infty^{B_D}. \end{aligned}$$

□

Proposition 4.26. For all $\Gamma \in B_{N,D}$, we have

$$\|\Gamma\|_\infty^{B_{N,D+1}} \leq 2\|\Gamma\|_\infty^{B_{N,D}}.$$

Proof. Let $\Gamma \in B_{N,D}$ be an N-piece Bézier curve of degree D with control points $P_{jD+i} \in \mathbb{R}^n$, $i = 0, \ldots, D$, $j = 0, \ldots, N-1$. So

$$\Gamma(t) = \begin{cases} \Gamma^{(0)}(Nt) = \displaystyle\sum_{i=0}^{D} P_i b_{i,D}(Nt) & \text{if } t \in \left[0, \frac{1}{N}\right], \\ \Gamma^{(j)}(Nt-j) = \displaystyle\sum_{i=0}^{D} P_{jD+i} b_{i,D}(Nt-j) & \text{if } t \in \left[\frac{j}{N}, \frac{j+1}{N}\right], \\ & \qquad j = 1, \ldots, N-1. \end{cases}$$

Each piece $\Gamma^{(j)}$ can be considered as a Bézier curve of degree $D+1$. This means that Γ can be considered as an N-piece Bézier curve of degree $D+1$. We have

$$\|\Gamma\|_\infty^{B_{N,D+1}} = \max_{j=0,\ldots,N-1} \|\Gamma^{(j)}\|_\infty^{B_{D+1}}.$$

Using Lemma 4.25, we obtain

$$\|\Gamma\|_\infty^{B_{N,D+1}} \leq \max_{j=0,\ldots,N-1} 2\|\Gamma^{(j)}\|_\infty^{B_D} = 2\|\Gamma\|_\infty^{B_{N,D}}.$$

□

Find a constant m such that $m\|\cdot\|_p^{B_{N,D}} \leq \|\cdot\|_p^{B_{N,D+1}}$ on $B_{N,D}$

Consider $p \in [1, \infty[$. To evaluate a lower bound for the norm $\|\cdot\|_p^{B_{D+1}}$ with respect to the norm $\|\cdot\|_p^{B_D}$ on the space B_D, we need to consider the parity of the degree D. Then we look for a constant m such that $m\|\cdot\|_p^{B_{N,D}} \leq \|\cdot\|_p^{B_{N,D+1}}$ on the space $B_{N,D}$.

Lemma 4.27. Let $p \in [1, \infty[$. For any $\Gamma \in B_D$, we have

$$\frac{1}{2(D+1)}\|\Gamma\|_p^{B_D} \leq \|\Gamma\|_p^{B_{D+1}}.$$

Proof. For any $\Gamma \in B_D$, we can assume that

$$\begin{aligned}\Gamma(t) =& B([P_0, \ldots, P_D], t) = \sum_{i=0}^{D} P_i b_{i,D}(t), \quad t \in [0,1] \\ =& B([Q_0, \ldots, Q_{D+1}], t) = \sum_{i=0}^{D+1} Q_i b_{i,D+1}(t), \quad t \in [0,1],\end{aligned}$$

where $P_i \in \mathbb{R}^n$, $i = 0, \ldots, D$, and $Q_i \in \mathbb{R}^n$, $i = 0, \ldots, D+1$, such that

$$Q_i = \begin{cases} P_0 & \text{if } i = 0, \\ \dfrac{i}{D+1}P_{i-1} + \dfrac{D+1-i}{D+1}P_i & \text{if } i = 1, \ldots, D, \\ P_D & \text{if } i = D+1. \end{cases}$$

We consider 2 cases.

- Case 1: D is an odd number. We have

$$\|\Gamma\|_p^{B_{D+1}} = \left(\sum_{i=0}^{D+1} \|Q_i\|_p^p\right)^{1/p} \geq \left(\sum_{i=0}^{(D+1)/2} \left\|\frac{i}{D+1}P_{i-1} + \frac{D+1-i}{D+1}P_i\right\|_p^p\right)^{1/p}.$$

Using the Minkowski inequality, we obtain

$$\begin{aligned}\|\Gamma\|_p^{B_{D+1}} \geq & \left(\sum_{i=0}^{(D+1)/2} \left\| \frac{D+1-i}{D+1} P_i \right\|_p^p \right)^{1/p} - \left(\sum_{i=0}^{(D+1)/2} \left\| \frac{i}{D+1} P_{i-1} \right\|_p^p \right)^{1/p} \\ \geq & \left(\sum_{i=0}^{\frac{D+1}{2}-1} \frac{D+1-i}{D+1} \|P_i\|_p^p \right)^{1/p} - \left(\sum_{i=0}^{\frac{D+1}{2}-1} \frac{i+1}{D+1} \|P_i\|_p^p \right)^{1/p} \\ \geq & \left(\sum_{i=0}^{\frac{D+1}{2}-1} \frac{D+3}{2(D+1)} \|P_i\|_p^p \right)^{1/p} - \left(\sum_{i=0}^{\frac{D+1}{2}-1} \frac{D+1}{2(D+1)} \|P_i\|_p^p \right)^{1/p} \\ \geq & \frac{1}{D+1} \left(\sum_{i=0}^{\frac{D+1}{2}-1} \|P_i\|_p^p \right)^{1/p}.\end{aligned}$$

Furthermore, we have

$$\|\Gamma\|_p^{B_{D+1}} = \left(\sum_{i=0}^{D+1} \|Q_i\|_p^p \right)^{1/p} \geq \left(\sum_{i=\frac{D+1}{2}+1}^{D+1} \left\| \frac{i}{D+1} P_{i-1} + \frac{D+1-i}{D+1} P_i \right\|_p^p \right)^{1/p}.$$

Using the Minkowski inequality, we obtain

$$\begin{aligned}\|\Gamma\|_p^{B_{D+1}} \geq & \left(\sum_{i=\frac{D+1}{2}+1}^{D+1} \left\| \frac{i}{D+1} P_{i-1} \right\|_p^p \right)^{1/p} - \left(\sum_{i=\frac{D+1}{2}+1}^{D+1} \left\| \frac{D+1-i}{D+1} P_i \right\|_p^p \right)^{1/p} \\ \geq & \left(\sum_{i=\frac{D+1}{2}}^{D} \frac{i+1}{D+1} \|P_i\|_p^p \right)^{1/p} - \left(\sum_{i=\frac{D+1}{2}}^{D} \frac{D+1-i}{D+1} \|P_i\|_p^p \right)^{1/p} \\ \geq & \left(\sum_{i=\frac{D+1}{2}}^{D} \frac{D+3}{2(D+1)} \|P_i\|_p^p \right)^{1/p} - \left(\sum_{i=\frac{D+1}{2}}^{D} \frac{D+1}{2(D+1)} \|P_i\|_p^p \right)^{1/p} \\ = & \frac{1}{D+1} \left(\sum_{i=\frac{D+1}{2}}^{D} \|P_i\|_p^p \right)^{1/p}.\end{aligned}$$

Then

$$\begin{aligned}2\|\Gamma\|_p^{B_{D+1}} \geq & \frac{1}{D+1} \left(\sum_{i=0}^{\frac{D+1}{2}-1} \|P_i\|_p^p \right)^{1/p} + \frac{1}{D+1} \left(\sum_{i=\frac{D+1}{2}}^{D} \|P_i\|_p^p \right)^{1/p} \\ \geq & \frac{1}{D+1} \left(\sum_{i=0}^{D} \|P_i\|_p^p \right)^{1/p} = \frac{1}{D+1} \Gamma\|_p^{B_D}.\end{aligned}$$

- Case 2: D is an even number. We have

$$\|\Gamma\|_p^{B_{D+1}} = \left(\sum_{i=0}^{D+1}\|Q_i\|_p^p\right)^{1/p} \geq \left(\sum_{i=0}^{D/2}\left\|\frac{i}{D+1}P_{i-1} + \frac{D+1-i}{D+1}P_i\right\|_p^p\right)^{1/p}.$$

Using the Minkowski inequality, we obtain

$$\begin{aligned}
\|\Gamma\|_p^{B_{D+1}} \geq & \left(\sum_{i=0}^{D/2}\left\|\frac{D+1-i}{D+1}P_i\right\|_p^p\right)^{1/p} - \left(\sum_{i=0}^{D/2}\left\|\frac{i}{D+1}P_{i-1}\right\|_p^p\right)^{1/p} \\
= & \left(\sum_{i=0}^{D/2}\frac{D+2}{2(D+1)}\|P_i\|_p^p\right)^{1/p} - \left(\sum_{i=0}^{\frac{D}{2}-1}\frac{D}{2(D+1)}\|P_i\|_p^p\right)^{1/p} \\
\geq & \left(\sum_{i=0}^{D/2}\frac{D+2}{2(D+1)}\|P_i\|_p^p\right)^{1/p} - \left(\sum_{i=0}^{D/2}\frac{D}{2(D+1)}\|P_i\|_p^p\right)^{1/p} \\
= & \frac{1}{D+1}\left(\sum_{i=0}^{D/2}\|P_i\|_p^p\right)^{1/p}.
\end{aligned}$$

Furthermore, we have

$$\|\Gamma\|_p^{B_{D+1}} = \left(\sum_{i=0}^{D+1}\|Q_i\|_p^p\right)^{1/p} \geq \left(\sum_{i=\frac{D}{2}+1}^{D+1}\left\|\frac{i}{D+1}P_{i-1} + \frac{D+1-i}{D+1}P_i\right\|_p^p\right)^{1/p}.$$

Using the Minkowski inequality, we obtain

$$\begin{aligned}
\|\Gamma\|_p^{B_{D+1}} \geq & \left(\sum_{i=\frac{D}{2}+1}^{D+1}\left\|\frac{i}{D+1}P_{i-1}\right\|_p^p\right)^{1/p} - \left(\sum_{i=\frac{D}{2}+1}^{D+1}\left\|\frac{D+1-i}{D+1}P_i\right\|_p^p\right)^{1/p} \\
\geq & \left(\sum_{i=D/2}^{D}\frac{D+2}{2(D+1)}\|P_i\|_p^p\right)^{1/p} - \left(\sum_{i=\frac{D}{2}+1}^{D}\frac{D}{2(D+1)}\|P_i\|_p^p\right)^{1/p} \\
\geq & \left(\sum_{i=\frac{D}{2}+1}^{D}\frac{D+2}{2(D+1)}\|P_i\|_p^p\right)^{1/p} - \left(\sum_{i=\frac{D}{2}+1}^{D}\frac{D}{2(D+1)}\|P_i\|_p^p\right)^{1/p} \\
= & \frac{1}{D+1}\left(\sum_{i=\frac{D}{2}+1}^{D}\|P_i\|_p^p\right)^{1/p}.
\end{aligned}$$

Then

$$2\|\Gamma\|_p^{B_{D+1}} \geq \frac{1}{D+1}\Big(\sum_{i=0}^{D/2}\|P_i\|_p^p\Big)^{1/p} + \frac{1}{D+1}\Big(\sum_{i=\frac{D}{2}+1}^{D}\|P_i\|_p^p\Big)^{1/p}$$
$$\geq \frac{1}{D+1}\Big(\sum_{i=0}^{D}\|P_i\|_p^p\Big)^{1/p} = \frac{1}{D+1}\Gamma\|_p^{B_D}.$$

From the above two cases, we get

$$\|\Gamma\|_1^{B_{D+1}} \geq \frac{1}{2(D+1)}\|\Gamma\|_1^{B_D}.$$

□

Next, we consider on the space $B_{N,D}$ of N-piece Bézier curve of degree D.

Proposition 4.28. Let $p \in [1, \infty[$. Then for all $\Gamma \in B_{N,D}$, we have

$$\frac{1}{2(D+1)}\|\Gamma\|_p^{B_{N,D}} \leq \|\Gamma\|_p^{B_{N,D+1}}.$$

Proof. Let $\Gamma \in B_{N,D}$ be an N-piece Bézier curve of degree D with control points $P_{jD+i} \in \mathbb{R}^n$, $i = 0, \ldots, D$, $j = 0, \ldots, N-1$. So

$$\Gamma(t) = \begin{cases} \Gamma^{(0)}(Nt) = \sum_{i=0}^{D} P_i b_{i,D}(Nt) & \text{if } t \in \Big[0, \frac{1}{N}\Big], \\ \Gamma^{(j)}(Nt-j) = \sum_{i=0}^{D} P_{jD+i} b_{i,D}(Nt-j) & \text{if } t \in \Big[\frac{j}{N}, \frac{j+1}{N}\Big], \\ & \quad j = 1, \ldots, N-1. \end{cases}$$

Each piece $\Gamma^{(j)}$ can be considered as a Bézier curve of degree $D+1$. This means that Γ can be considered as an N-piece Bézier curve of degree $D+1$. We have

$$\|\Gamma\|_p^{B_{N,D+1}} = \frac{1}{N^{1/p}}\Big(\sum_{j=0}^{N-1}\Big(\|\Gamma^{(j)}\|_p^{B_{D+1}}\Big)^p\Big)^{1/p}.$$

Using Lemma 4.27, we obtain

$$\|\Gamma\|_p^{B_{N,D+1}} \geq \frac{1}{N^{1/p}}\Big(\sum_{j=0}^{N-1}\Big(\frac{1}{2(D+1)}\|\Gamma^{(j)}\|_p^{B_D}\Big)^p\Big)^{1/p} = \frac{1}{2(D+1)}\|\Gamma\|_p^{B_{N,D}}.$$

□

Find a constant m such that $m\|\cdot\|_\infty^{B_{N,D}} \leq \|\cdot\|_\infty^{B_{N,D+1}}$ on $B_{N,D}$

Using the relation between control points, we determine a lower bound for the norm $\|\cdot\|_\infty^{B_{D+1}}$ with respect to the norm $\|\cdot\|_\infty^{B_D}$ on the space B_D. We then have a constant m such that $m\|\cdot\|_\infty^{B_{N,D}} \leq \|\cdot\|_\infty^{B_{N,D+1}}$ on the space $B_{N,D}$.

Lemma 4.29. For any $\Gamma \in B_D$, we have

$$\frac{1}{D+1}\|\Gamma\|_\infty^{B_D} \leq \|\Gamma\|_\infty^{B_{D+1}}.$$

Proof. For any $\Gamma \in B_D$, we can assume that

$$\begin{aligned}\Gamma(t) =& B([P_0,\dots,P_D],t) = \sum_{i=0}^{D} P_i b_{i,D}(t), \quad t\in[0,1]\\ =& B([Q_0,\dots,Q_{D+1}],t) = \sum_{i=0}^{D+1} Q_i b_{i,D+1}(t), \quad t\in[0,1],\end{aligned}$$

where $P_i \in \mathbb{R}^n$, $i = 0,\dots,D$, and $Q_i \in \mathbb{R}^n$, $i = 0,\dots,D+1$, such that

$$Q_i = \begin{cases} P_0 & \text{if } i = 0,\\ \dfrac{i}{D+1}P_{i-1} + \dfrac{D+1-i}{D+1}P_i & \text{if } i = 1,\dots,D,\\ P_D & \text{if } i = D+1.\end{cases}$$

We assume that $\|\Gamma\|_\infty^{B_D} = \|P_{i_0}\|_\infty$, where $i_0 \in \{0,\dots,D\}$.

- Case $0 \leq i_0 < \dfrac{D+1}{2}$. We have

$$\begin{aligned}\|\Gamma\|_\infty^{B_{D+1}} =& \max_{i=0,\dots,D+1}\{\|Q_i\|_\infty\} \geq \left\|\frac{i_0}{D+1}P_{i_0-1} + \frac{D+1-i_0}{D+1}P_{i_0}\right\|_\infty\\ \geq& \frac{D+1-i}{D+1}\|P_{i_0}\|_\infty - \frac{i_0}{D+1}\|P_{i_0-1}\|_\infty\\ =& \frac{D+1-2i_0}{D+1}\|P_{i_0}\|_\infty \geq \frac{1}{D+1}\|P_{i_0}\|_\infty = \frac{1}{D+1}\|\Gamma\|_\infty^{B_D}.\end{aligned}$$

- Case $i_0 = \dfrac{D+1}{2}$. (This case happens only if D is an even number.) We have

$$\begin{aligned}\|\Gamma\|_\infty^{B_{D+1}} &= \max_{i=0,\dots,D+1}\{\|Q_i\|_\infty\} \geq \left\|\frac{i_0+1}{D+1}P_{i_0} + \frac{D+1-(i_0+1)}{D+1}P_{i_0+1}\right\|_\infty \\ &\geq \frac{i_0+1}{D+1}\|P_{i_0}\|_\infty - \frac{D-i_0}{D+1}\|P_{i_0+1}\|_\infty \\ &= \frac{2i_0+1-D}{D+1}\|P_{i_0}\|_\infty \geq \frac{1}{D+1}\|P_{i_0}\|_\infty = \frac{1}{D+1}\|\Gamma\|_\infty^{B_D}.\end{aligned}$$

- Case $i_0 > \dfrac{D+1}{2}$. We have

$$\begin{aligned}\|\Gamma\|_\infty^{B_{D+1}} &= \max_{i=0,\dots,D+1}\{\|Q_i\|_\infty\} \geq \left\|\frac{i_0+1}{D+1}P_{i_0} + \frac{D+1-(i_0+1)}{D+1}P_{i_0+1}\right\|_\infty \\ &\geq \frac{i_0+1}{D+1}\|P_{i_0}\|_\infty - \frac{D-i_0}{D+1}\|P_{i_0+1}\|_\infty \\ &= \frac{2i_0+1-D}{D+1}\|P_{i_0}\|_\infty \geq \frac{1}{D+1}\|P_{i_0}\|_\infty = \frac{1}{D+1}\|\Gamma\|_\infty^{B_D}.\end{aligned}$$

From the above three cases, we get

$$\|\Gamma\|_\infty^{B_{D+1}} \geq \frac{1}{D+1}\|\Gamma\|_\infty^{B_D}.$$

□

Applying the above lemma to each piece of the N-piece Bézier curve of degree D, we have the following result.

Proposition 4.30. For all $\Gamma \in B_{N,D}$, we have

$$\frac{1}{D+1}\|\Gamma\|_\infty^{B_{N,D}} \leq \|\Gamma\|_\infty^{B_{N,D+1}}.$$

Proof. Let $\Gamma \in B_{N,D}$ be an N-piece Bézier curve of degree D with control points $P_{jD+i} \in \mathbb{R}^n$, $i = 0, \dots, D$, $j = 0, \dots, N-1$. So

$$\Gamma(t) = \begin{cases} \Gamma^{(0)}(Nt) = \displaystyle\sum_{i=0}^{D} P_i b_{i,D}(Nt) & \text{if } t \in \left[0, \frac{1}{N}\right], \\ \Gamma^{(j)}(Nt-j) = \displaystyle\sum_{i=0}^{D} P_{jD+i} b_{i,D}(Nt-j) & \text{if } t \in \left[\frac{j}{N}, \frac{j+1}{N}\right], \\ & \qquad j = 1, \dots, N-1. \end{cases}$$

Each piece $\Gamma^{(j)}$ can be considered as a Bézier curve of degree $D+1$. This means

that Γ can be considered as an N-piece Bézier curve of degree $D+1$. We have

$$\|\Gamma\|_{\infty}^{B_{N,D+1}} = \max_{j=0,\ldots,N-1} \|\Gamma^{(j)}\|_{\infty}^{B_{D+1}}.$$

Using Lemma 4.29, we get

$$\|\Gamma\|_{\infty}^{B_{N,D+1}} \geq \max_{j=0,\ldots,N-1} \frac{1}{D+1}\|\Gamma^{(j)}\|_{\infty}^{B_D} = \frac{1}{D+1}\|\Gamma\|_{\infty}^{B_{N,D}}.$$

□

Equivalence constants for the norms $\|\cdot\|_p^{B_{N,D+1}}$ and $\|\cdot\|_p^{B_{N,D}}$ on $B_{N,D}$

Combining the above propositions, we have the following theorem about the equivalence constants for the norm $\|\cdot\|_p^{B_{N,D+1}}$ and the norm $\|\cdot\|_p^{B_{N,D}}$ on the space $B_{N,D}$.

Theorem 4.2. Let $p \in [1,\infty[\cup\{\infty\}$. For all $\Gamma \in B_{N,D}$, we have

$$\frac{1}{2(D+1)}\|\Gamma\|_p^{B_{N,D}} \leq \|\Gamma\|_p^{B_{N,D+1}} \leq 2\|\Gamma\|_p^{B_{N,D}}.$$

Proof. Using Proposition 4.24, Proposition 4.28, Proposition 4.26 and Proposition 4.30, we have the proof of this theorem. □

From the above theorem, we obtain the corollary as follows

$$\frac{1}{2(D+1)} d_p^{B_{N,D}}(\Gamma,\Delta) \leq d_p^{B_{N,D+1}}(\Gamma,\Delta) \leq 2d_p^{B_{N,D}}(\Gamma,\Delta),$$

for any $\Gamma, \Delta \in B_{N,D}$.

4.2.5 Splitting N-piece cubic Bézier curves

When the curve object is complicated, we need more control points in order to give additional freedom for curve design. To solve this problem without increasing the degree of curves, we split N-piece cubic Bézier curves. Splitting N-piece cubic Bézier curves plays an important role in Algorithm 2 on page 86 in Chapter 5 using piecewise cubic Bézier curve. The current subsection is devoted to presenting how to split an N-piece cubic Bézier curve to become a $2N$-piece cubic Bézier curve. This means that an N-piece cubic Bézier curve can be considered as a $2N$-piece cubic Bézier curve and the norm $\|\cdot\|_p^{B_{2N,3}}$ is also a norm on the space $B_{N,3}$. We

then study the equivalence constants for the norm $\|\cdot\|_p^{B_{2N,3}}$ and the norm $\|\cdot\|_p^{B_{N,3}}$ on the space $B_{N,3}$.

Splitting N-piece cubic Bézier curves

The purpose of this paragraph is to rewrite an N-piece cubic Bézier curve as a new piecewise cubic Bézier curve such that the number of pieces in the new piecewise cubic Bézier curve is greater than N. We will see that when we split every piece of an N-piece cubic Bézier curve at the middle point of the piece, we get a $2N$-piece cubic Bézier curve.

Let $\Gamma \in B_3$ be a cubic Bézier curve with control points $P_i \in \mathbb{R}^n$, $i = 0, \ldots, 3$. So

$$\Gamma(t) = \sum_{i=0}^{3} P_i b_{i,3}(t), \quad t \in [0,1].$$

By ([26, chapter 9, p. 201]), we can split Γ at any $t_0 \in (0,1)$. When we split Γ at $t_0 \neq \frac{1}{2}$, we get 2 cubic Bézier curves but the point $\Gamma\Big(\frac{1}{2}\Big)$ is not the connecting point of the pieces. In order to get a uniform 2-piece cubic Bézier curve, we split Γ at $t = \frac{1}{2}$ and obtain a uniform two-piece cubic Bézier curve as follows

$$\Gamma(t) = \begin{cases} \Gamma^{(0)}(2t) = \sum\limits_{i=0}^{3} Q_i b_{i,3}(2t) & \text{if } t \in \Big[0, \frac{1}{2}\Big] \\ \Gamma^{(1)}(2t-1) = \sum\limits_{i=0}^{3} Q_{3+i} b_{i,3}(2t-1) & \text{if } t \in \Big[\frac{1}{2}, 1\Big], \end{cases} \tag{4.3}$$

where

$$\begin{cases} Q_i = \sum\limits_{l=0}^{i} b_{l,i}\Big(\frac{1}{2}\Big) P_{i-l}, & i = 0, \ldots, 3, \\ Q_{3+i} = \sum\limits_{l=0}^{i} b_{l,i}\Big(\frac{1}{2}\Big) P_{3-i+l}, & i = 0, \ldots, 3. \end{cases}$$

Then a cubic Bézier curve can be considered as a uniform two-piece cubic Bézier curve.

More generally, let $\Gamma \in B_{N,3}$ be an N-piece cubic Bézier curve with control points $P_{j3+i} \in \mathbb{R}^n$, $j = 0, \ldots, N-1$, $i = 0, \ldots, 3$. So

$$\Gamma(t) = \begin{cases} \Gamma^{(0)}(Nt) = \sum\limits_{i=0}^{3} P_i b_{i,3}(Nt) & \text{if } t \in \Big[0, \frac{1}{N}\Big], \\ \Gamma^{(j)}(Nt-j) = \sum\limits_{i=0}^{3} P_{j3+i} b_{i,3}(Nt-j) & \text{if } t \in \Big[\frac{j}{N}, \frac{j+1}{N}\Big], \\ & \qquad j = 1, \ldots, N-1. \end{cases} \tag{4.4}$$

If we just split a piece of Γ, we get $N+1$ pieces but some points at $t = \frac{j}{N+1}$, $j = 1, \ldots, N$, are not the connecting points of the pieces. Then we split every piece of Γ at the middle point of the piece and obtain a uniform $2N$-piece cubic Bézier curve as follows

$$\Gamma(t) = \begin{cases} \Delta^{(2j)}(2Nt-2j) = \sum\limits_{i=0}^{3} Q_{2j3+i} b_{i,3}(2Nt-2j) & \text{if } t \in \left[\frac{2j}{2N}, \frac{2j+1}{2N}\right] \\ \Delta^{(2j+1)}(2Nt-2j-1) = \sum\limits_{i=0}^{3} Q_{(2j+1)3+i} b_{i,3}(2Nt-2j-1) & \text{if } t \in \left[\frac{2j+1}{2N}, \frac{2j+2}{2N}\right], \\ & j = 0, \ldots, N-1, \end{cases} \tag{4.5}$$

where

$$\begin{cases} Q_{2j3+i} = \sum\limits_{l=0}^{i} b_{l,i}\Big(\frac{1}{2}\Big) P_{j3+i-l}, & i = 0, \ldots, 3, j = 0, \ldots, N-1, \\ Q_{(2j+1)3+i} = \sum\limits_{l=0}^{i} b_{l,i}\Big(\frac{1}{2}\Big) P_{j3+3-i+l}, & i = 0, \ldots, 3, j = 0, \ldots, N-1. \end{cases} \tag{4.6}$$

So, Γ can be considered as a $2N$-piece cubic Bézier curve. This means that the space $B_{N,3}$ is a subspace of the space $B_{2N,3}$ and the space $B_{N,3}$ inherits the norm $\|\cdot\|_p^{B_{2N,3}}$. We next study the equivalence constants for the norm $\|\cdot\|_p^{B_{N,3}}$ and the norm $\|\cdot\|_p^{B_{2N,3}}$ on the space $B_{N,3}$.

Find a constant M such that $\|\cdot\|_p^{B_{2N,3}} \leq M \|\cdot\|_p^{B_{N,3}}$ on $B_{N,3}$

We first estimate M in two cases $p \in [1, \infty[$ and $p = \infty$. We then combine the results of the two cases.

Lemma 4.31. Let $p \in [1, \infty[$. For any $\Gamma \in B_{N,3}$, we have

$$\|\Gamma\|_p^{B_{2N,3}} \leq 3^{1/p} \, \|\Gamma\|_p^{B_{N,3}}.$$

Proof. Let $\Gamma \in B_{N,3}$ be an N-piece cubic Bézier curve with control points $P_{j3+i} \in \mathbb{R}^n$, $i = 0, \ldots, 3$, $j = 0, \ldots, N-1$. So

$$\Gamma(t) = \begin{cases} \Gamma^{(0)}(Nt) = \sum\limits_{i=0}^{3} P_i b_{i,3}(Nt) & \text{if } \ t \in \Big[0, \frac{1}{N}\Big], \\ \Gamma^{(j)}(Nt-j) = \sum\limits_{i=0}^{3} P_{j3+i} b_{i,3}(Nt-j) & \text{if } \ t \in \Big[\frac{j}{N}, \frac{j+1}{N}\Big], \\ & j = 0, \ldots, N-1. \end{cases}$$

From (4.5), Γ can be considered as a $2N$-piece cubic Bézier curve as follows

$$\Gamma(t) = \begin{cases} \Delta^{(2j)}(2Nt-2j) = \sum\limits_{i=0}^{3} Q_{2j3+i} b_{i,3}(2Nt-2j) & \text{if } t \in \left[\frac{2j}{2N}, \frac{2j+1}{2N}\right] \\ \Delta^{(2j+1)}(2Nt-2j-1) = \sum\limits_{i=0}^{3} Q_{(2j+1)3+i} b_{i,3}(2Nt-2j-1) & \text{if } t \in \left[\frac{2j+1}{2N}, \frac{2j+2}{2N}\right], \\ & j = 0, \dots, N-1, \end{cases}$$

where

$$\begin{cases} Q_{2j3+i} = \sum\limits_{l=0}^{i} b_{l,i}\Big(\frac{1}{2}\Big) P_{j3+i-l}, & i = 0, \dots, 3, j = 0, \dots, N-1, \\ Q_{(2j+1)3+i} = \sum\limits_{l=0}^{i} b_{l,i}\Big(\frac{1}{2}\Big) P_{j3+3-i+l}, & i = 0, \dots, 3, j = 0, \dots, N-1. \end{cases}$$

Since

$$\begin{aligned} \Big(\|\Delta^{(2j)}\|_p^{B_3}\Big)^p &= \sum_{i=0}^{3} \Big\| \sum_{l=0}^{i} b_{l,i}\Big(\frac{1}{2}\Big) P_{j3+i-l} \Big\|_p^p \\ &\le 3 \max_{i=0,\dots,3} \|P_{j3+i}\|_p^p \le 3 \sum_{i=0}^{3} \|P_{j3+i}\|_p^p = 3\Big(\|\Gamma^{(j)}\|_p^{B_3}\Big)^p, \\ &\qquad \forall j = 0, \dots, N-1, \end{aligned}$$

and similarly

$$\Big(\|\Delta^{(2j+1)}\|_p^{B_3}\Big)^p = \sum_{i=0}^{3} \Big\| \sum_{l=0}^{i} b_{l,i}\Big(\frac{1}{2}\Big) P_{j_0 3+3-i+l} \Big\|_p^p \le 3\Big(\|\Gamma^{(j)}\|_p^{B_3}\Big)^p, \forall j = 0, \dots, N-1,$$

we get

$$\begin{aligned} \|\Gamma\|_p^{B_{2N,3}} &= \frac{1}{(2N)^{1/p}} \Bigg(\sum_{j=0}^{N} \Big(\|\Delta^{(2j)}\|_p^{B_3}\Big)^p + \Big(\|\Delta^{(2j+1)}\|_p^{B_3}\Big)^p \Bigg)^{1/p} \\ &\le \frac{1}{(2N)^{1/p}} \Bigg(\sum_{j=0}^{N} 6\Big(\|\Gamma^{(j)}\|_p^{B_3}\Big)^p \Bigg)^{1/p} \le 3^{1/p} \, \|\Gamma\|_p^{B_{N,3}}. \end{aligned}$$

□

Lemma 4.32. For any $\Gamma \in B_{N,3}$, we have

$$\|\Gamma\|_\infty^{B_{2N,3}} \le \|\Gamma\|_\infty^{B_{N,3}}.$$

Proof. Let $\Gamma \in B_{N,3}$ be an N-piece cubic Bézier curve with control points $P_{j3+i} \in \mathbb{R}^n$, $i = 0, \ldots, 3$, $j = 0, \ldots, N-1$. So

$$\Gamma(t) = \begin{cases} \Gamma^{(0)}(Nt) = \sum\limits_{i=0}^{3} P_i b_{i,3}(Nt) & \text{if } t \in \Big[0, \dfrac{1}{N}\Big], \\ \Gamma^{(j)}(Nt-j) = \sum\limits_{i=0}^{3} P_{j3+i} b_{i,3}(Nt-j) & \text{if } t \in \Big[\dfrac{j}{N}, \dfrac{j+1}{N}\Big], \\ & j = 0, \ldots, N-1. \end{cases}$$

From (4.5), Γ can be considered as a $2N$-piece cubic Bézier curve as follows

$$\Gamma(t) = \begin{cases} \Delta^{(2j)}(2Nt-2j) = \sum\limits_{i=0}^{3} Q_{2j3+i} b_{i,3}(2Nt-2j) & \text{if } t \in \Big[\frac{2j}{2N}, \frac{2j+1}{2N}\Big] \\ \Delta^{(2j+1)}(2Nt-2j-1) = \sum\limits_{i=0}^{3} Q_{(2j+1)3+i} b_{i,3}(2Nt-2j-1) & \text{if } t \in \Big[\frac{2j+1}{2N}, \frac{2j+2}{2N}\Big], \\ & j = 0, \ldots, N-1, \end{cases}$$

where

$$\begin{cases} Q_{2j3+i} = \sum\limits_{l=0}^{i} b_{l,i}\Big(\dfrac{1}{2}\Big) P_{j3+i-l}, & i = 0, \ldots, 3, j = 0, \ldots, N-1, \\ Q_{(2j+1)3+i} = \sum\limits_{l=0}^{i} b_{l,i}\Big(\dfrac{1}{2}\Big) P_{j3+3-i+l}, & i = 0, \ldots, 3, j = 0, \ldots, N-1. \end{cases}$$

Since

$$\|\Delta^{(2j)}\|_\infty^{B_3} = \max_{i=0,\ldots,3} \Big\| \sum_{l=0}^{i} b_{l,i}\Big(\frac{1}{2}\Big) P_{j3+i-l} \Big\|_\infty \le \max_{i=0,\ldots,3} \|P_{j3+i}\|_\infty = \|\Gamma^{(j)}\|_\infty^{B_3}, \quad \forall j = 0, \ldots, N-1,$$

and similarly

$$\|\Delta^{(2j+1)}\|_\infty^{B_3} = \max_{i=0,\ldots,3} \Big\| \sum_{l=0}^{i} b_{l,i}\Big(\frac{1}{2}\Big) P_{j3+i-l} \Big\|_\infty \le \|\Gamma^{(j)}\|_\infty^{B_3}, \ \ \forall j = 0, \ldots, N-1,$$

we get

$$\begin{aligned} \|\Gamma\|_\infty^{B_{2N,D}} &= \max_{j=0,\ldots,N-1} \max\Big\{ \|\Delta^{(2j)}\|_\infty^{B_D}, \|\Delta^{(2j+1)}\|_\infty^{B_D} \Big\} \\ &\le \max_{j=0,\ldots,N-1} \|\Gamma^{(j)}\|_\infty^{B_D} = \|\Gamma\|_\infty^{B_{N,D}}. \end{aligned}$$

□

From the above two lemmas, we have the following proposition.

Proposition 4.33. Let $p \in [1, \infty[\cup \{\infty\}$. For any $\Gamma \in B_{N,3}$, we have

$$\|\Gamma\|_p^{B_{2N,3}} \leq 3^{1/p} \, \|\Gamma\|_p^{B_{N,3}}.$$

Proof. Using Lemma 4.31 and Lemma 4.32, we get the proof of this proposition. □

Find a constant m such that $m\|\cdot\|_p^{B_{2N,3}} \leq \|\cdot\|_p^{B_{N,3}}$ on $B_{N,3}$

We also consider two cases $p \in [1, \infty[$ and $p = \infty$. Combining the results of the two cases, we get a constant m such that $m\|\cdot\|_p^{B_{2N,3}} \leq \|\cdot\|_p^{B_{N,3}}$ on the space $B_{N,3}$.

Lemma 4.34. Let $p \in [1, \infty[$. For any $\Gamma \in B_{N,3}$, we have

$$\frac{1}{24^{1/p}} \, \|\Gamma\|_p^{B_{N,3}} \leq \|\Gamma\|_p^{B_{2N,3}}.$$

Proof. Let $\Gamma \in B_{N,3}$ be an N-piece cubic Bézier curve with control points $P_{j3+i} \in \mathbb{R}^n$, $i = 0, \ldots, 3$, $j = 0, \ldots, N-1$. So

$$\Gamma(t) = \begin{cases} \Gamma^{(0)}(Nt) = \sum\limits_{i=0}^{3} P_i b_{i,3}(Nt) & \text{if } t \in \left[0, \frac{1}{N}\right], \\ \Gamma^{(j)}(Nt-j) = \sum\limits_{i=0}^{3} P_{j3+i} b_{i,3}(Nt-j) & \text{if } t \in \left[\frac{j}{N}, \frac{j+1}{N}\right], \\ & j = 0, \ldots, N-1. \end{cases}$$

From (4.5), Γ can be considered as a $2N$-piece cubic Bézier curve as follows

$$\Gamma(t) = \begin{cases} \Delta^{(2j)}(2Nt-2j) = \sum\limits_{i=0}^{3} Q_{2j3+i} b_{i,3}(2Nt-2j) & \text{if } t \in \left[\frac{2j}{2N}, \frac{2j+1}{2N}\right] \\ \Delta^{(2j+1)}(2Nt-2j-1) = \sum\limits_{i=0}^{3} Q_{(2j+1)3+i} b_{i,3}(2Nt-2j-1) & \text{if } t \in \left[\frac{2j+1}{2N}, \frac{2j+2}{2N}\right], \\ & j = 0, \ldots, N-1, \end{cases}$$

where

$$\begin{cases} Q_{2j3+i} = \sum\limits_{l=0}^{i} b_{l,i}\left(\frac{1}{2}\right) P_{j3+i-l}, & i = 0, \ldots, 3, j = 0, \ldots, N-1, \\ Q_{(2j+1)3+i} = \sum\limits_{l=0}^{i} b_{l,i}\left(\frac{1}{2}\right) P_{j3+3-i+l}, & i = 0, \ldots, 3, j = 0, \ldots, N-1. \end{cases}$$

We first consider $\left(\|\Delta^{(2j)}\|_p^{B_3}\right)^p + \left(\|\Delta^{(2j+1)}\|_p^{B_3}\right)^p$, $j = 0, \ldots, N-1$.

- Case 1: $\|P_{j3}\|_p = \max\Big\{\|P_{j3}\|_p, \frac{1}{2}\|P_{j3+1}\|_p, \frac{1}{2}\|P_{j3+2}\|_p, \|P_{j3+3}\|_p\Big\}$.
  We have

$$\Big(\|\Delta^{(2j)}\|_p^{B_3}\Big)^p + \Big(\|\Delta^{(2j+1)}\|_p^{B_3}\Big)^p \geq \Big(\|\Delta^{(2j)}\|_p^{B_3}\Big)^p \geq \|Q_{j3}\|_p^p = \|P_{j3}\|_p^p \geq \frac{1}{6}\sum_{i=3}^{3}\|P_{j3+i}\|_p^p = \frac{1}{6}\Big(\|\Gamma^{(j)}\|_p^{B_3}\Big)^p.$$

- Case 2: $\frac{1}{2}\|P_{j3+1}\|_p = \max\Big\{\|P_{j3}\|_p, \frac{1}{2}\|P_{j3+1}\|_p, \frac{1}{2}\|P_{j3+2}\|_p, \|P_{j3+3}\|_p\Big\}$.
  We have

$$\Big(\|\Delta^{(2j)}\|_p^{B_3}\Big)^p + \Big(\|\Delta^{(2j+1)}\|_p^{B_3}\Big)^p \geq \Big(\|\Delta^{(2j)}\|_p^{B_3}\Big)^p \geq \|Q_{2j3+1}\|_p^p = \Big\|\frac{1}{2}P_{j3} + \frac{1}{2}P_{j3+1}\Big\|_p^p \geq \frac{1}{4}\|P_{j3+1}\|_p^p \geq \frac{1}{12}\sum_{i=3}^{3}\|P_{j3+i}\|_p^p = \frac{1}{12}\Big(\|\Gamma^{(j)}\|_p^{B_3}\Big)^p.$$

- Case 3: $\frac{1}{2}\|P_{j3+2}\|_p = \max\Big\{\|P_{j3}\|_p, \frac{1}{2}\|P_{j3+1}\|_p, \frac{1}{2}\|P_{j3+2}\|_p, \|P_{j3+3}\|_p\Big\}$.
  In this case, we consider $\Delta^{(2j+1)}$. As similar to Case 2, we obtain

$$\Big(\|\Delta^{(2j)}\|_p^{B_3}\Big)^p + \Big(\|\Delta^{(2j+1)}\|_p^{B_3}\Big)^p \geq \Big(\|\Delta^{(j+1)}\|_p^{B_3}\Big)^p \geq \frac{1}{12}\Big(\|\Gamma^{(j)}\|_p^{B_3}\Big)^p.$$

- Case 4: $\|P_{j3+4}\|_p = \max\Big\{\|P_{j3}\|_p, \frac{1}{2}\|P_{j3+1}\|_p, \frac{1}{2}\|P_{j3+2}\|_p, \|P_{j3+3}\|_p\Big\}$.
  In this case, we consider $\Delta^{(2j+1)}$. As similar to Case 1, we obtain

$$\Big(\|\Delta^{(2j)}\|_p^{B_3}\Big)^p + \Big(\|\Delta^{(2j+1)}\|_p^{B_3}\Big)^p \geq \Big(\|\Delta^{(2j+1)}\|_p^{B_3}\Big)^p \geq \frac{1}{6}\Big(\|\Gamma^{(j)}\|_p^{B_3}\Big)^p.$$

From the above four cases, we get

$$\Big(\|\Delta^{(2j)}\|_p^{B_3}\Big)^p + \Big(\|\Delta^{(2j+1)}\|_p^{B_3}\Big)^p \geq \frac{1}{12}\Big(\|\Gamma^{(j)}\|_p^{B_3}\Big)^p, \quad \forall j = 0, \ldots, N-1.$$

Then

$$\|\Delta_{\Gamma,j_0}\|_p^{B_{2N,D}} = \frac{1}{(2N)^{1/p}}\left(\sum_{j=0}^{N-1}\Big(\|\Delta^{(2j)}\|_p^{B_3}\Big)^p + \Big(\|\Delta^{(2j+1)}\|_p^{B_3}\Big)^p\right)^{1/p} \geq \frac{1}{(2N)^{1/p}}\left(\sum_{j=0}^{N-1}\frac{1}{12}\Big(\|\Gamma^{(j)}\|_p^{B_3}\Big)^p\right)^{1/p} = \frac{1}{24^{1/p}}\|\Gamma\|_p^{B_{N,D}}.$$

□

Lemma 4.35. For any $\Gamma \in B_{N,3}$, we have

$$\frac{1}{4}\,\|\Gamma\|_\infty^{B_{N,3}} \leq \|\Gamma\|_\infty^{B_{2N,3}}.$$

Proof. Let $\Gamma \in B_{N,3}$ be an N-piece cubic Bézier curve with control points $P_{j3+i} \in \mathbb{R}^n$, $i = 0, \ldots, 3$, $j = 0, \ldots, N-1$. So

$$\Gamma(t) = \begin{cases} \Gamma^{(0)}(Nt) = \sum\limits_{i=0}^{3} P_i b_{i,3}(Nt) & \text{if } t \in \Big[0, \frac{1}{N}\Big], \\ \Gamma^{(j)}(Nt-j) = \sum\limits_{i=0}^{3} P_{j3+i} b_{i,3}(Nt-j) & \text{if } t \in \Big[\frac{j}{N}, \frac{j+1}{N}\Big], \\ & j = 0, \ldots, N-1. \end{cases}$$

From (4.5), Γ can be considered as a $2N$-piece cubic Bézier curve as follows

$$\Gamma(t) = \begin{cases} \Delta^{(2j)}(2Nt-2j) = \sum\limits_{i=0}^{3} Q_{2j3+i} b_{i,3}(2Nt-2j) & \text{if } t \in \Big[\frac{2j}{2N}, \frac{2j+1}{2N}\Big] \\ \Delta^{(2j+1)}(2Nt-2j-1) = \sum\limits_{i=0}^{3} Q_{(2j+1)3+i} b_{i,3}(2Nt-2j-1) & \text{if } t \in \Big[\frac{2j+1}{2N}, \frac{2j+2}{2N}\Big], \\ & j = 0, \ldots, N-1, \end{cases}$$

where

$$\begin{cases} Q_{2j3+i} = \sum\limits_{l=0}^{i} b_{l,i}\Big(\frac{1}{2}\Big) P_{j3+i-l}, & i = 0, \ldots, 3, j = 0, \ldots, N-1, \\ Q_{(2j+1)3+i} = \sum\limits_{l=0}^{i} b_{l,i}\Big(\frac{1}{2}\Big) P_{j3+3-i+l}, & i = 0, \ldots, 3, j = 0, \ldots, N-1. \end{cases}$$

We first consider $\max\Big\{\|\Delta^{(2j)}\|_\infty^{B_3}, \|\Delta^{(2j+1)}\|_\infty^{B_3}\Big\}$, $j = 0, \ldots, N-1$.

- Case 1: $\|P_{j3}\|_\infty = \max\Big\{\|P_{j3}\|_\infty, \frac{1}{2}\|P_{j3+1}\|_\infty, \frac{1}{2}\|P_{j3+2}\|_\infty, \|P_{j3+3}\|_\infty\Big\}$. We have

$$\max\Big\{\|\Delta^{(2j)}\|_\infty^{B_3}, \|\Delta^{(2j+1)}\|_\infty^{B_3}\Big\} \geq \|\Delta^{(2j)}\|_\infty^{B_3} \geq \|Q_{2j3}\|_\infty = \|P_{j3}\|_\infty = \|\Gamma^{(j)}\|_\infty^{B_3}.$$

- Case 2: $\frac{1}{2}\|P_{j3+1}\|_\infty = \max\Big\{\|P_{j3}\|_\infty, \frac{1}{2}\|P_{j3+1}\|_\infty, \frac{1}{2}\|P_{j3+2}\|_\infty, \|P_{j3+3}\|_\infty\Big\}$.

We have

$$\max\left\{\|\Delta^{(2j)}\|_\infty^{B_3}, \|\Delta^{(2j+1)}\|_\infty^{B_3}\right\} \geq \|\Delta^{(2j)}\|_\infty^{B_3} \geq \|Q_{2j3+1}\|_\infty = \left\|\frac{1}{2}P_{j3} + \frac{1}{2}P_{j3+1}\right\|_\infty$$
$$\geq \frac{1}{4}\|P_{j3+1}\|_\infty = \frac{1}{4}\|\Gamma^{(j)}\|_\infty^{B_3}.$$

- Case 3: $\frac{1}{2}\|P_{j3+2}\|_\infty = \max\left\{\|P_{j3}\|_\infty, \frac{1}{2}\|P_{j3+1}\|_\infty, \frac{1}{2}\|P_{j3+2}\|_\infty, \|P_{j3+3}\|_\infty\right\}$.
  In this case, we consider $\Delta^{(2j+1)}$. As similar to Case 2, we obtain

$$\max\left\{\|\Delta^{(2j)}\|_\infty^{B_3}, \|\Delta^{(2j+1)}\|_\infty^{B_3}\right\} \geq \|\Delta^{(2j+1)}\|_\infty^{B_3} \geq \frac{1}{4}\|\Gamma^{(j_0)}\|_\infty^{B_3}.$$

- Case 4: $\|P_{j3+3}\|_\infty = \max\left\{\|P_{j3}\|_\infty, \frac{1}{2}\|P_{j3+1}\|_\infty, \frac{1}{2}\|P_{j3+2}\|_\infty, \|P_{j3+3}\|_\infty\right\}$.
  In this case, we consider $\Gamma^{(1)}$. As similar to Case 1, we obtain

$$\max\left\{\|\Delta^{(2j)}\|_\infty^{B_3}, \|\Delta^{(2j+1)}\|_\infty^{B_3}\right\} \geq \|\Delta^{(2j+1)}\|_\infty^{B_3} \geq \|\Gamma^{(j)}\|_\infty^{B_3}.$$

From the above four cases, we get

$$\max\left\{\|\Delta^{(2j)}\|_\infty^{B_3}, \|\Delta^{(2j+1)}\|_\infty^{B_3}\right\} \geq \frac{1}{4}\|\Gamma^{(j)}\|_\infty^{B_3}. \tag{4.7}$$

Then

$$\|\Gamma\|_\infty^{B_{2N,D}} = \max_{j=0,\dots,N-1} \max\left\{\|\Delta^{(2j)}\|_\infty^{B_3}, \|\Delta^{(2j+1)}\|_\infty^{B_3}\right\}$$
$$\geq \max_{j=0,\dots,N-1} \frac{1}{4}\|\Gamma^{(j)}\|_\infty^{B_3} = \frac{1}{4}\|\Gamma\|_\infty^{B_{N,D}}.$$

□

From the above two lemmas, we have the following proposition.

Proposition 4.36. Let $p \in [1, \infty[\cup\{\infty\}$. For any $\Gamma \in B_{N,3}$, we have

$$\min\left\{\frac{1}{24^{1/p}}, \frac{1}{4}\right\}\|\Gamma\|_p^{B_{N,3}} \leq \|\Gamma\|_p^{B_{2N,3}}.$$

Proof. Using Lemma 4.34 and Lemma 4.35, we get the proof of this proposition. □

Equivalence constants for the norms $\|\cdot\|_p^{B_{2N,3}}$ and $\|\cdot\|_p^{B_{N,3}}$ on $B_{N,3}$

Combining the above two propositions, we have the following theorem.

Theorem 4.3. Let $p \in [1, \infty[\cup \infty$. For any $\Gamma \in B_{N,3}$, we have

$$\min\left\{\frac{1}{24^{1/p}}, \frac{1}{4}\right\}\|\Gamma\|_p^{B_{N,3}} \leq \|\Gamma\|_p^{B_{2N,3}} \leq 3^{1/p}\ \|\Gamma\|_p^{B_{N,3}}.$$

Proof. Using Proposition 4.33 and Proposition 4.36, we have the proof of this theorem. □

From the above theorem, we have the following corollary:

$$\min\left\{\frac{1}{24^{1/p}}, \frac{1}{4}\right\} d_p^{B_{N,3}}(\Gamma - \Delta) \leq d_p^{B_{2N,3}}(\Gamma - \Delta) \leq 3^{1/p}\ d_p^{B_{N,3}}(\Gamma - \Delta),$$

for any $\Gamma, \Delta \in B_{N,3}$.

From results in this chapter, we have the norm $\|\cdot\|_p^{B_{N,3}}$ on the space $B_{N,3}$. The equivalence constants for the norm $\|\cdot\|_p^{B_{N,3}}$ and the norm L_p do not depend on the number N of pieces. We can use the norm $\|\cdot\|_p^{B_{N,3}}$ to consider the convergence for sequences of piecewise cubic Bézier curves. An N-piece Bézier curve can be split and reparametrized to become an $N+1$-piece Bézier curve. This way creates extra control points in order to give additional freedom for curve design and avoids increasing the degree of the curve. Then we are going to propose an algorithm using piecewise cubic Bézier curves to find optimal trajectories in the next chapter. This method can be applied to approximate solution orbits of autonomous ordinary differential equations and control of autonomous ordinary differential equations.

Chapter 5

Application to trajectory optimization problems, autonomous ordinary differential equations and control of autonomous ordinary differential equations

In this chapter, we focus on using piecewise uniform cubic Bézier curves in order to approximate optimal trajectories. Optimal trajectory problem appears in many different domains as robotic ([16, 36, 37, 75]), astrophysics ([6, 76, 92, 94]) and the core of motion planning which is known to be a very difficult problem ([18, 35, 37, 74, 88]). Roughly, the optimal trajectory problem is an optimization problem when the "variable" is a curve. Using piecewise uniform cubic Bézier curves, we reduce an infinite-dimensional optimization problem to a finite-dimensional optimization problem and the smoothness can be integrated with using constraints. We use this idea in the context of geodesic for condition metric. Condition metric is an important aspect in the studies of complexity of numerical methods ([5, 10]). We also apply our method to approximate solution orbits of autonomous ordinary differential equations and control of autonomous ordinary differential equations. Our method is more effective than the Euler method and the Runge-Kutta method for finding solution orbits of autonomous ordinary differential equations (see Figures 5.48, 5.49, 5.50, 5.51, 5.52 and 5.53).

We have a general method which applies to many different problems using the same methodology. It gives a unifying approach to problems in optimal trajectory, autonomous ordinary differential equation and control theory. We will show this unifying approach on (hopefully) significant examples in this chapter.

5.1 Trajectory optimization

In this section, we propose an algorithm using piecewise uniform cubic Bézier curves to approximate optimal trajectories.

Let $F : C^0([0,1],\mathbb{R}^n) \to \mathbb{R}$ be a continuous function. We require that this objective function F should be invariant under reparametrization. An element $\gamma_0 \in C^0([0,1],\mathbb{R}^n)$ is called a local minimum of F if there exists $r > 0$ such that $F(\gamma_0) \leq F(\gamma)$ for all $\gamma \in B(\gamma_0, r)$ for the L_p-norm. For $N \in \mathbb{N}$, we denote by $F\mid_{B_{N,3}}$ the restriction of F to the space $B_{N,3}$ of uniform N-piece cubic Bézier curves. We first consider some properties about the convergence of a sequence to a local minimum.

Proposition 5.1. Let $F : C^0([0,1],\mathbb{R}^n) \to \mathbb{R}$ be a continuous function such that F is invariant under reparametrization. Let $\gamma_0 \in C^0([0,1],\mathbb{R}^n)$ be a local minimum of F and $r > 0$ be such that $F(\gamma_0) \leq F(\gamma)$ for all $\gamma \in B(\gamma_0, r)$ for the L_p-norm. Let $\tilde{\gamma}_N$ be a minimum of $F\mid_{B_{N,3}}$ on the set $B_{N,3} \cap B(\gamma_0, r)$. If the sequence $\{\tilde{\gamma}_N\}$ converges with respect to the norm L_p on the space $C^0([0,1],\mathbb{R}^n)$ and $\lim\limits_{N\to\infty} \tilde{\gamma}_N \in B(\gamma_0, r)$, then the limit $\lim\limits_{N\to\infty} \tilde{\gamma}_N$ is a local minimum of F.

Proof. We denote $\tilde{\gamma}_0 = \lim\limits_{N\to\infty} \tilde{\gamma}_N$.
If $F(\tilde{\gamma}_0) = F(\gamma_0)$, then $\tilde{\gamma}_0$ is a local minimum of the function F.
If $F(\tilde{\gamma}_0) \neq F(\gamma_0)$, we set $\epsilon = F(\tilde{\gamma}_0) - F(\gamma_0) > 0$. Since $\gamma_0 \in C^0([0,1],\mathbb{R}^n)$, there exists a sequence $\{\alpha_N\}$ such that $\alpha_N \in B_{N,3}$ and $\{\alpha_N\}$ converges to γ_0 with respect to the norm L_p.
We have $\gamma_0 \in B(\gamma_0, r)$, thus there exists $N_0 > 0$ such that

$$\forall N > N_0, \alpha_N \in B_{N,3} \cap B(\gamma_0, r).$$

Because the function F is continuous, α_N converges to γ_0 and $F(\gamma_0) \leq F(\gamma)$ for all $\gamma \in B(\gamma_0, r)$, there exists $N_1 \in \mathbb{N}$ such that

$$\forall N > N_1, F(\gamma_0) \leq F(\alpha_N) \leq F(\gamma_0) + \epsilon/2.$$

Taking $\lim_{N\to\infty}$, we have $F(\gamma_0) \leq F(\tilde{\gamma}_0) \leq F(\gamma_0)+\epsilon/2$. This contradicts with $F(\tilde{\gamma}_0) = F(\gamma_0) + \epsilon$. So $F(\tilde{\gamma}_0) = F(\gamma_0)$ and therefore the limit $\tilde{\gamma}_0 = \lim_{N\to\infty} \tilde{\gamma}_N$ is a local minimum of F. □

If we drop some hypotheses, Proposition 5.1 will be not true. We can see this in the following example.

Example 5.2. Let γ_0 be the upper half circle

$$\begin{aligned} \gamma_0 : [0,1] &\to \mathbb{R}^2 \\ t &\mapsto \gamma_0(t) = (\cos(\pi - t\pi), \sin(\pi - t\pi)) . \end{aligned}$$

Consider the continuous function

$$\begin{aligned} F : C^0\left([0,1], \mathbb{R}^2\right) \setminus \{\gamma_0\} &\to \mathbb{R} \\ \gamma &\mapsto \frac{-1}{\|\gamma - \gamma_0\|_{L_2}}. \end{aligned}$$

We have $F(\gamma_0) = -\infty$. So γ_0 is not a minimum of F. But $F\mid_{B_{N,3}}: B_{N,3} \to \mathbb{R}$ has a minimum $\tilde{\gamma}_N \in C^0([0,1], \mathbb{R}^2) \setminus \{\gamma_0\}$ such that $\tilde{\gamma}_N \to \gamma_0$ as $N \to \infty$.

Proposition 5.3. Let $F : C^0([0,1], \mathbb{R}^n) \to \mathbb{R}$ be a continuous function such that F is invariant under reparametrization. Let $\tilde{\gamma}_N$ be a minimum of $F\mid_{B_{N,3}}$ on the set $B_{N,3} \cap V_N$, where V_N is an open set of $C^0([0,1], \mathbb{R}^n)$ for the L_p-norm. If

- the sequence $\{\tilde{\gamma}_N\}$ converges with respect to the norm L_p on $C^0([0,1], \mathbb{R}^n)$,
- the limit $\lim_{N\to\infty} \tilde{\gamma}_N$ is in $C^0([0,1], \mathbb{R}^n)$,
- $\bigcap_N V_N$ is a non-empty open set of $C^0([0,1], \mathbb{R}^n)$ for the L_p-norm,

then the limit $\lim_{N\to\infty} \tilde{\gamma}_N$ is a local minimum of F.

Proof. We set $\tilde{\gamma}_0 = \lim_{N\to\infty} \tilde{\gamma}_N$ and $V_0 = \bigcap_N V_N$. Let γ be an element in V_0. Since γ is continuous, there exists a sequence $\{\alpha_N\}$ such that $\alpha_N \in B_{N,3}$ and $\{\alpha_N\}$ converges to γ with respect to the norm L_p.
We have $\gamma \in V_0$, thus there exists a positive integer N such that

$$\forall N > N_0, \alpha_N \in V_0.$$

Since $\tilde{\gamma}_N$ is a minimum of $F\mid_{B_{N,3}}$ on the set $B_{N,3} \cap V_N$ and $V_0 = \bigcap_N V_N$, we have

$$\forall N > N_0, F(\tilde{\gamma}_N) \leq F(\alpha_N).$$

Taking $\lim_{N\to\infty}$, we have $F(\tilde{\gamma}_0) \leq F(\gamma)$. Then $\tilde{\gamma}_0$ is a minimum of F on V_0. □

Combining Proposition 5.1, Proposition 5.3 and Theorem 4.1, we propose Algorithm 2 using piecewise uniform cubic Bézier curves to approximate optimal trajectories. In the Algorithm 2, the objective function F is invariant under reparametrization.

The idea is to improve the approximation of the trajectory by splitting pieces when they bring improvement. Along the algorithm, the current approximation is a list of pieces. The split procedure allows to replace one piece by two pieces without changing the curve. We run along the list of pieces and successively.

We first establish Algorithm 1. Algorithm 1 is a sub-algorithm of Algorithm 2. In Algorithm 1, we split a uniform N-piece cubic Bézier curve $\tilde{\gamma}_N$ at a fixed index i^{th} and reparametrize to become a uniform $N+1$-piece cubic Bézier curve γ_{N+1}. Since the objective function is invariant under reparametrization, we have $F(\gamma_{N+1}) = F(\tilde{\gamma}_N)$. This approach creates 3 extra control points in order to give additional freedom for curve design. Then we find $\tilde{\gamma}_{N+1}$ that is a local minimum of F on $B_{N+1,3}$ from the initial curve γ_{N+1}. This step is a finite-dimensional optimization problem. In numerical tests, we use **Fmincon** in Matlab to find the local minimum $\tilde{\gamma}_{N+1}$ of F on $B_{N+1,3}$. If $\|\tilde{\gamma}_{N+1} - \gamma_{N+1}\|_p^{B_{N+1,3}}$ is small enough, the difference $|F(\tilde{\gamma}_{N+1}) - F(\gamma_{N+1})|$ is very small. This means we can not improve the curve by splitting $\tilde{\gamma}_N$ at the i^{th} piece. We will save this index to avoid splitting this piece at next steps.

Algorithm 1 SPLIT-OPTIMAL $(F, \tilde{\gamma}, i, \epsilon, I)$ ▷ Split at a fixed piece and optimize a piecewise uniform cubic Bézier curve

Input $F : C^0([0,1], \mathbb{R}^n) \to \mathbb{R}$ is invariant under reparametrization, $\tilde{\gamma}$ is a piecewise uniform cubic Bézier curve, i is a piece index, ϵ is a constant, I is a set of piece indexes.

Output A piecewise uniform cubic Bézier curve and a set of piece indexes.

1: **Begin Procedure**
2: $N :=$ the number of pieces of $\tilde{\gamma}$
3: Split $\tilde{\gamma} \in B_{N,3}$ at the i^{th} piece and reparametrize to become $\gamma_{N+1} \in B_{N+1,3}$ ▷ We note that $F(\gamma_{N+1}) = F(\tilde{\gamma}_N)$
4: Find $\tilde{\gamma}_{N+1}$ being a local minimum of F on $B_{N+1,3}$ from the initial curve γ_{N+1}
5: **if** $\|\tilde{\gamma}_{N+1} - \gamma_{N+1}\|_p^{B_{N+1,3}} < \epsilon$ **then**
6: Put the piece indexes i^{th} and $(i+1)^{th}$ in the set I
7: **end if**
8: **return** $[\tilde{\gamma}_{N+1}, I]$
9: **End Procedure**

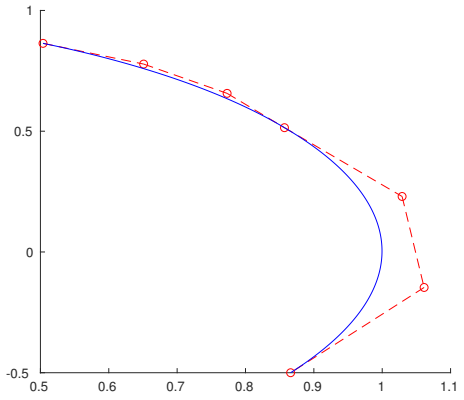

Fig. 5.1: A uniform 2-piece cubic Bézier curve γ_2.

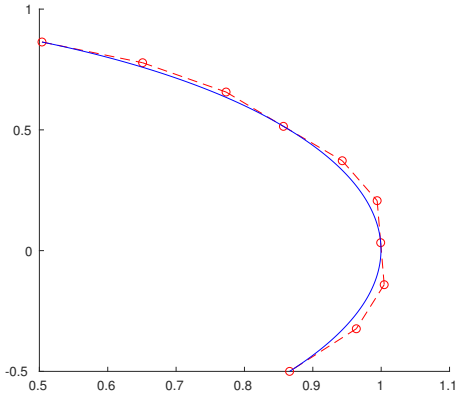

Fig. 5.2: Split γ_2 at the 2^{nd} piece.

We recall the way to split a uniform N-piece cubic Bézier curve at the j_0^{th} piece and reparametrize to become a uniform $N+1$-piece cubic Bézier curve. Let $\Gamma \in B_{N,3}$ be a uniform N-piece cubic Bézier curve with control points $P_{j3+i} \in \mathbb{R}^n$, $j = 0, \ldots, N-1$, $i = 0, \ldots, 3$. So

$$\Gamma(t) = \begin{cases} \Gamma^{(0)}(Nt) = \sum_{i=0}^{3} P_i b_{i,3}(Nt) & \text{if } t \in \left[0, \frac{1}{N}\right], \\ \Gamma^{(j)}(Nt-j) = \sum_{i=0}^{3} P_{j3+i} b_{i,3}(Nt-j) & \text{if } t \in \left[\frac{j}{N}, \frac{j+1}{N}\right], \\ & j = 1, \ldots, N-1. \end{cases}$$

By ([26, chapter 9, p. 201]), we can split Γ at the j_0^{th} piece and obtain

$$\Gamma(t) = \begin{cases} \Gamma^{(j)}(Nt-j) = \sum_{i=0}^{3} P_{j3+i} b_{i,3}(Nt-j) \text{ if } t \in \left[\frac{j}{N}, \frac{j+1}{N}\right], \forall j = 0, \ldots j_0 - 1 \\ \Delta^{(j_0)}(2Nt-2j_0) = \sum_{i=0}^{3} Q_{j_0 3+i} b_{i,3}(2Nt-2j_0) \text{ if } t \in \left[\frac{2j_0}{2N}, \frac{2j_0+1}{2N}\right] \\ \Delta^{(j_0+1)}(2Nt-2j_0-1) = \sum_{i=0}^{3} Q_{(j_0+1)3+i} b_{i,3}(2Nt-2j_0-1) \text{ if } t \in \left[\frac{2j_0+1}{2N}, \frac{2j_0+2}{2N}\right], \\ \Gamma^{(j)}(Nt-j) = \sum_{i=0}^{3} P_{j3+i} b_{i,3}(Nt-j) \text{ if } t \in \left[\frac{j}{N}, \frac{j+1}{N}\right], \forall j = j_0+1, \ldots N-1. \end{cases}$$

where

$$\begin{cases} Q_{j_0 3+i} = \sum_{l=0}^{i} b_{l,i}\left(\frac{1}{2}\right) P_{j_0 3+i-l}, & i = 0, \ldots, 3, \\ Q_{(j_0+1)3+i} = \sum_{l=0}^{i} b_{l,i}\left(\frac{1}{2}\right) P_{j_0 3+3-i+l}, & i = 0, \ldots, 3. \end{cases}$$

We reparametrize Γ to become a uniform $N+1$-piece cubic Bézier curve Δ as

follows

$$\Delta(t) = \begin{cases} \Delta^{(0)}((N+1)t) = \sum_{i=0}^{3} Q_i b_{i,3}(Nt) & \text{if } t \in \Big[0, \frac{1}{N+1}\Big], \\ \Delta^{(j)}((N+1)t - j) = \sum_{i=0}^{3} Q_{j3+i} b_{i,3}(Nt - j) & \text{if } t \in \Big[\frac{j}{N+1}, \frac{j+1}{N+1}\Big], \\ & j = 1, \ldots, N, \end{cases}$$

where

$$\begin{cases} Q_{j3+i} = P_{j3+i}, \forall j = 0, \ldots, j_0 - 1, i = 0, \ldots, 3, \\ Q_{j_0 3+i} = \sum_{l=0}^{i} b_{l,i}\Big(\frac{1}{2}\Big) P_{j_0 3+i-l}, i = 0, \ldots, 3, \\ Q_{(j_0+1)3+i} = \sum_{l=0}^{i} b_{l,i}\Big(\frac{1}{2}\Big) P_{j_0 3+3-i+l}, i = 0, \ldots, 3, \\ Q_{j3+i} = P_{(j-1)3+i}, \forall j = j_0 + 2, \ldots, N, i = 0, \ldots, 3. \end{cases}$$

In Algorithm 2, we split each piece of the curve and optimize respectively. At each step, we just split one piece and then optimize. The number of pieces increases one piece and the number of control points increases 3 points after each step. The algorithm will be stop if we can not improve the curve by splitting any pieces.

Algorithm 2 OPTIMAL (F, γ_1, ϵ) ▷ Using piecewise uniform cubic Bézier curves to approximate optimal trajectories

Input $F : C^0([0,1], \mathbb{R}^n) \to \mathbb{R}$ is invariant under reparametrization, $\gamma_{N_0} \in B_{N_0,3}$ and $\epsilon > 0$. ▷ $N_0 \in \mathbb{N}^+$

Output A piecewise uniform cubic Bézier curve.

Begin Procedure
$N = N_0$;
$I = []$; ▷ The indexes of pieces which are optimal
Find $\tilde{\gamma}_{N_0}$ being a local minimum of F on $B_{N_0,3}$ from the initial curve γ_{N_0}
while All piece indexes of the curves does not belong I **do**
    $j = 0$; ▷ The increasing in the number of pieces of the curve
    for $i := 1$ to N **do** ▷ We split each piece of the curve and optimize
        if $i + j \notin I$ **then**
            $[\tilde{\gamma}_{N+1}, I]$:= SPLIT-OPTIMAL ($F, \tilde{\gamma}_N, i + j, \epsilon, I$);
            $N := N + 1$;
            $j := j + 1$;
        end if
    end for
end while
return $\tilde{\gamma}_{N+1}$ ▷ The approximation of the optimal trajectory
End Procedure

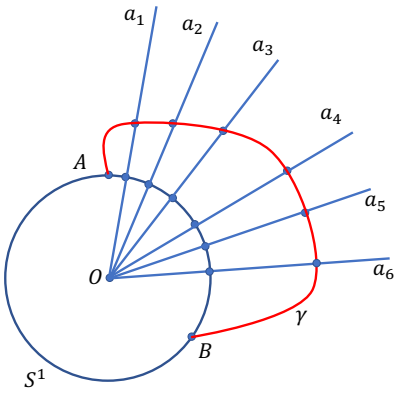

Fig. 5.3: Example 5.4.

We will now present some experiments in order to illustrate the efficiency of the proposed method. We will consider simple problems and progressively go to more and more advanced problems. The first problem is a geometric approximation of the arc of the unit circle.

Example 5.4. Let S^1 be the unit circle on the plane. Let $a_1, \ldots, a_6$ be six rays as follows

$$\begin{aligned}
(a_1) \quad & y = 8x, && x \geq 0 \\
(a_2) \quad & y = 3x, && x \geq 0 \\
(a_3) \quad & y = 1.5x, && x \geq 0 \\
(a_4) \quad & y = 0.7x, && x \geq 0 \\
(a_5) \quad & y = 0.4x, && x \geq 0 \\
(a_6) \quad & y = 0.1x, && x \geq 0.
\end{aligned}$$

For a curve $\gamma : [0,1] \to \mathbb{R}^2$, we define our objective function F by

$$F(\gamma) = \sum_{i=1}^{6} \|(\gamma \cap a_i) - (\gamma \cap S^1)\|_2.$$

We want to find a curve γ going from $A(0,1)$ to $B(\sqrt{3}/2, 0.5)$ such that $F(\gamma)$ is minimum. (See Figures 5.3)
It is easily seen that the arc α of the circle going from A to B realizes the minimum of F: we have $F(\alpha) = 0$.

We use piecewise uniform cubic Bézier curves and Algorithm 2 to find an approximation of the minimum of F. We run Algorithm 2 step by step and obtain

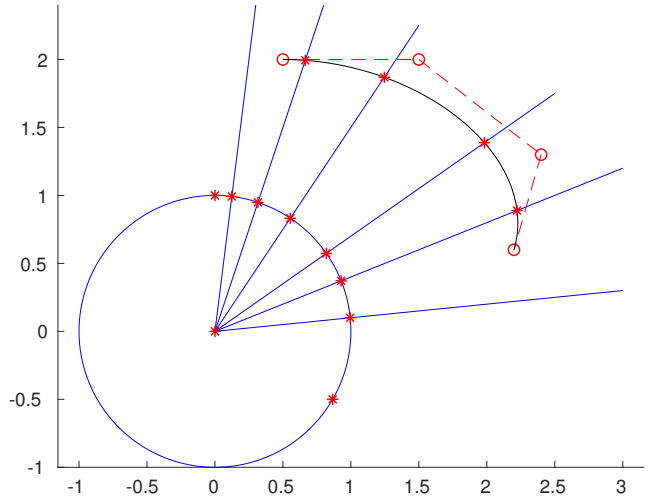

Fig. 5.4: Step 1 in Example 5.4: the initial curve $\gamma_1 \in B_{1,3}$.

the list of curves at each step (See Figure 5.4, Figure 5.5, Figure 5.6, Figure 5.7, Figure 5.8, Figure 5.9, Figure 5.10 and Figure 5.11).

Summary: We have a table of values and some notations when using Algorithm 2 to approximate the minimum of F in Example 5.4 as follows:

	$\lvert F(\tilde{\gamma}_i) - F(\alpha)\rvert$	$\lvert F(\tilde{\gamma}_i) - F(\gamma_i)\rvert$	$\frac{F(\tilde{\gamma}_i)}{F(\gamma_i)}$	$\lVert\tilde{\gamma}_i - \gamma_i\rVert_2^{B_{i,3}}$
$i = 1$	$4.7817.10^{-04}$	205.1609	$0.2330.10^{-5}$	2.8848
$i = 2$	$1.8505.10^{-07}$	$4.7798.10^{-4}$	$0.3870.10^{-3}$	0.0042
$i = 3$	$7.7819.10^{-08}$	$1.0723.10^{-7}$	0.4205	$4.6025.10^{-8}$
$i = 4$	$7.7819.10^{-08}$	0	1	0

- The arc α of the circle going from A to B realizes the minimum of F: we have $F(\alpha) = 0$.
- $\gamma_i \in B_{i,3}$ is a reparametrization of $\tilde{\gamma}_{i-1} \in B_{i-1,3}$. Since F is invariant under reparametrization, we have $F(\gamma_i) = F(\tilde{\gamma}_{i-1})$.
- Each step from $\tilde{\gamma}_i$ to $\tilde{\gamma}_{i+1}$, the number of pieces increases one piece and the number of control points increases 3 points.
- $\lvert F(\tilde{\gamma}_i - F(\gamma_i)\rvert \to 0$ as $i \to 4$.
- $\lVert\tilde{\gamma}_i - \gamma_i\rVert_2^{B_{i,3}} \to 0$ as $i \to 4$.

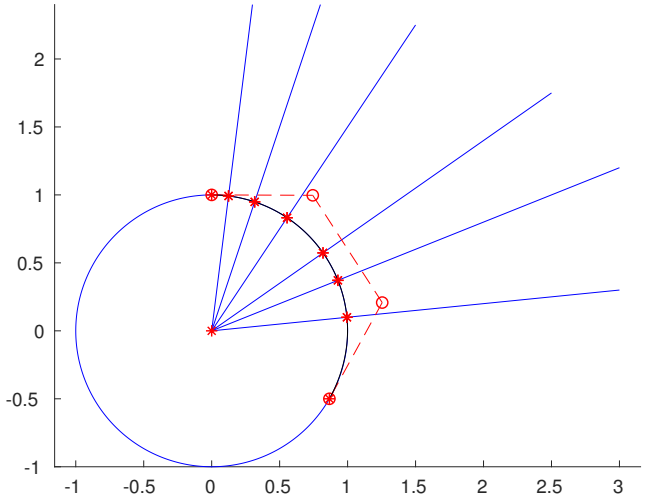

Fig. 5.5: Step 2 in Example 5.4: the local minimum $\tilde{\gamma}_1 \in B_{1,3}$ of $F\mid_{B_{1,3}}$ from the initial curve $\gamma_1 \in B_{1,3}$.

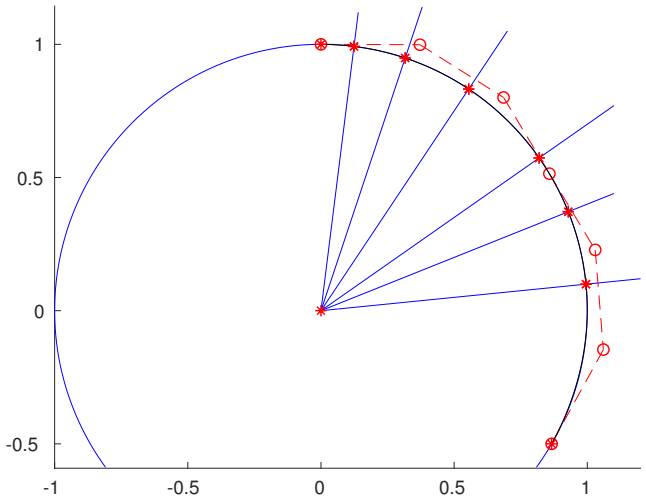

Fig. 5.6: Step 3 in Example 5.4: split and reparametrize $\tilde{\gamma}_1 \in B_{1,3}$ to become $\gamma_2 \in B_{2,3}$.

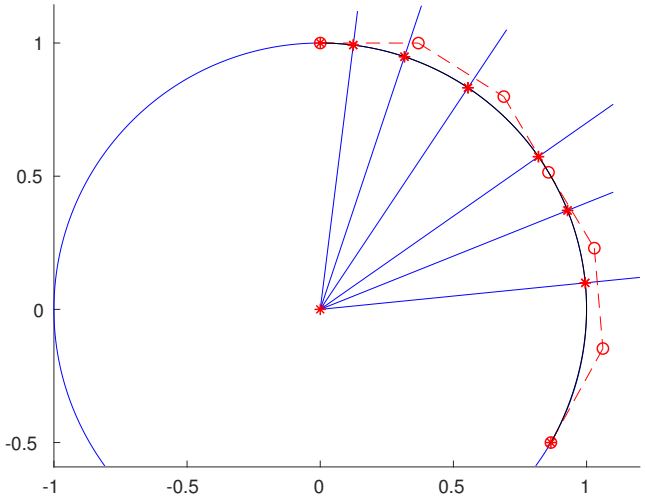

Fig. 5.7: Step 4 in Example 5.4: the local minimum $\tilde{\gamma}_2 \in B_{2,3}$ of $F\mid_{B_{2,3}}$ from the initial curve $\gamma_2 \in B_{2,3}$.

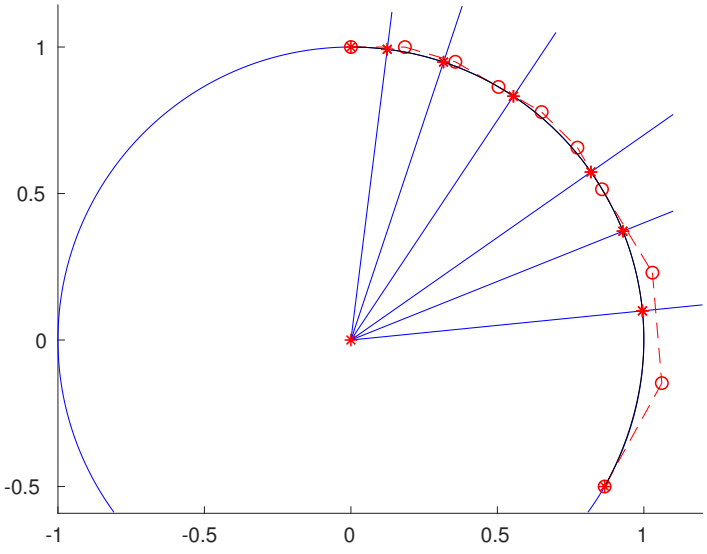

Fig. 5.8: Step 5 in Example 5.4: split at the first piece and reparametrize $\tilde{\gamma}_2$ to become $\gamma_3 \in B_{3,3}$.

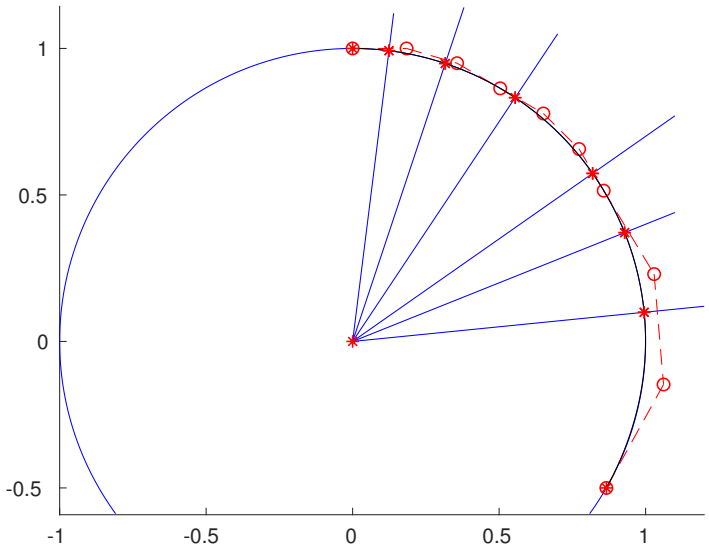

Fig. 5.9: Step 6 in Example 5.4: the local minimum $\tilde{\gamma}_3 \in B_{3,3}$ of $F\mid_{B_{2,3}}$ from the initial curve $\gamma_3 \in B_{3,3}$.

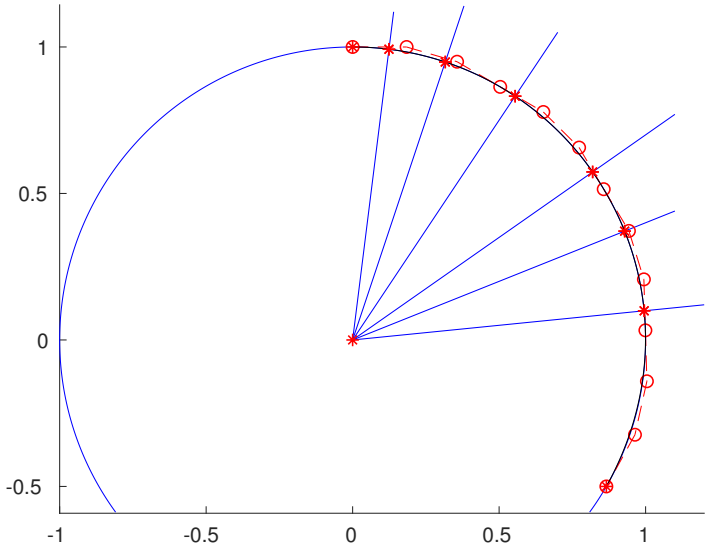

Fig. 5.10: Step 7 in Example 5.4 : split at the third piece and reparametrize $\tilde{\gamma}_3$ to become $\gamma_4 \in B_{4,3}$.

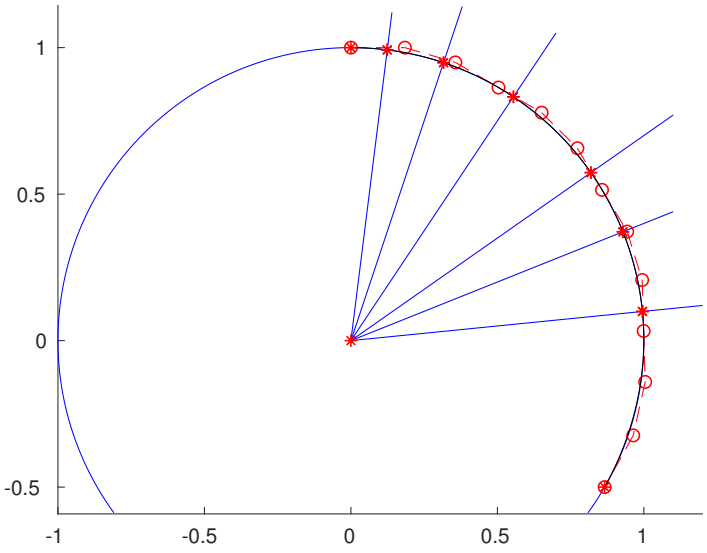

Fig. 5.11: Step 8 in Example 5.4: the local minimum $\tilde{\gamma}_4 \in B_{4,3}$ of $F\mid_{B_{4,3}}$ from the initial curve $\gamma_4 \in B_{4,3}$.

- $|F(\tilde{\gamma}_i) - F(\alpha)|$ approaches to nearly zero as $i \to 4$.
- The rate of decrease of $|F(\tilde{\gamma}_i) - F(\alpha)|$ slows down over each step.
- When the value of $\|\tilde{\gamma}_i - \gamma_i\|_2^{B_{i,3}}$ is small enough, $|F(\tilde{\gamma}_i) - F(\gamma_i)|$ is very small.
- At $i-1$, we split and reparametrize $\tilde{\gamma}_{i-1} \in B_{i-1,3}$ at one piece to become $\gamma_i \in B_{i,3}$. Then we use **Fmincon** in Matlab to find the local minimum $\tilde{\gamma}_i \in B_{i,3}$ from the initial curve $\gamma_i \in B_{i,3}$.
- At Step 5 and Step 6, we split $\tilde{\gamma}_2$ at the first piece, reparametrize to become $\gamma_3 \in B_{3,3}$ and then find the local minimum $\tilde{\gamma}_3 \in B_{3,3}$. We see that $\|\tilde{\gamma}_3 - \gamma_3\|_2^{B_{3,3}}$ and $|F(\tilde{\gamma}_3) - F(\gamma_3)|$ are very small. This means that we can not improve the curve by splitting the first piece of $\tilde{\gamma}_2$. So we remember the first piece and the second piece of $\tilde{\gamma}_3$ in the set I and stop splitting these pieces in the next steps.
- At Step 7 and Step 8, we split $\tilde{\gamma}_3$ at the third piece, reparametrize to become $\gamma_4 \in B_{3,3}$ and then find the local minimum $\tilde{\gamma}_4 \in B_{3,3}$. We see that $\|\tilde{\gamma}_4 - \gamma_4\|_2^{B_{4,3}}$ and $|F(\tilde{\gamma}_4) - F(\gamma_4)|$ are very small. This means that we can not improve the curve by splitting the third piece of $\tilde{\gamma}_3$. So we remember the third piece

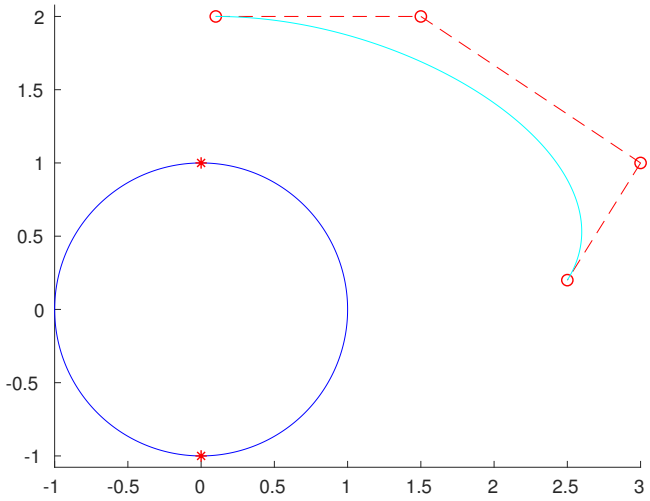

Fig. 5.12: Step 1 in Example 5.5: the initial curve $\gamma_1 \in B_{1,3}$.

and fourth piece of $\tilde{\gamma}_4$ in the set I and stop splitting these pieces in the next steps.

- After Step 8, all piece indexes of $\tilde{\gamma}_4$ belong to I. This means that we can not improve the curve. Then the algorithm stops and we obtain $\tilde{\gamma}_4$ as an approximation of α.

Example 5.5. We consider again the unit circle S^1 on the plane. For a curve $\gamma : [0,1] \to \mathbb{R}^2$, we define our objective function F by

$$\int_0^1 \|\dot{\gamma}(t)\|_2 . d(\gamma(t), S^1) dt,$$

where $d(\gamma(t), S^1) = \min_{A \in S^1} \|\gamma(t) - A\|_2$. We want to find a curve γ going from $A(0,1)$ to $B(0,-1)$ such that $F(\gamma)$ is minimum.

It is clear that the semi circle α going from A to B realizes the minimum of F.

We use piecewise uniform cubic Bézier curves and Algorithm 2 to find an approximation of the semi circle α. We run Algorithm 2 step by step and obtain the list of curves at each step (See Figure 5.12, Figure 5.13, Figure 5.14, Figure 5.15, Figure 5.16, Figure 5.17, Figure 5.18, Figure 5.19, Figure 5.20, Figure 5.21, Figure 5.22, Figure 5.23, Figure 5.24, Figure 5.25, Figure 5.26 and Figure 5.27).

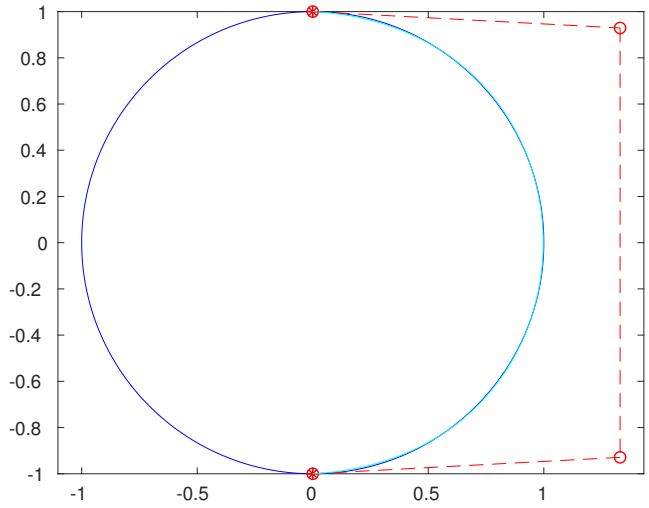

Fig. 5.13: Step 2 in Example 5.5: the local minimum $\tilde{\gamma}_1 \in B_{1,3}$ of $F\,|_{B_{1,3}}$ from the initial curve $\gamma_1 \in B_{1,3}$.

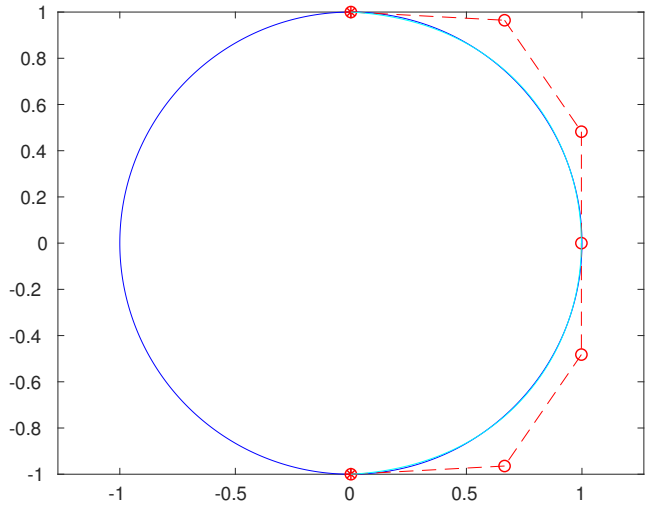

Fig. 5.14: Step 3 in Example 5.5: split and reparametrize $\tilde{\gamma}_1 \in B_{1,3}$ to become $\gamma_2 \in B_{2,3}$.

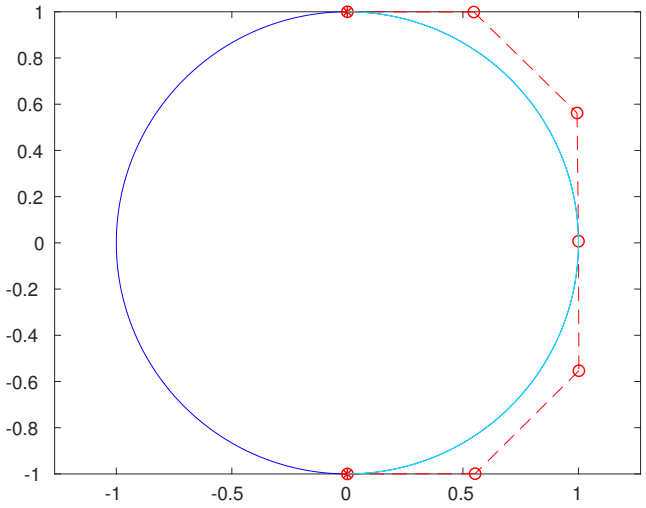

Fig. 5.15: Step 4 in Example 5.5: the local minimum $\tilde{\gamma}_2 \in B_{2,3}$ of $F\,|_{B_{2,3}}$ from the initial curve $\gamma_2 \in B_{2,3}$.

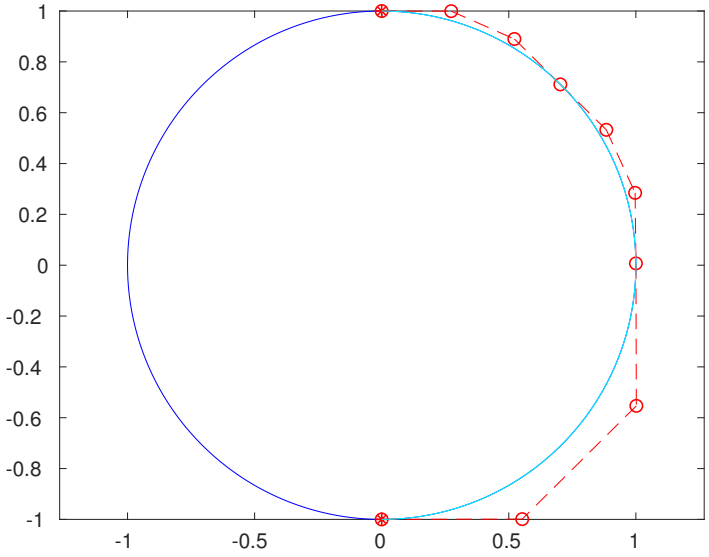

Fig. 5.16: Step 5 in Example 5.5: split at the first piece and reparametrize $\tilde{\gamma}_2$ to become $\gamma_3 \in B_{3,3}$.

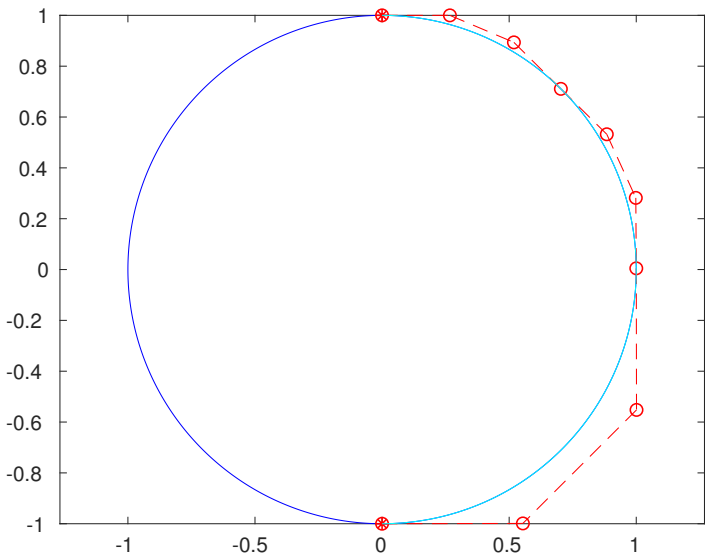

Fig. 5.17: Step 6 in Example 5.5: the local minimum $\tilde{\gamma}_3 \in B_{3,3}$ of $F\,|_{B_{3,3}}$ from the initial curve $\gamma_3 \in B_{3,3}$.

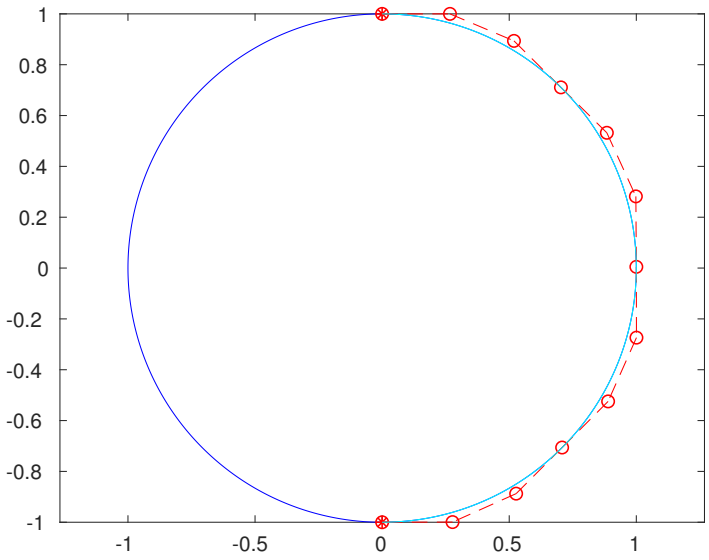

Fig. 5.18: Step 7 in Example 5.5: split at the third piece and reparametrize $\gamma_3 \in B_{3,3}$ to become $\gamma_4 \in B_{4,3}$.

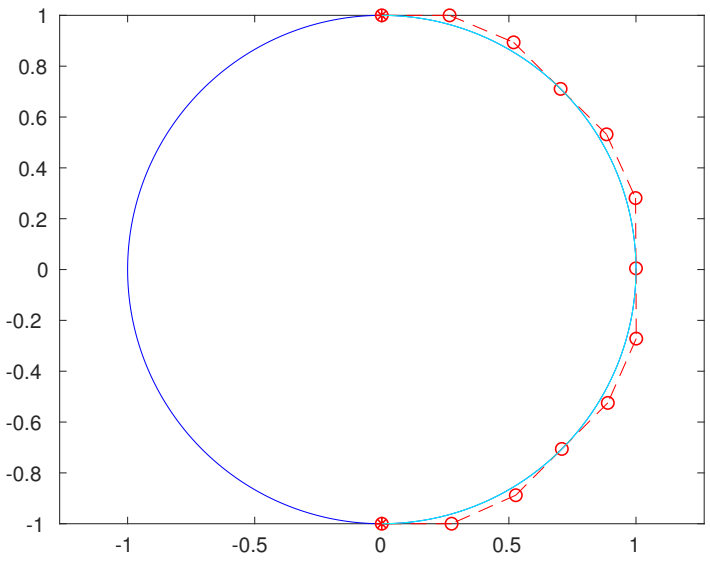

Fig. 5.19: Step 8 in Example 5.5: the local minimum $\tilde{\gamma}_4 \in B_{4,3}$ of $F\mid_{B_{4,3}}$ from the initial curve $\gamma_4 \in B_{4,3}$.

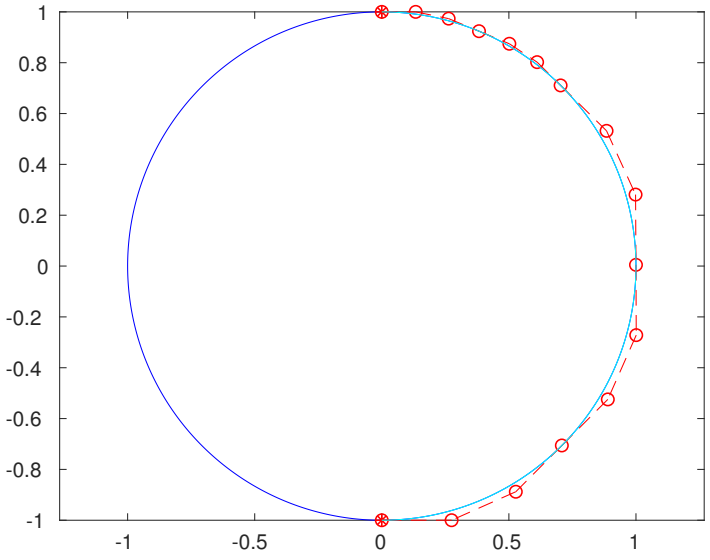

Fig. 5.20: Step 9 in Example 5.5: split at the first piece and parametrize $\gamma_4 \in B_{4,3}$ to become $\gamma_5 \in B_{5,3}$.

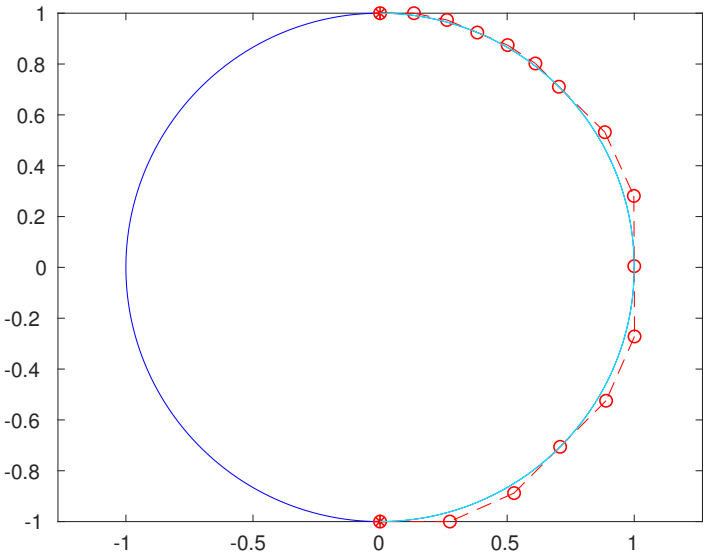

Fig. 5.21: Step 10 in Example 5.5: the local minimum $\tilde{\gamma}_5 \in B_{5,3}$ of $F\mid_{B_{5,3}}$ from the initial curve $\gamma_5 \in B_{5,3}$.

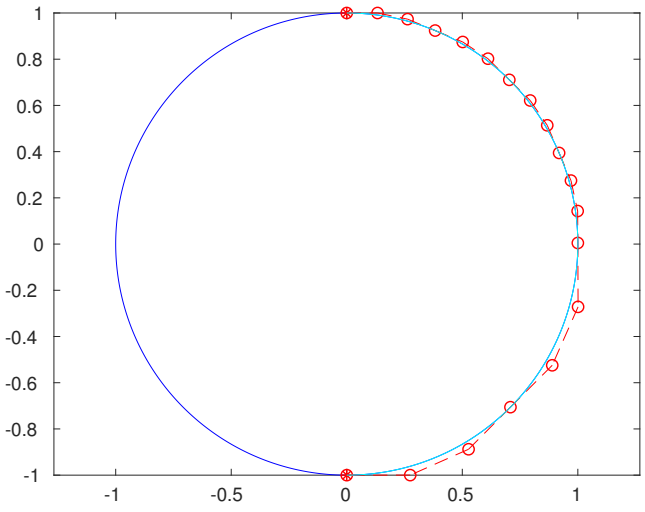

Fig. 5.22: Step 11 in Example 5.5: split at the third piece and reparametrize $\tilde{\gamma}_5 \in B_{5,3}$ to become $\gamma_6 \in B_{6,3}$.

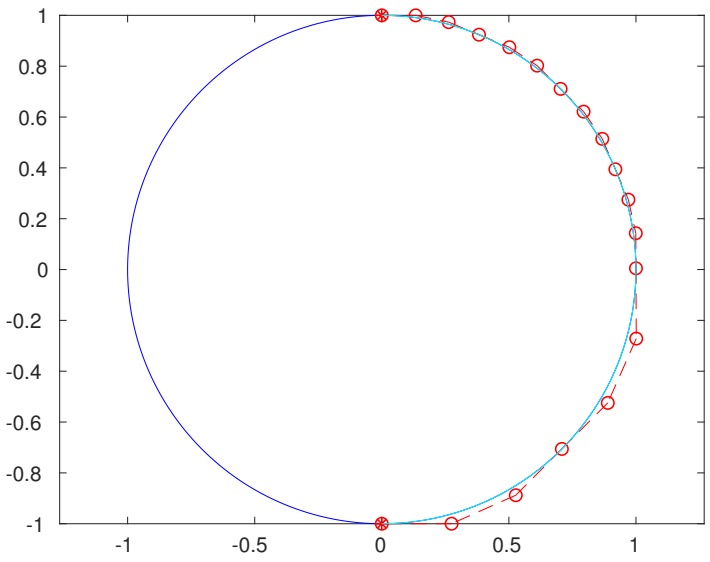

Fig. 5.23: Step 12 in Example 5.5: the local minimum $\tilde{\gamma}_6 \in B_{6,3}$ of $F\mid_{B_{6,3}}$ from the initial curve $\gamma_6 \in B_{6,3}$.

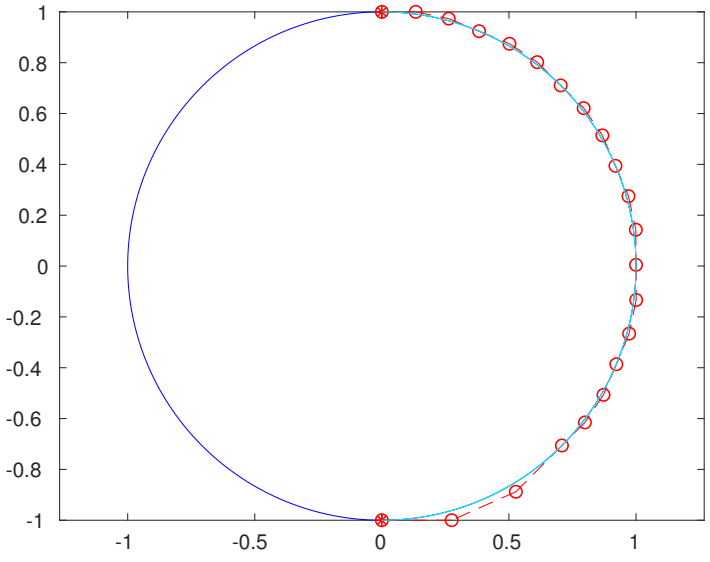

Fig. 5.24: Step 13 in Example 5.5: split at the fifth piece and reparametrize $\tilde{\gamma}_6 \in B_{6,3}$ to become $\gamma_7 \in B_{7,3}$.

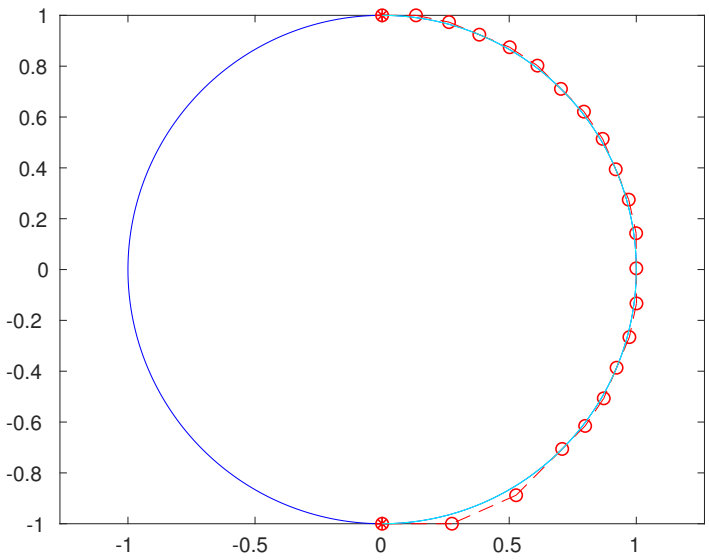

Fig. 5.25: Step 14 in Example 5.5: the local minimum $\tilde{\gamma}_7 \in B_{7,3}$ of $F\mid_{B_{7,3}}$ from the initial curve $\gamma_7 \in B_{7,3}$.

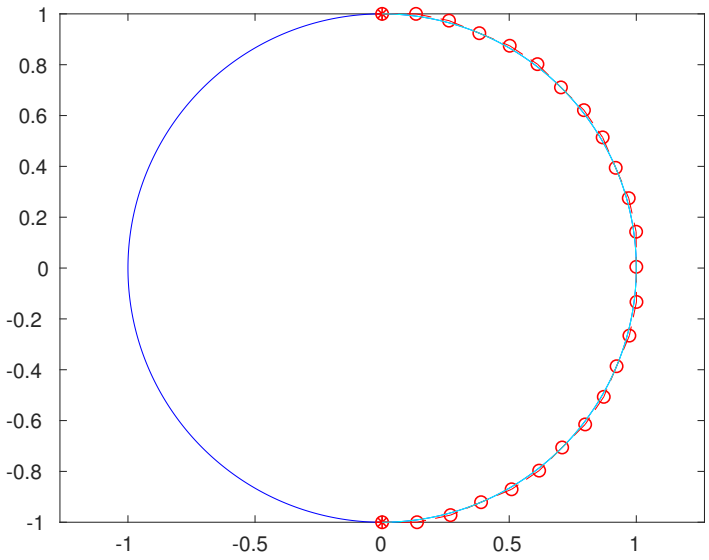

Fig. 5.26: Step 15 in Example 5.5: split at the seventh piece and reparametrize $\gamma_7 \in B_{7,3}$ to become $\gamma_8 \in B_{8,3}$.

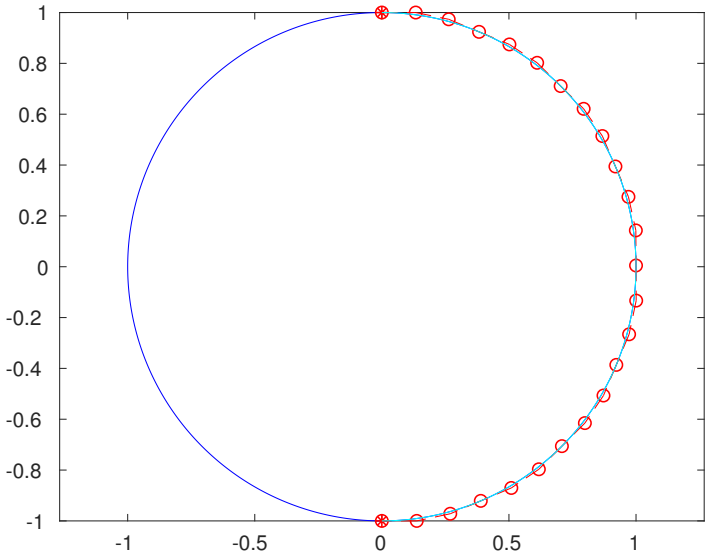

Fig. 5.27: Step 18 in Example 5.5: the local minimum $\tilde{\gamma}_8 \in B_{8,3}$ of $F\mid_{B_{8,3}}$ from the initial curve $\gamma_8 \in B_{8,3}$.

Summary: We have a table of values and some notations when using Algorithm 2 to approximate the optimal trajectory in Example 5.5:

	$\lvert F(\tilde{\gamma}_i) - F(\alpha)\rvert$	$\lvert F(\tilde{\gamma}_i) - F(\gamma_i)\rvert$	$\frac{F(\tilde{\gamma}_i)}{F(\gamma_i)}$	$\lVert\tilde{\gamma}_i - \gamma_i\rVert_2^{B_{i,3}}$
$i=1$	0.0074	4.6726	$1.5811.10^{-3}$	4.0479
$i=2$	$1.0438.10^{-04}$	0.0072	$1.4105.10^{-2}$	0.1423
$i=3$	$6.4337.10^{-05}$	$4.0043.10^{-5}$	0.6163	0.0056
$i=4$	$1.4791.10^{-05}$	$4.9546.10^{-5}$	0.2298	0.0017
$i=5$	$1.3482.10^{-05}$	$1.309.10^{-6}$	0.9115	$7.4317.10^{-05}$
$i=6$	$9.6766.10^{-06}$	$3.8054.10^{-6}$	0.7177	$1.1210.10^{-04}$
$i=7$	$6.4016.10^{-06}$	$3.275.10^{-6}$	0.6615	$5.5171.10^{-05}$
$i=8$	$2.3964.10^{-06}$	$4.0052.10^{-6}$	0.3743	$4.7458.10^{-05}$

- $\gamma_i \in B_{i,3}$ is a reparametrization of $\tilde{\gamma}_{i-1} \in B_{i-1,3}$. Since F is invariant under reparametrization, we have $F(\gamma_i) = F(\tilde{\gamma}_{i-1})$.
- Each step from $\tilde{\gamma}_i$ to $\tilde{\gamma}_{i+1}$, the number of pieces increases one piece and the number of control points increases 3 points.
- The decrease of $\lvert F(\tilde{\gamma}_i) - F(\alpha)\rvert$ at step $i = 3$ and at step $i = 4$ are quite

similar because these steps split each piece of $\tilde{\gamma}_2$ and optimize respectively.

- The value of $\|\tilde{\gamma}_i - \gamma_i\|_2^{B_{i,3}}$ at step $i = 3$ and at step $i = 4$ are quite similar because these steps split each piece of $\tilde{\gamma}_2$ and optimize respectively.

- The decrease of $|F(\tilde{\gamma}_i) - F(\alpha)|$ at step $i = 5$, at step $i = 6$, at step $i = 7$ and at step $i = 8$ are quite similar because these steps split each piece of $\tilde{\gamma}_4$ and optimize respectively.

- The value of $\|\tilde{\gamma}_i - \gamma_i\|_2^{B_{i,3}}$ at step $i = 5$, at step $i = 6$, at step $i = 7$ and at step $i = 8$ are quite similar because these steps split each piece of $\tilde{\gamma}_4$ and optimize respectively.

- When the value of $\|\tilde{\gamma}_i - \gamma_i\|_2^{B_{i,3}}$ is small enough, $|F(\tilde{\gamma}_i) - F(\gamma_i)|$ is very small.

- At $i - 1$, we split and reparametrize $\tilde{\gamma}_{i-1} \in B_{i-1,3}$ at one piece to become $\gamma_i \in B_{i,3}$. Then we use **Fmincon** in Matlab to find the local minimum $\tilde{\gamma}_i \in B_{i,3}$ from the initial curve $\gamma_i \in B_{i,3}$.

- At Step 9 and Step 10, we split $\tilde{\gamma}_4$ at the first piece, reparametrize to become $\gamma_5 \in B_{5,3}$ and then find the local minimum $\tilde{\gamma}_5 \in B_{5,3}$. We see that $\|\tilde{\gamma}_5 - \gamma_5\|_2^{B_{5,3}}$ and $|F(\tilde{\gamma}_5) - F(\gamma_5)|$ are very small. This means we can not improve the curve by splitting the first piece of $\tilde{\gamma}_4$. So we remember the first piece and the second piece of $\tilde{\gamma}_5$ in the set I and stop splitting these pieces in the next steps.

- At Step 11 and Step 12, we split $\tilde{\gamma}_5$ at the third piece, reparametrize to become $\gamma_6 \in B_{6,3}$ and then find the local minimum $\tilde{\gamma}_6 \in B_{6,3}$. We see that $\|\tilde{\gamma}_6 - \gamma_6\|_2^{B_{6,3}}$ and $|F(\tilde{\gamma}_6) - F(\gamma_6)|$ are very small. This means we can not improve the curve by splitting the third piece of $\tilde{\gamma}_5$. So we remember the third piece and the fourth piece of $\tilde{\gamma}_6$ in the set I and stop splitting these pieces in the next steps.

- At Step 13 and Step 14, we split $\tilde{\gamma}_6$ at the fifth piece, reparametrize to become $\gamma_7 \in B_{7,3}$ and then find the local minimum $\tilde{\gamma}_7 \in B_{7,3}$. We see that $\|\tilde{\gamma}_7 - \gamma_7\|_2^{B_{7,3}}$ and $|F(\tilde{\gamma}_7) - F(\gamma_7)|$ are very small. This means we can not improve the curve by splitting the third piece of $\tilde{\gamma}_6$. So we remember the fifth piece and the sixth piece of $\tilde{\gamma}_7$ in the set I and stop splitting these pieces in the next steps.

- At Step 15 and Step 16, we split $\tilde{\gamma}_7$ at the seventh piece, reparametrize to become $\gamma_8 \in B_{8,3}$ and then find the local minimum $\tilde{\gamma}_8 \in B_{8,3}$. We see that

$\|\tilde{\gamma}_8 - \gamma_8\|_2^{B_{8,3}}$ and $|F(\tilde{\gamma}_8) - F(\gamma_8)|$ are very small. This means we can not improve the curve by splitting the seventh piece of $\tilde{\gamma}_7$. So we remember the seventh piece and the eighth piece of $\tilde{\gamma}_8$ in the set I and stop splitting these pieces in the next steps.

- After Step 16, all piece indexes of $\tilde{\gamma}_8$ belongs I. This means that we can not improve the curve. Then the algorithm stops and we obtain an approximation $\tilde{\gamma}_8$ of the semi circle α going from A to B.

We next consider some examples of trajectory optimization problems.

5.2 Some examples of trajectory optimization problems

In this section, we present some instances of trajectory optimization problems. We are going to use piecewise uniform cubic Bézier curves and Algorithm 2 to approximate optimal trajectories. These trajectory optimization problems is applied to the movement of robots.

We consider the problem: Given two points $A, B \in \mathbb{R}^2$ and a compact set $\Sigma \subset \mathbb{R}^2$. For a continuously differentiable curve $\gamma : [0,1] \to \mathbb{R}^2$, we define our objective function F by

$$F(\gamma) = \int_0^1 \frac{\|\dot{\gamma}(t)\|_2}{d(\gamma(t), \Sigma)} dt,$$

where $\|\cdot\|_2$ is the Euclidean norm on $\mathbb{R}^2$ and $d(\gamma(t), \Sigma) = \min_{P \in \Sigma} \|\gamma(t) - P\|_2$ for $t \in [0,1]$. We want to find a continuously differentiable curve γ going from A to B such that γ is a local minimum of F.

Piecewise uniform cubic Bézier curves are continuously differentiable everywhere except at a countable set of points. We use piecewise uniform cubic Bézier curves, Algorithm 2 and Matlab to approximate optimal trajectories of this problem.

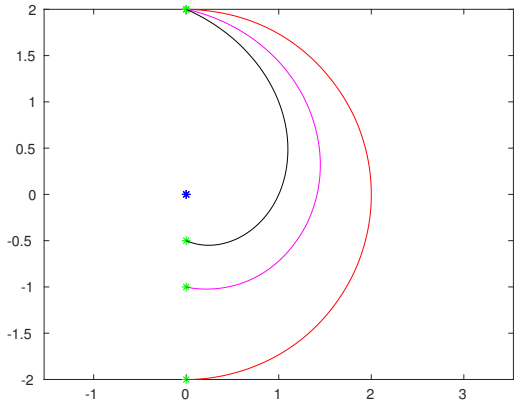

Fig. 5.28: Some locally optimal trajectories as Σ is a point $\Sigma := \{O(0,0)\}$.

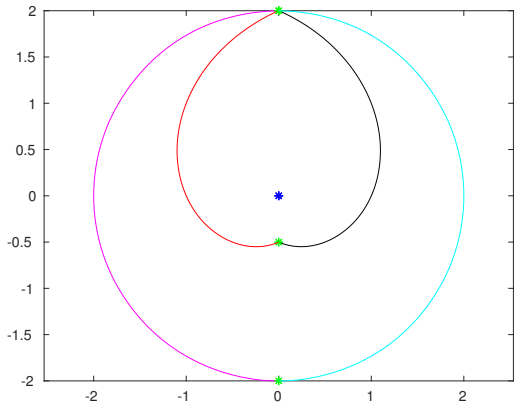

Fig. 5.29: Some locally optimal trajectories as Σ is a point $\Sigma := \{O(0,0)\}$.

5.2.1 Case Σ is a point

Given two points A, B and a set $\Sigma := \{O(0,0)\}$. For a continuously differentiable curve $\gamma : [0,1] \to \mathbb{R}^2$, we define our objective function F by

$$F(\gamma) = \int_0^1 \frac{\|\dot{\gamma}(t)\|_2}{\|\gamma(t) - O\|_2} dt.$$

We want to find a continuously differentiable curve γ going from A to B such that γ is a local minimum of F.

Using piecewise uniform cubic Bézier curves, Algorithm 2 and Matlab, we can approximate optimal trajectories of this problem (see Figures 5.28 and 5.29). We have some remarks about this problem as following:

Remark 5.6.

- We find a curve γ_0 connecting A and B such that γ_0 is as far $\Sigma := \{O\}$ as good and γ_0 is also as short as good.
- For two points A, B, there are two locally optimal trajectories connecting A and B.
- When the initial curve is near the locally optimal trajectory Γ_0, the output of the algorithm is an approximation of Γ_0.
- If γ contains O, then the code stops at γ since $F(\gamma) = \infty$. But γ containing M or N is not a locally optimal trajectory.
- If $d(A, O) = d(B, O)$, optimal trajectories are arcs of circles.
- An optimal trajectory is not always an arc of a circle.

5.2.2 Case Σ is two points

Given two points A, B and a set $\Sigma := \{M, N\}$. For a continuously differentiable curve $\gamma : [0, 1] \to \mathbb{R}^2$, we define our objective function F by

$$F(\gamma) = \int_0^1 \frac{\|\dot{\gamma}(t)\|_2}{d(\gamma(t), \Sigma)} dt,$$

where $d(\gamma(t), \Sigma) = \min\{\|\gamma(t) - M\|_2, \|\gamma(t) - N\|_2\}$. We want to find a continuously differentiable curve γ going from A to B such that γ is a local minimum of F.

Using piecewise uniform cubic Bézier curves, Algorithm 2 and Matlab, we can approximate optimal trajectories of this problem (see Figures 5.30 and 5.31). We have some remarks about this problem as following:

Remark 5.7.

- We find a curve γ_0 connecting A and B such that γ_0 is as far $\Sigma := \{M, N\}$ as good and γ_0 is also as short as good.
- This example has four locally optimal trajectories.
- When the initial curve is near the locally optimal trajectory Γ_0, the output of the algorithm is an approximation of Γ_0.

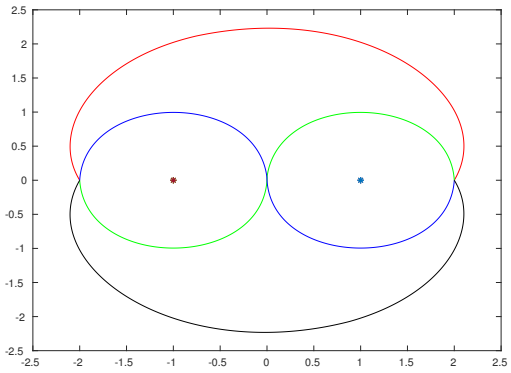

Fig. 5.30: Four locally optimal trajectories which go from $A(-2,0)$ to $B(2,0)$ as Σ is two points $\Sigma := \{M(-1,0), N(1,0)\}$.

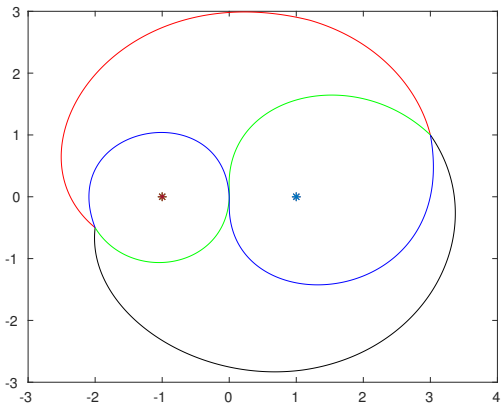

Fig. 5.31: Four locally optimal trajectories which go from $A(-2,-0.5)$ to $B(3,1)$ as Σ is two points $\Sigma := \{M(-1,0), N(1,0)\}$.

- At each $t \in [0,1]$, $d(\gamma(t), \Sigma)$ exists uniquely because $\Sigma := \{M, N\}$ is a compact set.
- If γ contains M or N, then the code stops at γ since $F(\gamma) = \infty$. But γ containing M or N is not a locally optimal trajectory.

We note that a local optimal trajectory of this problem is not always an arc of a circle. For example, let us consider $\Sigma := \{M(-1,0), N(1,0)\}$. We will consider two cases of A, B as follows:

- Case 1: $A = (1,2)$ and $B = (1,-2)$.

  In this case, we found a local optimal trajectory being a half circle (the magenta curve in Figure 5.32).

- Case 2: $A = (1,2)$ and $B = (1,-1)$.

  In this case, we found a local optimal trajectory γ_1 (the red curve in Figure 5.32) and we have $F(\gamma_1) = 3.2172$.

  The half circle γ_2 (the black curve in Figure 5.32) connecting A and B has the following formula

$$\begin{cases} x = 1 + 1.5\cos\left(\dfrac{\pi}{2} - \pi t\right) \\ y = 0.5 + 1.5\sin\left(\dfrac{\pi}{2} - \pi t\right), \end{cases} \quad t \in [0,1].$$

  We have $F(\gamma_2) = 3.2348 > F(\gamma_1) = 3.2172$.

  So, the arc γ_2 is not a local optimal trajectory.

5.2.3 Case Σ is a segment

Given two points A, B and a segment $\Sigma := \overline{MN}$. For a continuously differentiable curve $\gamma : [0,1] \to \mathbb{R}^2$, we define our objective function F by

$$F(\gamma) = \int_0^1 \frac{\|\dot{\gamma}(t)\|_2}{d(\gamma(t), \Sigma)} dt,$$

where $d(\gamma(t), \Sigma) = \min_{P \in \Sigma} \|\gamma(t) - P\|_2$. We want to find a continuously differentiable curve γ going from A to B such that γ is a local minimum of F.

Using piecewise uniform cubic Bézier curves, Algorithm 2 and Matlab, we can approximate optimal trajectories of this problem (see Figures 5.33 and 5.34). We have some remarks about this problem as following:

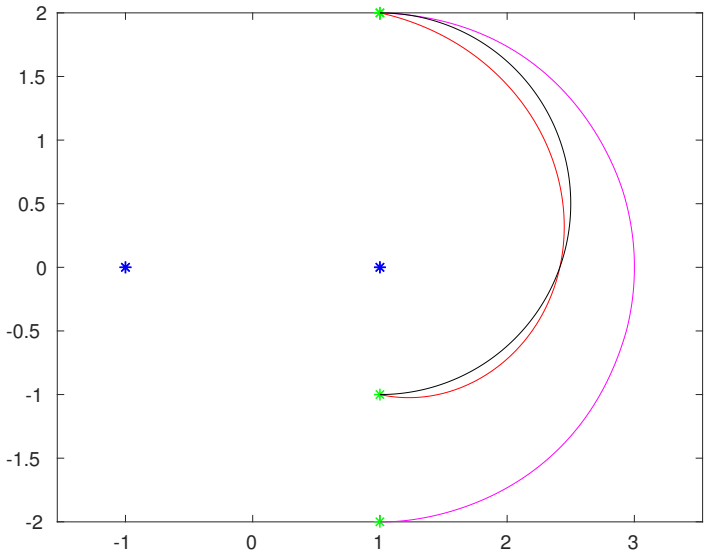

Fig. 5.32: $\Sigma := \{M(-1,0), N(1,0)\}$: red curve and magenta curve are two optimal trajectories, black curve (a half circle) is not a optimal trajectory.

Remark 5.8.

- We find a curve γ_0 connecting A and B such that γ_0 is as far the segment $\Sigma := \overline{MN}$ as good and γ_0 is also as short as good.
- This example has two locally optimal trajectories.
- When the initial curve is near the locally optimal trajectory Γ_0, the output of the algorithm is an approximation of Γ_0.
- At each $t \in [0,1]$, $d(\gamma(t), \Sigma)$ always exists uniquely because the segment $\Sigma := \overline{MN}$ is a compact set.
- If γ contains a point in the segment $\Sigma := \overline{MN}$, then the code stops at γ since $F(\gamma) = \infty$. But γ is not a locally optimal trajectory.

5.2.4 Case Σ is three points

Given two points A, B and a set $\Sigma = \{M, N, K\}$. For a continuously differentiable curve $\gamma : [0,1] \to \mathbb{R}^2$, we define our objective function F by

$$F(\gamma) = \int_0^1 \frac{\|\dot{\gamma}(t)\|_2}{d(\gamma(t), \Sigma)} dt,$$

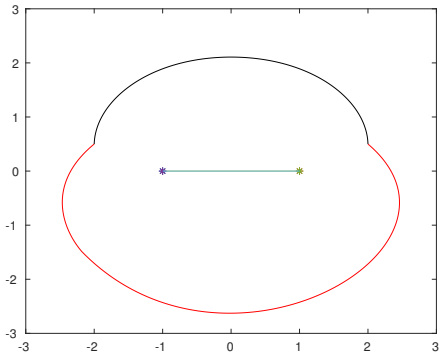

Fig. 5.33: Two locally optimal trajectories which go from $A(-2, 0.5)$ to $B(2, 0.5)$ as Σ is the segment $M(-1, 0)N(1, 0)$.

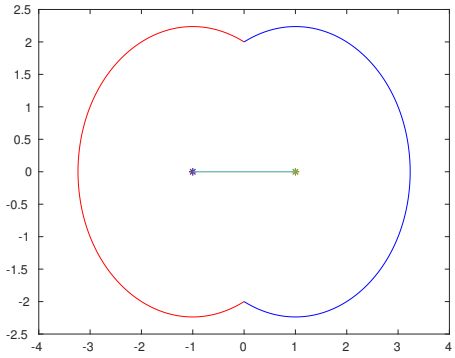

Fig. 5.34: Two locally optimal trajectories which go from $A(0, -2)$ to $B(0, 2)$ as Σ is the segment $M(-1, 0)N(1, 0)$.

where $d(\gamma(t)\Sigma) = \min\left\{\|\gamma(t) - M\|_2, \|\gamma(t) - N\|_2, \|\gamma(t) - K\|_2\right\}$. We want to find a continuously differentiable curve γ going from A to B such that γ is a local minimum of F.

Using piecewise uniform cubic Bézier curves, Algorithm 2 and Matlab, we can approximate optimal trajectories of this problem (see Figures 5.35). We have some remarks about this problem as following:

Remark 5.9.

- We find a curve γ_0 connecting A and B such that γ_0 is as far $\Sigma := \{M, N, K\}$ as good and γ_0 is also as short as good.
- This example has six locally optimal trajectories.

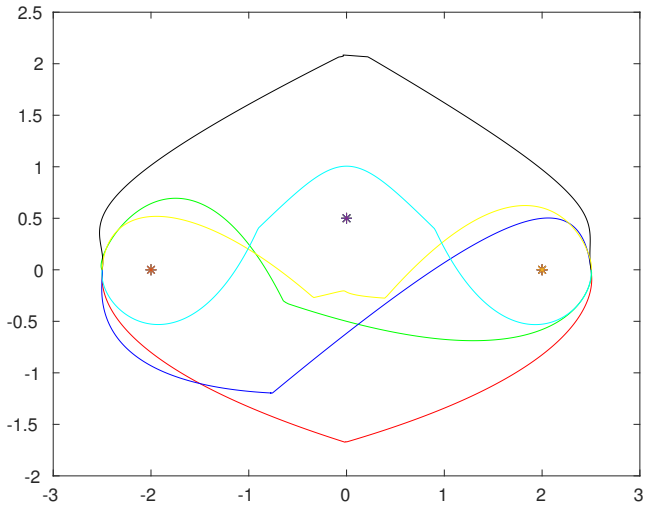

Fig. 5.35: Six locally optimal trajectories which go from $A(-2.5, 0)$ to $B(2.5, 0)$ as Σ is three points $M(-2, 0), N(2, 0), K(0, 0.5)$.

- When the initial curve is near the locally optimal trajectory Γ_0, the output of the algorithm is an approximation of Γ_0.
- At each $t \in [0, 1]$, $d(\gamma(t), \Sigma)$ always exists uniquely because $\Sigma := \{M, N, K\}$ is a compact set.
- If γ contains M or N or K, then the code stops at γ since $F(\gamma) = \infty$. But γ is not a locally optimal trajectory.

5.2.5 Case Σ is a triangle

Given two points A, B and a triangle $\Sigma := \triangle MNK$. For a continuously differentiable curve $\gamma : [0, 1] \to \mathbb{R}^2$, we define our objective function F by

$$F(\gamma) = \int_0^1 \frac{\|\dot{\gamma}(t)\|_2}{d(\gamma(t), \Sigma)} dt,$$

where $d(\gamma(t), \Sigma) = \min_{P \in \Sigma} \|\gamma(t) - P\|_2$. We want to find a continuously differentiable curve γ going from A to B such that γ is a local minimum of F.

Using piecewise uniform cubic Bézier curves, Algorithm 2 and Matlab, we can approximate optimal trajectories of this problem (see Figures 5.36 and 5.37). We have some remarks about this problem as following:

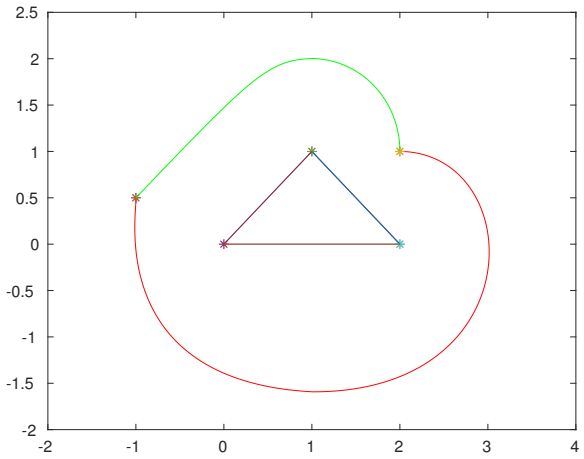

Fig. 5.36: Two locally optimal trajectories which go from $A(-1, 0.5)$ to $B(2, 1)$ as Σ is the triangle $M(0, 0)N(1, 1)K(2, 0)$

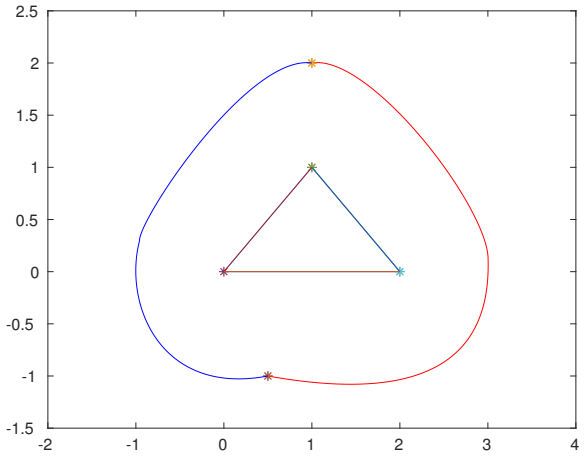

Fig. 5.37: Two locally optimal trajectories which go from $A(0.5, -1)$ to $B(1, 2)$ as Σ is the triangle $M(0, 0)N(1, 1)K(2, 0)$

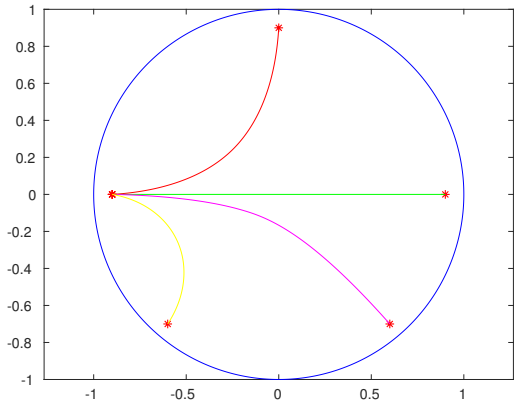

Fig. 5.38: Some optimal trajectories as Σ is the unit circle

Remark 5.10.

- We find a curve γ_0 connecting A and B such that γ_0 is as far $\Sigma := \triangle MNK$ as good and γ_0 is also as short as good.
- This example has two locally optimal trajectories.
- When the initial curve is near the locally optimal trajectory Γ_0, the output of the algorithm is an approximation of Γ_0.
- At each $t \in [0,1]$, $d(\gamma(t), \Sigma)$ always exists uniquely because the triangle $\Sigma := \triangle MNK$ is a compact set.
- If γ contains a point lying on the triangle $\triangle MNK$ then the code stops at γ since $F(\gamma) = \infty$. But γ is not a locally optimal trajectory.

5.2.6 Case Σ is the unit circle

Given the unit circle Σ on the plane and two points A, B inside the unit circle Σ. For a continuously differentiable curve $\gamma : [0,1] \to \mathbb{R}^2$, we define our objective function F by

$$F(\gamma) = \int_0^1 \frac{\|\dot{\gamma}(t)\|_2}{d(\gamma(t), \Sigma)} dt,$$

where $d(\gamma(t), \Sigma) = \min_{P \in \Sigma} \|\gamma(t) - P\|_2$. We want to find a continuously differentiable curve γ going from A to B such that γ is a local minimum of F.

Using piecewise uniform cubic Bézier curves, Algorithm 2 and Matlab, we can approximate optimal trajectories of this problem (see Figures 5.38). We have some remarks about this problem as following:

Remark 5.11.

- We find a curve γ_0 connecting A and B such that γ_0 is as far the unit circle Σ as good and γ_0 is also as short as good.

- For any two points A, B inside the unit circle, there is an optimal trajectory connecting A and B.

- At each $t \in [0, 1]$, $d(\gamma(t), \Sigma)$ always exists uniquely since the unit circle Σ is a compact set.

- If γ contains a point lying on the unit circle Σ, then the code stops at γ since $F(\gamma) = \infty$. But γ is not a optimal trajectory.

Given two district points A, B inside the unit circle, the optimal trajectory connecting A and B is the geodesic of them. The length of the geodesic is defined as the distance between A and B. The unit circle with this geodesic distance is called Poincaré disk model. The Poincaré disk model is a classical model of 2-dimensional hyperbolic geometry ([4, chapter 4, p. 117], [77, chapter 25, p. 489]).

5.3 Autonomous ordinary differential equation

In this section, we study the relation between the autonomous ordinary differential equation and the trajectory optimization problem. Then we propose a method to approximate orbits of autonomous ordinary differential equations.

The method is not really to compute solutions of the autonomous ODE. The interesting point is that we can compute orbits of autonomous ordinary differential equations in an accurate way avoiding some difficulties arising from parametrization.

Once the orbit is known, we do not need to compute quadrature formula to have numerical approximation of the solution. Locally, at any point, its enough to recall the derivative to have the same norm as the vector field.

5.3.1 Theoretical basis

An *autonomous ordinary differential equation* is a system of ordinary differential equations of the form

$$\dot{X}(t) = f(X(t)).$$

This system is said to be autonomous because the right hand side of the differential system does not depend explicitly on t.

We consider an autonomous ordinary differential equation together with initial condition as follows

$$\begin{cases} \dot{X}(t) = f(X(t)) \\ X(t_0) = X_0, \end{cases} \tag{5.1}$$

where $f : U \to TU$, $U \subset \mathbb{R}^n$, $I \subset \mathbb{R}$, $t_0 \in I$ and $X_0 \in U$.

We refer [91, Chapter 2, p. 7], [29, Chapter IX, p. 400] for a complete description of this problem.

Following [21, p. 2], they define the *orbit* of the solution $X : I \to U$ to be the set

$$\mathcal{O}_X := \{X(t) |\ t \in I\}.$$

We will propose a way to find solution orbits of the autonomous ordinary differential equation together with initial condition. Then we use our method using piecewise uniform cubic Bézier curves to approximate solution orbits.

Proposition 5.12. Let U be a subset in $\mathbb{R}^n$, $X_0 \in U$ and $I = [t_0, t_1) \subset \mathbb{R}$. Let $f : U \to TU$ be a Lipschitz continuous function. We consider the following autonomous ordinary differential equation together with initial condition

$$\begin{cases} \dot{X}(t) = f(X(t)), \forall t \in I \\ X(t_0) = X_0. \end{cases} \tag{5.2}$$

If $\gamma : [0, 1] \to U$ is a continuously differentiable function such that $\dot{\gamma}(v) \neq 0$ for all $v \in [0, 1]$ and

$$\begin{cases} F_f(\gamma) = \int\limits_0^1 (\|\dot{\gamma}(v)\|_2 . \|f(\gamma(v))\|_2 - \langle \dot{\gamma}(v), f(\gamma(v)) \rangle)\, dv = 0, \\ \gamma(0) = X_0, \end{cases} \tag{5.3}$$

then there exists an increasing differentiable function $\varphi : I \to [0, 1]$ such that $\gamma \circ \varphi$ is a solution of (5.2).

Proof. We have

$$F_f(\gamma) = \int_0^1 (\|\dot{\gamma}(v)\|_2.\|f(\gamma(v))\|_2 - \langle \dot{\gamma}(v), f(\gamma(v))\rangle)\, dv = 0.$$

Since γ and f are continuous,

$$\begin{aligned} &\|\dot{\gamma}(v)\|_2.\|f(\gamma(v))\|_2 - \langle \dot{\gamma}(v), f(\gamma(v))\rangle = 0, \forall v \in [0,1] \\ \Rightarrow &\cos(\dot{\gamma}(v), f(\gamma(v))) = 1, \forall v \in [0,1]. \end{aligned}$$

This means that for every $v \in [0,1]$, $\dot{\gamma}(v)$ and $f(\gamma(v))$ are collinear and in the same direction.

We need to show that there exists $\varphi : I \to [0,1]$ such that $\gamma \circ \varphi$ is a solution of 5.2. This means

$$\begin{aligned} &\begin{cases} (\dot{\gamma} \circ \varphi)(t).\dot{\varphi}(t) = f((\gamma \circ \varphi)(t)) \\ \varphi(t_0) = 0 \end{cases} \\ \Rightarrow &\begin{cases} \dot{\varphi}(t) = \dfrac{\|f((\gamma \circ \varphi)(t))\|_2}{\|(\dot{\gamma} \circ \varphi)(t)\|_2} \\ \varphi(t_0) = 0. \end{cases} \end{aligned}$$

We consider the following one-dimensional differential equation

$$\begin{cases} \dot{\varphi} = h(t, \varphi) \\ \varphi(t_0) = 0, \end{cases} \tag{5.4}$$

where $h(t,\varphi) = \dfrac{\|f(\gamma(\varphi))\|_2}{\|\dot{\gamma}(\varphi)\|_2}$.

From the assumption of f, γ and [33, Theorem 8.5, p. 96], [33, Theorem 8.6, p. 96], the function h satisfies Lipschitz condition in the variable φ. Following [91, Theorem 1.1, p. 3], (5.4) exists a unique solution $\varphi : I \to [0,1]$. It is clear that $\varphi(t) \geq 0, \forall t \in I$.

Otherwise, if $\varphi : I \to [0,1]$ is solution of 5.4, we have

$$\|(\dot{\gamma} \circ \varphi)(t)\|_2.\dot{\varphi}(t) = \|f((\gamma \circ \varphi)(t))\|_2, \forall t \in I$$

and $\varphi(t_0) = 0$. Combining the fact that $\dot{\gamma}(v)$ and $f(\gamma(v))$ are colinear and in the same direction for every $v \in [0,1]$, we find that $\gamma \circ \varphi$ is solution of (5.2). □

From Proposition 5.12, we see that the continuously differentiable solutions of the system 5.3 differ from the solutions of the autonomous ordinary differential equation 5.2 by an increasing differentiable function. The solutions of the system 5.3 can be simpler than the solution of the autonomous ordinary differential equation 5.2. Let us consider the following example.

Example 5.13. Let $X_0 \in \mathbb{R}^2 \setminus \{(0,0)\}$. We introduce a function

$$\begin{aligned} f : \mathbb{R}^2 &\to T\mathbb{R}^2 \\ M &\mapsto -M. \end{aligned}$$

We consider the following autonomous ordinary differential equation

$$\begin{cases} \dot{X}(t) = f(X(t)) = -X(t), \forall t \in [0, \infty[\\ X(0) = X_0. \end{cases} \tag{5.5}$$

From Proposition 5.12, we can translate 5.5 to the following problem

$$\begin{cases} F_f(\gamma) = \int\limits_0^1 \left(\|\dot{\gamma}(t)\|_2 . \|-\gamma(t)\|_2 - \langle \dot{\gamma}(t), -\gamma(t) \rangle \right) dt = 0 \\ \gamma(0) = X_0. \end{cases} \tag{5.6}$$

Case 1: The function

$$\gamma_0(t) = X_0 - tX_0, \ t \in [0,1]$$

satisfies $F_f(\gamma_0) = 0$ and $\gamma_0(0) = X_0$. However, γ_0 is not a solution of (5.5). We show that there exists an increasing differentiable function $\varphi : I \to [0,1]$ such that $\gamma_0 \circ \varphi$ is a solution of (5.5).

From the proof of Proposition 5.12, the function φ is a solution of the following one-dimensional differential equation

$$\begin{cases} \dot{\varphi}(t) = \dfrac{\|-(X_0 - \varphi(t)X_0)\|_2}{\|-X_0\|_2} \\ \varphi(t_0) = 0 \end{cases}$$

$$\Rightarrow \begin{cases} \dot{\varphi}(t) = |1 - \varphi(t)| \\ \varphi(0) = 0. \end{cases}$$

Since $\varphi(t) \leq 1$, we have

$$\begin{cases} \dot{\varphi}(t) = -\varphi(t) + 1 \\ \varphi(t_0) = 0 \\ \varphi(t) \in [0,1]. \end{cases}$$

This is a linear differential equation with constant coefficients and we have the solution

$$\varphi_0(t) = -e^{-t} + 1,\ t \in I \equiv [0, \infty[.$$

It is clear that

$$Y_0(t) = (\gamma_0 \circ \varphi_0)(t) = e^{-t} X_0,\ t \in I \equiv [0, \infty[$$

is a solution of (5.5).

Case 2: The function

$$\gamma_1(t) = X_0 - \frac{1}{2} t X_0,\ t \in [0,1]$$

satisfies $F_f(\gamma_1) = 0$ and $\gamma_1(0) = X_0$. However, γ_1 is not a solution of (5.5). We show that there exists an increasing differentiable function $\varphi : I \to [0,1]$ such that $\gamma_1 \circ \varphi$ is a solution of (5.5).

Similarly, φ is a solution of the following one-dimensional differential equation

$$\begin{cases} \dot{\varphi}(t) = \dfrac{\left\| -(X_0 - \frac{1}{2}\varphi(t) X_0) \right\|_2}{\left\| -\frac{1}{2} X_0 \right\|_2} \\ \varphi(0) = 0 \end{cases}$$

$$\Rightarrow \begin{cases} \dot{\varphi}(t) = |2 - \varphi(t)| \\ \varphi(t_0) = 0. \end{cases}$$

Since $\varphi(t) \leq 1$, we have

$$\begin{cases} \dot{\varphi}(t) = -\varphi(t) + 2 \\ \varphi(t_0) = 0 \\ \varphi(t) \in [0,1]. \end{cases}$$

This is a linear differential equation with constant coefficients and we obtain the solution

$$\varphi_1(t) = -2e^{-t} + 2,\ t \in I \equiv [0, \ln 2].$$

It is easily seen that

$$Y_1(t) = (\gamma_0 \circ \varphi_1)(t) = e^{-t}X_0,\ t \in I \equiv [0, \ln 2]$$

is the solution of (5.5).

We remark that $\gamma_0(t) = X_0 - tX_0,\ t \in [0,1]$ and $\gamma_1(t) = X_0 - \frac{1}{2}tX_0,\ t \in [0,1]$ are linear. They are simpler than the solution of (5.5).

We note that

$$F_f(\gamma) = \int_0^1 (\|\dot{\gamma}(v)\|_2.\|f(\gamma(v))\|_2 - \langle \dot{\gamma}(v), f(\gamma(v))\rangle)\, dv$$

is always non-negative and invariant under reparametrization. Then, the system 5.3 can be considered as the following trajectory optimization problem

$$\begin{cases} F_f(\gamma) = \int_0^1 (\|\dot{\gamma}(v)\|_2.\|f(\gamma(v))\|_2 - \langle \dot{\gamma}(v), f(\gamma(v))\rangle)\, dv \\ \gamma(0) = X_0. \end{cases} \tag{5.7}$$

This means that we can find solution orbits of the autonomous ordinary differential equation 5.2 from the trajectory optimization problem 5.7. Piecewise uniform cubic Bézier curves are continuously differentiable everywhere except at a countable set of points. Thus, we use piecewise uniform cubic Bézier curves and Algorithm 2 to approximate solution orbits of the autonomous ordinary differential equation. We consider the following example and run Algorithm 2 step by step in order to illustrate the efficiency of our method.

Example 5.14. We consider the autonomous ordinary differential equation together with initial condition

$$\begin{cases} y_1' = -\dfrac{y_1^2 - 1}{y_1 - y_2} \\ y_2' = -\dfrac{y_2^2 - 1}{y_2 - y_1} \\ (y_1(0), y_2(0)) = (-0.2, 5). \end{cases}$$

We find a reparametrization of the solution by finding the minimum of the following

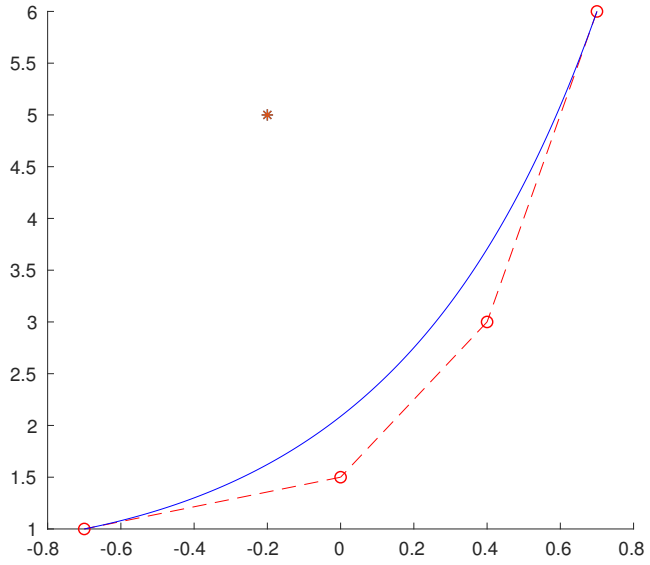

Fig. 5.39: Step 1 in Example 5.14: the initial curve $\gamma_1 \in B_{1,3}$.

problem

$$\begin{cases} F(\gamma) = \int_0^1 \left(\|\dot{\gamma}(t)\|_2 \, . \, \|f(\gamma(t))\|_2 - \langle \dot{\gamma}(t), f(\gamma(t)) \rangle \right) dt \\ \gamma(0) = (-0.2, 5), \end{cases}$$

where

$$\begin{aligned} f : \mathbb{R}^2 &\to T\mathbb{R}^2 \\ (y_1, y_2) &\mapsto \left(-\frac{y_1^2 - 1}{y_1 - y_2}, -\frac{y_2^2 - 1}{y_2 - y_1} \right). \end{aligned}$$

Using piecewise uniform cubic Bézier curves, Algorithm 2 and Matlab, we can approximate the solution orbit of this problem. We have the list of curves at each step (See Figures 5.39, Figures 5.40, Figures 5.41, Figures 5.42, Figures 5.43, Figures 5.44, Figures 5.45 and Figures 5.46).

Summary: We have a table of values and some notations when using Algorithm 2 to approximate the solution orbit in Example 5.14:

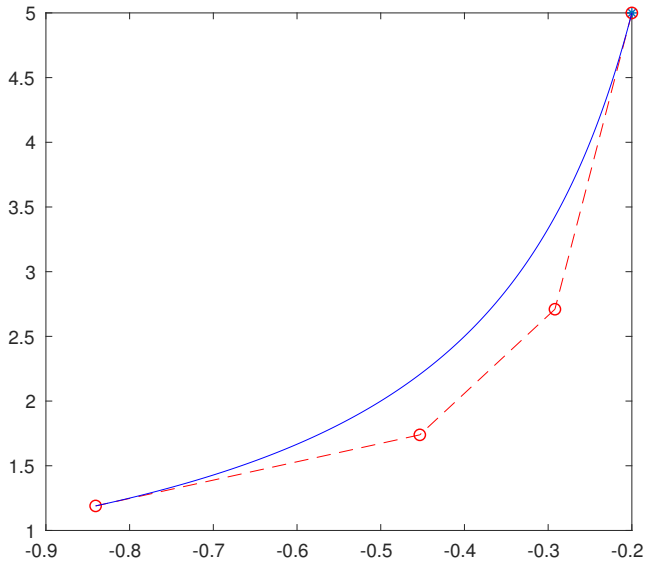

Fig. 5.40: Step 2 in Example 5.14: the local minimum $\tilde{\gamma}_1 \in B_{1,3}$ of $F\mid_{B_{1,3}}$ from the initial curve $\gamma_1 \in B_{1,3}$.

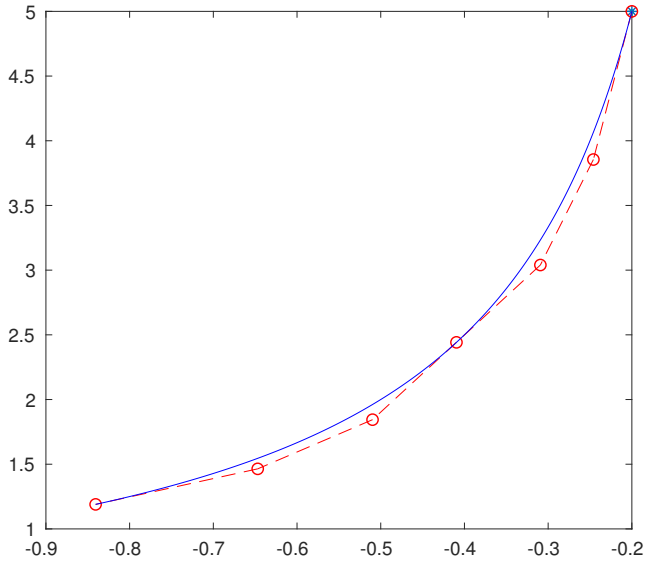

Fig. 5.41: Step 3 in Example 5.14: split and reparametrize $\tilde{\gamma}_1 \in B_{1,3}$ to become $\gamma_2 \in B_{2,3}$.

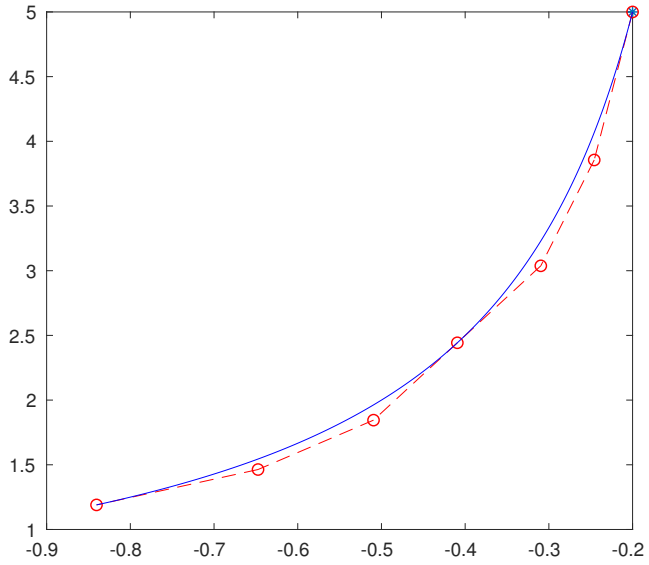

Fig. 5.42: Step 4 in Example 5.14: the local minimum $\tilde{\gamma}_2 \in B_{2,3}$ of $F\mid_{B_{2,3}}$ from the initial curve $\gamma_2 \in B_{2,3}$.

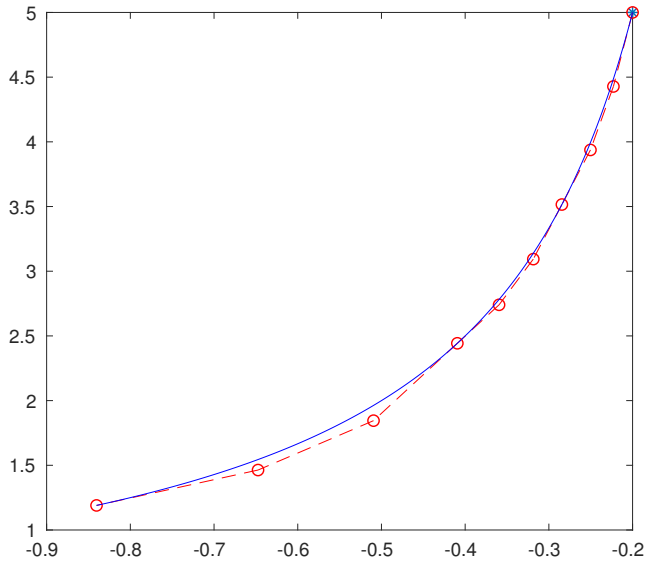

Fig. 5.43: Step 5 in Example 5.14: split at the first piece and reparametrize $\tilde{\gamma}_2 \in B_{2,3}$ to become $\gamma_3 \in B_{3,3}$.

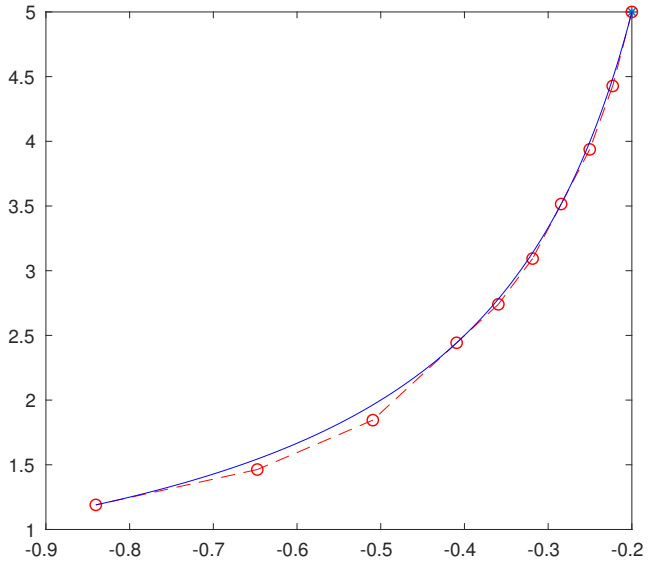

Fig. 5.44: Step 6 in Example 5.14: the local minimum $\tilde{\gamma}_3 \in B_{3,3}$ of $F\mid_{B_{3,3}}$ from the initial curve $\gamma_3 \in B_{3,3}$.

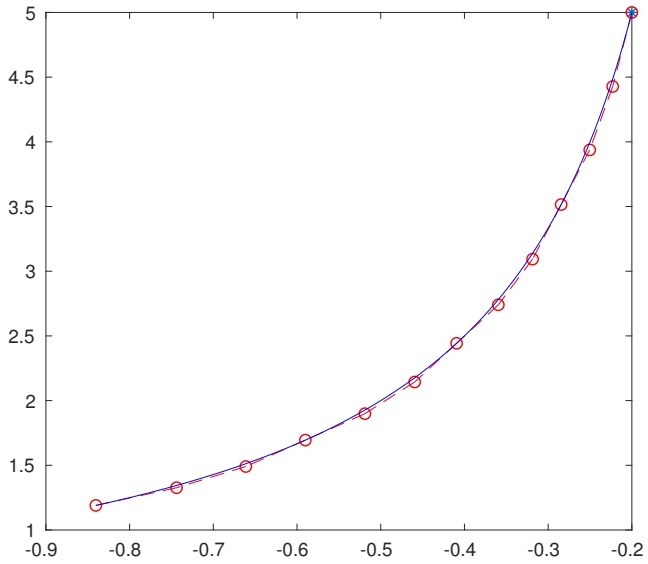

Fig. 5.45: Step 7 in Example 5.14: split at the third piece and reparametrize $\tilde{\gamma}_3 \in B_{3,3}$ to become $\gamma_4 \in B_{4,3}$.

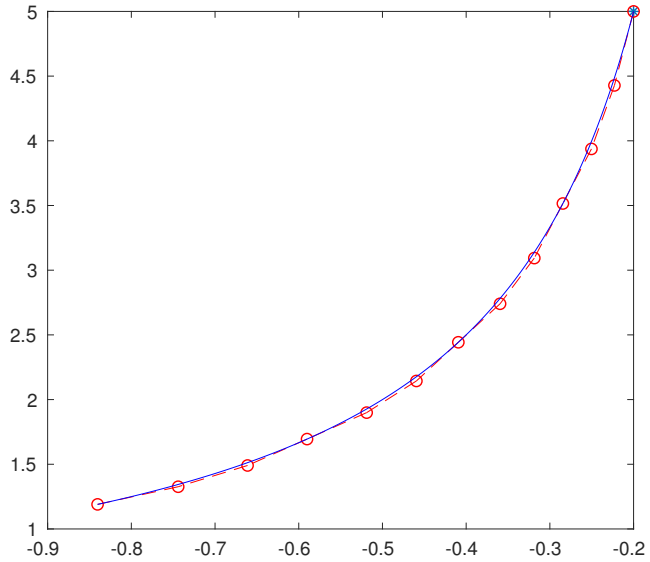

Fig. 5.46: Step 8 in Example 5.14: the local minimum $\tilde{\gamma}_4 \in B_{4,3}$ of $F\mid_{B_{4,3}}$ from the initial curve $\gamma_4 \in B_{4,3}$.

	$\lvert F(\tilde{\gamma}_i) - 0\rvert$	$\lvert F(\tilde{\gamma}_i) - F(\gamma_i)\rvert$	$\frac{F(\tilde{\gamma}_i)}{F(\gamma_i)}$	$\lVert\tilde{\gamma}_i - \gamma_i\rVert_2^{B_{i,3}}$
$i=1$	$2.9696.10^{-08}$	0.0989	$0.3002.10^{-6}$	1.6405
$i=2$	$3.2358.10^{-09}$	$2.6460.10^{-8}$	0.1089	0.0020
$i=3$	$2.3298.10^{-09}$	$0.906.10^{-9}$	0.7200	$1.3251.10^{-5}$
$i=4$	$1.7352.10^{-10}$	$2.1562.10^{-9}$	0.0744	$2.2561.10^{-4}$

- $\gamma_i \in B_{i,3}$ is a reparametrization of $\tilde{\gamma}_{i-1} \in B_{i-1,3}$. Since F is invariant under reparametrization, we have $F(\gamma_i) = F(\tilde{\gamma}_{i-1})$.
- Each step from $\tilde{\gamma}_i$ to $\tilde{\gamma}_{i+1}$, the number of pieces increases one piece and the number of control points increases 3 points.
- $\lvert F(\tilde{\gamma}_i) - F(\gamma_i)\rvert$ approaches to nearly zero as $i \to 4$.
- $\lVert\tilde{\gamma}_i - \gamma_i\rVert_2^{B_{i,3}}$ approaches to nearly zero as $i \to 4$.
- $F(\tilde{\gamma}_i)$ approaches to nearly zero as $i \to 4$.
- The rate of decrease of $\lvert F(\tilde{\gamma}_i) - 0\rvert$ slows down over each step.
- When the value of $\lVert\tilde{\gamma}_i - \gamma_i\rVert_2^{B_{i,3}}$ is small enough, $\lvert F(\tilde{\gamma}_i) - F(\gamma_i)\rvert$ is very small.

- The decrease of $|F(\tilde{\gamma}_i) - 0|$ at Step $i = 3$ and at Step $i = 4$ are quite similar because these steps split each piece of $\tilde{\gamma}_2$ and optimize respectively.

- The value of $\|\tilde{\gamma}_i - \gamma_i\|_2^{B_{i,3}}$ at Step $i = 3$ and at Step $i = 4$ are quite similar because these steps split each piece of $\tilde{\gamma}_2$ and optimize respectively.

- At $i - 1$, we split and reparametrize $\tilde{\gamma}_{i-1} \in B_{i-1,3}$ at one piece to become $\gamma_i \in B_{i,3}$. Then we use **Fmincon** in Matlab to find the local minimum $\tilde{\gamma}_i \in B_{i,3}$ from the initial curve $\gamma_i \in B_{i,3}$.

- At Step 5 and Step 6, we split $\tilde{\gamma}_2$ at the first piece, reparametrize to become $\gamma_3 \in B_{3,3}$ and then find the local minimum $\tilde{\gamma}_3 \in B_{3,3}$. We see that $\|\tilde{\gamma}_3 - \gamma_3\|_2^{B_{3,3}}$ and $|F(\tilde{\gamma}_3) - F(\gamma_3)|$ are very small. This means that we can not improve the curve by splitting the first piece of $\tilde{\gamma}_2$. So we remember the first piece and the second piece of $\tilde{\gamma}_3$ in the set I and stop splitting these pieces in the next steps.

- At Step 7 and Step 8, we split $\tilde{\gamma}_3$ at the third piece, reparametrize to become $\gamma_4 \in B_{3,3}$ and then find the local minimum $\tilde{\gamma}_4 \in B_{3,3}$. We see that $\|\tilde{\gamma}_4 - \gamma_4\|_2^{B_{4,3}}$ and $|F(\tilde{\gamma}_4) - F(\gamma_4)|$ are very small. This means that we can not improve the curve by splitting the third piece of $\tilde{\gamma}_3$. So we remember the third piece and fourth piece of $\tilde{\gamma}_4$ in the set I and stop splitting these pieces in the next steps.

- After Step 8, all piece indexes of $\tilde{\gamma}_4$ belong to I. This means that we can not improve the curve. Then the algorithm stops and we obtain $\tilde{\gamma}_4$ as an approximation of the solution orbit.

- The image of the curve found by our method is a piece of the solution orbit.

5.3.2 The choice of functions for the orbit approximation

We note that the choice $F_f(\gamma) = \int_0^1 (\|\dot{\gamma}(v)\|_2.\|f(\gamma(v))\|_2 - \langle \dot{\gamma}(v), f(\gamma(v))\rangle)\, dv$ is important because it removes "time" from the problem. It is clear that $F_f(\gamma) = F_f(\gamma \circ \delta)$ for all $\delta \in \mathrm{Diff}^+([0,1])$. Thus the function F_f is well defined over $\mathfrak{C}$. Our algorithm using F_f will stop when it reaches a parametrization of the solution. This means that our algorithm using F_f is to approximate solution orbits of autonomous ordinary differential equations.

It is not the case for $G_f(\gamma) = \int_0^1 \|\dot{\gamma}(v) - f(\gamma(v))\|_2 dv$. If we use G_f, the algorithm find a curve γ such that $\dot{\gamma}(v) = f(\gamma(v))$ for every $v \in [0,1]$. Thus the algorithm using G_f is to approximate the solution. It is obvious that the algorithm using G_f has more constraints than our method using F_f. This leads to some types of problems:

- Solutions given by the algorithm using G_f can be very local.
- Solutions given by the algorithm using G_f can be unstable.

Then the use F_f is more convenient to approximate the solution orbits of autonomous ordinary differential equations than the use G_f. Let us consider the following example to see the efficiency of F_f towards G_f.

Example 5.15. We consider the following autonomous ordinary differential equation

$$\begin{cases} x' = 1.5 + \cos 4x \\ y' = 0 \\ (x(0), y(0)) = (1, 0). \end{cases} \tag{5.8}$$

We run our method using $F_f(\gamma) = \int_0^1 \left(\|\dot{\gamma}(v)\|_2 . \|f(\gamma(v))\|_2 - \langle \dot{\gamma}(v), f(\gamma(v)) \rangle\right) dv$ and the method using $G_f(\gamma) = \int_0^1 \|\dot{\gamma}(v) - f(\gamma)\|_2 dv$ with the same inputs: the starting curve, ϵ using to stop the algorithm and then we get the results (see Figure 5.47). We have some remarks as follows:

Remark 5.16.

- The curve found by our method using F_f is longer than the curve found by the method using G_f.
- The curve found by our method using F_f is nearer the solution orbit than the curve found by the method using G_f.

Our approach is general. The regularity of F_f depends on the regularity of f. For instance, if $F_f(\gamma(t))$, for $\gamma \in B_{N,3}$, is differentiable with respect to the coordinates of control points, then we use gradient descent to find a local minimum of F_f. If $F_f(\gamma(t))$, for $\gamma \in B_{N,3}$, is two times differentiable, then we use, for instance, Newton's method to find a local minimum of F_f.

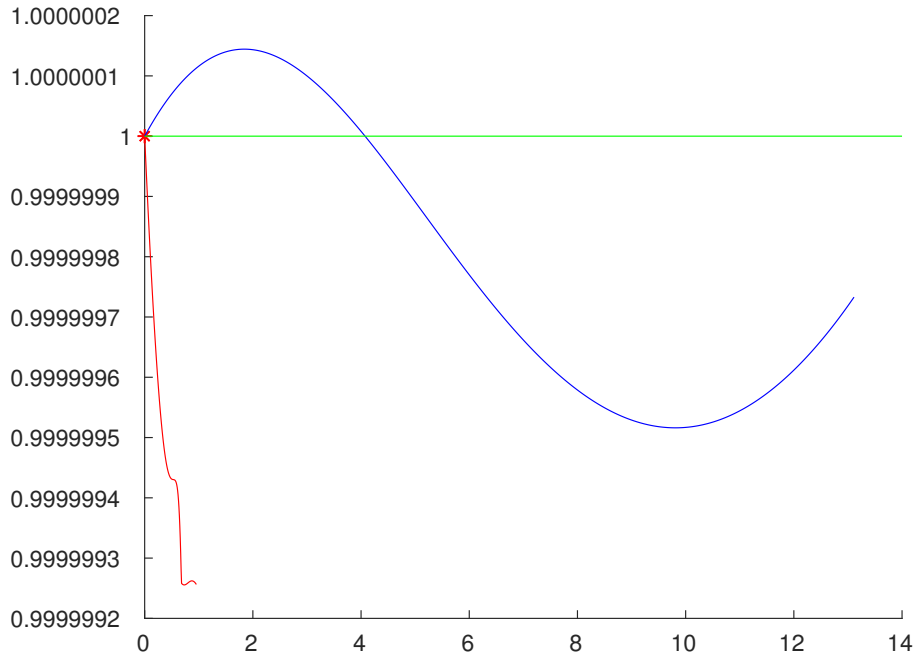

Fig. 5.47: The curve (blue curve) found by using F_f, the curve (red curve) found by using G_f and the solution orbit (green curve) of (5.8).

5.3.3 Computing a maximal solution

In this subsection, we introduce two methods in order to compute solution over a wide interval or a maximal solution when it is possible. One of the main drawback on the method proposed above is that we do not know the interval on which we are looking for a solution. The first ideas is to exploit the link between the length of the curve and the interval. The second idea is based on continuation method. Let us denote $E_{x_0} = \{\gamma \in Emb([0,1], U\}$. By

5.3.4 Comparison with classical methods

In this subsection, we compare our method and some classical methods. Note that we focus attention on orbits of autonomous ordinary differential equation. The Euler method and the Runge-Kutta method are two classical methods to approximate solutions of ordinary differential equations. We will present some examples such that our method is more effective than the Euler method and the Runge-Kutta method.

Example 5.17. We consider the following autonomous ordinary differential

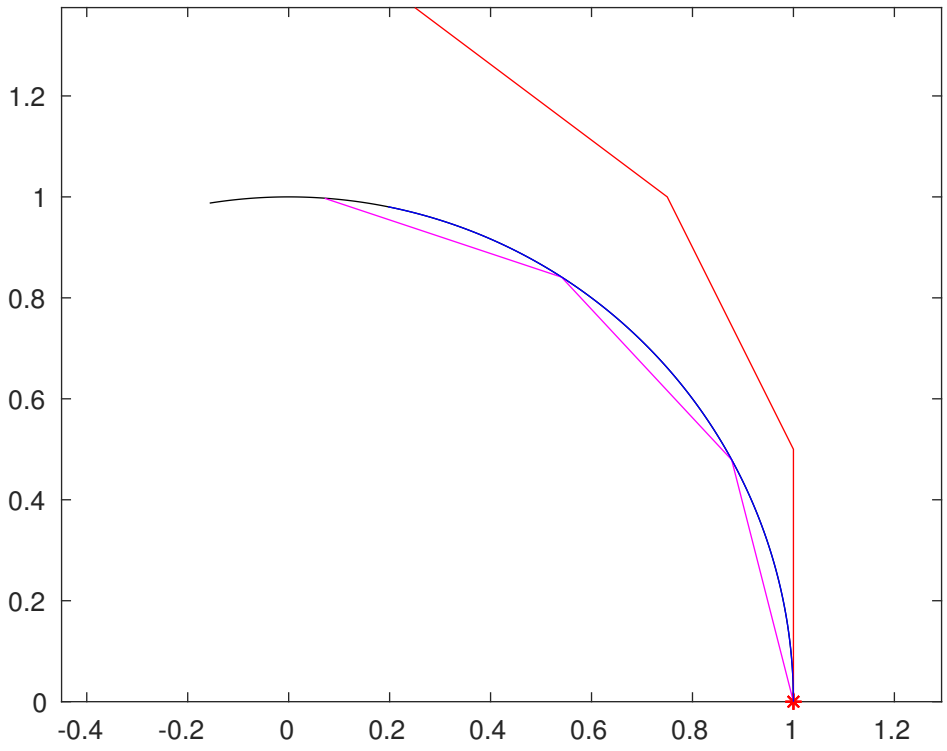

Fig. 5.48: Our method (blue curve) using $\epsilon = 0.5$, Euler method (red curve) using the step size $h = 0.5$, Runge–Kutta method (magenta curve) using the step size $h = 0.5$ and the exact solution (black curve) of (5.9) in Example 5.17.

equation

$$\begin{cases} x' = -y \\ y' = x \\ (x(0), y(0)) = (1, 0). \end{cases} \tag{5.9}$$

This autonomous ordinary differential equation has the solution

$$X(t) = \begin{pmatrix} \cos t \\ \sin t \end{pmatrix}, \quad t \in \mathbb{R}.$$

We use our method, the Euler method and the Runge-Kutta method to approximate the solution of (5.9) (see Figure 5.48 and Figure 5.49). We have some remarks when using our method, the Euler method and the Runge-Kutta method as follows:

Remark 5.18.

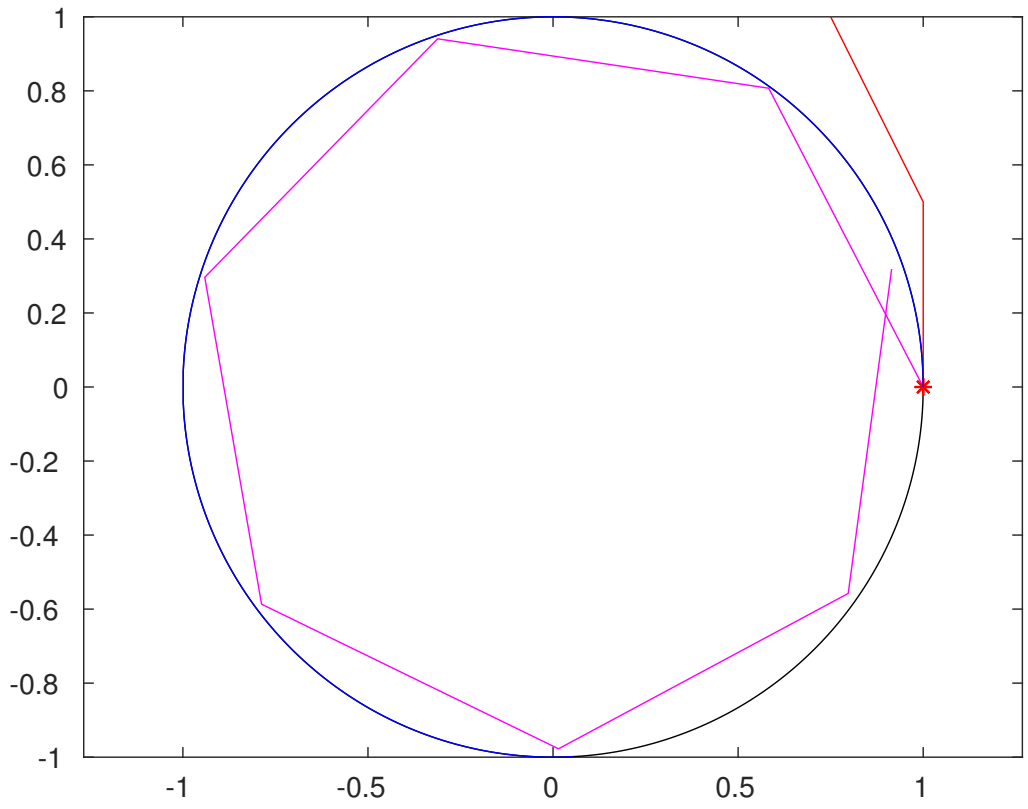

Fig. 5.49: Our method (blue curve) using $\epsilon = 0.95$, Euler method (red curve) using the step size $h = 0.5$, Runge–Kutta method (magenta curve) using the step size $h = 0.95$ and the exact solution (black curve) of (5.9) in Example 5.17.

- The orbits found by our method coincides with a portion of the solution when we use $\epsilon = 0.5$ (in Figure 5.48) or $\epsilon = 0.95$ (in Figure 5.49) to stop the algorithm.

- The orbit found by the Euler method does not coincide the solution when we use the step size $h = 0.5$ (see Figure 5.48 and Figure 5.49).

- The orbits found by the Runge-Kutta method do not coincide the solution when we use the step size $h = 0.5$ (in Figure 5.48) or the step size $h = 0.95$ (in Figure 5.49).

Example 5.19. We consider the following autonomous ordinary differential equation

$$\begin{cases} x' = -x - 8y \\ y' = 8x - y \\ (x(0), y(0)) = (1, 0). \end{cases} \tag{5.10}$$

This autonomous ordinary differential equation has the solution

$$X(t) = \begin{pmatrix} e^{-t}\cos 8t \\ e^{-t}\sin 8t \end{pmatrix}, \quad t \in \mathbb{R}.$$

We use our method, the Euler method and the Runge-Kutta method to approximate the solution of (5.10) (see Figure 5.50). We have some remarks when using our method, the Euler method and the Runge-Kutta method as follows:

Remark 5.20.

- The orbit found by our method coincides with a portion of the solution when we use $\epsilon = 0.5$ to stop the algorithm.

- The orbits found by the Euler method and the Runge-Kutta method do not coincide the solution when we use the step size $h = 0.05$.

Example 5.21. We consider the following autonomous ordinary differential equation

$$\begin{cases} x' = x - 8y \\ y' = 8x + y \\ (x(0), y(0)) = (1, 0). \end{cases} \tag{5.11}$$

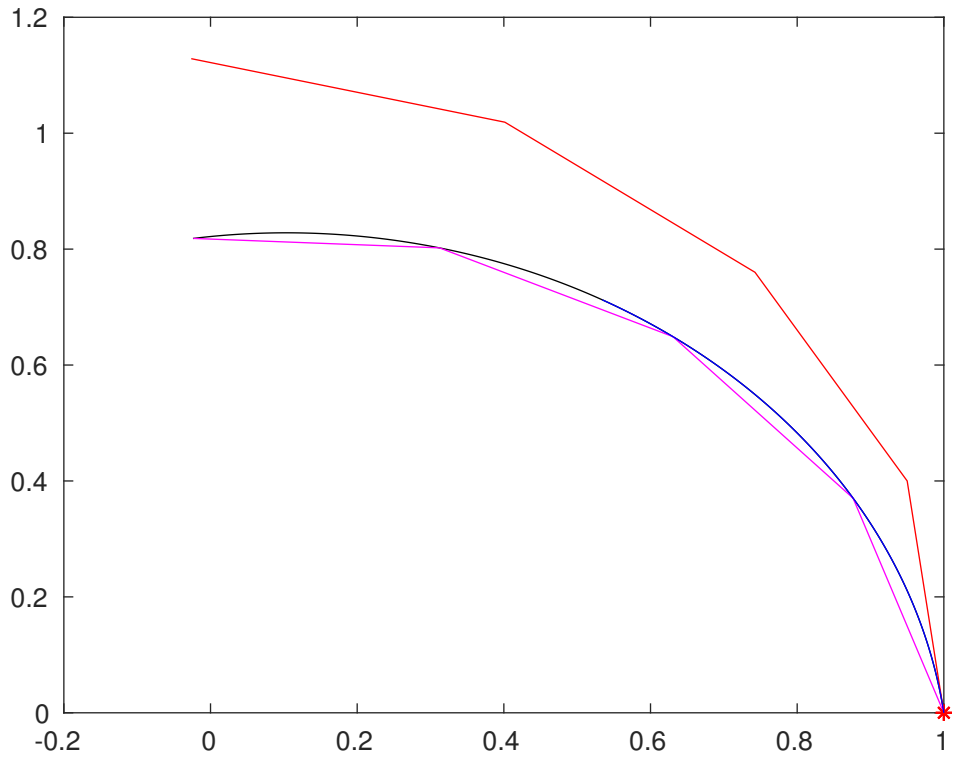

Fig. 5.50: Our method (blue curve) using $\epsilon = 0.5$, Euler method (red curve) using the step size $h = 0.05$, Runge–Kutta method (magenta curve) using the step size $h = 0.05$ and the exact solution (black curve) of (5.10) in Example 5.19.

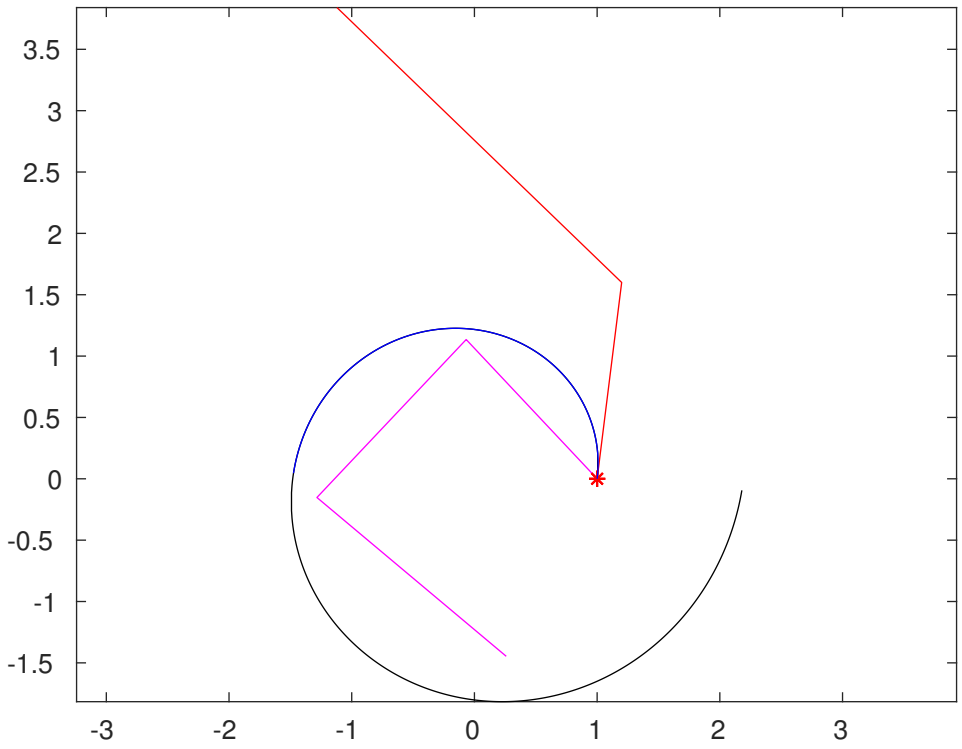

Fig. 5.51: Our method (blue curve) using $\epsilon = 0.2$, Euler method (red curve) using the step size $h = 0.2$, Runge–Kutta method (magenta curve) using the step size $h = 0.2$ and the exact solution (black curve) of (5.11) in Example 5.21.

This autonomous ordinary differential equation has the solution

$$X(t) = \begin{pmatrix} e^t \cos 8t \\ e^t \sin 8t \end{pmatrix}, \quad t \in \mathbb{R}.$$

We use our method, the Euler method and the Runge-Kutta method to approximate the solution of (5.11) (see Figure 5.51 and Figure 5.52). We have some remarks when using our method, the Euler method and the Runge-Kutta method as follows:

Remark 5.22.

- The orbit found by our method coincides with a portion of the solution when we use $\epsilon = 0.2$ (in Figure 5.51) or $\epsilon = 0.5$ (in Figure 5.52)) to stop the algorithm.
- The orbits found by the Euler method do not coincide the solution when we

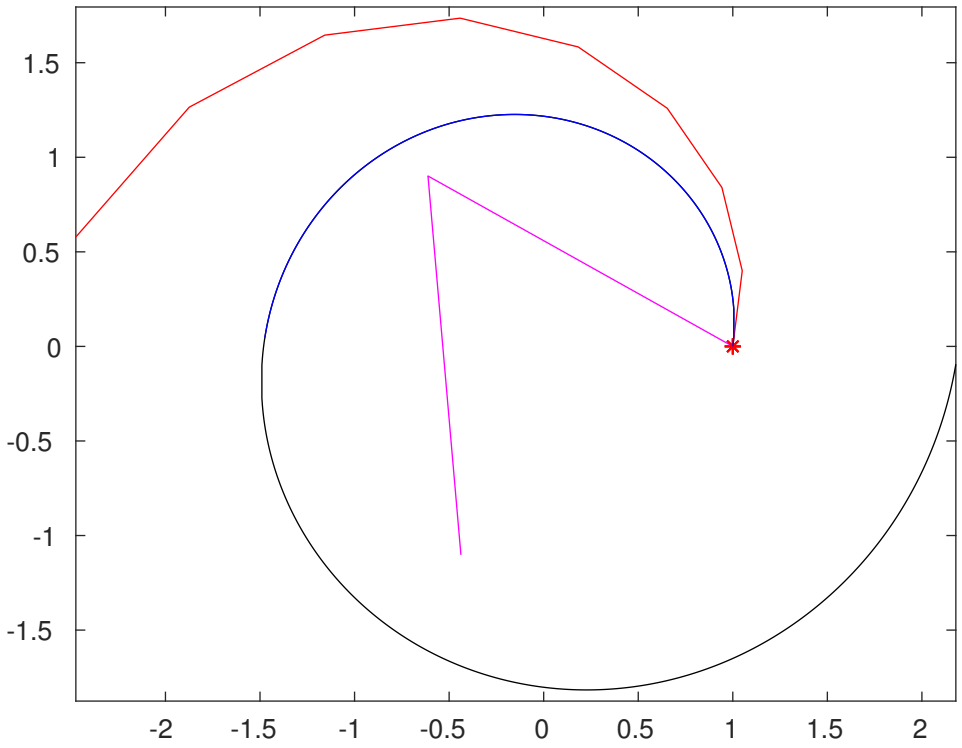

Fig. 5.52: Our method (blue curve) using $\epsilon = 0.5$, Euler method (red curve) using the step size $h = 0.05$, Runge–Kutta method (magenta curve) using the step size $h = 0.25$ and the exact solution (black curve) of (5.11) in Example 5.21.

use the step size $h = 0.2$ (in Figure 5.51) or $h = 0.05$ (in Figure 5.52)).

- The orbits found by the Runge–Kutta method do not coincide the solution when we use the step size $h = 0.2$ (in Figure 5.51) or $h = 0.25$ (in Figure 5.52)).

Example 5.23. We consider the following autonomous ordinary differential equation

$$\begin{cases} x' = 1 \\ y' = y \sin^2 x \\ (x(0), y(0)) = (0, 1). \end{cases} \tag{5.12}$$

This autonomous ordinary differential equation has the solution

$$X(t) = \begin{pmatrix} t \\ e^{0.5(t - \sin t \cos t)} \end{pmatrix}, \quad t \in \mathbb{R}.$$

We use our method, the Euler method and the Runge-Kutta method to approximate the solution of (5.12) (see Figure 5.53). We have some remarks when using our method, the Euler method and the Runge-Kutta method as follows:

Remark 5.24.

- The orbit found by our method coincides with a portion of the solution when we use $\epsilon = 0.9$ to stop the algorithm.

- The orbits found by the Euler method and the Runge-Kutta method do not coincide the solution when we use the step size $h = 0.9$.

Euler method and Runge-Kutta method do approximation with piecewise linear. In Euler and Runge-Kutta methods, each sampling point must be satisfied two constrains: the direction and the length (speed). In our method, each point just need one constrain: the direction. We do not care the speed in our method. This means that our method has less constrains than the Euler method and Runge-Kutta method. We have a table about the Euler method, the Runge-Kutta method and our method as follows:

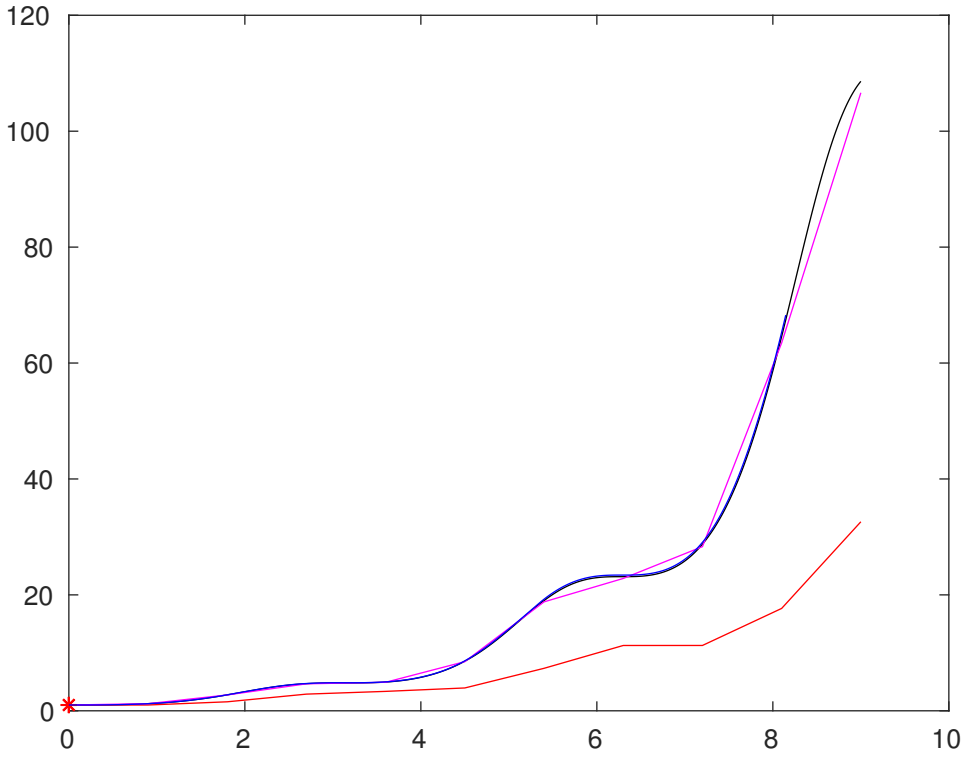

Fig. 5.53: Our method (blue curve) using $\epsilon = 0.9$, Euler method (red curve) using the step size $h = 0.9$, Runge–Kutta method (magenta curve) using the step size $h = 0.9$ and the exact solution (black curve) of (5.12) in Example 5.23.

	The Euler method and the Runge-Kutta method	Our method
Result	Solutions of autonomous ODEs	Trajectories of autonomous ODEs
Constrain	Each point must be satisfied the autonomous ODE $\Rightarrow$ many constrains	Each point is the same direction with the solution $\Rightarrow$ less constrains
How does it woks	x_{i+1} is determined from x_i and the step size h $\Rightarrow$ the error at x_{i+1} is greater than x_i	Find the optimal trajectory in the space of curves
The error depends on	The step size h and the number of steps	The starting curve and ϵ using to stop the algorithm

From Example 5.17, Example 5.19 and Example 5.23, we can see that our method is better than the Euler method and the Runge-Kutta method for finding solution orbits of autonomous ordinary differential equations. Consequently, piecewise uniform cubic Bézier curves and Algorithm 2 are useful to approximate optimal trajectories and solution orbits of autonomous ordinary differential equations. We next consider some numerical examples.

5.4 Some examples of autonomous ordinary differential equations

This section presents some autonomous ordinary differential equations. We will apply Proposition 5.12 and Algorithm 2 to approximate solution orbits of autonomous ordinary differential equations.

5.4.1 Example 1

We consider the autonomous ordinary differential equation together with initial condition

$$\begin{cases} x' = -x \\ y' = -y \\ (x(0), y(0)) = (x_0, y_0). \end{cases} \tag{5.13}$$

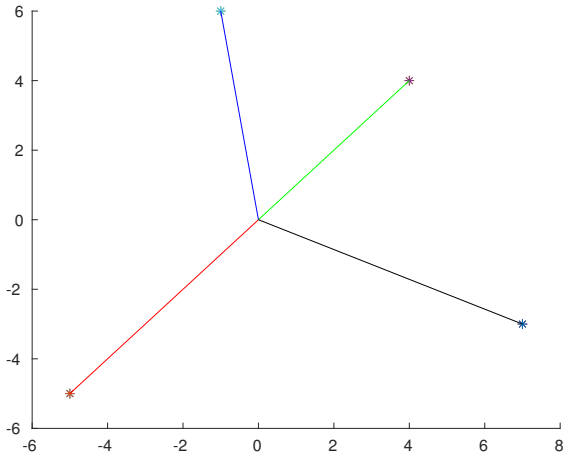

Fig. 5.54: Some solution orbits in Example 1.

We find a reparametrization of the solution by finding the minimum curve of the following problem

$$\begin{cases} F(\gamma) = \int_0^1 \left(\|\dot{\gamma}(t)\|_2 \,.\, \|-\gamma(t)\|_2 - \langle \dot{\gamma}(t), -\gamma(t) \rangle \right) dt \\ \gamma(0) = (x_0, y_0), \end{cases} \tag{5.14}$$

where

$$\begin{aligned} f : \mathbb{R}^2 &\to T\mathbb{R}^2 \\ (x, y) &\mapsto (-x, -y). \end{aligned}$$

Using piecewise uniform cubic Bézier curves, Algorithm 2 and Matlab, we can approximate solution orbits of (5.13) (see Figures 5.54). We have some remarks about this problem as follows:

Remark 5.25.

- We know that (5.13) has the following solution

$$\begin{cases} x = x_0.e^{-t} \\ y = y_0.e^{-t}. \end{cases}$$

- The image of the curve found by our method is a piece of the solution orbit of (5.13).

- For each initial point (x_0, y_0), (5.13) has a solution orbit.
- The solution orbits of (5.13) is a segment from (x_0, y_0) to $(0, 0)$.
- The equation 5.13 has a fix point $(0, 0)$.

5.4.2 Example 2

We consider the autonomous ordinary differential equation together with initial condition

$$\begin{cases} x' = -y \\ y' = x \\ (x(0), y(0)) = (x_0, y_0). \end{cases} \tag{5.15}$$

We find a reparametrization of the solution by finding the minimum curve of the following problem

$$\begin{cases} F(\gamma) = \int_0^1 \left(\|\dot{\gamma}(t)\|_2 . \|f(\gamma(t))\|_2 - \langle \dot{\gamma}(t), f(\gamma(t)) \rangle \right) dt \\ \gamma(0) = (x_0, y_0), \end{cases} \tag{5.16}$$

where

$$\begin{aligned} f : \mathbb{R}^2 &\to T\mathbb{R}^2 \\ (x, y) &\mapsto (-y, x). \end{aligned}$$

Using piecewise uniform cubic Bézier curves, Algorithm 2 and Matlab, we can approximate solution orbits of (5.15) (see Figures 5.55). We have some remarks about this problem as follows:

Remark 5.26.

- Solution orbits of (5.15) is a circle which has center $O(0, 0)$ and goes through point (x_0, y_0).
- The image of the curve found by our method is a piece of the solution orbit of (5.15).
- For each initial point (x_0, y_0), (5.15) has a solution orbit.

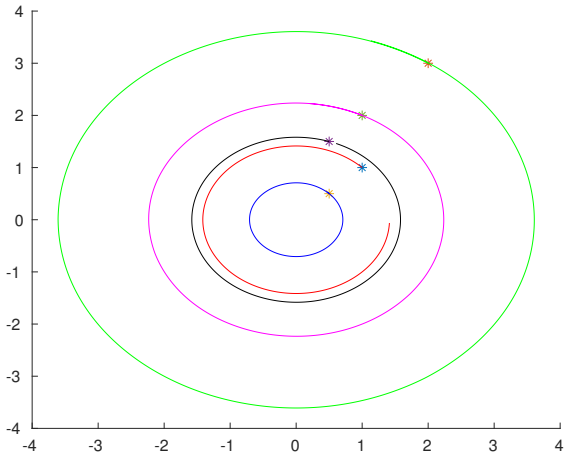

Fig. 5.55: Some solution orbits in Example 2.

5.4.3 Example 3

We consider the autonomous ordinary differential equation together with initial condition

$$\begin{cases} x' = 0.5x \\ y' = -0.5y \\ (x(0), y(0)) = (x_0, y_0). \end{cases} \tag{5.17}$$

We find a reparametrization of the solution by finding the minimum curve of the following problem

$$\begin{cases} F(\gamma) = \int_0^1 \left(\|\dot{\gamma}(t)\|_2 \cdot \|f(\gamma(t))\|_2 - \langle \dot{\gamma}(t), f(\gamma(t)) \rangle \right) dt \\ \gamma(0) = (x_0, y_0), \end{cases} \tag{5.18}$$

where

$$\begin{aligned} f : \mathbb{R}^2 &\to T\mathbb{R}^2 \\ (x, y) &\mapsto (0.5x, -0.5y). \end{aligned}$$

Using piecewise uniform cubic Bézier curves, Algorithm 2 and Matlab, we can approximate solution orbits of (5.17) (see Figures 5.56). We have some remarks about this problem as follows:

Remark 5.27.

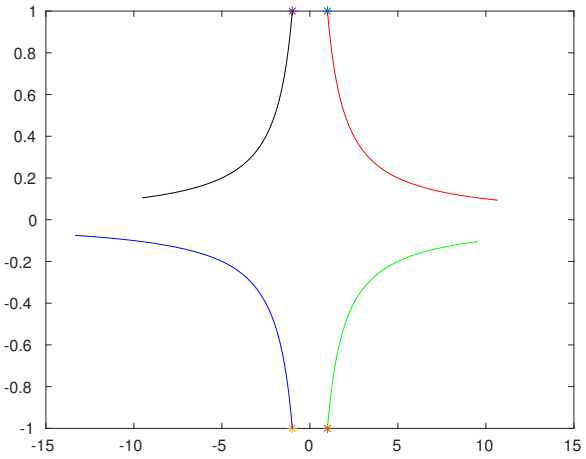

Fig. 5.56: Solution orbits in Example 3.

- We know that (5.17) has the following solution

$$\begin{cases} x = x_0 e^{0.5t} \\ y = y_0 e^{-0.5t}. \end{cases}$$

- The image of the curve found by our method is a piece of the solution orbit of (5.17).

- For each initial point (x_0, y_0), (5.17) has a solution orbit.

- The code stops if γ contains the origin $O(0, 0)$. So, we can not find the minimum curve in this case.

5.4.4 Example 4

We consider the autonomous ordinary differential equation together with initial condition

$$\begin{cases} x' = \dfrac{\sqrt{2}}{2}x + \dfrac{\sqrt{2}}{2}y \\ y' = -\dfrac{\sqrt{2}}{2}x + \dfrac{\sqrt{2}}{2}y \\ (x(0), y(0)) = (x_0, y_0). \end{cases} \tag{5.19}$$

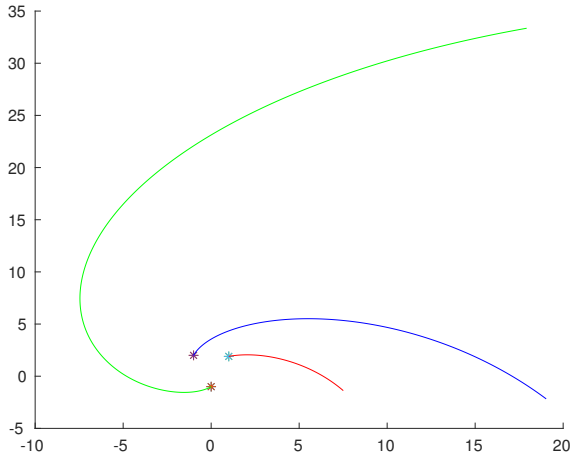

Fig. 5.57: Some solution orbits in Example 4.

We find a reparametrization of the solution by finding the minimum curve of the following problem

$$\begin{cases} F(\gamma) = \int_0^1 \left(\|\dot{\gamma}(t)\|_2 \, . \, \|f(\gamma(t))\|_2 - \langle \dot{\gamma}(t), f(\gamma(t)) \rangle \right) dt \\ \gamma(0) = (x_0, y_0), \end{cases} \tag{5.20}$$

where

$$\begin{aligned} & f : \mathbb{R}^2 \to T\mathbb{R}^2 \\ & (x, y) \mapsto \left(\frac{\sqrt{2}}{2}x + \frac{\sqrt{2}}{2}y, -\frac{\sqrt{2}}{2}x + \frac{\sqrt{2}}{2}y \right). \end{aligned}$$

Using piecewise uniform cubic Bézier curves, Algorithm 2 and Matlab, we can approximate solution orbits of (5.19) (see Figures 5.57). We have some remarks about this problem as follows:

Remark 5.28.

- The image of the curve found by our method is a piece of the solution orbit of (5.19).

- For each initial point (x_0, y_0), (5.19) has a solution orbit.

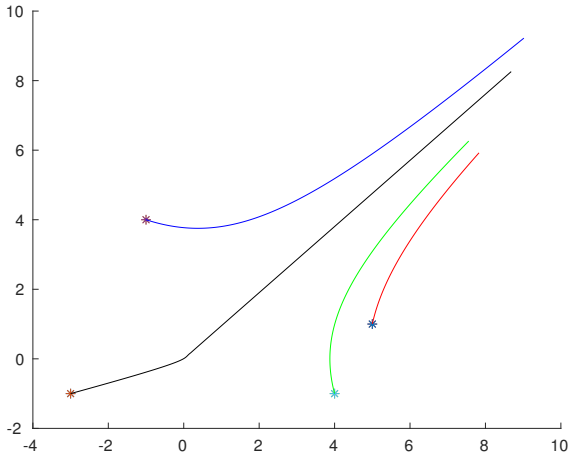

Fig. 5.58: Some solution orbits in Example 5.

5.4.5 Example 5

We consider the autonomous ordinary differential equation together with initial condition

$$\begin{cases} x' = y \\ y' = x - 0.1y \\ (x(0), y(0)) = (1, 0). \end{cases} \tag{5.21}$$

We find a reparametrization of the solution by finding the minimum curve of the following problem

$$\begin{cases} F(\gamma) = \int_0^1 \left(\|\dot{\gamma}(t)\|_2 \,.\, \|f(\gamma(t))\|_2 - \langle \dot{\gamma}(t), f(\gamma(t)) \rangle \right) dt \\ \gamma(0) = (1, 0), \end{cases} \tag{5.22}$$

where

$$\begin{aligned} f : \mathbb{R}^2 &\to T\mathbb{R}^2 \\ (x, y) &\mapsto (y, x - 0.1y)\,. \end{aligned}$$

Using piecewise uniform cubic Bézier curves, Algorithm 2 and Matlab, we can approximate solution orbits of this problem (see Figures 5.58). We have some remarks about this problem as follows:

Remark 5.29.

- The image of the curve found by our method is a piece of the solution orbit

of (5.21).

- For each initial point (x_0, y_0), (5.21) has a solution orbit.

5.4.6 Example 6

We consider the autonomous ordinary differential equation together with initial condition

$$\begin{cases} y_1' = -\dfrac{y_1^2 - 1}{y_1 - y_2} \\ y_2' = -\dfrac{y_2^2 - 1}{y_2 - y_1} \\ (y_1(0), y_2(0)) = (a, b). \end{cases} \tag{5.23}$$

We find a reparametrization of the solution by finding the minimum curve of the following problem

$$\begin{cases} F(\gamma) = \int_0^1 \left(\|\dot{\gamma}(t)\|_2 \,.\, \|f(\gamma(t))\|_2 - \langle \dot{\gamma}(t), f(\gamma(t)) \rangle \right) dt \\ \gamma(0) = (a, b), \end{cases} \tag{5.24}$$

where

$$\begin{aligned} f : \mathbb{R}^2 &\to T\mathbb{R}^2 \\ (y_1, y_2) &\mapsto \left(-\frac{y_1^2 - 1}{y_1 - y_2}, -\frac{y_2^2 - 1}{y_2 - y_1} \right). \end{aligned}$$

Using piecewise uniform cubic Bézier curves, Algorithm 2 and Matlab, we can approximate solution orbits of this problem (see Figures 5.59, 5.60, 5.61 and 5.62). We have some remarks about this problem as follows:

Remark 5.30.

- The image of the curve found by our method is a piece of the solution orbit of (5.23).
- If there exists $t \in [0, 1]$ such that two coordinates of $\gamma(t)$ are the same, then $f(\gamma(t)) = \infty$. So, we can not the minimum curve in this case.
- The equation 5.23 has two fix points $(-1, 1)$ and $(1, -1)$.

On the autonomous ordinary differential equation together with initial condition, we do not control the interval which the solution is defined. Then we

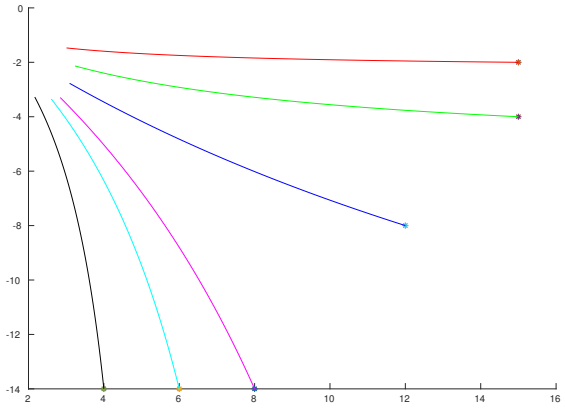

Fig. 5.59: Some solution orbits in Example 6.

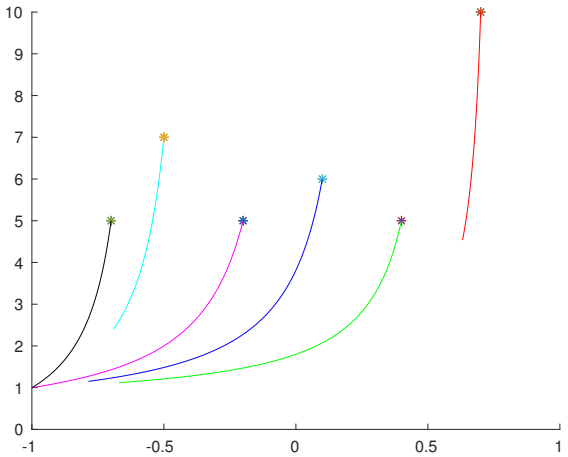

Fig. 5.60: Some solution orbits in Example 6.

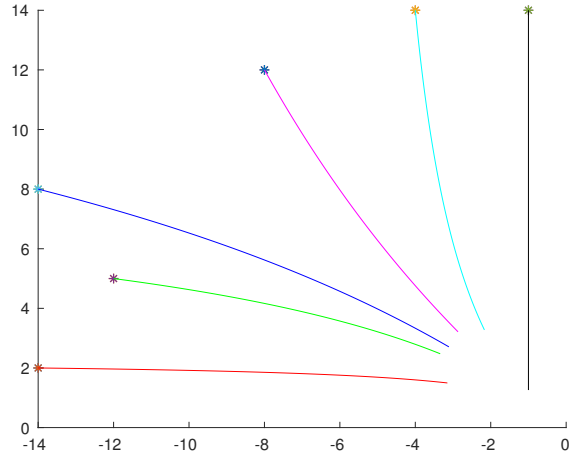

Fig. 5.61: Some solution orbits in Example 6.

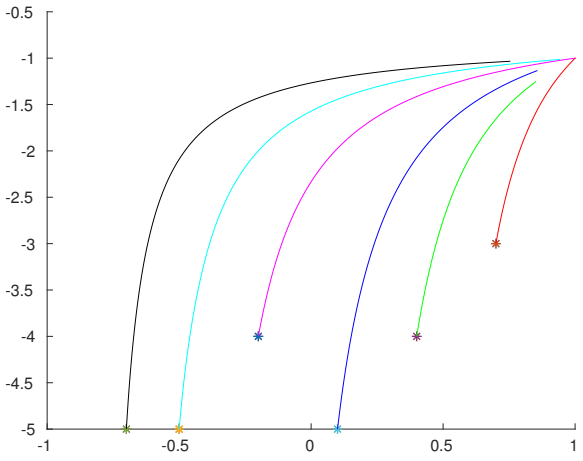

Fig. 5.62: Some solution orbits in Example 6.

have a piece of the solution orbit of the autonomous ordinary differential equation only when applying this method.

5.5 Control of autonomous ordinary differential equations

In this section, we apply our method to approximate solution orbits of control of autonomous ordinary differential equations.

We consider the following control of autonomous ordinary differential equation

$$\begin{cases} \dot{X}(t) = f(X(t), Y(t)), \forall t \in I \\ X(t_0) = X_0 \\ X_1 \in X(I), \end{cases}$$

where $f : U \times V \to T\mathbb{R}^n$, $U \subset \mathbb{R}^n$, $V \subset \mathbb{R}^m$, $X_0, X_1 \in U$ and $I = [t_0, \infty[\subset \mathbb{R}$. The function Y is called the control function. The function Y is used to control the function X such that X passes through X_1. We have a proposition as follows:

Proposition 5.31. Let U be a subset in $\mathbb{R}^n$, $V \subset \mathbb{R}^m$, $X_0 \in U$, $X_1 \in U$, and $I = [t_0, \infty[\subset \mathbb{R}$. Let $f : U \times V \to TU$ be a Lipschitz continuous function such that $f(x, y) \neq 0$ for $(x, y) \in U \times V$. We consider the following control of autonomous ordinary differential equation

$$\begin{cases} \dot{X}(t) = f(X(t), Y(t)), \forall t \in I \\ X(t_0) = X_0 \\ X_1 \in X(I). \end{cases} \tag{5.25}$$

If $\gamma : [0, 1] \to U$ and $\beta : [0, 1] \to V$ are continuously differentiable functions such that $\dot{\gamma}(v) \neq 0$ for all $v \in [0, 1]$ and

$$\begin{cases} F_f(\gamma, \beta) = \int_0^1 (\|\dot{\gamma}(v)\|_2 . \|f(\gamma(v), \beta(v)\|_2 - \langle \dot{\gamma}(v), f(\gamma(v), \beta(v)) \rangle) \, dv = 0 \\ \gamma(0) = X_0 \\ \gamma(1) = X_1, \end{cases} \tag{5.26}$$

then there exists an increasing differentiable function $\varphi : I \to [0, 1]$ such that $(\gamma \circ \varphi, \beta \circ \varphi)$ is a solution of (5.25).

The proof of this proposition is similar to that of Proposition 5.12.

From Proposition 5.31, we see that the continuously differentiable solutions of the system 5.26 are reparametrizations of the solutions of the control of autonomous ordinary differential equation 5.25. We note that

$$F_f(\gamma,\beta) = \int_0^1 (\|\dot{\gamma}(v)\|_2.\|f(\gamma(v),\beta(v)\|_2 - \langle\dot{\gamma}(v), f(\gamma(v),\beta(v)\rangle)\, dv$$

is always non-negative and invariant under reparametrization. Then, the system 5.26 can be considered as the following trajectory optimization problem

$$\begin{cases} F_f(\gamma,\beta) = \int_0^1 (\|\dot{\gamma}(v)\|_2.\|f(\gamma(v),\beta(v)\|_2 - \langle\dot{\gamma}(v), f(\gamma(v),\beta(v)\rangle)\, dv \\ \gamma(0) = X_0 \\ \gamma(1) = X_1. \end{cases} \tag{5.27}$$

This means that we can find solution orbits of the control of autonomous ordinary differential equation 5.25 from the trajectory optimization problem 5.27. Piecewise uniform cubic Bézier curves are continuously differentiable everywhere except at a countable set of points. Thus, we use piecewise uniform cubic Bézier curves and Algorithm 2 to approximate solution orbits of the control of autonomous ordinary differential equation 5.25. Let us consider some numerical examples. The control functions in these examples are from simple to more complex.

5.5.1 Example 1

This subsection presents an example with nonlinear autonomous ordinary differential equation and linear control.

We consider the control of autonomous ordinary differential equation

$$\begin{cases} X' = \begin{pmatrix} x' \\ y' \end{pmatrix} = \begin{pmatrix} 1 \\ -\dfrac{e^{1-x^2}-1}{e-1} \end{pmatrix} + \begin{pmatrix} u_1 \\ u_2 \end{pmatrix} \\ X(0) = \begin{pmatrix} x(0) \\ y(0) \end{pmatrix} = \begin{pmatrix} -1 \\ -1 \end{pmatrix} \\ \begin{pmatrix} 4 \\ 2 \end{pmatrix} \in X(\mathbb{R}^+). \end{cases} \tag{5.28}$$

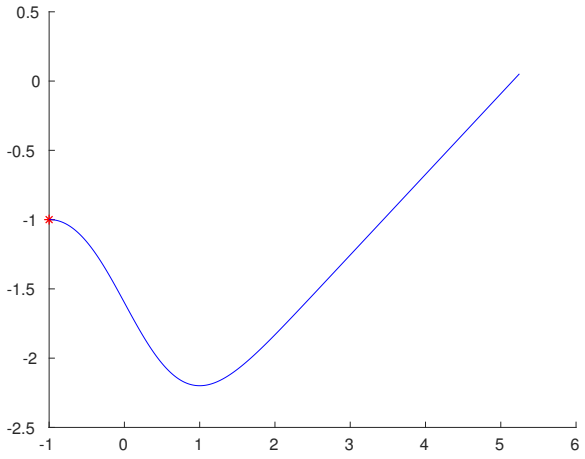

Fig. 5.63: The solution orbit (blue curve) of (5.29) without control.

The control of autonomous ordinary differential equation 5.28 is derived directly from the following autonomous ordinary differential equation

$$\begin{cases} X' = \begin{pmatrix} x' \\ y' \end{pmatrix} = \begin{pmatrix} 1 \\ -\dfrac{e^{1-x^2}-1}{e-1} \end{pmatrix} \\ X(0) = \begin{pmatrix} x(0) \\ y(0) \end{pmatrix} = \begin{pmatrix} -1 \\ -1 \end{pmatrix}. \end{cases} \tag{5.29}$$

The autonomous ordinary differential equation 5.29 is nonlinear. The solution of the autonomous ordinary differential equation 5.29 does not pass through the point $(4, 2)$ (see Figures 5.63). Then we add a control function (u_1, u_2) such that the solution of (5.28) passes through the point $(4, 2)$. This control function is simple and natural.

We find a reparametrization of the solution of (5.28) from the following trajectory optimization problem

$$\begin{cases} F_f(\gamma, \alpha) = \int\limits_0^1 \left(\|\dot{\gamma}(v)\|_2 . \|f(\gamma(v), u(v))\|_2 - \langle \dot{\gamma}(v), f(\gamma(v), \alpha(v)) \rangle \right) dv \\ \gamma(0) = (-1, -1) \\ \gamma(1) = (4, 2), \end{cases}$$

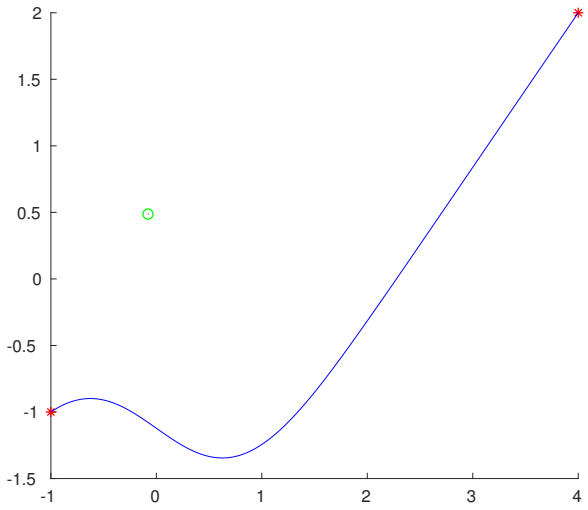

Fig. 5.64: A solution orbit (blue curve) and an orbit of control function (green point) of (5.28) in Example 1 as the control function is a point (i.e., a constant function).

where

$$f : \mathbb{R}^2 \times \mathbb{R}^2 \to T\mathbb{R}^2$$
$$(x, y) \times (u_1, u_2) \mapsto \left(1 + u_1, -\frac{e^{1-x^2} - 1}{e - 1} + u_2\right).$$

Using piecewise uniform cubic Bézier curves, Algorithm 2 and Matlab, we can approximate solution orbits of (5.28) (see Figures 5.64, 5.65 and 5.66). We have some remarks about this problem as follows:

Remark 5.32.

- The image of the curve found by our method is a portion of the solution orbit from $(-1, -1)$ to $(4, 2)$.
- When the control function is a point (i.e., a constant function), (5.28) has a unique solution orbit.
- When the control function is a linear Bézier curve, (5.28) has many solution orbits.

5.5.2 Example 2

This subsection presents an example with nonlinear autonomous ordinary differential equation and linear control.

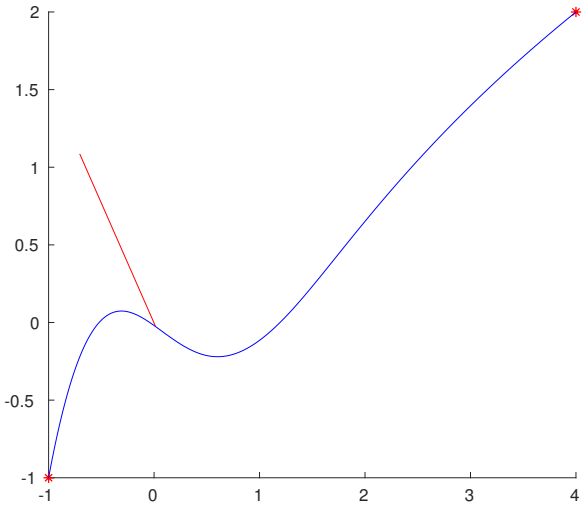

Fig. 5.65: A solution orbit (blue curve) and an orbit of control function (red curve) of (5.28) in Example 1 as the control function is a linear Bézier curve.

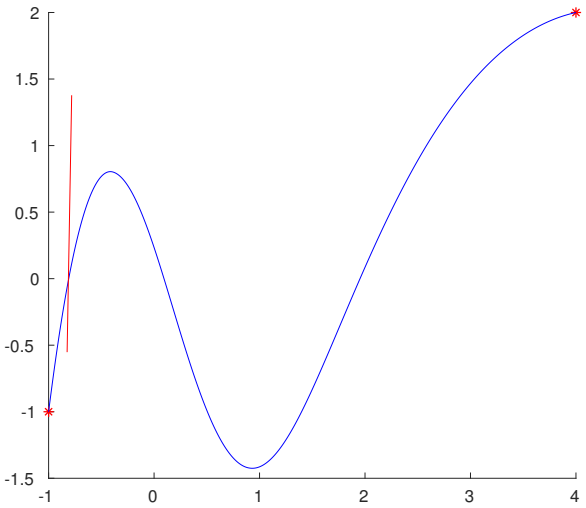

Fig. 5.66: A solution orbit (blue curve) and an orbit of control function (red curve) of (5.28) in Example 1 as the control function is a linear Bézier curve.

We consider the control of autonomous ordinary differential equation

$$\begin{cases} X' = \begin{pmatrix} x' \\ y' \end{pmatrix} = \begin{pmatrix} y \\ -2x^3 \end{pmatrix} + \begin{pmatrix} u_1 \\ u_2 \end{pmatrix} \\ X(0) = \begin{pmatrix} x(0) \\ y(0) \end{pmatrix} = \begin{pmatrix} 1 \\ 0 \end{pmatrix} \\ \begin{pmatrix} -3 \\ 3 \end{pmatrix} \in X(\mathbb{R}^+). \end{cases} \tag{5.30}$$

The control of autonomous ordinary differential equation 5.30 is derived directly from the following autonomous ordinary differential equation

$$\begin{cases} X' = \begin{pmatrix} x' \\ y' \end{pmatrix} = \begin{pmatrix} y \\ -2x^3 \end{pmatrix} \\ X(0) = \begin{pmatrix} x(0) \\ y(0) \end{pmatrix} = \begin{pmatrix} 1 \\ 0 \end{pmatrix}. \end{cases} \tag{5.31}$$

The solution of the autonomous ordinary differential equation 5.31 is a portion of the closed curve $x^4 + y^2 = 1$ (see [29, Chapter IX, p. 409]). It is clear that the solution of (5.31) does not pass through the point $(-3, 3)$. Then we add a control function (u_1, u_2) such that the solution of (5.30) passes through the point $(-3, 3)$. This control function is simple and natural.

We find a reparametrization of the solution of (5.30) the solution from the following trajectory optimization problem

$$\begin{cases} F_f(\gamma, \alpha) = \int\limits_0^1 \left(\|\dot{\gamma}(v)\|_2 . \|f(\gamma(v), u(v))\|_2 - \langle \dot{\gamma}(v), f(\gamma(v), \alpha(v)) \rangle \right) dv \\ \gamma(0) = (1, 0) \\ \gamma(1) = (-3, 3), \end{cases}$$

where

$$\begin{aligned} f : \mathbb{R}^2 \times \mathbb{R}^2 &\to T\mathbb{R}^2 \\ (x, y) \times (u_1, u_2) &\mapsto (y + u_1, -2x^3 + u_2). \end{aligned}$$

Using piecewise uniform cubic Bézier curves, Algorithm 2 and Matlab, we can approximate solution orbits of (5.30) (see Figures 5.67, 5.68 and 5.69). We have

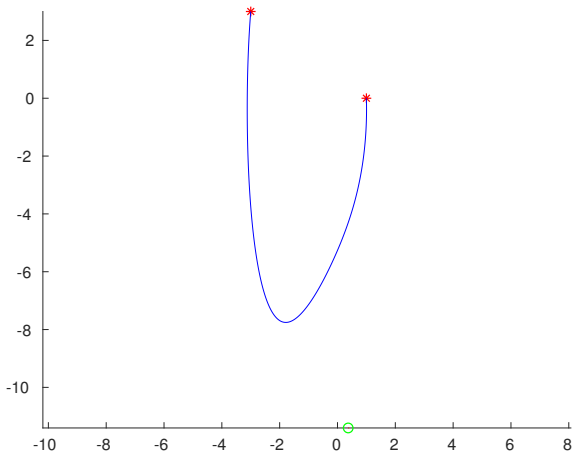

Fig. 5.67: A solution orbit (blue curve) and an orbit of control function (green point) of (5.30) in Example 2 as the control function is a point (i.e., a constant function).

some remarks about this problem as follows:

Remark 5.33.

- The image of the curve found by our method is a portion of the solution orbit from $(1, 0)$ to $(-3, 3)$.
- When the control function is a point (i.e., a constant function), (5.30) has a unique solution orbit.
- When the control function is a linear Bézier curve, (5.30) has many solution orbits.

5.5.3 Example 3

This subsection presents an example with linear autonomous ordinary differential equation and linear control.

We consider the control of autonomous ordinary differential equation

$$\begin{cases} X' = \begin{pmatrix} x' \\ y' \end{pmatrix} = \begin{pmatrix} -x \\ -y \end{pmatrix} + \begin{pmatrix} u_1 - u_2 \\ u_2 + 1 \end{pmatrix} \\ X(0) = \begin{pmatrix} x(0) \\ y(0) \end{pmatrix} = \begin{pmatrix} 9 \\ 9 \end{pmatrix} \\ \begin{pmatrix} -5 \\ 4 \end{pmatrix} \in X(\mathbb{R}^+). \end{cases} \tag{5.32}$$

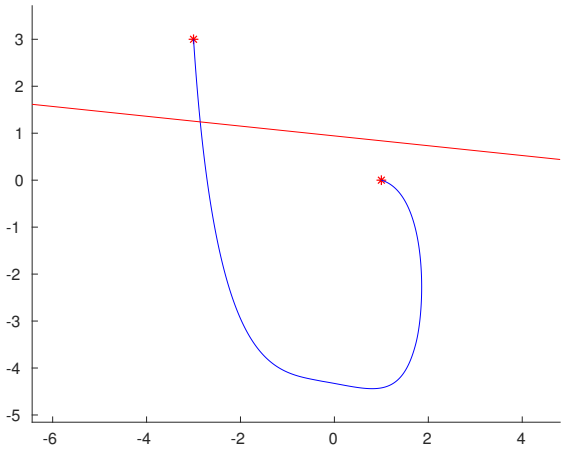

Fig. 5.68: A solution orbit (blue curve) and an orbit of control function (red curve) of (5.30) in Example 2 as the control function is a linear Bézier curve.

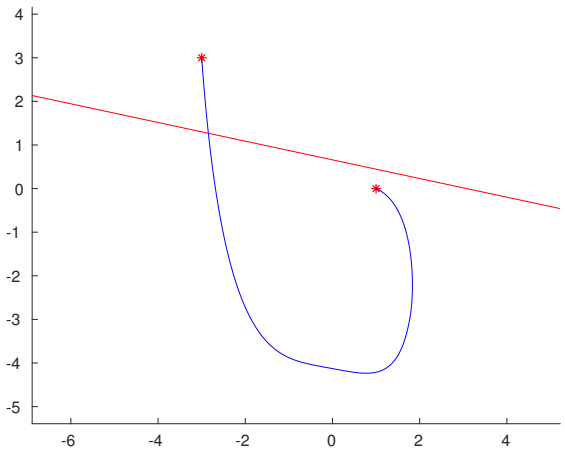

Fig. 5.69: A solution orbit (blue curve) and an orbit of control function (red curve) of (5.30) in Example 2 as the control function is a linear Bézier curve.

The control of autonomous ordinary differential equation 5.32 is derived directly from the following autonomous ordinary differential equation

$$\begin{cases} X' = \begin{pmatrix} x' \\ y' \end{pmatrix} = \begin{pmatrix} -x \\ -y \end{pmatrix} \\ X(0) = \begin{pmatrix} x(0) \\ y(0) \end{pmatrix} = \begin{pmatrix} 9 \\ 9 \end{pmatrix}. \end{cases} \tag{5.33}$$

The solution of the autonomous ordinary differential equation 5.33 is the segment connecting the point $(9, 9)$ and the origin $O(0, 0)$ (see Figure 5.54 in Subsection 5.4.1). It is clear that the solution of (5.33) does not pass through the point $(-5, 4)$. Then we add a control function $(u_1 - u_2, u_2 + 1)$ such that the solution of (5.32) passes through the point $(-5, 4)$. The control function $(u_1 - u_2, u_2 + 1)$ is linear.

We find a reparametrization of the solution of (5.32) from the following trajectory optimization problem

$$\begin{cases} F_f(\gamma, \alpha) = \int\limits_0^1 (\|\dot{\gamma}(v)\|_2.\|f(\gamma(v), u(v))\|_2 - \langle \dot{\gamma}(v), f(\gamma(v), \alpha(v))\rangle)\, dv \\ \gamma(0) = (9, 9) \\ \gamma(1) = (-5, 4), \end{cases}$$

where

$$\begin{aligned} f : \mathbb{R}^2 \times \mathbb{R}^2 &\to T\mathbb{R}^2 \\ (x, y) \times (u_1, u_2) &\mapsto (-x + u_1 - u_2, -y + u_2 + 1). \end{aligned}$$

Using piecewise uniform cubic Bézier curves, Algorithm 2 and Matlab, we can approximate solution orbits of (5.32) (see Figures 5.70, 5.71 and 5.71). We have some remarks about this problem as follows:

Remark 5.34.

- The image of the curve found by our method is a portion of the solution orbit from $(9, 9)$ to $(-5, 4)$.

- When the control function is a point (i.e., a constant function), (5.32) has a unique solution orbit.

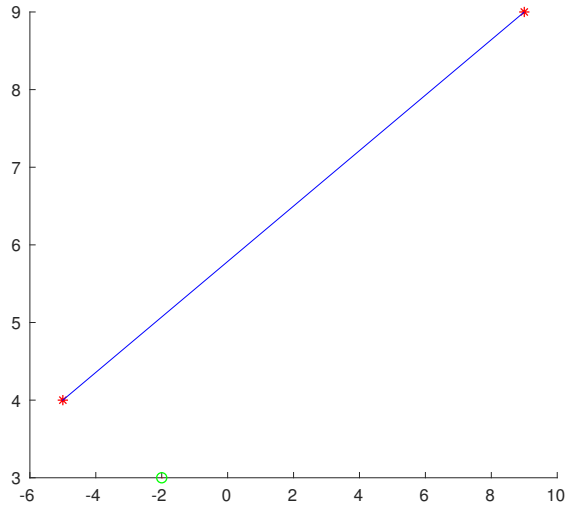

Fig. 5.70: A solution orbit (blue curve) and an orbit of control function (green point) of (5.32) in Example 2 as the control function is a point (i.e., a constant function).

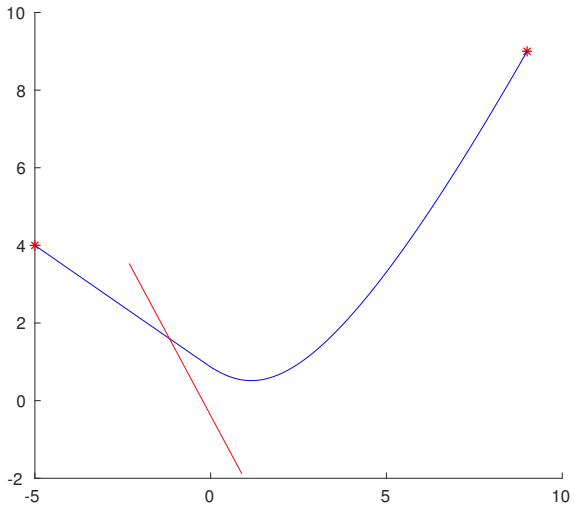

Fig. 5.71: A solution orbit (blue curve) and an orbit of control function (red curve) of (5.32) in Example 3 as the control function is a linear Bézier curve.

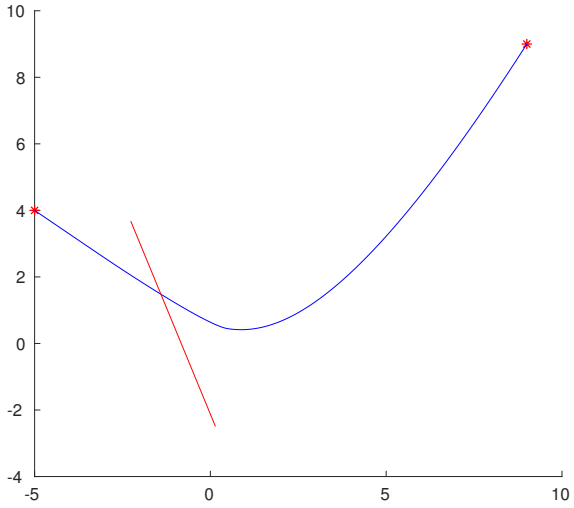

Fig. 5.72: A solution orbit (blue curve) and an orbit of control function (red curve) of (5.32) in Example 3 as the control function is a linear Bézier curve.

- When the control function is a linear Bézier curve, (5.32) has many solution orbits.

5.5.4 Example 4

This subsection presents an example with linear autonomous ordinary differential equation and nonlinear control.

We consider the control of autonomous ordinary differential equation

$$\begin{cases} X' = \begin{pmatrix} x' \\ y' \end{pmatrix} = \begin{pmatrix} -y \\ x \end{pmatrix} + \begin{pmatrix} u_1^2 + 2 \\ -2u_2^2 + u_2 \end{pmatrix} \\ X(0) = \begin{pmatrix} x(0) \\ y(0) \end{pmatrix} = \begin{pmatrix} 1 \\ 0 \end{pmatrix} \\ \begin{pmatrix} -3 \\ 0 \end{pmatrix} \in X(\mathbb{R}^+). \end{cases} \tag{5.34}$$

The control of autonomous ordinary differential equation 5.34 is derived directly

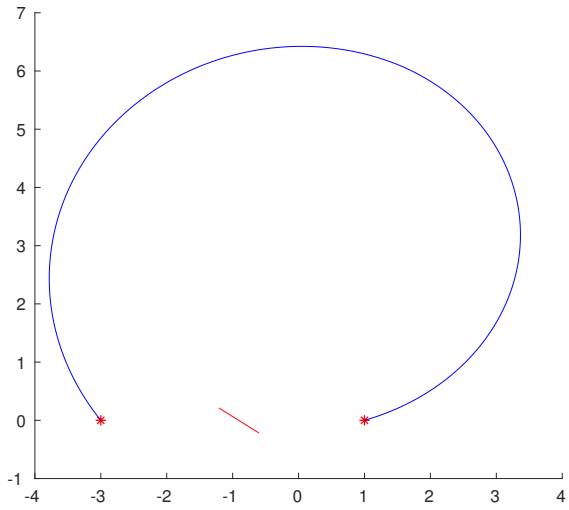

Fig. 5.73: A solution orbit (blue curve) and an orbit of control function (red curve) of (5.34) in Example 4 as the control function is a linear Bézier curve.

from the following autonomous ordinary differential equation

$$\begin{cases} X' = \begin{pmatrix} x' \\ y' \end{pmatrix} = \begin{pmatrix} -y \\ x \end{pmatrix} \\ X(0) = \begin{pmatrix} x(0) \\ y(0) \end{pmatrix} = \begin{pmatrix} 1 \\ 0 \end{pmatrix}. \end{cases} \tag{5.35}$$

The solution of the autonomous ordinary differential equation 5.35 is a circle with center $O(0,0)$ and radius 1 (see Figures 5.55 in Subsection 5.4.2). It is clear that the solution of (5.35) does not pass through the point $(-3,0)$. Then we add a control function $(u_1^2+2, -2u_2^2+u_2)$ such that the solution of (5.34) passes through the point $(-3,0)$. The autonomous ordinary differential equation 5.35 is classical but the control function $(u_1^2+2, -2u_2^2+u_2)$ is nonlinear.

We find a reparametrization of the solution of (5.34) from the following trajectory optimization problem

$$\begin{cases} F_f(\gamma,\alpha) = \int\limits_0^1 \left(\|\dot{\gamma}(v)\|_2.\|f(\gamma(v),u(v))\|_2 - \langle\dot{\gamma}(v), f(\gamma(v),\alpha(v))\rangle\right) dv \\ \gamma(0) = (1,0) \\ \gamma(1) = (-3,0), \end{cases}$$

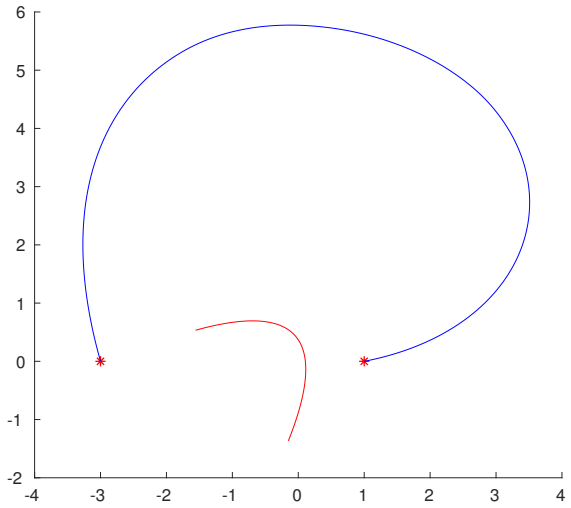

Fig. 5.74: A solution orbit (blue curve) and an orbit of control function (red curve) of (5.34) in Example 4 as the control function is a quadratic Bézier curve.

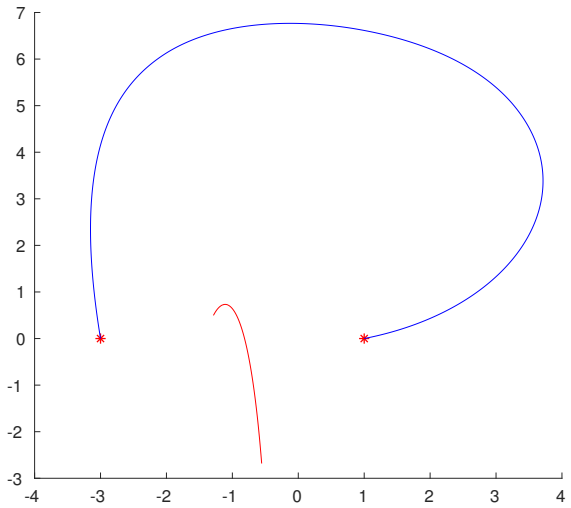

Fig. 5.75: A solution orbit (blue curve) and an orbit of control function (red curve) of (5.34) in Example 4 as the control function is a cubic Bézier curve.

where

$$f : \mathbb{R}^2 \times \mathbb{R}^2 \to T\mathbb{R}^2$$
$$(x, y) \times (u_1, u_2) \mapsto (-y + u_1^2 + 2, x - 2u_2^2 + u_2).$$

Using piecewise uniform cubic Bézier curves, Algorithm 2 and Matlab, we can approximate solution orbits of (5.34) (see Figures 5.73, 5.74 and 5.75). We have some remarks about this problem as follows:

Remark 5.35.

- The image of the curve found by our method is a portion of the solution orbit from $(1, 0)$ to $(-3, 0)$.
- When the control function is a point (i.e., a constant function), (5.34) has no solution.
- When the control function is a linear Bézier curve, (5.34) has a unique solution orbit.
- When the control function is a quadratic Bézier curve, (5.34) has many solution orbits.

5.5.5 Example 5

This subsection presents an example with linear autonomous ordinary differential equation and nonlinear control.

We consider the control of autonomous ordinary differential equation

$$\begin{cases} X' = \begin{pmatrix} x' \\ y' \end{pmatrix} = \begin{pmatrix} \frac{\sqrt{2}}{2}x + \frac{\sqrt{2}}{2}y \\ -\frac{\sqrt{2}}{2}x + \frac{\sqrt{2}}{2}y \end{pmatrix} + \begin{pmatrix} -2u_1^2 - u_2 \\ u_2^2 - u_1 + 1 \end{pmatrix} \\ X(0) = \begin{pmatrix} x(0) \\ y(0) \end{pmatrix} = \begin{pmatrix} 1 \\ 0 \end{pmatrix} \\ \begin{pmatrix} 4 \\ 3 \end{pmatrix} \in X(\mathbb{R}^+). \end{cases} \tag{5.36}$$

The control of autonomous ordinary differential equation 5.36 is derived directly

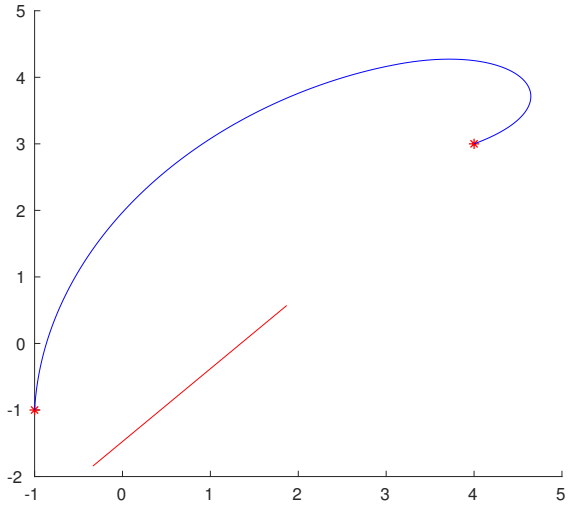

Fig. 5.76: A solution orbit (blue curve) and an orbit of control function (red curve) of (5.36) in Example 5 as the control function is a linear Bézier curve.

from the following autonomous ordinary differential equation

$$\begin{cases} X' = \begin{pmatrix} x' \\ y' \end{pmatrix} = \begin{pmatrix} \frac{\sqrt{2}}{2}x + \frac{\sqrt{2}}{2}y \\ -\frac{\sqrt{2}}{2}x + \frac{\sqrt{2}}{2}y \end{pmatrix} \\ X(0) = \begin{pmatrix} x(0) \\ y(0) \end{pmatrix} = \begin{pmatrix} 1 \\ 0 \end{pmatrix}. \end{cases} \tag{5.37}$$

The autonomous ordinary differential equation 5.37 is studied in Subsection 5.4.4. We add a control function $(-2u_1^2 - u_2, u_2^2 - u_1 + 1)$ such that the solution of (5.36) passes through the point $(4, 3)$. The control function $(-2u_1^2 - u_2, u_2^2 - u_1 + 1)$ is nonlinear.

We find a reparametrization of the solution of (5.36) from the following trajectory optimization problem

$$\begin{cases} F_f(\gamma, \alpha) = \int_0^1 (\|\dot{\gamma}(v)\|_2 . \|f(\gamma(v), u(v))\|_2 - \langle \dot{\gamma}(v), f(\gamma(v), \alpha(v)) \rangle)\, dv \\ \gamma(0) = (1, 0) \\ \gamma(1) = (4, 3), \end{cases}$$

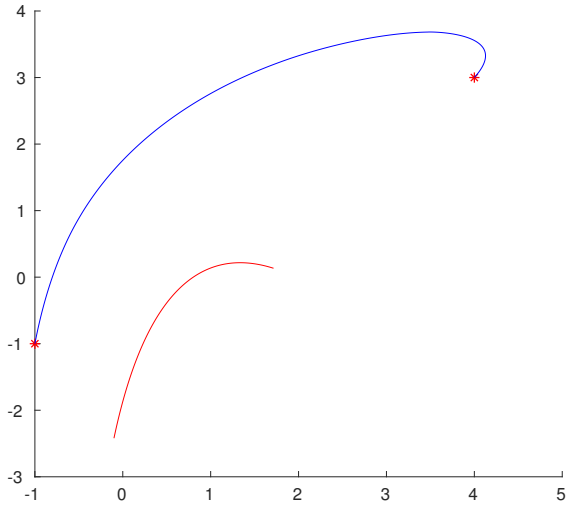

Fig. 5.77: A solution orbit (blue curve) and an orbit of control function (red curve) of (5.36) in Example 5 as the control function is a quadratic Bézier curve.

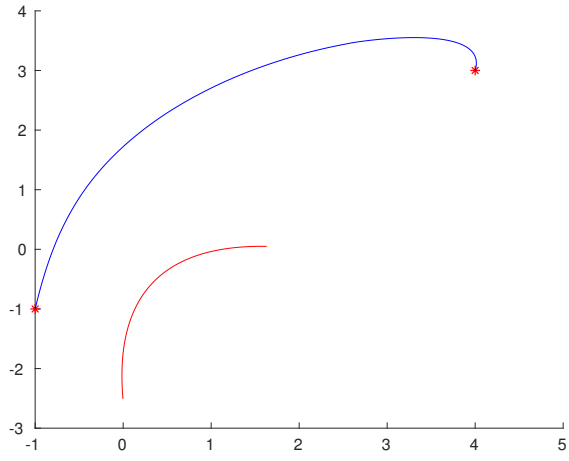

Fig. 5.78: A solution orbit (blue curve) and an orbit of control function (red curve) of (5.36) in Example 5 as the control function is a quadratic Bézier curve.

where

$$f : \mathbb{R}^2 \times \mathbb{R}^2 \to T\mathbb{R}^2$$
$$(x, y) \times (u_1, u_2) \mapsto \Big(\frac{\sqrt{2}}{2}x + \frac{\sqrt{2}}{2}y - 2u_1^2 - u_2, -\frac{\sqrt{2}}{2}x + \frac{\sqrt{2}}{2}y + u_2^2 - u_1 + 1\Big).$$

Using piecewise uniform cubic Bézier curves, Algorithm 2 and Matlab, we can approximate solution orbits of (5.36) (see Figures 5.76, 5.77 and 5.78). We have some remarks about this problem as follows:

Remark 5.36.

- The image of the curve found by our method is a portion of the solution orbit from $(1, 0)$ to $(4, 3)$.
- When the control function is a point (i.e., a constant function), (5.36) has no solution.
- When the control function is a linear Bézier curve, we have a unique solution orbit.
- When the control function is a quadratic Bézier curve, (5.36) has many solution orbits.

5.5.6 Example 6

This subsection presents an example with linear autonomous ordinary differential equation and linear control.

We consider the control of autonomous ordinary differential equation

$$\begin{cases} X' = \begin{pmatrix} x' \\ y' \end{pmatrix} = \begin{pmatrix} u_1 y \\ u_2(x - 0.1y) \end{pmatrix} \\ X(0) = \begin{pmatrix} x(0) \\ y(0) \end{pmatrix} = \begin{pmatrix} 4 \\ -1 \end{pmatrix} \\ \begin{pmatrix} -4 \\ 1 \end{pmatrix} \in X(\mathbb{R}^+). \end{cases} \tag{5.38}$$

The control of autonomous ordinary differential equation 5.38 is derived directly

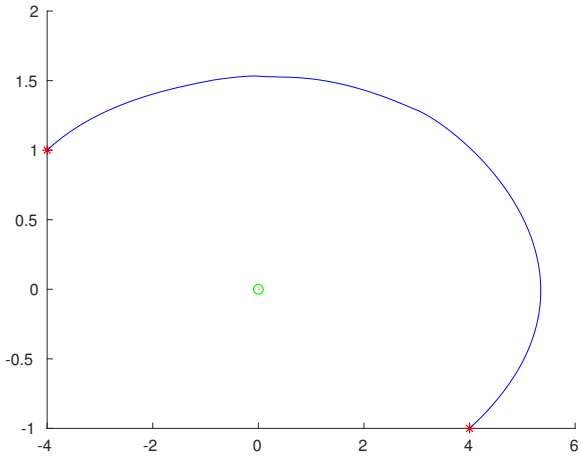

Fig. 5.79: A solution orbit (blue curve) and an orbit of control function (green point) of (5.38) in Example 6 as the control function is a point (i.e., a constant function).

from the following autonomous ordinary differential equation

$$\begin{cases} X' = \begin{pmatrix} x' \\ y' \end{pmatrix} = \begin{pmatrix} y \\ x - 0.1y \end{pmatrix} \\ X(0) = \begin{pmatrix} x(0) \\ y(0) \end{pmatrix} = \begin{pmatrix} 4 \\ -1 \end{pmatrix}. \end{cases} \tag{5.39}$$

The autonomous ordinary differential equation 5.39 is studied in Subsection 5.4.5. We use a control function (u_1, u_2) such that the solution of (5.38) passes through the point $(-4, 1)$. In this problem, we multiply the control function and the autonomous ordinary differential equation. The control of autonomous ordinary differential equation 5.38 is nonlinear.

We find a reparametrization of the solution of (5.38) from the following trajectory optimization problem

$$\begin{cases} F_f(\gamma, \alpha) = \int_0^1 \left(\|\dot{\gamma}(v)\|_2 . \|f(\gamma(v), u(v))\|_2 - \langle \dot{\gamma}(v), f(\gamma(v), \alpha(v)) \rangle \right) dv \\ \gamma(0) = (1, 0) \\ \gamma(1) = (4, 3), \end{cases}$$

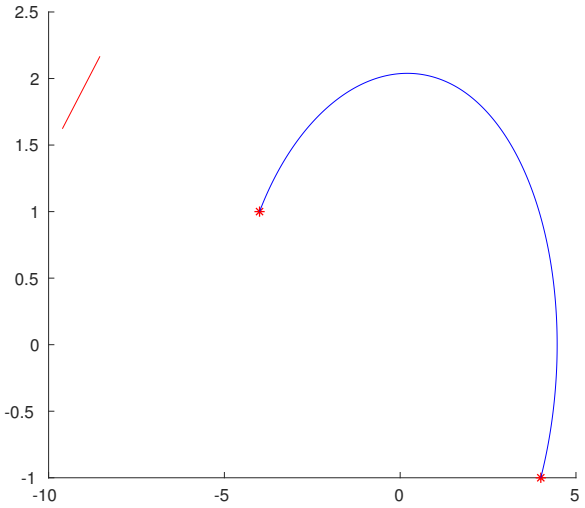

Fig. 5.80: A solution orbit (blue curve) and an orbit of control function (red curve) of (5.38) in Example 6 as the control function is a linear Bézier curve.

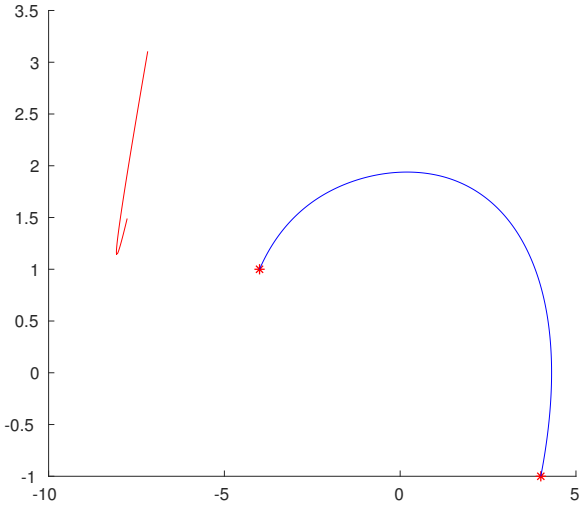

Fig. 5.81: A solution orbit (blue curve) and an orbit of control function (red curve) of (5.38) in Example 6 as the control function is a quadratic Bézier curve.

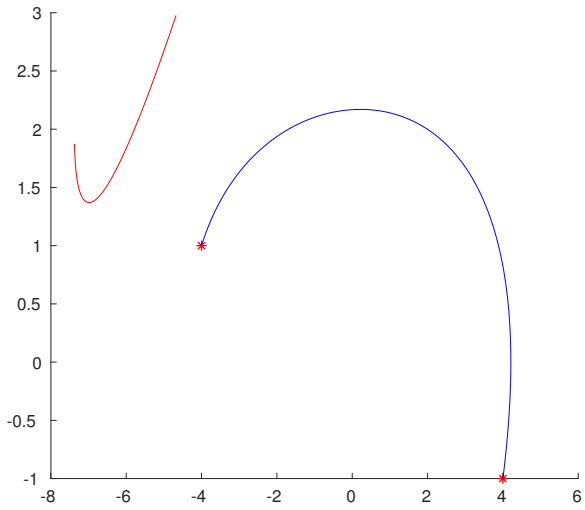

Fig. 5.82: A solution orbit (blue curve) and an orbit of control function (red curve) of (5.38) in Example 6 as the control function is a quadratic Bézier curve.

where

$$f : \mathbb{R}^2 \times \mathbb{R}^2 \to T\mathbb{R}^2$$
$$(x, y) \times (u_1, u_2) \mapsto (u_1 y, u_2(x - 0.1y)).$$

Using piecewise uniform cubic Bézier curves, Algorithm 2 and Matlab, we can approximate solution orbits of (5.38) (see Figures 5.79, 5.80, 5.81 and 5.82). We have some remarks about this problem as follows:

Remark 5.37.

- The image of the curve found by our method is a portion of the solution orbit from $(4, -1)$ to $(-4, 1)$.
- When the control function is a point (i.e., a constant function), (5.38) has a unique solution orbit.
- When the control function is a linear Bézier curve or a quadratic Bézier curve, (5.38) has many solution orbits.

5.5.7 Example 7

This subsection presents an example with linear autonomous ordinary differential equation and linear control.

We consider the control of autonomous ordinary differential equation

$$\begin{cases} X' = \begin{pmatrix} x' \\ y' \end{pmatrix} = \begin{pmatrix} -u_1 x - 8y \\ 8x - u_2 y \end{pmatrix} \\ X(0) = \begin{pmatrix} x(0) \\ y(0) \end{pmatrix} = \begin{pmatrix} 1 \\ 0 \end{pmatrix} \\ \begin{pmatrix} 0.2 \\ 0 \end{pmatrix} \in X(\mathbb{R}^+). \end{cases} \tag{5.40}$$

The control of autonomous ordinary differential equation 5.40 is derived directly from the following autonomous ordinary differential equation

$$\begin{cases} X' = \begin{pmatrix} x' \\ y' \end{pmatrix} = \begin{pmatrix} -x - 8y \\ 8x - y \end{pmatrix} \\ X(0) = \begin{pmatrix} x(0) \\ y(0) \end{pmatrix} = \begin{pmatrix} 1 \\ 0 \end{pmatrix}. \end{cases} \tag{5.41}$$

The solution orbit of the autonomous ordinary differential equation 5.41 is a two-dimensional spiral about the origin (see [29, Chapter IX, p. 404]). We add a control function (u_1, u_2) such that the solution of (5.40) passes through the point $(-0.2, 0)$. In this problem, we multiply the control function and some elements of the autonomous ordinary differential equation. The control of autonomous ordinary differential equation 5.40 is nonlinear.

We find a reparametrization of the solution of (5.40) from the following trajectory optimization problem

$$\begin{cases} F_f(\gamma, \alpha) = \int\limits_0^1 \left(\|\dot{\gamma}(v)\|_2 . \|f(\gamma(v), u(v))\|_2 - \langle \dot{\gamma}(v), f(\gamma(v), \alpha(v)) \rangle \right) dv \\ \gamma(0) = (1, 0) \\ \gamma(1) = (-0.2, 0), \end{cases}$$

where

$$\begin{aligned} f : \mathbb{R}^2 \times \mathbb{R}^2 &\to T\mathbb{R}^2 \\ (x, y) \times (u_1, u_2) &\mapsto (-u_1 x - 8y, 8x - u_2 y). \end{aligned}$$

Using piecewise uniform cubic Bézier curves, Algorithm 2 and Matlab, we can

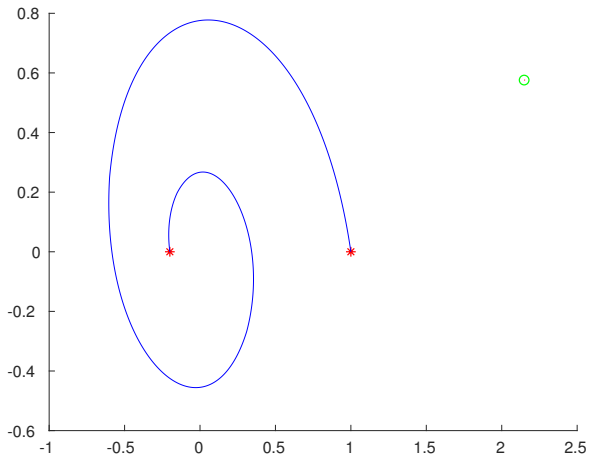

Fig. 5.83: A solution orbit (blue curve) and an orbit of control function (green point) of (5.40) in Example 7 as the control function is a point (i.e., a constant function).

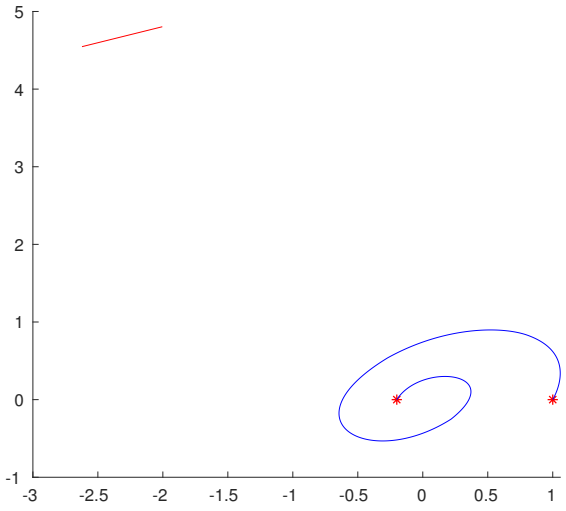

Fig. 5.84: A solution orbit (blue curve) and an orbit of control function (read curve) of (5.40) in Example 7 as the control function is a linear Bézier curve.

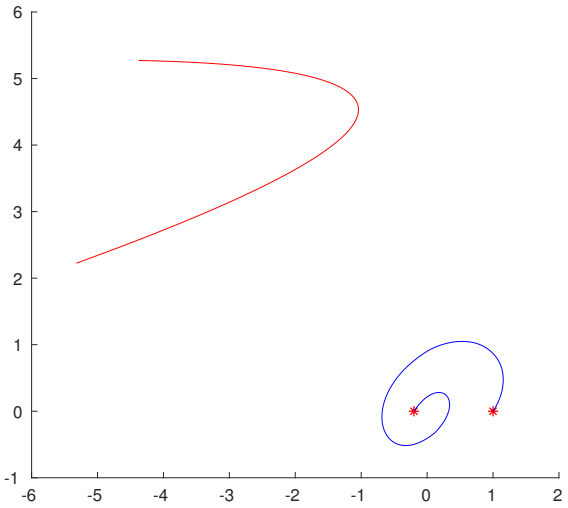

Fig. 5.85: A solution orbit (blue curve) and an orbit of control function (red curve) of (5.40) in Example 7 as the control function is a quadratic Bézier curve.

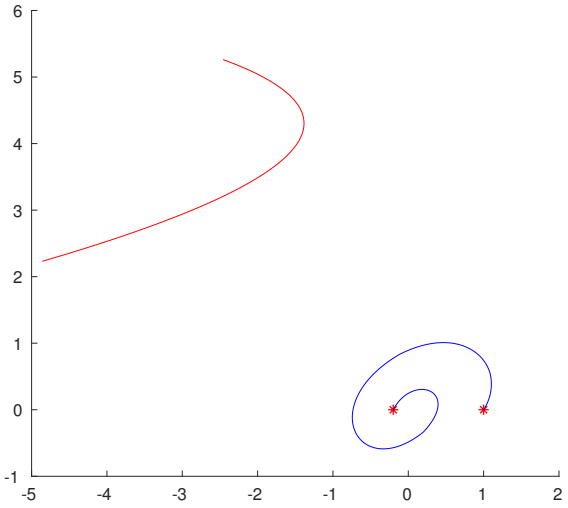

Fig. 5.86: A solution orbit (blue curve) and an orbit of control function (red curve) of (5.40) in Example 7 as the control function is a quadratic Bézier curve.

approximate solution orbits of (5.40) (see Figures 5.83, 5.84, 5.85 and 5.86). We have some remarks about this problem as follows:

Remark 5.38.

- The image of the curve found by our method is a portion of the solution orbit from $(1, 0)$ to $(-0.2, 0)$.
- When the control function is a point (i.e., a constant function), (5.40) has a unique solution orbit.
- When the control function is a linear Bézier curve or a quadratic Bézier curve, (5.40) has many solution orbits.

5.5.8 Example 8

This subsection presents an example with nonlinear autonomous ordinary differential equation and nonlinear control.

We consider the control of autonomous ordinary differential equation

$$\begin{cases} X' = \begin{pmatrix} x' \\ y' \end{pmatrix} = \begin{pmatrix} \frac{2}{3}x - \frac{4}{3}xy \\ xy - y \end{pmatrix} + \begin{pmatrix} u_1^3 + 1 \\ -2u_2^3 + u_1^2 \end{pmatrix} \\ X(0) = \begin{pmatrix} x(0) \\ y(0) \end{pmatrix} = \begin{pmatrix} 1.8 \\ 1.8 \end{pmatrix} \\ \begin{pmatrix} 2 \\ 0.7 \end{pmatrix} \in X(\mathbb{R}^+). \end{cases} \tag{5.42}$$

The control of autonomous ordinary differential equation 5.42 is derived directly from the following autonomous ordinary differential equation

$$\begin{cases} X' = \begin{pmatrix} x' \\ y' \end{pmatrix} = \begin{pmatrix} \frac{2}{3}x - \frac{4}{3}xy \\ xy - y \end{pmatrix} \\ X(0) = \begin{pmatrix} x(0) \\ y(0) \end{pmatrix} = \begin{pmatrix} 1.8 \\ 1.8 \end{pmatrix}. \end{cases} \tag{5.43}$$

This autonomous ordinary differential equation is a Lotka–Volterra equation (see [29, Chapter IX, p. 435], [73, Chapter 3, p. 79]). We add a control function

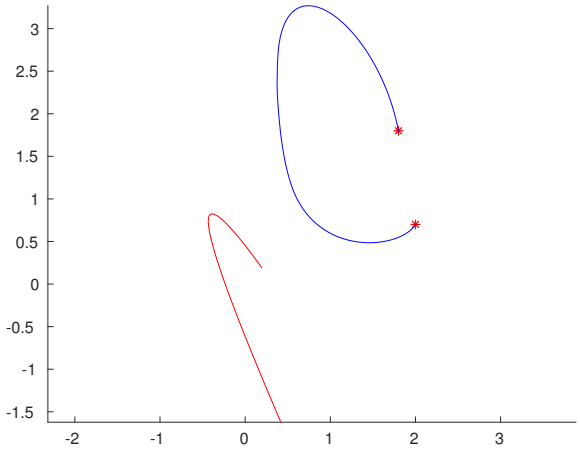

Fig. 5.87: A solution orbit (blue curve) and an orbit of control function (red curve) of (5.42) in Example 8 as the control function is a quadratic Bézier curve.

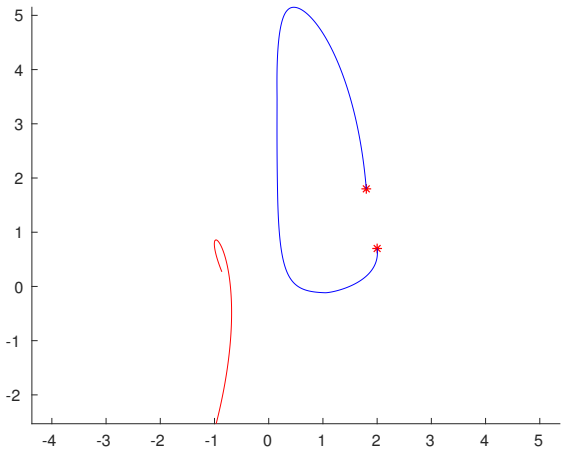

Fig. 5.88: A solution orbit (blue curve) and an orbit of control function (red curve) of (5.42) in Example 8 as the control function is a cubic Bézier curve.

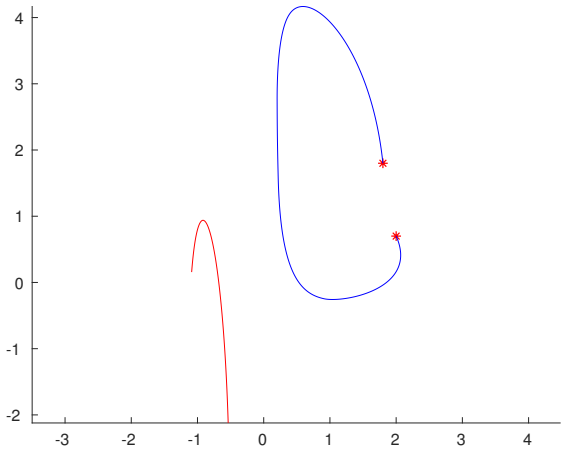

Fig. 5.89: A solution orbit (blue curve) and an orbit of control function (red curve) of (5.42) in Example 8 as the control function is a cubic Bézier curve.

$(u_1^3+1, -2u_2^3+u_1^2)$ such that the solution of (5.42) passes through the point $(2, 0.7)$. The control of autonomous ordinary differential equation 5.42 is nonlinear.

We find a reparametrization of the solution of (5.42) from the following trajectory optimization problem

$$\begin{cases} F_f(\gamma,\alpha) = \int\limits_0^1 \left(\|\dot{\gamma}(v)\|_2.\|f(\gamma(v),u(v))\|_2 - \langle\dot{\gamma}(v), f(\gamma(v),\alpha(v))\rangle\right) dv \\ \gamma(0) = (1.8, 1.8) \\ \gamma(1) = (2, 0.7), \end{cases}$$

where

$$\begin{aligned} f : \mathbb{R}^2 \times \mathbb{R}^2 &\to T\mathbb{R}^2 \\ (x,y) \times (u_1,u_2) &\mapsto \Big(\frac{2}{3}x - \frac{4}{3}xy + u_1^3 + 1, xy - y - 2u_2^3 + u_1^2\Big). \end{aligned}$$

Using piecewise uniform cubic Bézier curves, Algorithm 2 and Matlab, we can approximate solution orbits of (5.42) (see Figures 5.87, 5.88 and 5.89). We have some remarks about this problem as follows:

Remark 5.39.

- The image of the curve found by our method is a portion of the solution orbit from $(1.8, 1.8)$ to $(2, 0.7)$.
- When the control function is a point (i.e., a constant function), (5.42) has

no solution.

- When the control function is a linear Bézier curve, (5.42) has no solution.
- When the control function is a quadratic Bézier curve, (5.42) has a unique solution orbit.
- When the control function is a cubic Bézier curve, (5.42) has many solution orbits.

5.5.9 Relation between our approach and the shooting method

In this section, we want to give a simple comparison with the most commonly used method for non linear control, the shooting method. Interested reader can refer to [87] to have a complete presentation of the subject. We give a quick idea on how the shooting method work and we will give an idea of why our method is interesting compare to this one. Consider a special case of ODE control problem:

$$\begin{cases} \dot{X}(t) = F(X(t), U(t)) \\ X(0) = X_0 \\ X(T) = X_1 \end{cases} \tag{5.44}$$

where X_0 and X_1 are given points on E. I assume here that a solution exist, i.e. that X_1 is feasible and at the time T. A simple idea is to consider X_U, the solution of the Cauchy problem:

$$\begin{cases} \dot{X}_U(t) = F(X_U(t), U(t)) \\ X_U(0) = X_0 \end{cases} \tag{5.45}$$

and denote $G(U, X_0) = X_U(T) - X_1$. The indirect method consist in finding U such that $G(U) = 0$. The most classical strategy consists in discretizing both F and U in order to have a finite number of variables and then to use the Newton method. This approach is called the indirect method. The presentation here is adapted to control and not for optimal control for which the optimality condition can be used to eliminate U from the definition of G. The main problem of this approach is linked to stability of X_1 that can make it "repealing" for the Newton method. The approach we propose here, by only considering trajectories rather than parameterizations get rid of some problem of stability problems since we can fix $X(1)$ to be X_1 has experiments have shown.

In short, we have a method using piecewise uniform cubic Bézier curves to approximate optimal trajectories. This method can be also applied to approximate solution orbits of autonomous ordinary differential equations and control of autonomous ordinary differential equations.

Chapter 6

Conclusion

In this thesis, we focused on the optimization on the set of curves $\mathfrak{C}$ and on using piecewise uniform cubic Bézier curves to approximate optimal trajectories and solution orbits.

In our first contribution, we provided the normalization on $\mathrm{Emb}([0,1],\mathbb{R}^n)$ with respect to the action of $\mathrm{Diff}^+([0,1])$. Then, we identified the set of curves $\mathfrak{C}$ by the set of normal forms. The distance between curves is defined by using its normal forms. This distance is independent of the chosen parametrizations. From this distance, we researched topologies and differential structures on the set of curves.

Our second main contribution is to define a norm on the space of piecewise uniform cubic Bézier curves. This norm is determined through control points of piecewise uniform cubic Bézier curves. We studied the relation between this norm and some classical norms on the space of piecewise uniform cubic Bézier curves.

In our final contribution, we proposed a general method for trajectory optimization problems, autonomous ordinary differential equations and control of autonomous ordinary differential equations. Our method uses piecewise uniform cubic Bézier curves to approximate optimal trajectories. We can apply our method to find approximations of solution orbits of autonomous ordinary differential equations. In order to see the efficiency of our method, we compared our method and some classical methods. We then applied our method to control of autonomous ordinary differential equations.

Bibliography

[1] M. Adachi. *Embeddings and immersions*, volume 124 of *Translations of Mathematical Monographs*. American Mathematical Society, Providence, RI, 1993. ISBN 0-8218-4612-4. Translated from the 1984 Japanese original by Kiki Hudson.

[2] A. Akhmedov and M. P. Cohen. Some applications of hölder's theorem in groups of analytic diffeomorphisms of 1-manifolds. *Topology and its Applications*, 180:85 – 90, 2015. ISSN 0166-8641. doi: https://doi.org/10.1016/j.topol.2014.11.002. URL http://www.sciencedirect.com/science/article/pii/S0166864114004258.

[3] G. Allaire. *Shape optimization by the homogenization method*, volume 146 of *Applied Mathematical Sciences*. Springer-Verlag, New York, 2002. ISBN 0-387-95298-5. doi: 10.1007/978-1-4684-9286-6. URL https://doi-org.ezproxy.unilim.fr/10.1007/978-1-4684-9286-6.

[4] J. W. Anderson. *Hyperbolic geometry*. Springer Undergraduate Mathematics Series. Springer-Verlag London, Ltd., London, second edition, 2005. ISBN 1-85233-934-9.

[5] D. Armentano, C. Beltrán, P. Bürgisser, F. Cucker, and M. Shub. Condition length and complexity for the solution of polynomial systems. *Found. Comput. Math.*, 16(6):1401–1422, 2016. ISSN 1615-3375. doi: 10.1007/s10208-016-9309-9. URL https://doi-org.ezproxy.unilim.fr/10.1007/s10208-016-9309-9.

[6] M. Badiale and G. Tarantello. A Sobolev-Hardy inequality with applications to a nonlinear elliptic equation arising in astrophysics. *Arch. Ration. Mech. Anal.*, 163(4):259–293, 2002. ISSN 0003-9527. doi: 10.1007/s002050200201. URL https://doi-org.ezproxy.unilim.fr/10.1007/s002050200201.

[7] T. Banchoff and S. Lovett. *Differential geometry of curves and surfaces*. CRC Press, Boca Raton, FL, second edition, 2016. ISBN 978-1-4822-4734-3.

[8] M. Bauer, M. Bruveris, P. Harms, and P. W. Michor. Vanishing geodesic distance for the Riemannian metric with geodesic equation the KdV-equation. *Ann. Global Anal. Geom.*, 41(4):461–472, 2012. ISSN 0232-704X. doi: 10.1007/s10455-011-9294-9. URL https://doi-org.ezproxy.unilim.fr/10.1007/s10455-011-9294-9.

[9] M. Bauer, M. Bruveris, P. Harms, and P. W. Michor. Geodesic distance for right invariant Sobolev metrics of fractional order on the diffeomorphism group. *Ann. Global Anal. Geom.*, 44(1):5–21, 2013. ISSN 0232-704X. doi: 10.1007/s10455-012-9353-x. URL https://doi-org.ezproxy.unilim.fr/10.1007/s10455-012-9353-x.

[10] C. Beltrán and A. Leykin. Robust certified numerical homotopy tracking. *Found. Comput. Math.*, 13(2):253–295, 2013. ISSN 1615-3375. doi: 10.1007/s10208-013-9143-2. URL https://doi-org.ezproxy.unilim.fr/10.1007/s10208-013-9143-2.

[11] R. Bhatia. *Matrix analysis*, volume 169 of *Graduate Texts in Mathematics*. Springer-Verlag, New York, 1997. ISBN 0-387-94846-5. doi: 10.1007/978-1-4612-0653-8. URL https://doi-org.ezproxy.unilim.fr/10.1007/978-1-4612-0653-8.

[12] E. Binz and H. R. Fischer. The manifold of embeddings of a closed manifold. In *Differential geometric methods in mathematical physics (Proc. Internat. Conf., Tech. Univ. Clausthal, Clausthal-Zellerfeld, 1978)*, volume 139 of *Lecture Notes in Phys.*, pages 310–329. Springer, Berlin-New York, 1981. With an appendix by P. Michor.

[13] P. Bonnelie. *Déformations libres de contours pour l'optimisation de formes et application en électromagnétisme*. PhD thesis, Université de Limoges, 2017.

[14] H. Brezis. *Functional analysis, Sobolev spaces and partial differential equations*. Universitext. Springer, New York, 2011. ISBN 978-0-387-70913-0.

[15] D. Bucur and G. Buttazzo. *Variational methods in some shape optimization problems*. Appunti dei Corsi Tenuti da Docenti della Scuola. [Notes of Courses Given by Teachers at the School]. Scuola Normale Superiore, Pisa, 2002.

[16] F. Bullo, J. Cortés, and S. Martínez. *Distributed control of robotic networks*. Princeton Series in Applied Mathematics. Princeton University Press, Princeton, NJ, 2009. ISBN 978-0-691-14195-4. doi: 10.1515/9781400831470. URL https://doi-org.ezproxy.unilim.fr/10.1515/9781400831470. A mathematical approach to motion coordination algorithms.

[17] H. Busemann. *The geometry of geodesics*. Academic Press Inc., New York, N. Y., 1955.

[18] J. Canny. *The complexity of robot motion planning*, volume 1987 of *ACM Doctoral Dissertation Awards*. MIT Press, Cambridge, MA, 1988. ISBN 0-262-03136-1.

[19] P. Cardaliaguet, G. Carlier, and B. Nazaret. Geodesics for a class of distances in the space of probability measures. *Calc. Var. Partial Differential Equations*, 48(3-4):395–420, 2013. ISSN 0944-2669. doi: 10.1007/s00526-012-0555-7. URL https://doi-org.ezproxy.unilim.fr/10.1007/s00526-012-0555-7.

[20] V. Cervera, F. Mascaró, and P. W. Michor. The action of the diffeomorphism group on the space of immersions. *Differential Geom. Appl.*, 1(4):391–401, 1991. ISSN 0926-2245. doi: 10.1016/0926-2245(91)90015-2. URL https://doi-org.ezproxy.unilim.fr/10.1016/0926-2245(91)90015-2.

[21] C. Chicone. *Ordinary differential equations with applications*, volume 34 of *Texts in Applied Mathematics*. Springer, New York, second edition, 2006. ISBN 978-0387-30769-5; 0-387-30769-9.

[22] G. Coeuré. *Analytic functions and manifolds in infinite dimensional spaces*. North-Holland Publishing Co., Amsterdam-London; American Elsevier Publishing Co., Inc., New York, 1974. North-Holland Mathematics Studies, Vol. 11.

[23] R. Coleman. *Calculus on normed vector spaces*. Universitext. Springer, New York, 2012. ISBN 978-1-4614-3893-9. doi: 10.1007/978-1-4614-3894-6. URL https://doi-org.ezproxy.unilim.fr/10.1007/978-1-4614-3894-6.

[24] G. Corach, H. Porta, and L. Recht. Convexity of the geodesic distance on spaces of positive operators. *Illinois J. Math.*, 38(1):87–94, 1994. ISSN 0019-2082. URL http://projecteuclid.org.ezproxy.unilim.fr/euclid.ijm/1255986889.

[25] M. D. Crossley. *Essential topology*. Springer Undergraduate Mathematics Series. Springer-Verlag London, Ltd., London, 2005. ISBN 978-1-85233-782-7; 1-85233-782-6. doi: 10.1007/1-84628-194-6. URL https://doi-org.ezproxy.unilim.fr/10.1007/1-84628-194-6.

[26] I. Danaila, P. Joly, S. M. Kaber, and M. Postel. *An introduction to scientific computing*. Springer, New York, 2007. ISBN 978-0-387-30889-0; 0-387-30889-X. doi: 10.1007/978-0-387-49159-2. URL https://doi-org.ezproxy.unilim.fr/10.1007/978-0-387-49159-2. Twelve computational projects solved with MATLAB.

[27] F. de Gournay, G. Allaire, and F. Jouve. Shape and topology optimization of the robust compliance via the level set method. *ESAIM Control Optim. Calc. Var.*, 14(1):43–70, 2008. ISSN 1292-8119. doi: 10.1051/cocv:2007048. URL https://doi-org.ezproxy.unilim.fr/10.1051/cocv:2007048.

[28] M. P. do Carmo. *Differential geometry of curves and surfaces*. Prentice-Hall, Inc., Englewood Cliffs, N.J., 1976. Translated from the Portuguese.

[29] R. D. Driver. *Ordinary and delay differential equations*. Springer-Verlag, New York-Heidelberg, 1977. ISBN 0-387-90231-7. Applied Mathematical Sciences, Vol. 20.

[30] L. P. Eisenhart. *A treatise on the differential geometry of curves and surfaces*. Dover Publications, Inc., New York, 1960.

[31] H. I. Eliasson. Geometry of manifolds of maps. *J. Differential Geometry*, 1:169–194, 1967. ISSN 0022-040X. URL http://projecteuclid.org.ezproxy.unilim.fr/euclid.jdg/1214427887.

[32] R. Engelking. *Outline of general topology*. Translated from the Polish by K. Sieklucki. North-Holland Publishing Co., Amsterdam; PWN-Polish Scientific Publishers, Warsaw; Interscience Publishers Division John Wiley & Sons, Inc., New York, 1968.

[33] D. Estep. *Practical analysis in one variable*. Undergraduate Texts in Mathematics. Springer-Verlag, New York, 2002. ISBN 0-387-95484-8.

[34] M. Fabian, P. Habala, P. Hájek, V. Montesinos, and V. Zizler. *Banach space theory*. CMS Books in Mathematics/Ouvrages de Mathématiques de la SMC. Springer, New York, 2011. ISBN 978-1-4419-7514-0. doi:

10.1007/978-1-4419-7515-7. URL https://doi-org.ezproxy.unilim.fr/10.1007/978-1-4419-7515-7. The basis for linear and nonlinear analysis.

[35] M. Farber. Topological complexity of motion planning. *Discrete Comput. Geom.*, 29(2):211–221, 2003. ISSN 0179-5376. doi: 10.1007/s00454-002-0760-9. URL https://doi-org.ezproxy.unilim.fr/10.1007/s00454-002-0760-9.

[36] M. Farber. *Invitation to topological robotics*. Zurich Lectures in Advanced Mathematics. European Mathematical Society (EMS), Zürich, 2008. ISBN 978-3-03719-054-8. doi: 10.4171/054. URL https://doi-org.ezproxy.unilim.fr/10.4171/054.

[37] M. Farber, S. Tabachnikov, and S. Yuzvinsky. Topological robotics: motion planning in projective spaces. *Int. Math. Res. Not.*, (34):1853–1870, 2003. ISSN 1073-7928. doi: 10.1155/S1073792803210035. URL https://doi-org.ezproxy.unilim.fr/10.1155/S1073792803210035.

[38] G. Farin. *Curves and surfaces for computer-aided geometric design*. Computer Science and Scientific Computing. Academic Press, Inc., San Diego, CA, fourth edition, 1997. ISBN 0-12-249054-1. A practical guide, Chapter 1 by P. Bézier; Chapters 11 and 22 by W. Boehm, With 1 IBM-PC floppy disk (3.5 inch; HD).

[39] J. Gallier. *Curves and surfaces in geometric modeling*. The Morgan Kaufmann Series in Computer Graphics and Geometric Modeling. Morgan Kaufmann, San Francisco, CA, 2000. ISBN 1-55860-599-1. Theory and algorithms.

[40] F. R. Gantmacher. *The theory of matrices. Vols. 1, 2*. Translated by K. A. Hirsch. Chelsea Publishing Co., New York, 1959.

[41] H. Glöckner and K.-H. Neeb. Diffeomorphism groups of compact convex sets. *Indagationes Mathematicae*, 28(4):760 – 783, 2017. ISSN 0019-3577. doi: https://doi.org/10.1016/j.indag.2017.04.004. URL http://www.sciencedirect.com/science/article/pii/S0019357717300320.

[42] G. H. Golub and C. F. Van Loan. *Matrix computations*. Johns Hopkins Studies in the Mathematical Sciences. Johns Hopkins University Press, Baltimore, MD, third edition, 1996. ISBN 0-8018-5413-X; 0-8018-5414-8.

[43] J. Gravesen. Adaptive subdivision and the length and energy of Bézier curves. *Comput. Geom.*, 8(1):13–31, 1997. ISSN 0925-7721. doi: 10.1016/0925-7721(95)00054-2. URL https://doi-org.ezproxy.unilim.fr/10.1016/0925-7721(95)00054-2.

[44] J. Gravesen. De Casteljau's algorithm revisited. In *Mathematical methods for curves and surfaces, II (Lillehammer, 1997)*, Innov. Appl. Math., pages 221–228. Vanderbilt Univ. Press, Nashville, TN, 1998.

[45] J. K. Hale and S. M. Verduyn Lunel. *Introduction to functional-differential equations*, volume 99 of *Applied Mathematical Sciences*. Springer-Verlag, New York, 1993. ISBN 0-387-94076-6. doi: 10.1007/978-1-4612-4342-7. URL https://doi-org.ezproxy.unilim.fr/10.1007/978-1-4612-4342-7.

[46] R. S. Hamilton. The inverse function theorem of Nash and Moser. *Bull. Amer. Math. Soc. (N.S.)*, 7(1):65–222, 1982. ISSN 0273-0979. doi: 10.1090/S0273-0979-1982-15004-2. URL https://doi-org.ezproxy.unilim.fr/10.1090/S0273-0979-1982-15004-2.

[47] B. Hartley and T. O. Hawkes. *Rings, modules and linear algebra. A further course in algebra describing the structure of Abelian groups and canonical forms of matrices through the study of rings and modules*. Chapman and Hall, Ltd., London, 1970.

[48] J. Haslinger and R. A. E. Mäkinen. *Introduction to shape optimization*, volume 7 of *Advances in Design and Control*. Society for Industrial and Applied Mathematics (SIAM), Philadelphia, PA, 2003. ISBN 0-89871-536-9. doi: 10.1137/1.9780898718690. URL https://doi-org.ezproxy.unilim.fr/10.1137/1.9780898718690. Theory, approximation, and computation.

[49] F. Hiai and D. Petz. *Introduction to matrix analysis and applications*. Universitext. Springer, Cham; Hindustan Book Agency, New Delhi, 2014. ISBN 978-3-319-04149-0; 978-3-319-04150-6; 978-93-80250-60-1. doi: 10.1007/978-3-319-04150-6. URL https://doi-org.ezproxy.unilim.fr/10.1007/978-3-319-04150-6.

[50] R. A. Horn and C. R. Johnson. *Matrix analysis*. Cambridge University Press, Cambridge, second edition, 2013. ISBN 978-0-521-54823-6.

[51] S. H. Joshi, J. Su, Z. Zhang, and B. Ben Amor. Elastic shape analysis of functions, curves and trajectories. In *Riemannian computing in computer vision*, pages 211–231. Springer, Cham, 2016.

[52] J. L. Kelley. *General topology*. D. Van Nostrand Company, Inc., Toronto-New York-London, 1955.

[53] P. a. Kiciak. *Geometric continuity of curves and surfaces*, volume 25 of *Synthesis Lectures on Visual Computing*. Morgan & Claypool Publishers, [Williston], VT, 2017. ISBN 978-1-62705-905-3; 978-1-62705-467-6.

[54] W. Klingenberg. *Lectures on closed geodesics*. Springer-Verlag, Berlin-New York, 1978. ISBN 3-540-08393-6. Grundlehren der Mathematischen Wissenschaften, Vol. 230.

[55] S. Kobayashi and K. Nomizu. *Foundations of differential geometry. Vol. I*. Wiley Classics Library. John Wiley & Sons, Inc., New York, 1996. ISBN 0-471-15733-3. Reprint of the 1963 original, A Wiley-Interscience Publication.

[56] S. Kobayashi and K. Nomizu. *Foundations of differential geometry. Vol. II*. Wiley Classics Library. John Wiley & Sons, Inc., New York, 1996. ISBN 0-471-15732-5. Reprint of the 1969 original, A Wiley-Interscience Publication.

[57] A. Kriegl and P. W. Michor. *The convenient setting of global analysis*, volume 53 of *Mathematical Surveys and Monographs*. American Mathematical Society, Providence, RI, 1997. ISBN 0-8218-0780-3. doi: 10.1090/surv/053. URL https://doi-org.ezproxy.unilim.fr/10.1090/surv/053.

[58] S. Lang. *Undergraduate analysis*. Undergraduate Texts in Mathematics. Springer-Verlag, New York, 1983. ISBN 0-387-90800-5. doi: 10.1007/978-1-4757-1801-0. URL https://doi-org.ezproxy.unilim.fr/10.1007/978-1-4757-1801-0.

[59] S. Lang. *Differential and Riemannian manifolds*, volume 160 of *Graduate Texts in Mathematics*. Springer-Verlag, New York, third edition, 1995. ISBN 0-387-94338-2. doi: 10.1007/978-1-4612-4182-9. URL https://doi-org.ezproxy.unilim.fr/10.1007/978-1-4612-4182-9.

[60] W. F. Langford and P. Yu, editors. *Computation of normal forms and applications*. Watam Press, Waterloo, ON, 2001. Dyn. Contin. Discrete Impuls. Syst. Ser. A Math. Anal. **8** (2001), no. 4.

[61] J. M. Lee. *Introduction to smooth manifolds*, volume 218 of *Graduate Texts in Mathematics*. Springer, New York, second edition, 2013. ISBN 978-1-4419-9981-8.

[62] X. Liao and P. Yu. *Absolute stability of nonlinear control systems*, volume 25 of *Mathematical Modelling: Theory and Applications*. Springer, New York, second edition, 2008. ISBN 978-1-4020-8481-2. doi: 10.1007/978-1-4020-8482-9. URL https://doi-org.ezproxy.unilim.fr/10.1007/978-1-4020-8482-9.

[63] J. Lines and A. Bagnall. Time series classification with ensembles of elastic distance measures. *Data Min. Knowl. Discov.*, 29(3):565–592, 2015. ISSN 1384-5810. doi: 10.1007/s10618-014-0361-2. URL https://doi-org.ezproxy.unilim.fr/10.1007/s10618-014-0361-2.

[64] D. Marsh. *Applied geometry for computer graphics and CAD*. Springer Undergraduate Mathematics Series. Springer-Verlag London, Ltd., London, second edition, 2005. ISBN 1-85233-801-6.

[65] J. E. McIntyre. *Guidance, flight mechanics and trajectory optimization. Vol. VII: The Pontryagin maximum principle*. Report No. SID 65-1200-7. NASA CR-1006. National Aeronautics and Space Administration, Washington, D.C., 1968.

[66] D. R. Merkin. *Introduction to the theory of stability*, volume 24 of *Texts in Applied Mathematics*. Springer-Verlag, New York, 1997. ISBN 0-387-94761-2. Translated from the third (1987) Russian edition, edited and with an introduction by Fred F. Afagh and Andrei L. Smirnov.

[67] P. Michor. Manifolds of smooth maps. III. The principal bundle of embeddings of a noncompact smooth manifold. *Cahiers Topologie Géom. Différentielle*, 21(3):325–337, 1980. ISSN 0008-0004.

[68] P. W. Michor. *Manifolds of differentiable mappings*, volume 3 of *Shiva Mathematics Series*. Shiva Publishing Ltd., Nantwich, 1980. ISBN 0-906812-03-8.

[69] P. W. Michor and D. Mumford. Vanishing geodesic distance on spaces of submanifolds and diffeomorphisms. *Doc. Math.*, 10:217–245, 2005. ISSN 1431-0635.

[70] B. Mohammadi and O. Pironneau. Shape optimization in fluid mechanics. In *Annual review of fluid mechanics. Vol. 36*, volume 36 of *Annu. Rev. Fluid Mech.*, pages 255–279. Annual Reviews, Palo Alto, CA, 2004. doi: 10.1146/annurev.fluid.36.050802.121926. URL https://doi-org.ezproxy.unilim.fr/10.1146/annurev.fluid.36.050802.121926.

[71] B. Mohammadi and O. Pironneau. *Applied shape optimization for fluids*. Numerical Mathematics and Scientific Computation. Oxford University Press, Oxford, second edition, 2010. ISBN 978-0-19-954690-9.

[72] H. P. Moreton and C. H. Séquin. Minimum variation curves and surfaces for computer-aided geometric design. In *Designing fair curves and surfaces*, Geom. Des. Publ., pages 123–159. SIAM, Philadelphia, PA, 1994.

[73] J. D. Murray. *Mathematical biology. I*, volume 17 of *Interdisciplinary Applied Mathematics*. Springer-Verlag, New York, third edition, 2002. ISBN 0-387-95223-3. An introduction.

[74] R. M. Murray and S. S. Sastry. Nonholonomic motion planning: steering using sinusoids. *IEEE Trans. Automat. Control*, 38(5):700–716, 1993. ISSN 0018-9286. doi: 10.1109/9.277235. URL https://doi-org.ezproxy.unilim.fr/10.1109/9.277235.

[75] R. N. Murray, Z. X. Li, and S. S. Sastry. *A mathematical introduction to robotic manipulation*. CRC Press, Boca Raton, FL, 1994. ISBN 0-8493-7981-4.

[76] G. Rein. Collisionless kinetic equations from astrophysics—the Vlasov-Poisson system. In *Handbook of differential equations: evolutionary equations. Vol. III*, Handb. Differ. Equ., pages 383–476. Elsevier/North-Holland, Amsterdam, 2007. doi: 10.1016/S1874-5717(07)80008-9. URL https://doi-org.ezproxy.unilim.fr/10.1016/S1874-5717(07)80008-9.

[77] J. Richter-Gebert. *Perspectives on projective geometry*. Springer, Heidelberg, 2011. ISBN 978-3-642-17285-4. doi: 10.1007/978-3-642-17286-1. URL https://doi-org.ezproxy.unilim.fr/10.1007/978-3-642-17286-1. A guided tour through real and complex geometry.

[78] I. K. Sabitov. *Isometric immersions and embeddings of locally Euclidean metrics*, volume 13 of *Reviews in Mathematics and Mathematical Physics*. Cambridge Scientific Publishers, Cambridge, 2008. ISBN 978-1-904868-62-0.

[79] T. W. Sederberg. Applications to computer aided geometric design. In *Applications of computational algebraic geometry (San Diego, CA, 1997)*, volume 53 of *Proc. Sympos. Appl. Math.*, pages 67–89. Amer. Math. Soc., Providence, RI, 1998. doi: 10.1090/psapm/053/1602355. URL https://doi-org.ezproxy.unilim.fr/10.1090/psapm/053/1602355.

[80] G. E. Shilov. *Linear algebra*. Dover Publications, Inc., New York, english edition, 1977. ISBN 0-486-63518-X. Translated from the Russian and edited by Richard A. Silverman.

[81] J. Sokoł owski and J.-P. Zolésio. *Introduction to shape optimization*, volume 16 of *Springer Series in Computational Mathematics*. Springer-Verlag, Berlin, 1992. ISBN 3-540-54177-2. doi: 10.1007/978-3-642-58106-9. URL https://doi-org.ezproxy.unilim.fr/10.1007/978-3-642-58106-9. Shape sensitivity analysis.

[82] M. Spivak. *A comprehensive introduction to differential geometry. Vol. I.* Publish or Perish, Inc., Wilmington, Del., second edition, 1979. ISBN 0-914098-83-7.

[83] M. Spivak. *A comprehensive introduction to differential geometry. Vol. II.* Publish or Perish, Inc., Wilmington, Del., second edition, 1979. ISBN 0-914098-83-7.

[84] M. Spivak. *A comprehensive introduction to differential geometry. Vol. III.* Publish or Perish, Inc., Wilmington, Del., second edition, 1979. ISBN 0-914098-83-7.

[85] M. Spivak. *A comprehensive introduction to differential geometry. Vol. IV.* Publish or Perish, Inc., Wilmington, Del., second edition, 1979. ISBN 0-914098-83-7.

[86] M. Spivak. *A comprehensive introduction to differential geometry. Vol. V.* Publish or Perish, Inc., Wilmington, Del., second edition, 1979. ISBN 0-914098-83-7.

[87] J. Stoer and R. Bulirsch. *Introduction to numerical analysis*, volume 12 of *Texts in Applied Mathematics*. Springer-Verlag, New York, third edition, 2002. ISBN 0-387-95452-X. doi: 10.1007/978-0-387-21738-3. URL https://doi-org.ezproxy.unilim.fr/10.1007/978-0-387-21738-3. Translated from the German by R. Bartels, W. Gautschi and C. Witzgall.

[88] I. Streinu. A combinatorial approach to planar non-colliding robot arm motion planning. In *41st Annual Symposium on Foundations of Computer Science (Redondo Beach, CA, 2000)*, pages 443–453. IEEE Comput. Soc. Press, Los Alamitos, CA, 2000. doi: 10.1109/SFCS.2000.892132. URL https://doi-org.ezproxy.unilim.fr/10.1109/SFCS.2000.892132.

[89] M. Umehara and K. Yamada. *Differential geometry of curves and surfaces*. World Scientific Publishing Co. Pte. Ltd., Hackensack, NJ, 2017. ISBN 978-981-4740-23-4. doi: 10.1142/9901. URL https://doi-org.ezproxy.unilim.fr/10.1142/9901. Translated from the second (2015) Japanese edition by Wayne Rossman.

[90] M. A. van Wyk and W.-H. Steeb. *Chaos in electronics*, volume 2 of *Mathematical Modelling: Theory and Applications*. Kluwer Academic Publishers, Dordrecht, 1997. ISBN 0-7923-4576-2. doi: 10.1007/978-94-015-8921-5. URL https://doi-org.ezproxy.unilim.fr/10.1007/978-94-015-8921-5.

[91] F. Verhulst. *Nonlinear differential equations and dynamical systems*. Universitext. Springer-Verlag, Berlin, second edition, 1996. ISBN 3-540-60934-2. doi: 10.1007/978-3-642-61453-8. URL https://doi-org.ezproxy.unilim.fr/10.1007/978-3-642-61453-8. Translated from the 1985 Dutch original.

[92] J. von Neumann. *Collected works. Vol. VI: Theory of games, astrophysics, hydrodynamics and meteorology*. General editor: A. H. Taub. A Pergamon Press Book. The Macmillan Co., New York, 1963.

[93] F. W. Warner. *Foundations of differentiable manifolds and Lie groups*. Scott, Foresman and Co., Glenview, Ill.-London, 1971.

[94] K. J. Worsley. Boundary corrections for the expected Euler characteristic of excursion sets of random fields, with an application to astrophysics. *Adv. in Appl. Probab.*, 27(4):943–959, 1995. ISSN 0001-8678. doi: 10.2307/1427930. URL https://doi-org.ezproxy.unilim.fr/10.2307/1427930.

[95] L. Younes. A distance for elastic matching in object recognition. *C. R. Acad. Sci. Paris Sér. I Math.*, 322(2):197–202, 1996. ISSN 0764-4442.

[96] L. Younes. Computable elastic distances between shapes. *SIAM J. Appl. Math.*, 58(2):565–586, 1998. ISSN 0036-1399. doi: 10.

1137/S0036139995287685. URL https://doi-org.ezproxy.unilim.fr/10.1137/S0036139995287685.

[97] L. Younes. *Shapes and diffeomorphisms*, volume 171 of *Applied Mathematical Sciences*. Springer-Verlag, Berlin, 2010. ISBN 978-3-642-12054-1. doi: 10.1007/978-3-642-12055-8. URL https://doi-org.ezproxy.unilim.fr/10.1007/978-3-642-12055-8.

Titre thèse anglais: Distance and geometry of the set of curves and approximation of optimal trajectories

Abstract: Optimization problems on the set of curves appear in many fields of applications such as industry, robotic, path-planning and aerospace. This thesis is devoted to study the set of curves and propose a general method for trajectory optimization problems, autonomous ODEs and control of autonomous ODEs. In the first part, we provide a normalization of parametrized curves up to increasing diffeomorphism and use it to define a distance between curves. Then, we study topologies and differential structures on the set of curves. The second part defines a norm on spaces of piecewise cubic Bézier curves and estimates equivalence constants for this norm and some classical norms. The last part proposes a general method to approximate optimal trajectories using piecewise cubic Bézier curves. This idea is applied to autonomous ODEs and control of autonomous ODEs.

Keywords: the set of curves, Bézier curves, piecewise Bézier curves, distance, norm, normal form, normalization, autonomous ODE, control of autonomous ODE, optimal trajectory, orbit.

Titre thèse français: La distance et la géométrie de l'ensemble des courbes et l'approximation des trajectoires optimales

Résumé:

Les problèmes d'optimisation sur l'ensemble des courbes apparaissent dans de nombreux domaines d'applications l'industrielles comme la robotique, la planification de mouvements et l'aérospatiale. Dans cette thèse, nous nous étudions l'ensemble des courbes et proposons une méthode générale pour problèmes d'optimisation de trajectoires, équations différentielles ordinaires autonome et commande des équations différentielles ordinaires autonome. Dans la première partie, nous fournissons une normalisation des courbes paramétrisées sous l'action des difféomorphismes croissants et nous utilisons cette normalisation pour définir une distance entre les courbes paramétrées. Nous étudions ensuite la topologie et la structure différentielle sur l'ensemble des courbes. Dans la seconde partie nous définissons une norme sur l'espace des courbes de Bézier cubique par morceaux et nous estimons quelques constantes d'équivalence pour cette norme et certaines normes classiques. La dernière partie de cette thèse est propose une méthode générale pour approximer des trajectoires optimales en utilisant des courbes de Bézier cubiques par morceaux. Cette idèe est appliquée aux équations différentielles autonomes et au contrôle des équations différentielles autonomes.

Mots clés : ensemble des courbes paramétrées, courbes de Bézier, courbes de Bézier cubiques par morceaux, distance, norme, forme normale, normalisation, équations différentielles autonome, contrôle des équations différentielles autonome, trajectoire optimale, orbite.